เมแทบอไลต์ทุติยภูมิจากราเอนโดไฟต์ที่คัดเลือก
ซึ่งมีฤทธิ์เสริมยากลุ่มเอโซลในการต้าน *Candida albicans*

นางจตุพร เผ่าพงษ์ไทย

วิทยานิพนธ์นี้เป็นส่วนหนึ่งของการศึกษาตามหลักสูตรปริญญาวิทยาศาสตรดุษฎีบัณฑิต
สาขาวิชาเภสัชเวท ภาควิชาเภสัชเวทและเภสัชพฤกษศาสตร์
คณะเภสัชศาสตร์ จุฬาลงกรณ์มหาวิทยาลัย
ปีการศึกษา 2554
ลิขสิทธิ์ของจุฬาลงกรณ์มหาวิทยาลัย

บทคัดย่อและแฟ้มข้อมูลฉบับเต็มของวิทยานิพนธ์ตั้งแต่ปีการศึกษา 2554 ที่ให้บริการในคลังปัญญาจุฬาฯ (CUIR)
เป็นแฟ้มข้อมูลของนิสิตเจ้าของวิทยานิพนธ์ที่ส่งผ่านทางบัณฑิตวิทยาลัย
The abstract and full text of theses from the academic year 2011 in Chulalongkorn University Intellectual Repository(CUIR)
are the thesis authors' files submitted through the Graduate School.

SECONDARY METABOLITES FROM SELECTED ENDOPHYTIC FUNGI EXHIBITING SYNERGISTIC ACTIVITY WITH AZOLE DRUGS AGAINST *CANDIDA ALBICANS*

Mrs. Jatuporn Phaopongthai

A Dissertation Submitted in Partial Fulfillment of the Requirements
for the Degree of Doctor of Philosophy Program in Pharmacognosy
Department of Pharmacognosy and Pharmaceutical Botany
Faculty of Pharmaceutical Sciences
Chulalongkorn University
Academic Year 2011

Copyright of Chulalongkorn University

Thesis Title	SECONDARY METABOLITES FROM SELECTED ENDOPHYTIC FUNGI EXHIBITING SYNERGISTIC ACTIVITY WITH AZOLE DRUGS AGAINST *CANDIDA ALBICANS*
By	Mrs. Jatuporn Phaopongthai
Field of Study	Pharmacognosy
Thesis Advisor	Khanit Suwanborirux, Ph.D.
Thesis Co-Advisor	Associate Professor Nongluksna Sriubolmas, Ph.D.

Accepted by the Faculty of Pharmaceutical Sciences, Chulalongkorn University in Partial Fulfillment of the Requirements for the Doctoral Degree

……Dean of the Faculty of Pharmaceutical Sciences

(Associate Professor Pintip Pongpech, Ph.D.)

THESIS COMMITTEE

…….. Chairman

(Professor Kittisak Likhitwitayawuid, Ph.D.)

……. Thesis Advisor

(Khanit Suwanborirux, Ph.D.)

…….. Thesis Co-Advisor

(Associate Professor Nongluksna Sriubolmas, Ph.D.

…….. Examiner

(Associate Professor Rutt Suttisri, Ph.D.)

…….. Examiner

(Associate Professor Surattana Ammuoypol, Ph.D.)

…….. External Examiner

(Assistant Professor Suthep Wiyakrutta, Ph.D.)

จตุพร เผ่าพงษ์ไทย : เมแทบอไลต์ทุติยภูมิจากราเอนโดไฟต์ที่คัดเลือกซึ่งมีฤทธิ์เสริมยากลุ่มเอโซลในการต้าน *CANDIDA ALBICANS* (SECONDARY METABOLITES FROM SELECTED ENDOPHYTIC FUNGI EXHIBITING SYNERGISTIC ACTIVITY WITH AZOLE DRUGS AGAINST *CANDIDA ALBICANS*) อ.ที่ปรึกษาวิทยานิพนธ์หลัก: อ. ดร. คณิต สุวรรณบริรักษ์, อ.ที่ปรึกษาวิทยานิพนธ์ร่วม: รศ. ดร. นงลักษณ์ ศรีอุบลมาศ, 162 หน้า.

จากการศึกษาลักษณะทางกายภาพร่วมกับลำดับนิวคลีโอไทด์บริเวณจีนอาร์เอ็นเอไรโบโซม สามารถพิสูจน์เอกลักษณ์ราเอนโดไฟต์ ๒ ชนิด เป็น *Nodulisporium* sp. Aann-134 และ *Alternaria alternata* Tche-153 ซึ่งแยกได้จากใบโกฐจุฬาลำพา (*Artemisia annua* L.) และสมอไทย (*Terminalia chebula* Retz.) ตามลำดับ สารสกัดเอธิลอะซิเตทจากน้ำเลี้ยงเชื้อของราทั้งสองมีฤทธิ์เสริมยา ketoconazole ในการต้าน *Candida albicans* จึงได้ทำการแยกเมแทบอไลต์ทุติยภูมิจากสารสกัดทั้งสองด้วยคอลัมน์โครมาโทกราฟีควบคู่กับการตรวจสอบฤทธิ์ต้านเชื้อรา และทำการพิสูจน์โครงสร้างทางเคมีของสารด้วยการวิเคราะห์ข้อมูลสเปคโตสโคปี ทำให้สามารถแยกสารจำนวน ๗ ชนิดได้จากสารสกัดของราเอนโดไฟต์ *Nodulisporium* sp. Aann-134 และพิสูจน์ได้ว่าเป็นสาร polyketides กลุ่ม resorcinols จำนวน ๔ ชนิด ได้แก่ สาร 1′-(2,6-dihydroxyphenyl)butanone สาร 1′-(2,6-dihydroxyphenyl)-3′-hydroxy butanone สาร 1′-(2,6-dihydroxyphenyl)ethanone และสารชนิดใหม่ nodulisporin G สารกลุ่ม napthalenes จำนวน ๒ ชนิด ได้แก่ สาร 1,8-dimethoxynaphthalene และสาร 1,8-dihydroxynaphthalene และสาร phenylacetic acid รวมทั้งสามารถแยกสารจำนวน ๔ ชนิดได้จากสารสกัดของราเอนโดไฟต์ *Alternaria alternata* Tche-153 และพิสูจน์ได้ว่าเป็นสาร polyketides กลุ่ม salicylates จำนวน ๓ ชนิด ได้แก่ สาร altenusin สาร isoochracinic acid และสาร altenuic acid ร่วมกับสาร 2,5-dimethyl-7-hydroxychromone

โดยการใช้วิธี disk diffusion และวิธี chequerboard พบว่าสาร 1′-(2,6-dihydroxy phenyl)butanone และสาร 1,8-dihydroxynaphthalene มีฤทธิ์ที่แรงในการเสริมฤทธิ์ยา fluconazole ต้านเชื้อรา *C. albicans* โดยมีค่าดัชนีสัดส่วนความเข้มข้นในการต้านเชื้อที่ ๐.๒๕๐ และ ๐.๓๗๕ ตามลำดับ และสาร altenusin มีฤทธิ์ที่แรงมากในการเสริมฤทธิ์ยา ketoconazole fluconazole หรือ itraconazole ต้านเชื้อรา *C. albicans* โดยมีค่าดัชนีสัดส่วนความเข้มข้นในการต้านเชื้อในช่วง ๐.๐๗๘ ถึง ๐.๑๘๘

ภาควิชา: เภสัชเวทและเภสัชพฤกษศาสตร์ ลายมือชื่อนิสิต .....

สาขาวิชา เภสัชเวท ลายมือชื่อ อ.ที่ปรึกษาวิทยานิพนธ์หลัก .....

ปีการศึกษา 2554 ลายมือชื่อ อ.ที่ปรึกษาวิทยานิพนธ์ร่วม .....

4976952033: MAJOR PHARMACOGNOSY
KEYWORDS: AZOLE-SYNERGISM/ *NODULISPORIUM* SP./ 1'-(2,6-DIHYDROXY PHENYL)BUTANONE/ 1,8-DIHYDROXYNAPHTHALENE/ *ALTERNARIA ALTERNATA*/ ALTENUSIN

JATUPORN PHAOPONGTHAI: SECONDARY METABOLITES FROM SELECTED ENDOPHYTIC FUNGI EXHIBITING SYNERGISTIC ACTIVITY WITH AZOLE DRUGS AGAINST *CANDIDA ALBICANS*. ADVISOR: KHANIT SUWANBORIRUX, Ph.D., CO-ADVISOR: ASSOC. PROF. NONGLUKSNA SRIUBOLMAS, Ph.D., 162 pp.

Based on morphological characteristics and nucleotide sequences of the ribosomal RNA gene region, two endophytic fungi obtained from leaf of *Artemisia annua* L. and *Terminalia chebula* Retz. were identified as *Nodulisporium* sp. Aann-134 and *Alternaria alternata* Tche-153, respectively. The ethylacetate extracts of the culture broths from both fungi significantly exhibited synergistic activity with ketoconazole against *Candida albicans*. Bioassay-guided fractionation using column chromatographic technique together with analyses of spectroscopic data led to the isolation and identification of seven secondary metabolites from the *Nodulisporium* extract; including four resorcinol polyketides, 1′-(2,6-dihydroxyphenyl)butanone, 1′-(2,6-dihydroxyphenyl)-3′-hydroxybutanone, 1′-(2,6-dihydroxy phenyl)ethanone, and a new compound nodulisporin G; two napthalenes, 1,8-dimethoxy naphthalene and 1,8-dihydroxynaphthalene; and phenylacetic acid. In addition, three polyketide salicylates, including altenusin, isoochracinic acid, and altenuic acid, as well as a chromone, 2,5-dimethyl-7-hydroxychromone were identified from the fungus *Alternaria alternata* extract.

By employing the disk diffusion method and the chequerboard technique, 1′-(2,6-dihydroxyphenyl)butanone and 1,8-dihydroxynaphthalene exhibited synergistic activity with fluconazole against *C. albicans* with the fractional inhibitory concentration indices of 0.250 and 0.375, respectively. In the same manner, altenusin, in combination with ketoconazole, fluconazole, or itraconazole, displayed potent synergistic activity against *C. albicans* with the fractional inhibitory concentration index in the range of 0.078 to 0.188.

Department : Pharmacognosy and Pharmaceutical Botany	Student's Signature .....
Field of Study : Pharmacognosy	Advisor's Signature .....
Academic Year : 2011	Co-Advisor's Signature .....

ACKNOWLEDGEMENTS

I would like to express my thanks to my thesis advisor, Dr. Khanit Suwanborirux of the Department of Pharmacognosy and Pharmaceutical Botany, my thesis co-advisor, Associate Professor Dr. Nongluksna Sriubolmas of the Department of Biochemistry and Microbiology, Faculty of Pharmaceutical Sciences, Chulalongkorn University, for their excellent suggestion, guidance, kindness, encouragement and support throughout the course of this study.

I would like to express my thanks to Assistant Professor Dr. Suthep Wiyakrutta of the Department of Microbiology, Faculty of Science, Mahidol University, for his suggestion, guidance, and support throughout the research study.

I am particularly grateful to chairman of thesis committee, Professor Dr. Kittisak Likhitwitayawuid, Associate Professor Dr. Rutt Suttisri, and Associate Professor Dr. Surattana Ammuoypol as committee and for their editorial assistance and comments.

I would like to thank my friends and all members of the Department of Pharmacognosy and Pharmaceutical Botany, Faculty of Pharmaceutical Sciences and the Department of Chemistry, Faculty of Science, Chulalongkorn University for their valuable advice and helps.

I would like to acknowledge my thanks to Scientific and Technological Research Equipment Center, Chulalongkorn University, National Center for Genetic Engineering and Biotechnology (BIOTEC) and National Metal, and Materials Technology Center (MTEC).

This work was financially supported by Grant-in-Aid from National Research Council of Thailand (NRCT 2009-113). Thank to the Graduate School, Chulalongkorn University and Rajamangala University of Technology Thanyaburi for her thesis supporting grants.

Finally, my deepest gratitude is to all my family and my friends members for their support, understanding, and assistance.

CONTENTS

CHAPTER Page

CHAPTER Page

CHAPTER Page

LIST OF TABLES

LIST OF FIGURES

Figure Page

LIST OF SCHEMES

LIST OF ABBREVIATIONS

$[\alpha]_D^t$	=	specific rotation at t°C and sodium D line (589 nm)
bp	=	base pairs
°C	=	degree Celsius
^{13}C-NMR	=	carbon-13 nuclear magnetic resonance
Calcd for	=	calculated for
cm	=	centimeter
CC	=	column chromatography
CFU	=	colony forming unit
δ	=	chemical shift
d	=	doublet (for NMR spectral data)
dd	=	doublet of doublets (for NMR spectral data)
DNA	=	deoxyribonucleic acid
DEPT	=	distortionless enhancement by polarization transfer
ε	=	molar absorptivity
e.g.	=	for example
EI-MS	=	electron impact mass spectrometry
et al.	=	and other
ESI-TOF	=	electronspray ionization time of flight
FIC	=	fractional inhibitory concentration
g	=	gram
µg	=	microgram
h	=	hour
^{1}H-^{1}H COSY	=	homonuclear (proton-proton) correlation spectroscopy
^{1}H NMR	=	proton nuclear magnetic resonance
HMBC	=	^{1}H-detected heteronuclear multiple bond correlation
HMQC	=	^{1}H-detected heteronuclear multiple quantum coherence
Hz	=	hertz
IC_{50}	=	inhibitory concentration required for 50% inhibition of growth

IR	=	infrared
ITS	=	internally transcribed spacers
J	=	coupling constant
L	=	liter
µl	=	microliter
λ_{max}	=	wavelength at maximum absorption
M	=	molar
$[M+Na]^+$	=	pseudomolecular ion
m	=	multiplet (for NMR spectral data)
MCzB	=	malt czapek broth
mg	=	milligram
MIC	=	minimum inhibitory concentration
min	=	minute
ml	=	milliliter
mm	=	millimeter
mM	=	millimolar
MHz	=	megahertz
m.p.	=	melting point
MS	=	mass spectroscopy
MTPA	=	methoxytrifluoromethylphenylacetic acid
m/z	=	mass to charge ratio
nm	=	nanometer
NMR	=	nuclear magnetic resonance
OPC	=	oropharyngeal candidiasis
PCR	=	polymerase chain reaction
PDA	=	potato dextrose agar
PDB	=	potato dextrose broth
PLC	=	preperative thin layer chromatography
ppm	=	part per million
q	=	quartet (for NMR spectral data)

Rf	=	rate of flow
RPMI	=	Roswell Park memorial Institute medium
rRNA	=	ribosomal ribonucleic acid
s	=	singlet (for NMR spectral data)
SDA	=	sabouraud's dextrose agar
sp.	=	species
t	=	triplet (for NMR spectral data)
TLC	=	thin layer chromatography
U	=	unit
UV	=	ultraviolet
V	=	volt
v	=	volume
w	=	weight
YCzB	=	yeast czapek broth
YES	=	yeast extract sucrose

CHAPTER I

INTRODUCTION

Candida spp. are opportunistic fungal pathogens which can cause diverse diseases ranging from mucocutaneous infection to severe invasive candidiasis. Oropharyngeal candidiasis (OPC) is commonly seen in patients with human immunodeficiency virus (HIV) infection, (Greenspan, 1994) or cancer (Gligorov *et al*., 2011). Immunocompromised persons especially patients with hematopoietic cell and solid organ transplantations, are particularly susceptible to invasive candidiasis (Kriengkauykiat *et al*., 2011). Candidemia is a life-threatening infection in critically ill patients and *Candida albicans* is globally the most common species causing bloodstream infection (Lim *et al*., 2011; Pfaller *et al*., 2011). Azoles are one group of systemic antifungal agents available for treatment of candidiasis. Fluconazole and itraconazole are used commonly for treatment of OPC and invasive candidiasis. In addition, ketoconazole is mainly used for OPC treatment while voriconazole used in invasive candidiasis (Patton *et al*., 2001; Kriengkauykiat *et al*., 2011). Azole-resistant *Candida* spp. have been reported in HIV-infected patients and other immunocompromised patients (Rex *et al*., 1995; Marr *et al*., 1997; Pfaller *et al*., 2010, 2011). Therefore several approaches have been investigated to combat these azole-resistant *Candida*, involving the search for new antifungal entities (Sangamwar *et al*., 2007; Tempone *et al*., 2007; Eilenberg, 2010), the innovation of new dosage formulations (Ricci *et al*., 2004; Pfaller *et al*., 2005), and the search for new combination therapy to improve the antifungal efficacy (Ghannoum *et al*., 1995; Karwa & Wargo, 2009). A number of studies on combination therapy with well-known azole drugs showing synergistic effect against *C. albicans* have been reported (Ghannoum, 1997; Feser *et al*., 1998; Quan et al., 2006; Guo *et al*., 2008; Li *et al*., 2008; Karwa & Wargo, 2009; Nishi *et al*., 2009). In addition, some natural products exhibited synergistic effect with azoles such as combinations of fluconazole and allicin from *Allium sativum* (Guo *et al*., 2009), essential oil from *Ocimum sanctum* (Amber *et al*., 2010), and curvularide B

from the endophytic fungus *Curvularia geniculata* (Chomcheon *et al*., 2010); ketoconazole and xanthorrhizol from *Curcuma xanthorrhiza* (Rukayadi *et al*., 2009); azoles and retigeric acid B from the lichen *Lobaria kurokawae* (Sun *et al*., 2010), and curcumin from the rhizomes of *Curcuma longa* (Sharma *et al*., 2010).

In the course of screening program for azole-synergistic effect of endophytic fungi (Nongluksna Sriubolmas and Suthep Wiyakruttha, unpublished result), the crude EtOAc extracts from the endophytic fungi Aann-134 and Tche-153 showed significant synergistic activity with ketoconazole against *C. albicans*. The endophytic fungus Aann-134 was isolated from a fresh leaf of *Artemisia annua* L. a Thai medicinal plant (Figure 1). The leaves of *A. annua* have been traditionally used as digestive bitter, mild relaxant, carminative and as a treatment for cough and diarrhea (Bunyapraphatsara & Chokechaijaroenporn, 2000). The endophytic fungus Tche-153 was isolated from a fresh leaf of another Thai medicinal plant, *Terminalia chebula* Retz (Figure 2). The leaves of *T. chebula* have been traditionally used as mild laxative, antipyretic and carminative (Bunyapraphatsara & Chokechaijaroenporn, 2000).

The objectives of this study were as follows:

1. to identify the endophytic fungal isolates Aann-134 from *A. annua* and Tche-153 from *T. chebula*
2. to isolate and identify secondary metabolites from the endophytic fungal isolates Aann-134 and Tche-153 and
3. to determine azole-synergistic activity against *Candida albicans* of the isolated secondary metabolites from the endophytic fungal isolates Aann-134 and Tche-153.

Figure 1 *Artemisia annua* L. (Asteraceae)

Figure 2 *Terminalia chebula* Retz. (Combretaceae)

CHAPTER II

LITERATURE REVIEW

An increase in the number of people in the world having health problems has been caused by various cancers, drug-resistant bacteria, parasitic protozoans, and fungi. An intensive search for new and more effective agents to deal with these diseases is now under way and endophyte fungi are a novel source of potentially useful medicinal compounds. (Strobel and Daisy, 2003).

2.1 Endophytic fungi

Endophytic fungi are ascomycetes or conidial fungi living asymptomatically and inconspicuously in plant tissues (Strobel and Daisy, 2003). Symbiotic interaction in which the fungi produce metabolites to protect and/or to promote the growth of the host plants which in turn provide nutritional benefit to the fungi has been hypothesized (Tan and Zou, 2001). These endophytic fungi have been recognized as a new source of diverse bioactive secondary metabolites with potentially pharmacological and agrochemical properties (Strobel, 2002).

The relationships between the endophytic fungi and the host plants may range from the endophytes improving ecological adaptability of the hosts by enhancing their tolerance to environmental stresses and their resistance to phytopathogens and/or herbivores such as insects feeding on the host plants. Endophyte-infected grasses usually possess an increased tolerance to drought and aluminium toxicity. Furhermore, some endophytes are able to provide the host plants with protection against some nematodes, manmals and herbivores as well as bacterial and fungal pathogens (Tan and Zou, 2001).

2.2 Bioactive metabolites from endophytic fungi

Fungal endophytes provide a broad variety of other bioactive secondary metabolites with unique structures, including alkaloids, benzopyranones, flavonoids,

phenolic acids, quinones, steroids, terpenoids, xanthones and others (Tan and Zou, 2001). Such bioactive metabolites find wide-ranging applications as agrochemical, antibiotic, immunosuppressant, antiparasitic, antioxidant and anticancer agents (Gunatilaka, 2006). Interestingly, some endophytic fungi have been reported to produce bioactive compounds (Figure 3) previously isolated from their host plants, including the therapeutic anticancer drugs taxol **[1]** (Stierle *et al*., 1993, 1995; Strobel *et al*., 1996), vincristine **[2]** (Yang *et al*., 2004), podophyllotoxin **[3]** (Eyberger *et al*., 2006; Puri *et al*., 2006), camptothecin **[4]** (Puri *et al*., 2005) and hypericin **[5]** (Kusari *et al*., 2008).

Taxol was firstly isolated from the bark of *Taxus brevifolia*, a tree belonging to the family Taxaceae (Wani *et al.,* 1971). Nevertheless, these trees are rare, slow growing and produce small amount of taxol, which explain its high price in the market when obtained from this natural source (Stierle *et al*., 1993; Strobel *et al*., 1996). Besides, in the context of environmental degradation, the use of plant source as unique option have limited the supply of this drug due to the destructive collection of yew trees (Guo *et al*., 2008). Several reports about other sources for the production of taxol have been investigated. The isolation of taxol-producing endophyte *Taxomyces andreanae* has provided an alternative approach to obtain a cheaper and more available product *via* microorganism fermentation (Stierle *et al*., 1993). Subsequently, taxol has also been found in a number of different fungal endophytes either associated or not associated to yew trees, including *Taxodium distichum* (Lie *et al*., 1996),and *Wollemia nobilis* (Strobel *et al*., 1997).

Some endophytic fungi were reported to produce secondary metabolites with anti-*C. albicans* activity (Figure 4). An endophytic fungus *Cryptosporiopsis cf.* quercina from *Triterigium wilfordii*, produced cryptocandin **[6]** with MIC between 0.03-0.07 μg/ml (Strobel *et al.,* 1999). *Neoplaconema napellum* IFB-EO16 an endophytic fungus isolated from *Hopea hainanensis* leaf, produced neoplaether **[7]** having MIC of 6.2 μg/ml (Wang *et al.,* 2006). *Penicillium* sp., isolated from *H. hainanensis* leaf, produced 3,5-dichloro-*p*-anisic acid **[8]** with MIC of 15 μg/ml (Wang *et al*., 2008); an endophytic fungus E99291, isolated from *Cistus salvifolius* root, produced arundifungin **[9]** ascosteroside A **[10]** and

ascosteroside B **[11]** having diameters of inhibition zones 16, 17 and 14 mm., respectively (Roland *et al*., 2007); *Aspergillus niger* EN-13 isolated from marine brown alga *Colpomenia sinuosa* produced sphingolipid asperamides A **[12]** having diameter of inhibition zone 12 mm. (Zhang *et al*., 2007); Xylaria sp. PSU-D14 isolated from *Garcinia dulcis* leaf produced sordaricin **[13]** having MIC 32 µg/ml (Pongcharoen *et al*., 2008) and endophytic fungus *Xylaria* sp. YX-28 isolated from *Ginkgo biloba* twig produced 7-amino-4-methylcoumarin **[14]** having MIC 15 µg/ml (Liu *et al*., 2008).

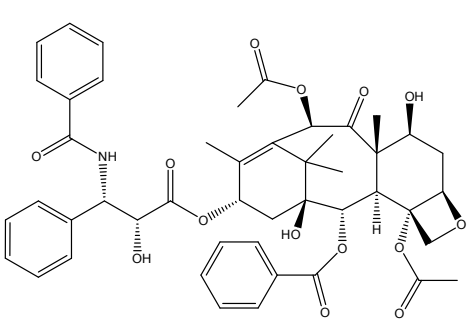

Taxol **[1]**

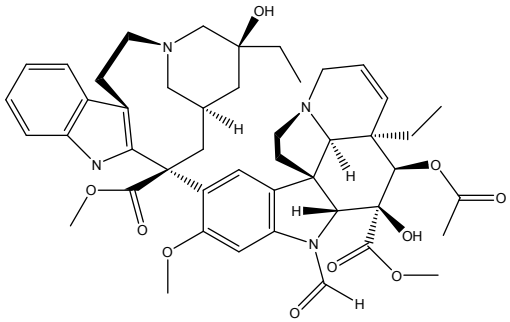

Vincristine **[2]**

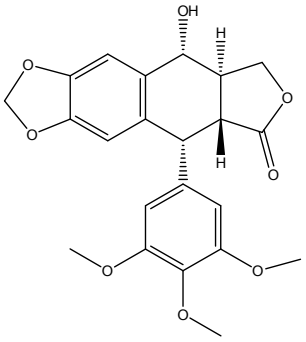

Podophyllotoxin **[3]**

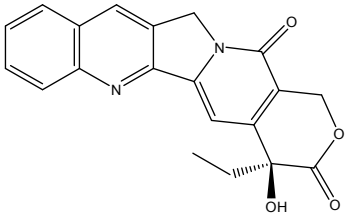

Camptothecin **[4]**

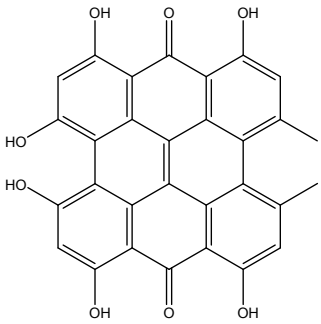

Hypericin **[5]**

Figure 3. Bioactive metabolites from endophytic fungi

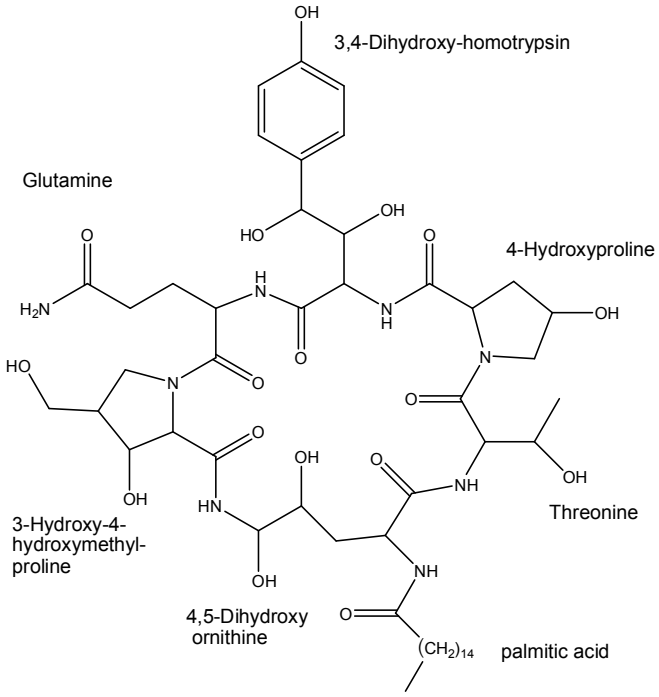

Cryptocandin **[6]**

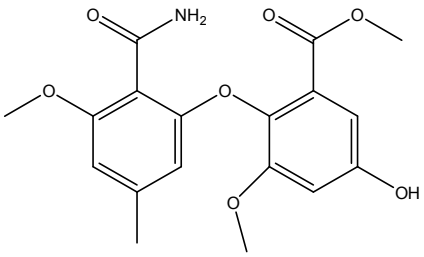

Neoplaether **[7]**

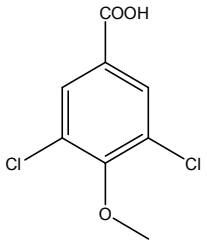

3,5-Dichloro-*p*-anisic acid **[8]**

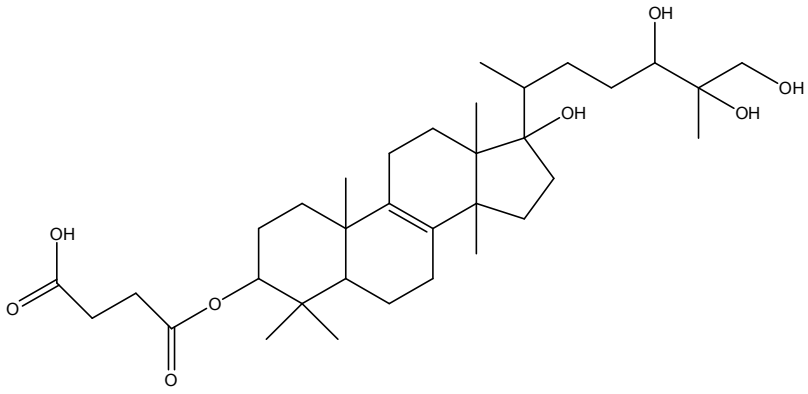

Arundifungin **(9)**

Figure 4 Anti-*Candida albican*s metabolites from endophytic fungi

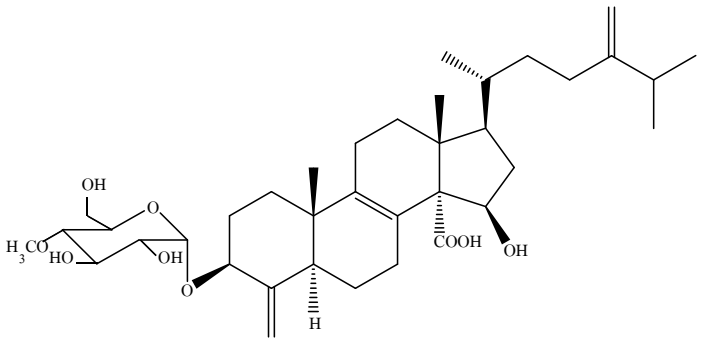

Ascosteroside A [10]

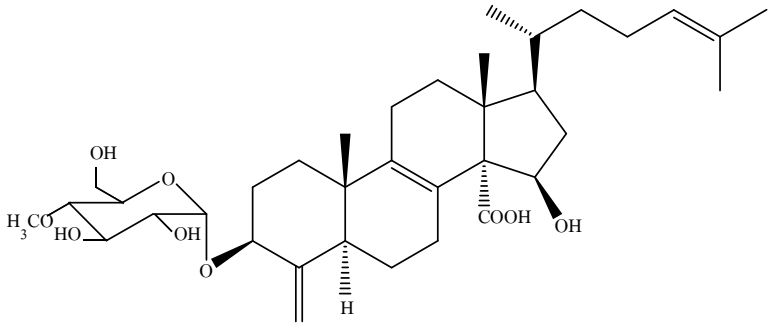

Ascosteroside B [11]

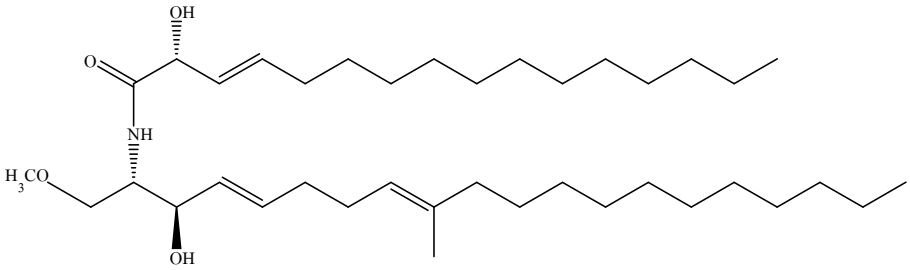

Asperamide [12]

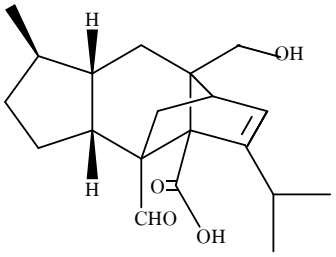

Sordaricin [13]

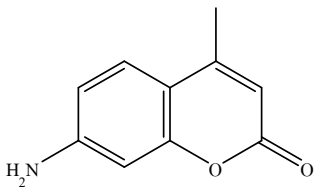

7-Amino-4-methylcoumarin [14]

Figure 4 (continued)

2.3 Secondary metabolites from the endophytic fungi *Nodulisporium* spp.

The endophytic fungus *Nodulisporium* belonging to Xylariaceae family was mainly obtained from the host plants *Erica arborea* (Ericaceae) and *Juniperus cedre* (Cupressaceae). The secondary metabolites isolated from the fungus are mainly polyketides and chemically classified as phenylbutanones and the related phenyl-methylpyrans, naphthalenes, bisnaphthalenes, and phenylbutanone-naphthalenes. The compounds and their biological activities together with the host plants are summarized in Table 1. The chemical structures are shown in Figure 5.

Table1 Secondary metabolites from the endophytics fungi *Nodulisporium* spp.

Compounds	Host plants	Biological activities	References
Helicascolide A **[15]**	*Erica arborea*	-	Dai *et al.,* 2009
5-Hydroxy-2-methyl-4*H*-chromen-4- one **[16]**	*E. arborea*, *Juniperus cedre*	anti-*Microbotryum violaceum*, anti-*Septoria tritici*, anti-*Chlorella fusca*	Dai *et al.,* 2006; 2009
8-Methoxynaphthalen-1-ol **[17]**	*E. arborea*, *J. cedre*	anti-*Microbotryum violaceum*, anti-*Chlorella fusca*	Dai *et al.,* 2006; 2009
1,8-Dimethoxynaphthalene **[18]**	*E. arborea*, *J. cedre*	anti-*Microbotryum violaceum*, anti-*Septoria tritici*, anti-*Chlorella fusca*	Dai *et al.,* 2006; 2009
1'-(2,6-Dihydroxyphenyl) -3'-hydroxybutanone**[19]**	*E. arborea*, *J. cedre*	antibacterial	Dai *et al.,* 2006; 2009
1'-(2,6-Dihydroxyphenyl) butanone **[20]**	*E. arborea, J. cedre*	anti-*Microbotryum violaceum*, anti-*Septoria tritici*, anti-*Chlorella fusca*	Dai *et al.,* 2006; 2009

Table 1 (continued)

Compounds	Host plants	Biological activities	References
Benzene-1,2,3-triol **[21]**	*E. arborea*	antifungal, antialgal, antibacterial	Dai *et al*., 2009
3-(2,3-Dihydroxy phenoxy)-butanoic acid **[22]**	*E. arborea*	antifungal, antialgal, antibacterial	Dai *et al*., 2009
5-Hydroxy-2-hydroxy methyl-4H-chromen-4-one **[23]**	*E. arborea*	antifungal, antialgal, antibacterial	Dai *et al*., 2009
2,4,6-Trimethyloct-6-ene-3,5-diol **[24]**	*E. arborea*	antifungal, antialgal, antibacterial	Dai *et al*., 2009
Nodulisporins F **[25]**	*E. arborea*	antifungal, antialgal, antibacterial	Dai *et al*., 2009
Nodulisporins E **[26**	*E. arborea*	antifungal, antialgal, antibacterial	Dai *et al*., 2009
Nodulisporins D **[27]**	*E. arborea*	antifungal antialgal antibacterial	Dai *et al*., 2009
(4*E*,6*E*)-2,4,6-Trimethylocta-4,6-dien-3-one **[28]**	*J. cedre*	anti-*Microbotryum violaceum*, anti-*Septoria tritici*, anti-*Chlorella fusca*	Dai *et al.,* 2006
Nodulisporin C **[29]**	*J. cedre*	anti-*Microbotryum violaceum*	Dai *et al.,* 2006
Daldinol **[30]**	*J. cedre*	anti-*Chlorella fusca*	Dai *et al.,* 2006
Nodulisporin B **[31]**	*J. cedre*	anti-*Microbotryum violaceum*, anti-*Chlorella fusca*	Dai *et al*., 2006
Nodulisporin A **[32]**	*J. cedre*	anti-*Microbotryum violaceum*	Dai *et al.,* 2006

Table 1 (continued)

Compounds	Host plants	Biological activities	References
1'-(2-Hydroxy-6-methoxy phenyl)butanone **[33]**	*J. cedre*	anti-*Microbotryum violaceum*, anti-*Septoria tritici*, anti-*Chlorella fusca*	Dai *et al.,* 2006
2,3-Dihydro-5-hydroxy-2-methylchromen-4-one **[34]**	*J. cedre*	anti-*Microbotryum violaceum*, anti-*Chlorella fusca*	Dai *et al*., 2006
2,3-Dihydro-5-methoxy-2-methylchromen-4-one **[35]**	*J. cedre*	anti-*Microbotryum violaceum*, anti-*Septoria tritici*, anti-*Chlorella fusca*	Dai *et al*., 2006
Ergosterol **[36]**	*J. cedre*	-	Dai *et al*., 2006
5α,8α-Epidioxyergosterol **[37]**	*J. cedre*	-	Dai *et al*., 2006

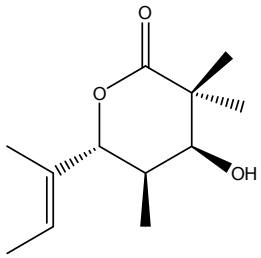

Helicascolide A **[15]**

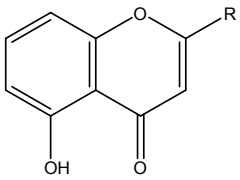

5-Hydroxy-2-methyl-4*H*-chromen-4- one **[16]** : R=CH_3

5-Hydroxy-2-hydroxymethyl-4H-chromen-4-one **[23]** : R=CH_2OH

Figure 5 Structures of secondary metabolites from *Nodulisporium* spp.

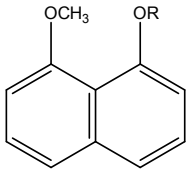

8-Methoxynaphthalen-1-ol **[17]** : R=H

1,8-Dimethoxynaphthalene **[18]** : R=CH_3

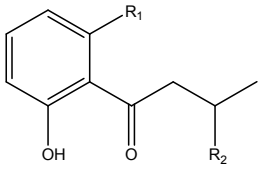

1'-(2,6-Dihydroxyphenyl)-3'-hydroxybutanone **[19]** : R_1=OH, R_2=OH

1'-(2,6-Dihydroxyphenyl)butanone **[20]** : R_1=OH, R_2=H

1'-(2-Hydroxy-6-methoxyphenyl)butanone **[33]** : R_1=OCH_3, R_2=H

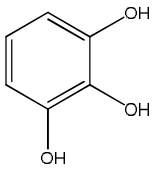

Benzene-1,2,3-triol **[21]**

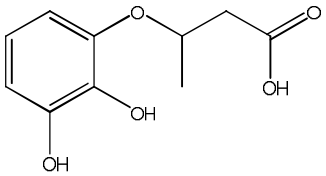

3-(2,3-Dihydroxyphenoxy)-butanoic acid **[22]**

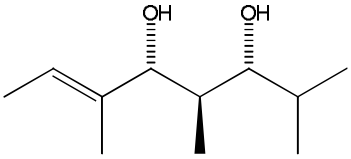

2,4,6-Trimethyloct-6-ene-3,5-diol **[24]**

Figure 5 (continued)

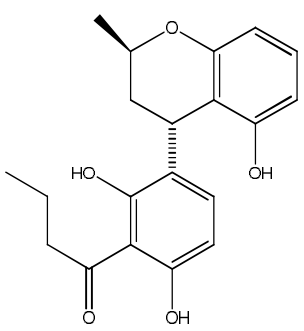

Nodulisporins F **[25]**

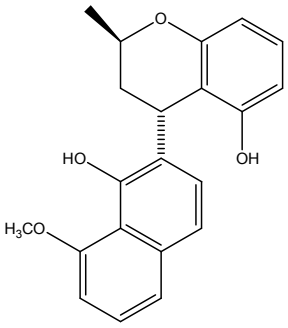

Nodulisporins E **[26]**

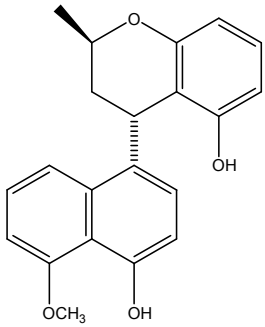

Nodulisporins D **[27]**

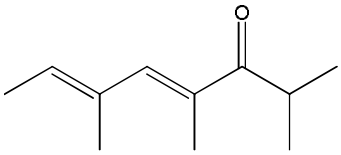

(4*E*,6*E*)-2,4,6-Trimethylocta-4,6-dien-3-one **[28]**

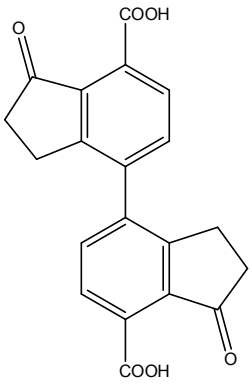

Nodulisporin C **[29]**

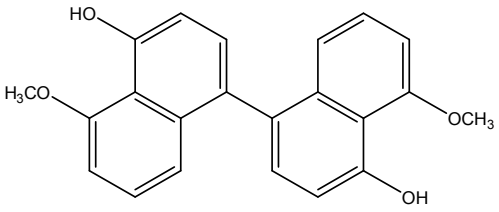

Daldinol **[30]**

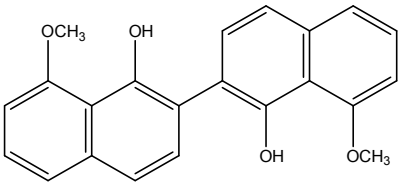

Nodulisporin B **[31]**

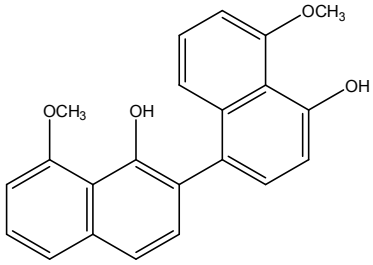

Nodulisporin A **[32]**

Figure 5 (continued)

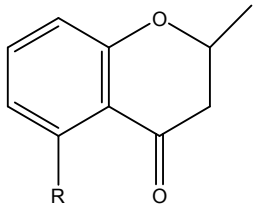

2,3-Dihydro-5-hydroxy-2-methylchromen-4-one **[34]** : R=OH

2,3-Dihydro-5-methoxy-2-methylchromen-4-one **[35]** : R=OCH_3

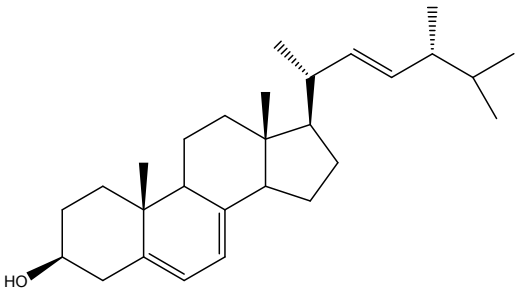

Ergosterol **[36]**

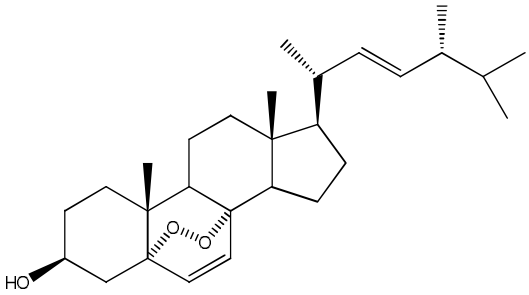

5α,8α-Epidioxyergosterol **[37]**

Figure 5. (continued)

2.4 Secondary metabolites from the endophytic fungus *Alternaria* spp.

The endophytic fungus *Alternaria* is a member of the family Pleosporaceae and has been found associated with the host plants *Polygonum senegalense* (Polygonaceae) and *Malus halliana* (Rosaceae). The secondary metabolites produced by these fungi are biphenyl derivatives (Figure 6). The compounds, the host plants and their biological activities are summarized in Table 2.

Table 2. Secondary metabolites from endophytic fungus *Alternaria* spp.

Compounds	Endophytic fungi	Host plants	Biological activities	References
Alternariol **[38]**	*Alternaria* sp.,	*Polygonum senegalense,*	cytotoxic	Aly *et al.* 2008a
	A. brassicicola ML-P08	*Malus halliana*	xanthine oxidase hibitory	Gu, 2009
Alternariol-5-*O*-sulphate **[39]**	*Alternaria* sp.	*P. senegalense*	cytotoxic	Aly *et al.* 2008a
Alternariol-5-*O*-methyl ether**[40]**	*Alternaria* sp.	*P. senegalense*	cytotoxic	Aly *et al.* 2008a
Alternariol-5-*O*-methyl ether-4`-*O*-sulphate **[41]**	*Alternaria* sp.	*P. senegalense*	-	Aly *et al.* 2008a
3`-Hydroxy alternariol -5-*O*-methyl ether**[42]**	*Alternaria* sp.	*P. senegalense*	-	Aly *et al.* 2008a
Altenusin **[43]**	*Alternaria* sp.	*P. senegalense*	cytotoxic inhibit several enzymes: trypanothione reductase cFMS kinase and pp60c-SRc kinase,	Aly *et al*., 2008a; Cota *et al*., 2008 Oyama *et al.,* 2004

Table 2 (continued)

Compounds	Endophytic fungi	Host plants	Biological activities	References
			HIV-1 integrase myosin light chain kinase, antioxidant	Singh *et al*., 2003 Nakanishi *et al*., 1995; Hirai *et al*., 1990;
Desmethylalternusin **[44]**	*Alternaria* sp.	*P. senegalense*	cytotoxic	Aly *et al.* 2008
Alterlactone **[45]**	*Alternaria* sp.	*P. senegalense*	-	Aly *et al.* 2008a
Talaroflavone **[46]**	*Alternaria* sp.	*P. senegalense*	-	Aly *et al.* 2008a
Alternaric acid **[47]**	*Alternaria* sp.	*P. senegalense*	-	Aly *et al.* 2008a
Altenuene **[48]**	*Alternaria* sp.	*P. senegalense*	-	Aly *et al.* 2008a
4'-epialtenuene **[49]**	*Alternaria* sp.	*P. senegalense*	-	Aly *et al.* 2008a
2,5-Dimethyl-7-hydroxychromone **[50]**	*Alternaria* sp.	*P. senegalense*	-	Aly *et al.* 2008a
Altertoxin I [51]	*Alternaria sp.*	*P. senegalense*	-	Aly et al. 2008a

Table 2 (continued)

Compounds	Endophytic fungi	Host plants	Biological activities	References
Tenuazonic acid **[52]**	*Alternaria* sp.	*P. senegalense*	-	Aly *et al.*, 2008a
Altenuic acid **[53]**	*A. tenusis*	-	-	Williams and Thomas, 1973
Isoochracinic acid **[54]**	*A. kikuchiana*;	-	phytotoxin	Kameda and Namiki, 1947

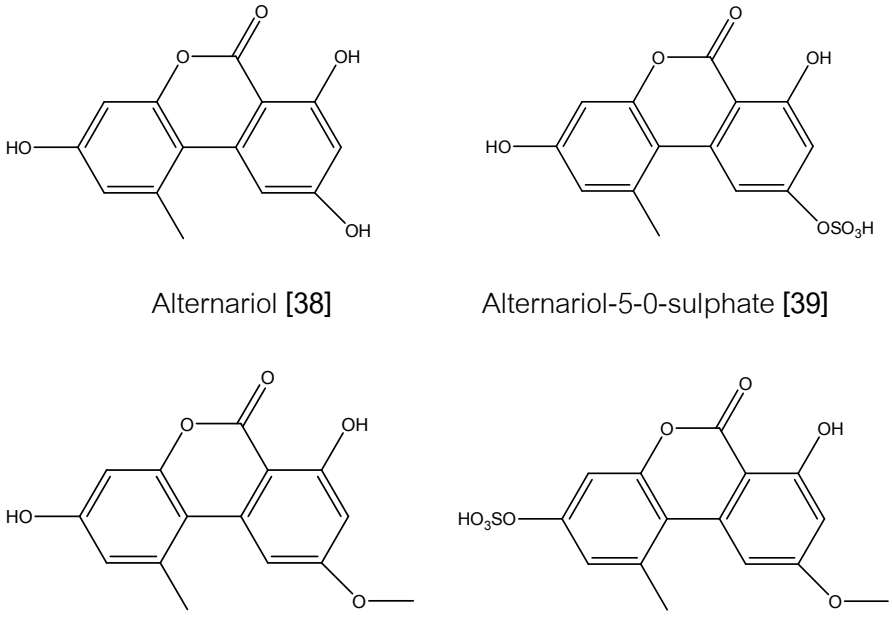

Figure 6 Structures of secondary metabolites from *Alternaria* spp.

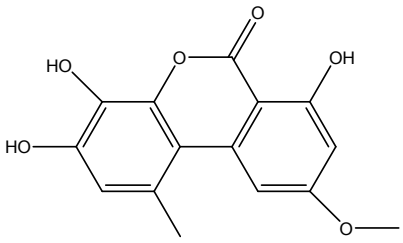

3'-Hydroxyalternariol-5-0- methyl ether **[42]**

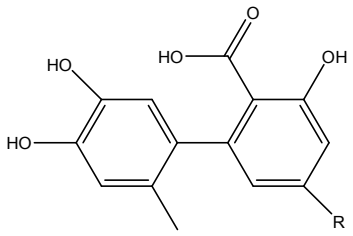

Altenusin **[43]** : R=OCH_3

Desmethylaltenusin **[44]** : R=OH

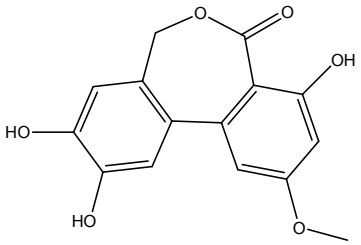

Alterlactone **[45]**

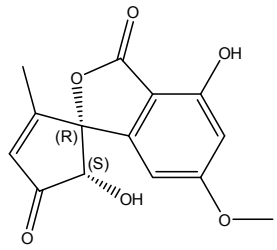

Alaroflavone **[46]**

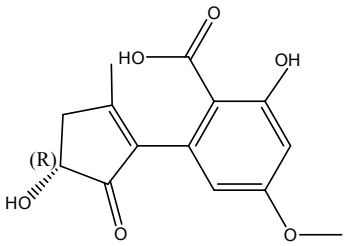

Alternaric acid **[47]**

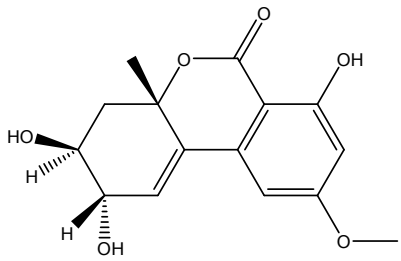

Altenuene **[48]**

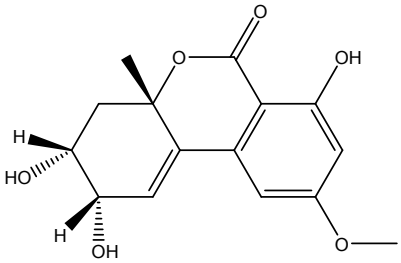

4'-Epialtenuene **[49]**

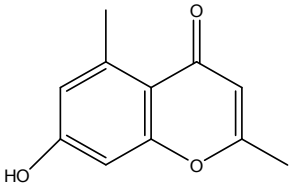

2,5-Dimethyl-7-hydroxychromone **[50]**

Figure 6 (continued)

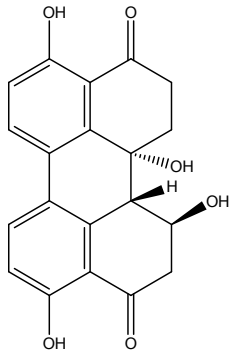

Altertoxin I **[51]**

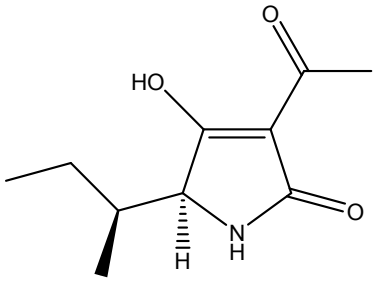

Tenuazonic acid **[52]**

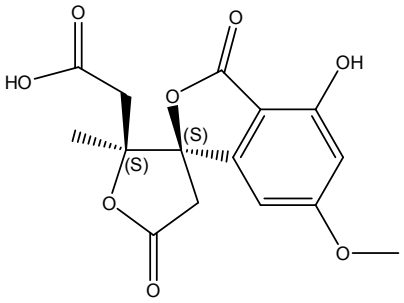

1S, 4S-Altenuic acid **[53]**

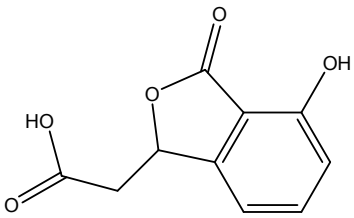

Isoochracinic acid **[54]**

Figure 6 (continued)

2.5 Natural compounds having synergistic activity with azole antifungals against *Candida albican*s

The search for new combination therapy an the interesting approach to improve the antifungal efficacy of antifungal agents (Ghannoum *et al*., 1995; Karwa and Wargo, 2009). A number of studies on combination therapy with well-known azole drugs have shown synergistic effect against *C. albicans*, for examples, combination of fluconazole with amphotericin B (Ghannoum, 1997), nitric oxide (Feser *et al*., 1998), berberine chloride (Quan *et al.,* 2006), amiodarone (Guo *et al*., 2008), cyclosporine (Li *et al*., 2008), efungumab (Karwa and Wargo, 2009), or micafungin (Nishi *et al*., 2009). In addition, some natural products exhibited synergistic effect with azoles such as fluconazole and allicin **[55]** from *Allium sativum* (Guo *et al.,* 2009); ketoconazole and

xanthorrhizol **[56]** from *Curcuma xanthorrhiza* (Rukayadi *et al*., 2009); azoles and retigeric acid B **[57]** isolated from the lichen *Lobaria kurokawae* (Sun *et al*., 2010); azoles and curcumin **[58]** from the rhizomes of *Curcuma longa* (Sharma *et al*., 2010); fluconazole and essential oil from *Ocimum sanctum* (Amber *et al.,* 2010); fluconazole and curvularide B **[59]** from the endophytic fungus *Curvularia geniculata* (Chomcheon *et al*., 2010). Structures of some natural products exhibiting synergistic effect with azoles are shown in Figure **7**.

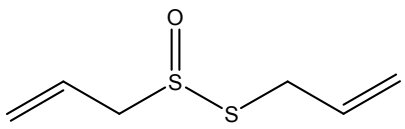

Allicin **[55]**

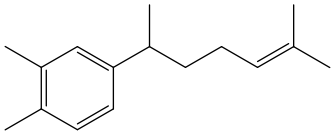

Xanthorrhizol **[56]**

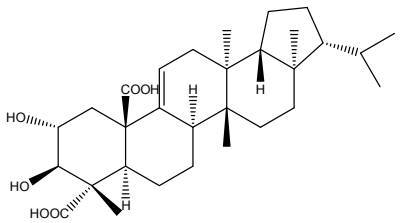

Retigeric acid B **[57]**

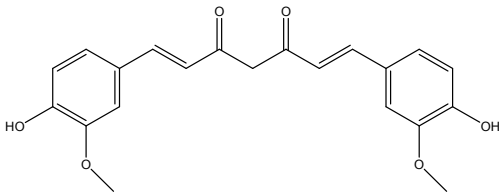

Curcumin **[58]**

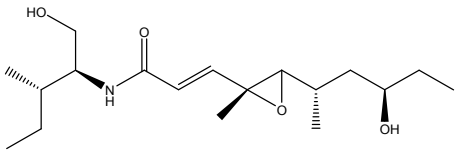

Curvularide B **[59]**

Figure 7 Structures of some natural products exhibiting synergistic effect with azoles against *Candida albicans*

CHAPTER III

MATERIALS AND METHODS

3.1 Instruments and Equipments

3.1.1 Ultraviolet (UV) spectra

UV (in methanol) spectra were obtained on a Shimadzu UV-2550 spectrophotometer (Faculty of Science, Chulalongkorn University).

3.1.2 Infrared (IR) spectra

IR spectra (KBr disc and film) were recorded on a Perkin Elmer FT-IR 1760X spectrometer (Faculty of Science and Technology, Rajamangala University of Technology, Thanyaburi).

3.1.3 Mass spectra (MS)

Electron impact mass spectra (EIMS) were obtained on a JEOL JMS-700 mass spectrometer (Meiji Pharmaceutical University, Japan) and electrospray ionization time of flight mass spectra (ESI-TOF-MS) on a Micromass LCT mass spectrometer (National Center for Genetic Engineering and Biotechnology, BIOTEC).

3.1.4 Proton and carbon-13 nuclear magnetic resonance (^{1}H and ^{13}C NMR) spectra

^{1}H NMR (300 MHz) and ^{13}C NMR (75 MHz) spectra were obtained on a Bruker Avance DPX-300 FT-NMR spectrometer (Faculty of Pharmaceutical Sciences, Chulalongkorn University).

^{1}H NMR (400 MHz) and ^{13}C NMR (100 MHz) spectra were obtained on a Varian Mercury^{+} 400 NMR spectrometer (Faculty of Science, Chulalongkorn University).

^{1}H NMR (500 MHz) and ^{13}C NMR (125 MHz) spectra were obtained on a JEOL JMN-A 500 NMR spectrometer (Scientific and Technological Research Equipment

Center, Chulalongkorn University) and a Bruker Biospin Avance AV-500 Digital NMR Spectrometer (National Metal and Materials Technology Center, MTEC)

Solvents for NMR spectra were deuterated chloroform ($CDCl_3$), deuterated dimethyl sulfoxide (DMSO-d_6) or deuterated methanol (CD_3OD). Chemical shifts were reported in ppm scale using the chemical shifts of the solvents as internal references.

3.1.5 Melting points

Melting points were obtained on a Fisher-Johns melting point apparatus (Faculty of Science, Chulalongkorn University).

3.1.6 Optical rotations

Optical rotations were measured on a Jasco P1010 polarimeter (Faculty of Science, Chulalongkorn University).

3.2 Chromatographic techniques

3.2.1 Analytical thin-layer chromatography (TLC)

Technique	:	One dimension, ascending
Adsorbent	:	Silica gel F_{254} (E. Merck) precoated plate
Layer thickness	:	0.2 mm
Distance	:	7.0 cm
Temperature	:	Laboratory temperature (28-35 °C)
Detection	:	1. Ultraviolet light (254 and 366 nm)
		2. Anisaldehyde reagent and heating at 105 °C for 10 min

3.2.2 Preparative thin-layer chromatography (PLC)

Technique	:	One dimension, ascending
Adsorbent	:	Silica gel F_{254} (E. Merck) precoated plate
Layer thickness	:	0.5 mm
Distance	:	7.0 cm
Temperature	:	Laboratory temperature (28-35 °C)

Detection : Ultraviolet light (254 and 366 nm)

3.2.3 Column chromatography

3.2.3.1 Quick column chromatography

Adsorbent : Silica gel 60 GF 254 for thin-layer chromatography (Art.7731, E. Merck)

Packing method : Dry packing

Sample loading : The sample was dissolved in a small amount of organic solvent, mixed with a small quantity of adsorbent, triturated, dried and then placed gently on top of the column.

Detection : Fractions were examined by TLC observing under UV light (254 and 366 nm).

3.2.3.2 Flash column chromatography

Adsorben : Silica gel 60 (No.9385) particle size 0.040-0.063 mm (230-400 mesh ASTM) (E. Merck)

Packing method : Wet packing

Sample loading : The sample was dissolved in a small amount of the eluent and then applied gently on top of the column.

Detection : Fractions were examined in the same manner as described in Section 3.2.3.1.

3.2.3.3 Gel filtration chromatography

Adsorbent : Sephadex LH-20 (Amersham)

Packing method : Gel was suspended in the eluent and left standing to swell for 24 hours prior to use. It was poured into the column and allowed to set tightly.

Sample loading : The sample was dissolved in a small amount of the eluent and applied gently on top of the column.

Detection : Fractions were examined in the same manner as described in Section 3.2.3.1.

3.3 Culture media and chemicals

3.3.1 Culture media

Culture media used for cultivation of endophytic fungi were potato dextrose agar (PDA) (Merck), Sabouraud's dextrose agar (SDA) (Merck), potato dextrose broth (PDB) (Merck), yeast Czapek broth (CzYB), yeast extract sucrose broth (YSB), yeast extract powder (Merck), and agar base (agar-agar ultrapure granulated, Merck). The formula are shown in Appendix B.

3.3.2 Chemicals

Chemicals used in this study are as follows: n-hexane (Labscan, AR), methylene chloride (Labscan, AR), ethyl acetate (Labscan, AR), methanol (Labscan, AR), $CDCl_3$ (Merck), CD_3OD (Merck), and DMSO-d_6 (Merck).

Throughout this work, all organic solvents were analytical grade and the commercial grade solvents were redistilled prior to use.

3.4 Isolation of endophytic fungi

Apparently healthy leaves of *Artemisia annua* L. (Family Asteraceae) and *Terminaria chebula* Retz. (Family Combretaceae) were collected from Thamaka Natural Agricultural Center, Kanjanaburi Province, and Suanluang Rama IX Public Park, Bangkok, respectively. The leaf samples were cleaned under running tap water and then air-dried. The cleaned leaves were repeatedly surface-sterilized in 70% ethanol for 1 min, sodium hypochlorite solution (5.25% available chlorine) for 5 min and washed in sterile distilled water for 1 min three times. The surface-sterilized leaves were cut into small pieces using a sterile blade and placed on sterile water agar for incubation at 30°C (Wiyakrutta et al., 2004). The fungal isolates designated Aann-134 from *A. annua* and Tche-153 from *T. chebula* were selected for further studies.

The endophytic fungal isolates Aann-134 and Tche-153 were deposited at the Bioactive Metabolite Unit (B600), Department of Microbiology, Faculty of Science,

Mahidol University. For short-term storage (< 1 year), the fungi were placed in distilled H_2O, and they were kept frozen at -70°C in 15 % glycerol for longer term storage.

3.5 Identification of the endophytic fungal isolates Aann-134 and Tche-153

3.5.1 Conventional method

Aann-134 and Tche-153 were grown on potato dextrose agar (PDA) plates and water agar plates with 5-6 small pieces of sterilized banana leaf at 25°C. Their macroscopic and microscopic characteristics were observed.

3.5.2 Molecular method

Both Aann-134 and Tche-153 were grown in potato dextrose broth. After cultivation for 5 days, fresh mycelium of each fungus (50 mg) was collected, washed twice with sterile normal saline solution and homogenized in 250 µl of sterile water. The mycelial homogenate was applied evenly to an FTA card matrix, allowed to dry at room temperature, and a 2-mm disk containing the fungal mycelia was punched from the FTA card. Total cellular DNA of fungal mycelia on the disk was extracted and purified using the FTA® Plant Kit (Whatman®) according to the manufacturer's instruction. Briefly, the disk was placed in a PCR tube, washed three times with FTA Purification Reagent and washed twice with TE buffer (10 mM Tris, pH 8.0). The washed disk was transferred to a PCR tube and the ITS1-5.8S-ITS2 ribosomal RNA gene region of fungal genomic DNA was amplified using ITS5 (GGAAGTAAAAGTCGTAACAAGG) and ITS4 (TCCTCCGCTTATTGATATGC) primers (White *et al*., 1990). PCR amplification was performed in a 50 µl reaction volume which contained Taq PCR Master Mix (USB Corp., USA) using an automated thermal cycler (Mastercycler gradient, Eppendorf, Hamburg, Germany). The thermocycling program was as follows: 3 min at 95°C followed by 30 cycles of 50 sec at 95°C, 40 sec at 45°C and 40 sec at 72°C, with a final extension period of 10 min at 72°C. The PCR products were gel purified and directly subjected to DNA sequencing (Bioservice Unit, NSTDA, Bangkok, Thailand) in both directions, primed with either of the two primers used to originally amplify the fragment. The DNA sequence of ITS1-5.8S-ITS2 rRNA gene obtained was used as the query sequence to search for similar sequences in GenBank using BLASTN 2.2.24+ (Zhang *et al*., 2000).

3.6 Cultivation of the endophytic fungi *Nodulisporium* sp. Aann-134 and *Alternaria alternata* Tche-153

The endophytic fungi *Nodulisporium* sp. Aann-134 and *Alternaria alternata* Tche-153 were cultivated on PDA agar plates at 25°C for 7 days. Six pieces (@ 0.5 x 0.5 cm) of mycelial agar plugs from each culture as seedlings were inoculated into a 1000-ml Erlenmeyer flask containing 200 ml of Czapek yeast broth (CzYB) for Aann-134 and yeast extract sucrose (YES) broth for Tche-153 (Paterson & Bridge, 1994) and incubated at 25°C under still condition for 21 days. Two batches of the Aann-134 isolate were cultivated, each twenty liters of the broth, and respectively designated as Aann-134 (1) and Aann-134 (2), while twenty liters of the Tche-153 culture broth was prepared for further isolation and purification of fungal metabolites.

3.7 Extraction of the culture broths from *Nodulisporium* sp. Aann-134

The first batch of *Nodulisporium* sp. Aann-134 culture broth [Aann-134(1)] was passed through four layers of cheese cloth and exhaustively pressed. The filtrate was extracted by partitioning with an equal volume of ethyl acetate 5 times. The ethyl acetate layers were combined and the solvent was then removed by evaporation at 50°C under reduced pressure until dryness. The crude EtOAc extract of the Aann-134(1) broth was obtained as a dark brown mass (3 g, 0.015 % w:v of the broth). The extraction of the Aann-134(1) culture broth is shown in Scheme 1.

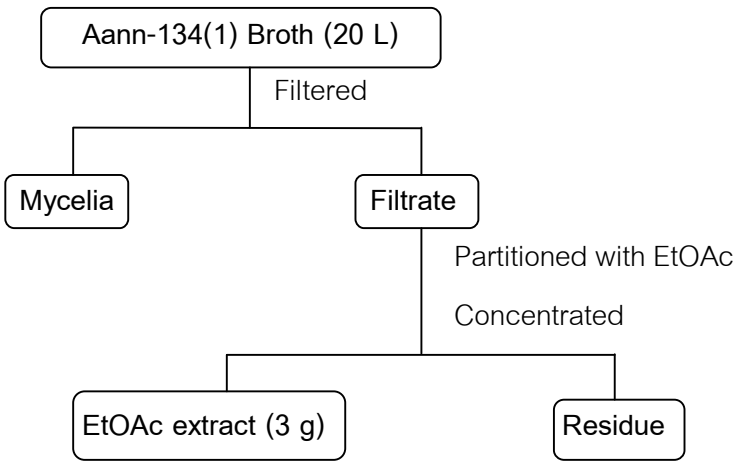

Scheme1 Extraction of the Aann-134(1) culture broth from *Nodulisporium* sp. Aann-134

The second-batch of *Nodulisporium* sp. Aann-134 culture broth [Aann-134(2)] was treated similar to the first batch to yield the EtOAc extract as a brown viscous oil (3 g). The EtOAc extract was further partitioned in MeOH: n-hexane (1:1, 5 times). Each layer was then evaporated at 50°C under reduced pressure until dryness. The MeOH and n-hexane extracts were obtained as a dark brown mass (2.5 g, 0.0125 % w/v of the broth) and a brown viscous liquid (0.5 g, 0.0025 % w/v of the broth), respectively. The extraction of the Aann-134(2) culture broth is shown in Scheme 2.

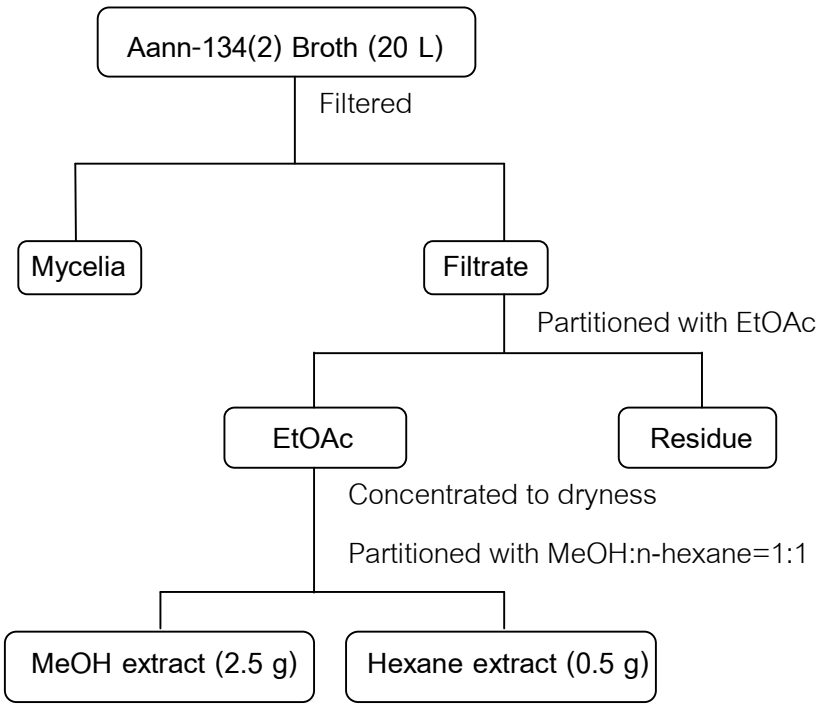

Scheme 2 Extraction of the Aann-134(2) culture broth from *Nodulisporium* sp. Aann-134

3.8 Extraction of the culture broth from *Alternaria alternata* Tche-153

The culture broth from *A. alternata* Tche-153 was treated in the same manner as Aann-134(1)culture broth. The crude EtOAc extract of the isolate Tche-153 was obtained as a dark brown mass (10 g, 0.05 % w/v of the broth). The extraction of the culture broth of the Tche-153 isolate is shown in Scheme 3.

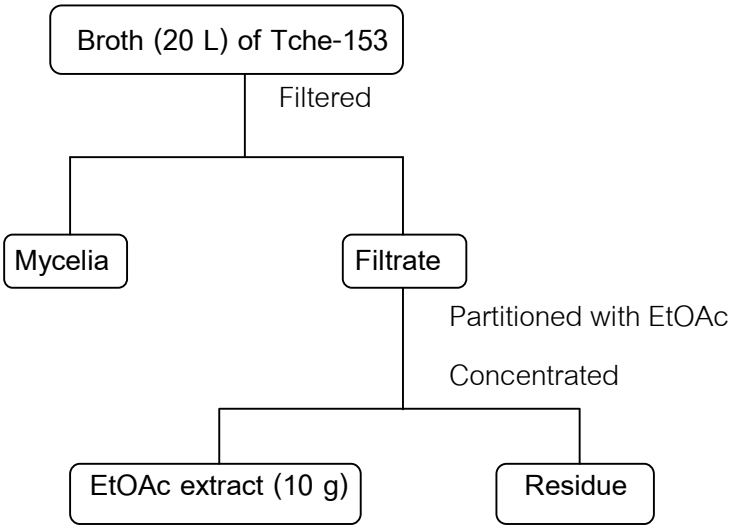

Scheme 3 Extraction of the culture broth of *Alternaria alternata* Tche-153

3.9 Isolation of secondary metabolites from *Nodulisporium* sp. Aann-134

3.9.1 Isolation of secondary metabolites from the EtOAc extract of *Nodulisporium* sp. Aann-134

The ethyl acetate extract (3 g) of the Aann-134(1) broth, designated as **AC,** was subjected to fractionation by quick column chromatography using a sintered glass filter column (10 x 5.5 cm) of silica gel (No. 7731, 200 g). Elution was performed in a polarity gradient manner with mixtures of n-hexane:CH_2Cl_2 (1:0, 50 ml; 1:1, 50 ml; 0:1, 50 ml), CH_2Cl_2:EtOAc (9:1, 350 ml) and EtOAc:MeOH (1:0, 50 ml; 9:1, 300 ml). The fractions (50 ml each) were collected and examined by TLC (silica gel, CH_2Cl_2:MeOH = 39:1). Twenty four fractions were obtained and the fractions showing similar chromatographic patterns were pooled to yield ten fractions: AC-001 - AC-010 (Figure 8, Table 3 and Scheme 4).

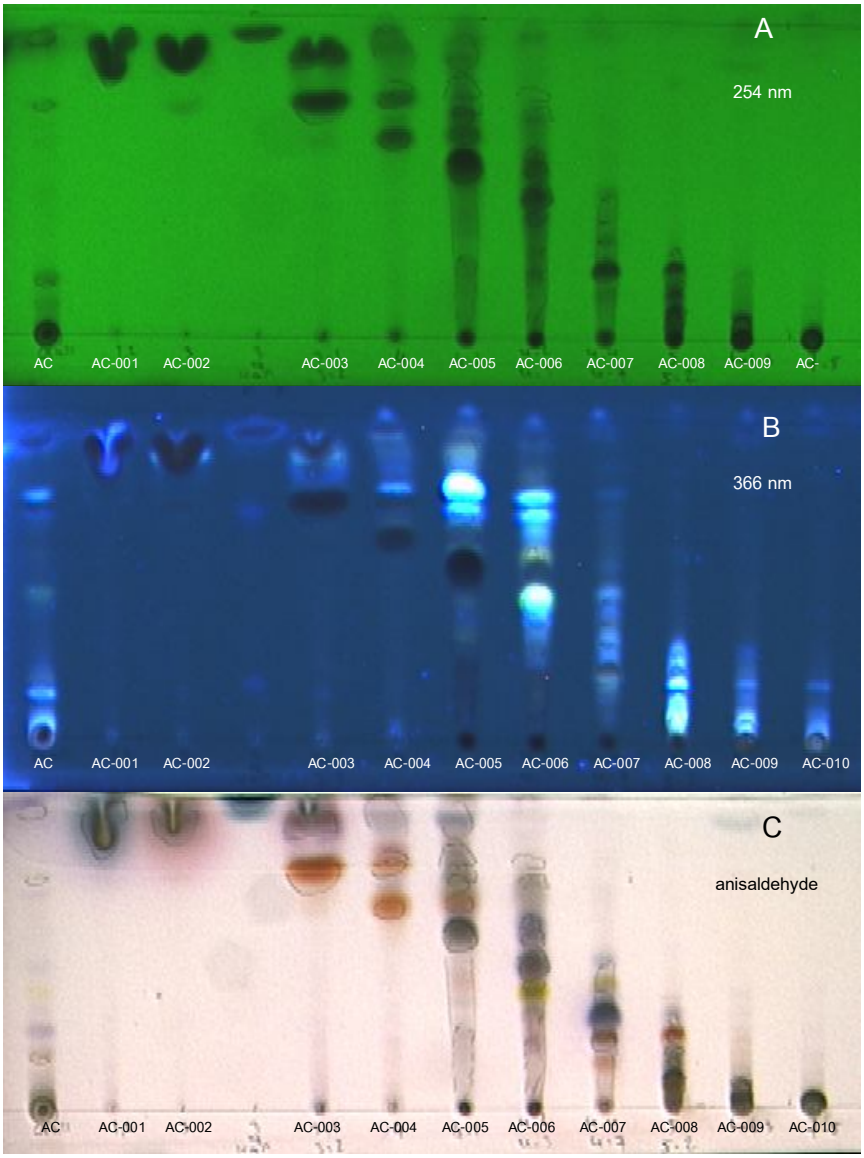

Figure 8 Thin-layer chromatogram (CH_2Cl_2: MeOH=39: 1) of fractions obtained from the EtOAc extract of *Nodulisporium* sp. Aann-134

A) detected under UV 254 nm;

B) detected under UV 366 nm, and

C) detected by anisaldehyde reagent

Table 3 Fractions obtained from the EtOAc extract of *Nodulisporium* sp. Aann-134.

Fraction code	Eluate volume (ml)	Weight (mg)
AC-001	100	74
AC-002	50	235
AC-003	100	810
AC-004	50	42
AC-005	50	121
AC-006	100	464
AC-007	200	63
AC-008	150	550
AC-009	150	307
AC-010	250	117

3.9.1.1 1,8-Dimethoxynaphthalene

Fraction AC-002 (235 mg) was crystallized from n-hexane:CH_2Cl_2 to give 3.6 mg of colorless needles (R_f 0.93, silica gel, CH_2Cl_2:MeOH = 39:1). It was subsequently identified as 1,8-dimethoxynaphthalene **[18]** (Scheme 4). The compound was also obtained from the hexane and the MeOH extracts of the second batch (Schemes 8 and 9).

3.9.1.2 1'-(2,6-Dihydroxyphenyl)butanone

The anti-*Candida albicans* active fraction (AC-003, 810 mg) was further separated by a Sephadex LH-20 column (1 x 45 cm) using n-hexane:CH_2Cl_2:MeOH (2:2:1) as the eluent. Fractions (10-30 ml each) were collected and examined by TLC (silica gel, CH_2Cl_2:MeOH = 39:1). Fractions with similar chromatographic patterns were combined to yield seven fractions: AC-011 - AC-017 (Table 4 and Scheme 5). The active fraction (AC-013, 90.7 mg) was repeatedly purified by a Sephadex LH-20 column (1 x 42 cm) eluted with n-hexane:CH_2Cl_2:MeOH (2:2:1). The eluates fractions (10-30 ml each) were collected and examined by TLC (silica gel, CH_2Cl_2:MeOH = 39:1). Fractions with similar chromatographic patterns were combined to yield four fractions: AC-018 - AC-021 (Table 5 and Scheme 5).

The anti-*C. albicans* fraction (AC-019, 15 mg) was subjected to crystallize from n-hexane:CH_2Cl_2 (1:1) to give 1'-(2,6-dihydroxyphenyl)butanone (6 mg) **[20]**. The compound was also obtained from the MeOH extract of the second batch (Scheme 12).

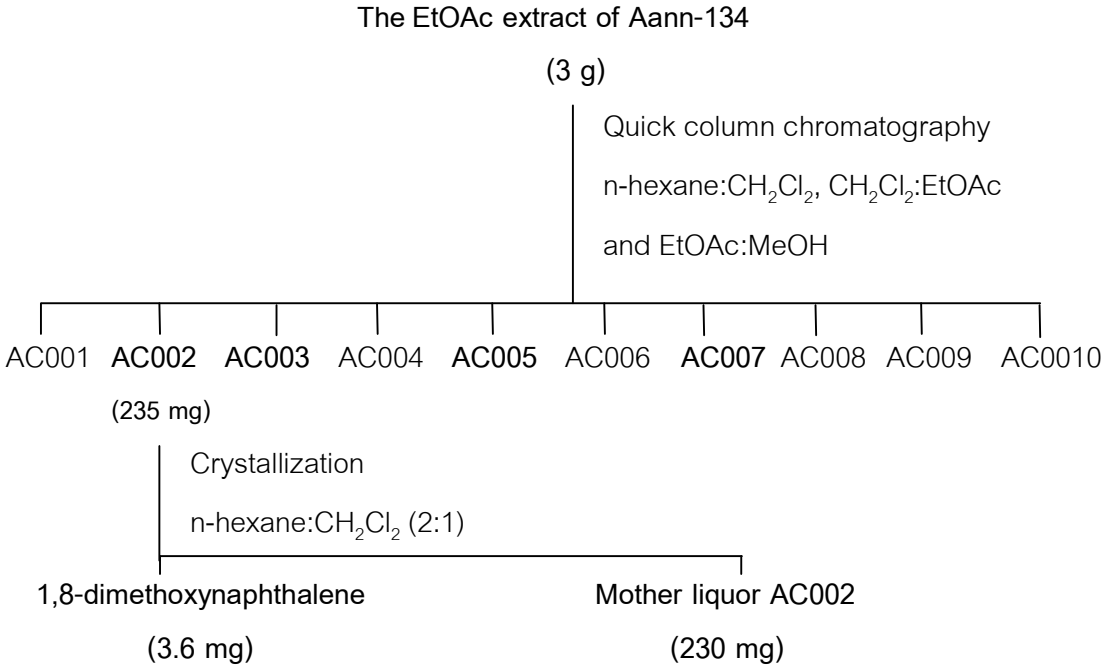

Scheme 4 Fractionation of the EtOAc extract and Isolation of 1,8-dimethoxy naphthalene from the Aann-134(1) culture broth

Table 4 Fractions obtained from fraction AC-003 of the Aann-134(1) culture broth.

Fraction code	Eluate volume (ml)	Weight (mg)
AC-011	30	61
AC-012	90	114
AC-013	90	90
AC-014	200	59
AC-015	120	43
AC-016	90	23
AC-017	100	158

Table 5 Fractions obtained from fraction AC-013 of the Aann-134(1) culture broth.

Fraction code	Eluate volume (ml)	Weight (mg)
AC-018	100	11
AC-019	90	15
AC-020	250	38
AC-021	30	13

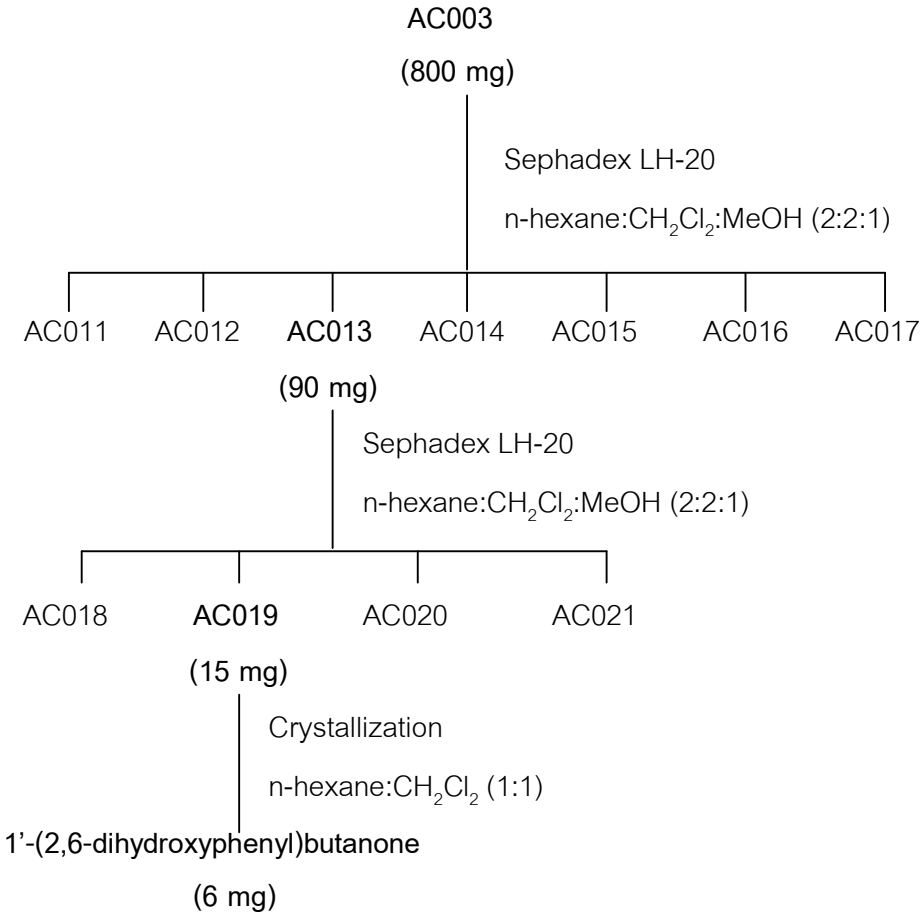

Scheme 5 Isolation of 1'-(2,6-dihydroxyphenyl)butanone from the Aann-134(1) culture broth

3.9.1.3 1'-(2,6-Dihydroxyphenyl)ethanone

Fraction AC-005 (121 mg) was repeatedly separated by a Sephadex LH-20 column (1 x 45 cm) using n-hexane:CH_2Cl_2:MeOH (2:2:1). Fractions (10-30 ml each) were collected and examined by TLC (silica gel, CH_2Cl_2:MeOH = 39:1). Fractions with

similar chromatographic patterns were combined to yield six fractions: AC-022 - AC-027, (Table 6 and Scheme 6).

Fraction AC-026 (16.9 mg) was crystallized in n-hexane:CH_2Cl_2 (1:1) to give 1'-(2,6-dihydroxyphenyl)ethanone (2.6 mg) **[60]**. The compound was also obtained from the MeOH extract of the second batch (Scheme 6).

Table 6 Fractions obtained from fraction AC-005 of the Aann-134(1) culture broth.

Fraction code	Eluate volume (ml)	Weight (mg)
AC-022	50	31
AC-023	50	24
AC-024	20	14
AC-025	30	14
AC-026	30	16
AC-027	150	22

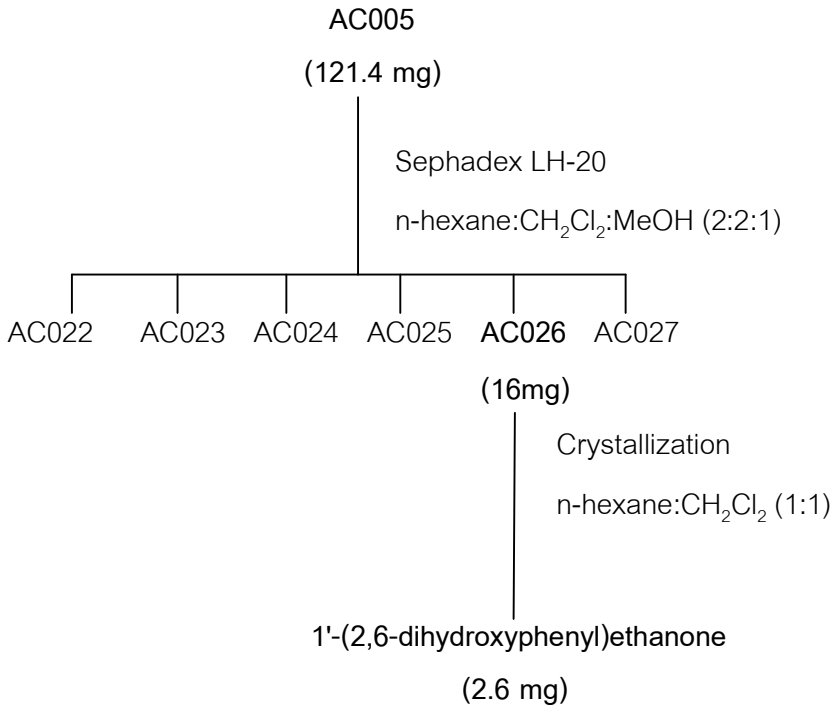

Scheme 6 Isolation of 1'-(2,6-dihydroxyphenyl)etanone from the Aann-134(1) culture broth

3.9.1.4 1'-(2,6-Dihydroxyphenyl)-3'-hydroxybutanone

Fraction AC-007 (63 mg) was repeatedly chromatographed on a Sephadex LH-20 column (1 x 45 cm) using n-hexane:CH_2Cl_2:MeOH (2:2:1) as the eluent. Fractions (10-30 ml each) were collected and examined by TLC (silica gel, CH_2Cl_2:MeOH = 39:1). Fractions with similar chromatographic patterns were combined to yield six fractions: AC-031 - AC-036 (Table 7 and Scheme 7).

Fraction AC-035 (6 mg) was crystallized from n-hexane:CH_2Cl_2:MeOH (2:2:1) to give 1'-(2,6-dihydroxyphenyl)-3'-hydroxybutanone (3.7 mg) **[19]**.

Table 7 Fractions obtained from fraction AC-007 of the Aann-134(1) culture broth.

Fraction code	Eluate volume (ml)	Weight (mg)
AC-031	40	9
AC-032	20	10
AC-033	20	20
AC-034	10	6
AC-035	20	6
AC-036	40	11

3.9.1.5 Phenylacetic acid

Fraction AC-033 (20 mg) was repeatedly chromatographed on a Sephadex LH-20 column (1 x 45 cm) using n-hexane:CH_2Cl_2:MeOH (2:2:1) as the eluent. Fractions (10-30 ml each) were collected and examined by TLC (silica gel, CH_2Cl_2:MeOH = 39:1). Fractions with similar chromatographic patterns were combined to yield three fractions: AC-044 - AC-046 (Table 8 and Scheme 7).

Fraction AC-045 (6mg) was crystallized from n-hexane:CH_2Cl_2 (1:2) to give phenylacetic acid (4.3 mg) **[61]**.

Table 8 Fractions obtained from fractions AC-033 from the Aann-134(1) culture broth

Fraction code	Eluate volume (ml)	Weight (mg)
AC-044	60	8
AC-045	20	6
AC-046	50	5

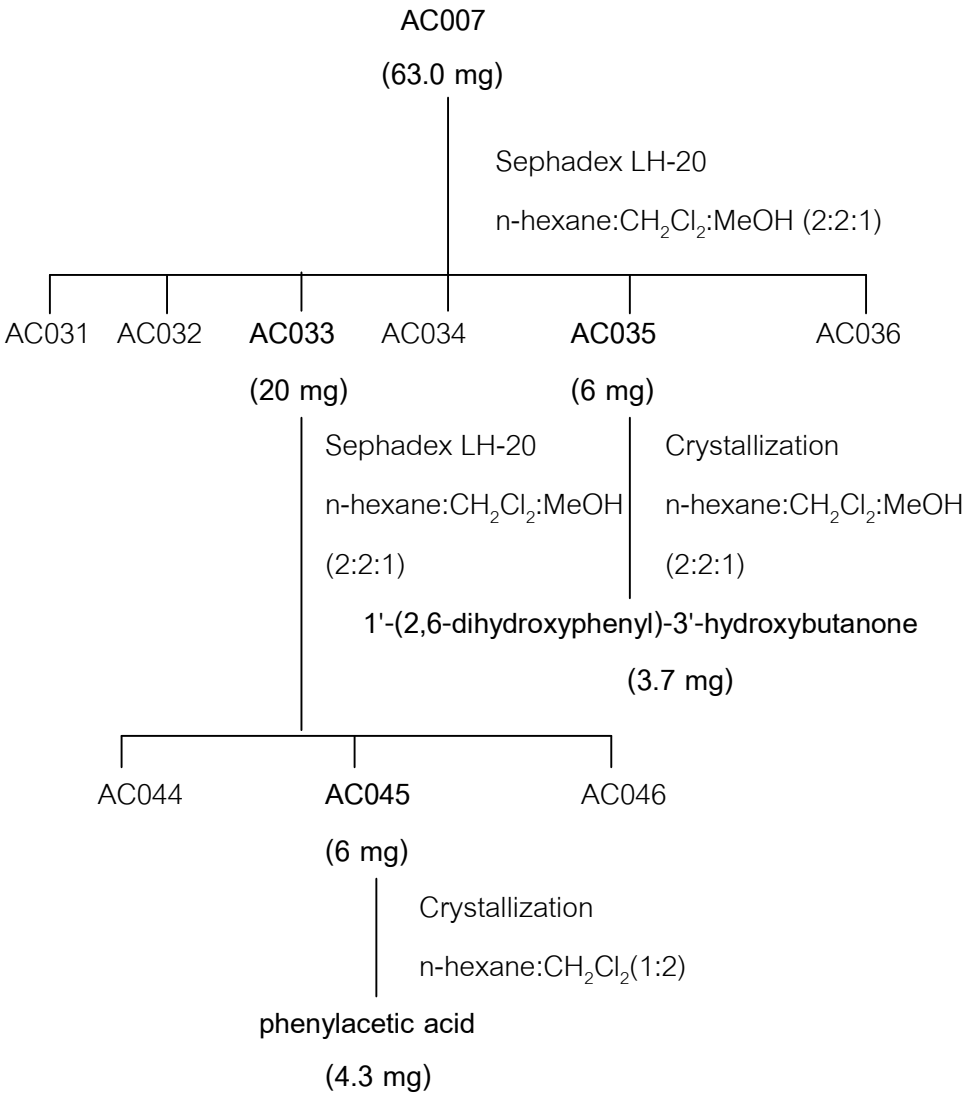

Scheme 7 Isolation of 1'-(2,6-dihydroxyphenyl)-3'-hydroxybutanone and phenylacetic acid from the Aann-134(1) culture broth.

3.9.2 Isolation of secondary metabolites from the hexane extract of *Nodulisporium* sp. Aann-134

The hexane extract (0.5 g) of the Aann-134 (2) culture broth was fractionated by quick column chromatography using a sintered glass filter column (4 x 4 cm) of silica gel (No. 7731, 80 g). Elution was performed in a polarity gradient manner with mixtures of n-hexane:CH_2Cl_2 (1:0, 100 ml; 1:1, 50 ml; 0:1, 100 ml) and CH_2Cl_2:EtOAc (1:0, 50 ml; 1:1, 50 ml; 0:1, 100 ml). Fractions (50 ml each) were collected and examined by TLC (silica gel, n-hexane:CH_2Cl_2=1:1) to yield six fractions: ACC-001 - ACC-006 (Table 9 and Scheme 8).

Table 9 Fractions obtained from the hexane extract of *Nodulisporium* sp. Aann-134.

Fraction code	Eluate volume (ml)	Weight (mg)
ACC-001	100	50
ACC-002	50	10
ACC-003	100	32
ACC004	50	45
ACC-005	50	50
ACC-006	100	37

3.9.2.1 1,8-Dimethoxynaphthalene

Fraction ACC-002 (10 mg) was crystallized from n-hexane:CH_2Cl_2 (2:1) to give 2.0 mg of colorless needles (R_f 0.93, silica gel, CH_2Cl_2:MeOH = 39:1). It was subsequently identified as 1,8-dimethoxynaphthalene (2.0 mg) **[18]** (Scheme 8). The compound was also obtained from the EtOAc extract of the first batch and the MeOH extract of the second batch (Schemes 4 and 9).

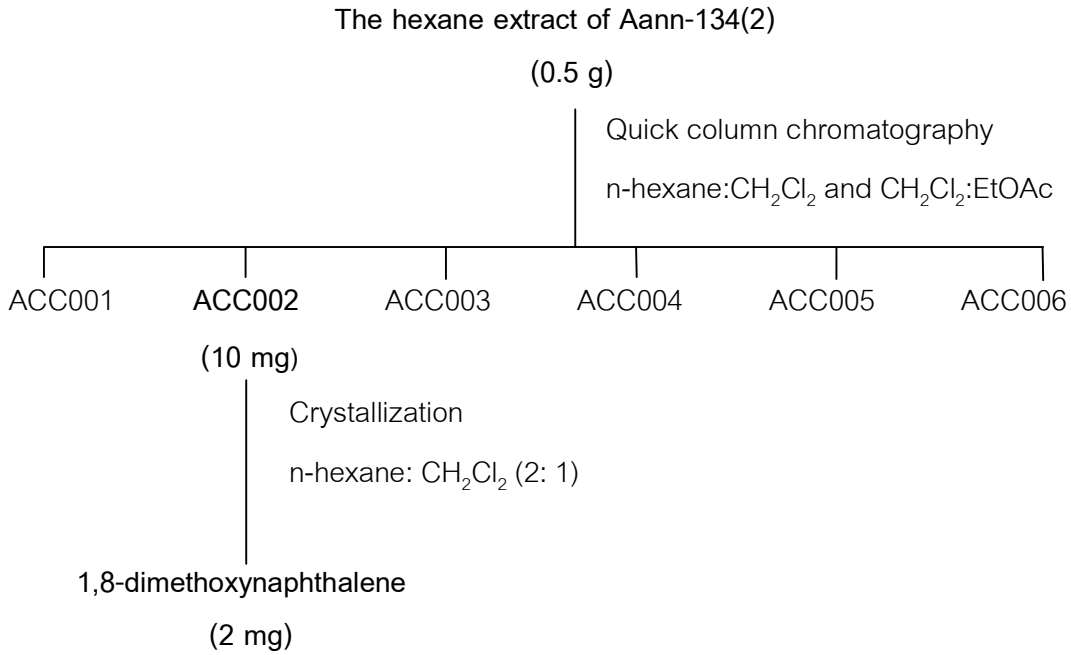

Scheme 8 Fractionation of the hexane extract and isolation of 1,8-dimethoxy-naphthalene from the Aann-134(2) culture broth.

3.9.3 Isolations of secondary metabolites from the methanol extract of *Nodulisporium* sp. Aann-134

The methanol extract (2.5 g) of the Aann-134 (2) culture broth was fractionated by quick column chromatography using a sintered glass filter column (10 x 5.5 cm) of silica gel (No. 7731, 200 g). Elution was performed in a polarity gradient manner with mixtures of n-hexane:CH_2Cl_2 (1:0, 50 ml; 1:1, 50 ml; 0:1, 150 ml), CH_2Cl_2:EtOAc (9:1, 200 ml; 1:1, 100 ml) and EtOAc:MeOH (1:0, 200 ml; 9:1, 200 ml). Fractions (50 ml each) were collected and examined by TLC (silica gel, CH_2Cl_2:MeOH = 39:1). Twenty-one fractions were obtained and the fractions showing similar chromatographic patterns were pooled to yield seven fractions: ACC-007 - ACC-013 (Table 10 and Scheme 9).

Table 10 Fractions obtained from the methanol extract of *Nodulisporium* sp. Aann-134.

Fraction code	Eluate volume (ml)	Weight (mg)
ACC-007	100	52
ACC-008	150	150
ACC-009	200	155
ACC-010	100	50
ACC-011	100	55
ACC-012	200	200
ACC-013	200	50

3.9.3.1 1,8-Dimethoxynaphthalene

Fraction ACC-007 (52 mg) was crystallized from n-hexane:CH_2Cl_2 to give 1.0 mg of colorless needles (R_f 0.93, silica gel, CH_2Cl_2:MeOH = 39:1). It was subsequently identified as a 1,8-dimethoxynaphthalene **[18]** (Scheme 9). The compound was also obtained from the EtOAc extract of the first batch and the hexane extract of the second batch (Schemes 4 and 8).

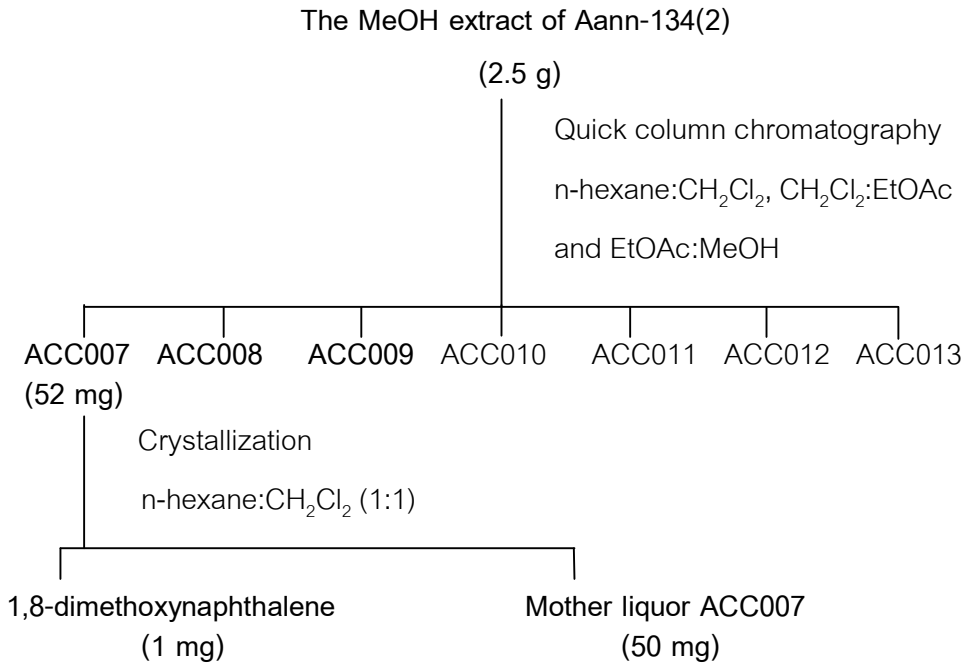

Scheme 9 Fractionation of the methanol extract and isolation of 1,8-dimethoxy naphthalene from the Aann-134(2) culture broth.

3.9.3.2 Nodulisporin G

Mother liquors of fractions AC-002 (230 mg) and ACC-007 (50 mg) were combined into fraction ACC-007-0 (280 mg) which was repeatedly gel-filtered on a Sephadex LH-20 column (1 x 45 cm) using n-hexane:CH_2Cl_2:MeOH (2:2:1) as eluent to yield six fractions: ACC-007-1 - ACC-007-6 (Table 11 and Scheme 10).

Fraction ACC-007-4 was further purified by preparative TLC using n-hexane:CH_2Cl_2 (9:1 and 20:1) as the solvent systems to give 13 mg of a yellow viscous liquid (R_f 0.87, silica gel, CH_2Cl_2:MeOH = 39:1). It was subsequently identified as nodulisporin G **[62]** (Scheme 10).

Table 11 Fractions obtained from fraction ACC-007-0 of the Aann-134(2) culture broth.

Fraction code	Eluate volume (ml)	Weight (mg)
ACC-007-1	20	70
ACC-007-2	10	53
ACC-007-3	5	15
ACC-007-4	10	55
ACC-007-5	5	3
ACC-007-6	15	7

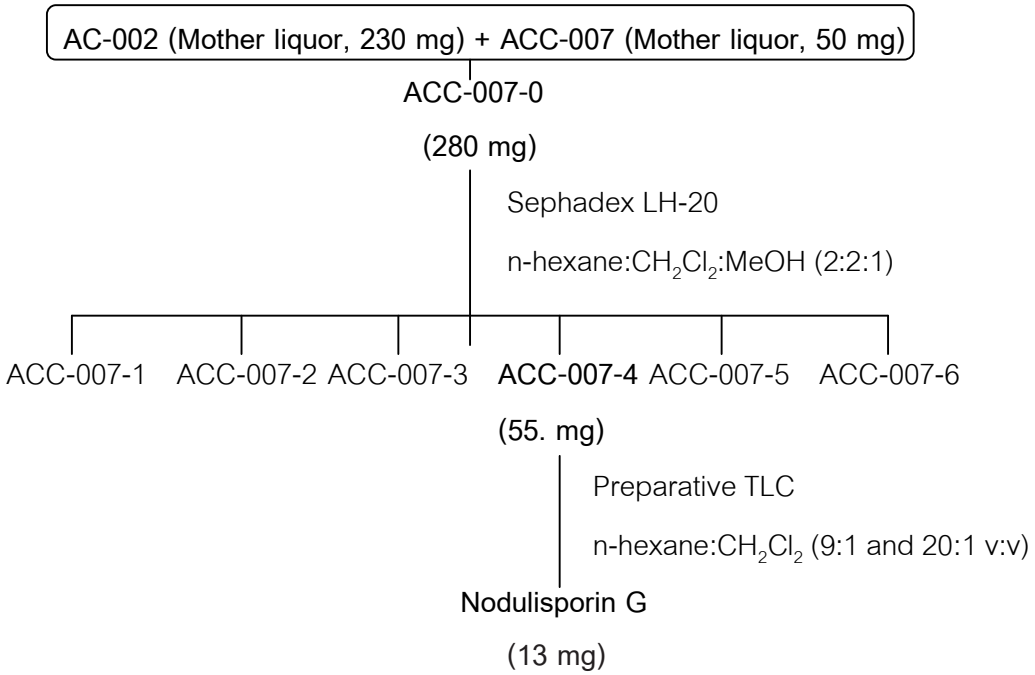

Scheme 10 Isolation of nodulisporin G from the Aann-134(1, 2) culture broth.

3.9.3.3 1,8-dihydroxynaphthalene

The anti-*Candida albicans* fraction (ACC-009, 155 mg) was repeatedly separated by silica gel (No. 9385, 40 g) flash column chromatography (1 x 30 cm). Elution was performed in a polarity gradient manner with mixtures of n-hexane:CH_2Cl_2 (1:1, 150 m; 0:1, 50 ml) and CH_2Cl_2: MeOH (39:1, 100 ml; 19:1, 100 ml; 9:1, 100 ml). Fractions (25 ml each) were collected and examined by TLC (silica gel, CH_2Cl_2:MeOH = 39:1). Fractions with similar chromatographic patterns were combined to yield three fractions: ACC-014-ACC-016 (Table 12 and Scheme 11).

The active fraction ACC-015 (20 mg) was crystallized from hexane:CH_2Cl_2 (1:2) to give 5.3 mg of colorless needles (R_f 0.43, silica gel, CH_2Cl_2:MeOH = 39:1). It was subsequently identified as 1,8-dihydroxynaphthalene (5.3 mg) **[63]** (Scheme 11).

Table 12 Fractions obtained from fraction ACC-009 of the Aann-134(2) culture broth.

Fraction code	Eluate volume (ml)	Weight (mg)
ACC-014	150	15
ACC-015	50	20
ACC-016	300	10

3.9.3.4 1'-(2,6-dihydroxyphenyl)ethanone

Fraction ACC-014 (15 mg) was crystallized from n-hexane:CH_2Cl_2 (1:1) to give 2.0 mg of colorless needles (R_f 0.5, silica gel, CH_2Cl_2:MeOH = 39:1). It was subsequently identified as 1'-(2,6-dihydroxyphenyl)ethanone (2 mg) **[60]**, as shown in Scheme 11. The compound was also obtained from the EtOAc extract of the first batch (Scheme 6).

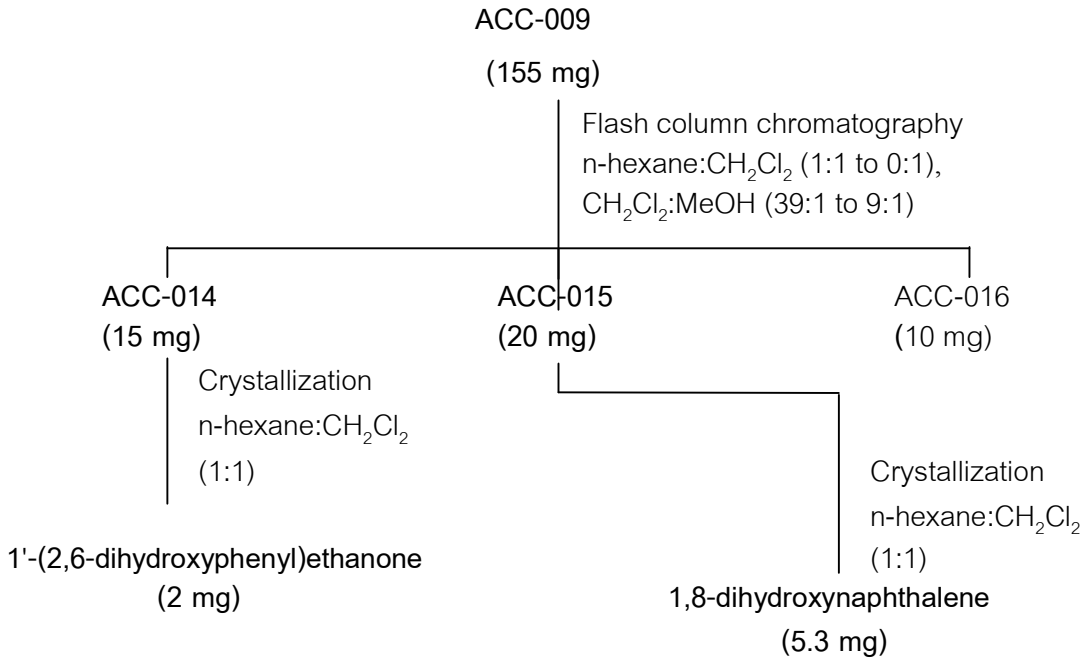

Scheme 11 Isolation of 1'-(2,6-dihydroxyphenyl)ethanone and 1,8-dihydroxy-naphthalene from the Aann-134(2) culture broth.

3.9.3.5 1'-(2,6-Dihydroxyphenyl)butanone

The anti-*C. albicans* fraction (ACC-008, 150 mg) was repeatedly chromatographed on a Flash column (1 x 30 cm) of silica gel (No. 9385, 40 g). Elution was performed in a polarity gradient manner with mixtures of n-hexane:CH_2Cl_2 (1:1, 50 ml; 0:1, 25 ml) and CH_2Cl_2:MeOH (39:1, 50 ml; 9:1,100 ml). The eluates fractions (25 ml each) were examined by TLC (silica gel, CH_2Cl_2:MeOH = 39:1). Fractions with similar chromatographic patterns were combined to yield five fractions: ACC-017 - ACC-021 (Table 13 and Scheme 12).

The active fraction (ACC 019, 10 mg) was crystallized from n-hexane:CH_2Cl_2 (1:1) to give 3 mg of colorless needles (R_f 0.71, silica gel, CH_2Cl_2:MeOH = 39:1). It was

subsequently identified as 1'-(2,6-dihydroxyphenyl)butanone **[20]** (Scheme 12). The compound was also obtained from the EtOAc extract of the first batch (Scheme 5).

Table 13 Fractions obtained from fraction ACC-008 of the Aann-134(2) culture broth.

Fraction code	Eluate volume (ml)	Weight (mg)
ACC-017	25	12
ACC-018	25	7
ACC-019	25	10
ACC-020	50	30
ACC-021	100	90

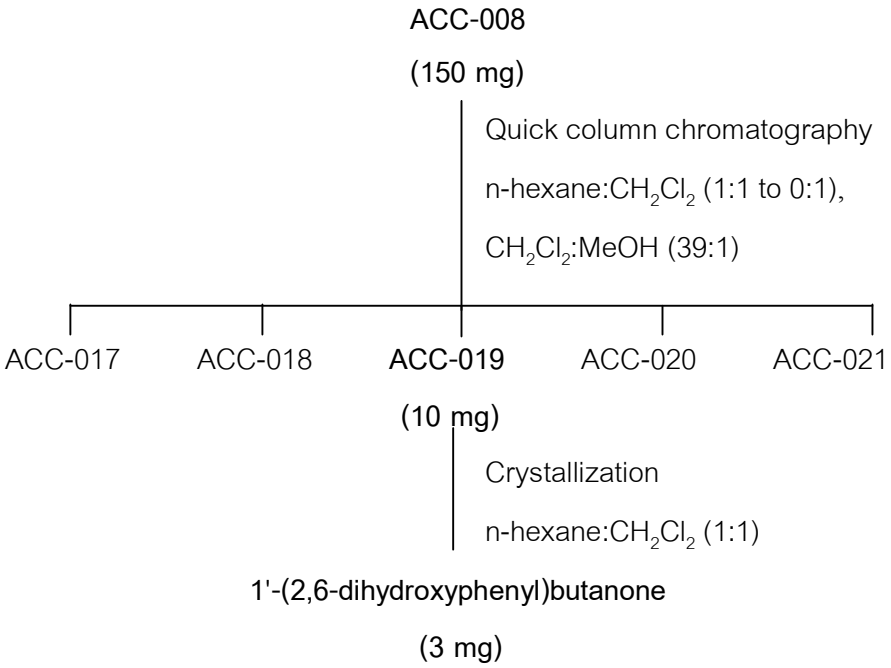

Scheme 12 Isolation of 1'-(2,6-dihydroxyphenyl)butanone from the Aann-134(2) culture broth.

3.10 Isolation of secondary metabolites from *Alternaria alternata* Tche-153

The EtOAc extract (10 g) was chromatographed over a Sephadex LH-20 column (2.5 cm x 150 cm) using n-hexane:CH_2Cl_2:MeOH (2:2:1) as solvent system. Fractions (50 ml each) were collected and examined by TLC (silica gel, CH_2Cl_2:MeOH = 39:1).

Fractions with similar chromatographic patterns were combined to yield fourteen fractions: TS-001-TS-014 (Figure 9, Table 14 and Scheme 13).

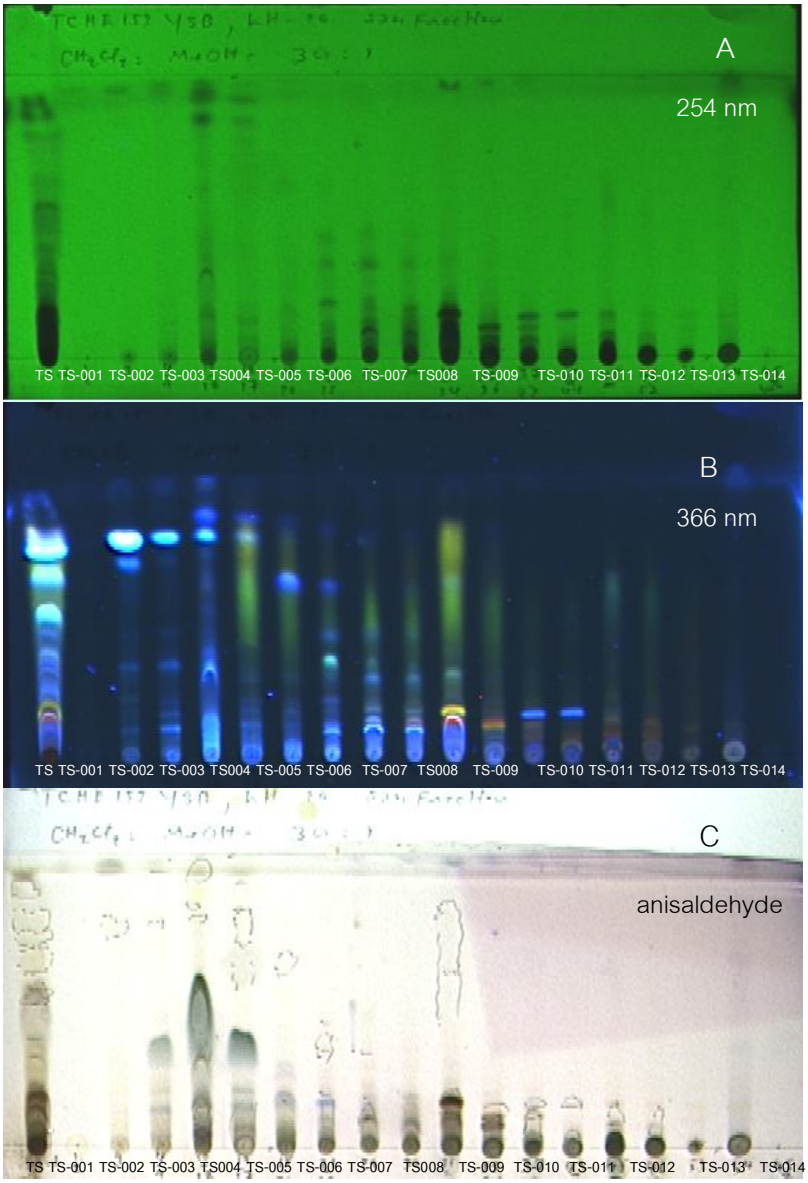

Figure 9 Thin-layer chromatogram system of fractions obtained from the EtOAc extract of *A. alternata* Tche-153.

A) detected under UV 254 nm;

B) detected under UV 366 nm, and

C) detected by anisaldehyde reagent

Table 14 Fractions obtained from the EtOAc extract of the Tche-153 culture broth.

Fraction code	Eluate volume (ml)	Weight (mg)
TS-001	100	98
TS-002	50	61
TS-003	300	180
TS -004	150	214
TS -005	250	271
TS -006	150	362
TS -007	400	1,379
TS 008	100	900
TS -009	200	1,911
TS -010	100	424
TS -011	300	599
TS -012	100	334
TS -013	50	255
TS -014	250	528

3.10.1 Isoochracinic acid

Fraction TS-009 (1,911 mg) was further fractionated by a sintered glass filter column (10 x 5.5 cm) of silica gel (No. 7731, 200 g). Elution was performed in a polarity gradient manner with mixtures of n-hexane :CH_2Cl_2 (1:0,100 ml; 1:1, 100 ml; 0:1, 100 ml), CH_2Cl_2:EtOAc (9:1, 1400 ml; 3:2, 200 ml; 1:1, 200 ml; 0:1, 400 ml) and EtOAc:MeOH (39:1, 100 ml; 9:1, 100 ml; 8:2, 300 ml). The eluates were collected as Thirty-one fractions and examined by TLC (silica gel, CH_2Cl_2:MeOH = 39:1). Fractions with similar chromatographic patterns were combined into eight fractions: TS-015-TS-022 (Table 15 and Scheme 13).

Fraction TS-017 (386 mg) was crystallized from CH_2Cl_2 :EtOAc (9:1) to give 6 mg of a colorless amorphous powder (R_f 0.6, silica gel, EtOAc:MeOH = 39:1). It was subsequently identified as isoochracinic acid **[54]** (Scheme 13).

Table 15 Fractions obtained from fraction TS-009 of the Tche-153 culture broth

Fraction code	Eluate volume (ml)	Weight (mg)
TS-015	300	187
TS-016	400	210
TS-017	300	386
TS-018	300	260
TS-019	200	235
TS-020	300	201
TS-021	200	156
TS-022	1,100	358

3.10.2 Altenuic acid

Fractions TS-018 to TS-020 (697 mg) were combined and crystallized from CH_2Cl_2:EtOAc (9:1) to give 33 mg of colorless needles (R_f 0.05, silica gel, CH_2Cl_2:MeOH = 39:1). The compound was subsequently identified as altenuic acid **[53]** (Scheme 13).

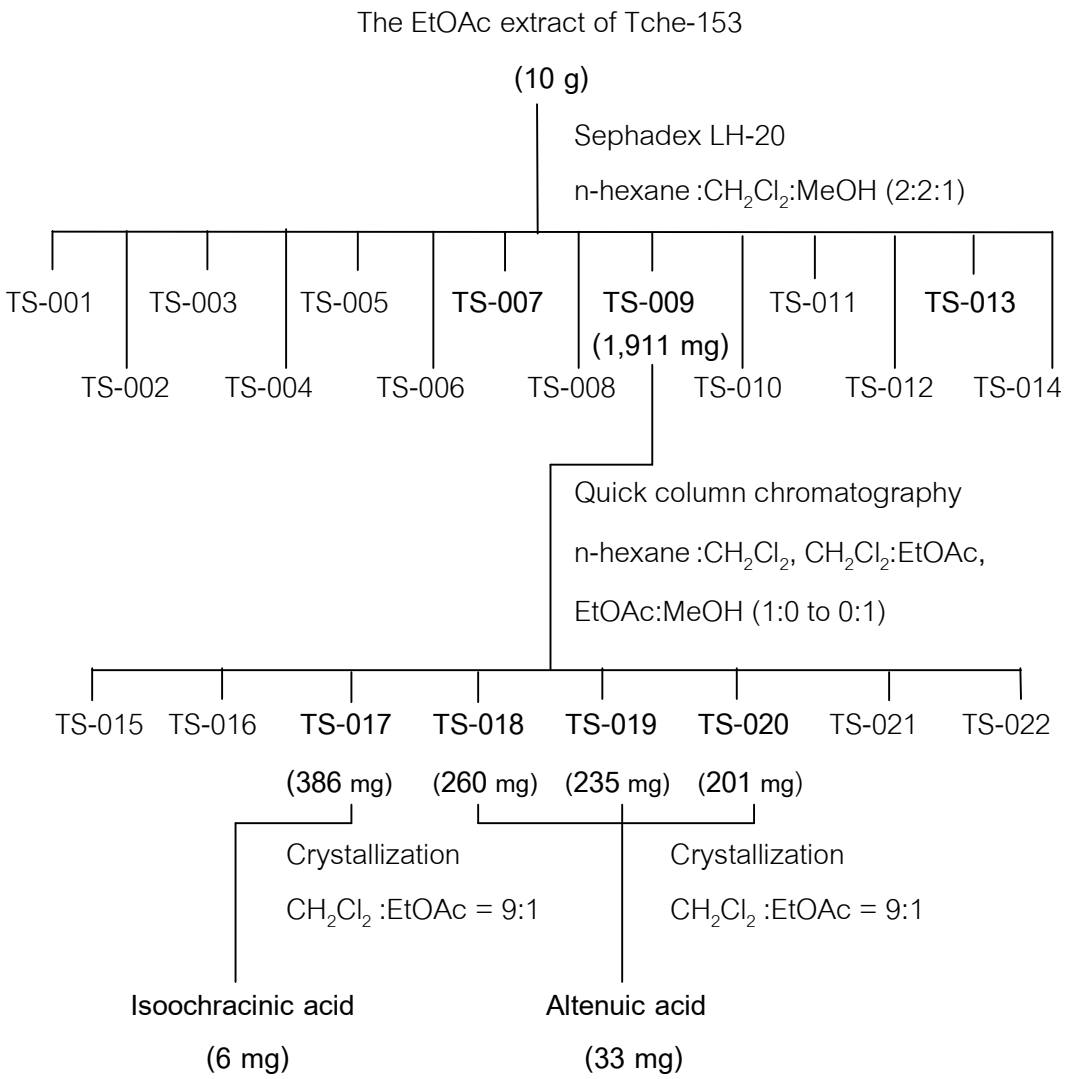

Scheme 13 Fractionation of the EtOAc extract and Isolation of altenuic acid and isoochracinic acid from the Tche-153 culture broth

3.10.3 2,5-Dimethyl-7-hydroxychromone

Fraction TS-007 (1379 mg) was separated by gel filtration chromatography over a Sephadex LH-20 column (1 x 50 cm) using n-hexane:CH_2Cl_2:MeOH (2:2:1) as the eluent. Fractions (50 ml each) were collected and examined by TLC (silica gel, CH_2Cl_2:MeOH = 39:1). Fractions with similar chromatographic patterns were combined to yield three fractions: TS-023 - TS-025 (Table 16 and Scheme 15). Fraction TS-024 (1,070 mg) was further separated by quick column chromatography using a sintered glass filter column (4x5 cm) of silica gel (No. 7731, 80 g). Elution was performed in a polarity gradient

manner with mixtures of n-hexane:CH_2Cl_2 (1:0,50 ml; 1:1, 250 ml; 0:1, 50 ml), CH_2Cl_2: EtOAc (9:1, 100 ml; 1:1, 50 ml; 0:1, 50 ml) and EtOAc :MeOH (19:1, 50 ml; 9:1, 50 ml). Fractions (50 ml each) were collected and examined by TLC (silica gel, CH_2Cl_2:MeOH = 39:1. Fractions with similar chromatographic patterns were combined to yield five fractions: TS-039 - TS-043 (Table 17 and Scheme 14).

Fraction TS-041 (35 mg) was crystallized from CH_2Cl_2;MeOH (99:1) to give 3.1 mg of reddish needles (R_f 0.27, silica gel, CH_2Cl_2:MeOH = 39:1). It was subsequently identified as 2,5-dimethyl-7-hydroxychromone **[50]** (Scheme 14).

Table 16 Fractions obtained from fraction TS-007 of the Tche-153 culture broth

Fraction code	Eluate volume (ml)	Weight (mg)
TS-023	100	40
TS-024	300	1,070
TS-025	500	160

Table 17 Fractions obtained from fraction TS-024 of the Tche-153 culture broth

Fraction code	Eluate volume (ml)	Weight (mg)
TS-039	150	10
TS040	150	83
TS-041	50	35
TS-042	100	94
TS-043	250	411

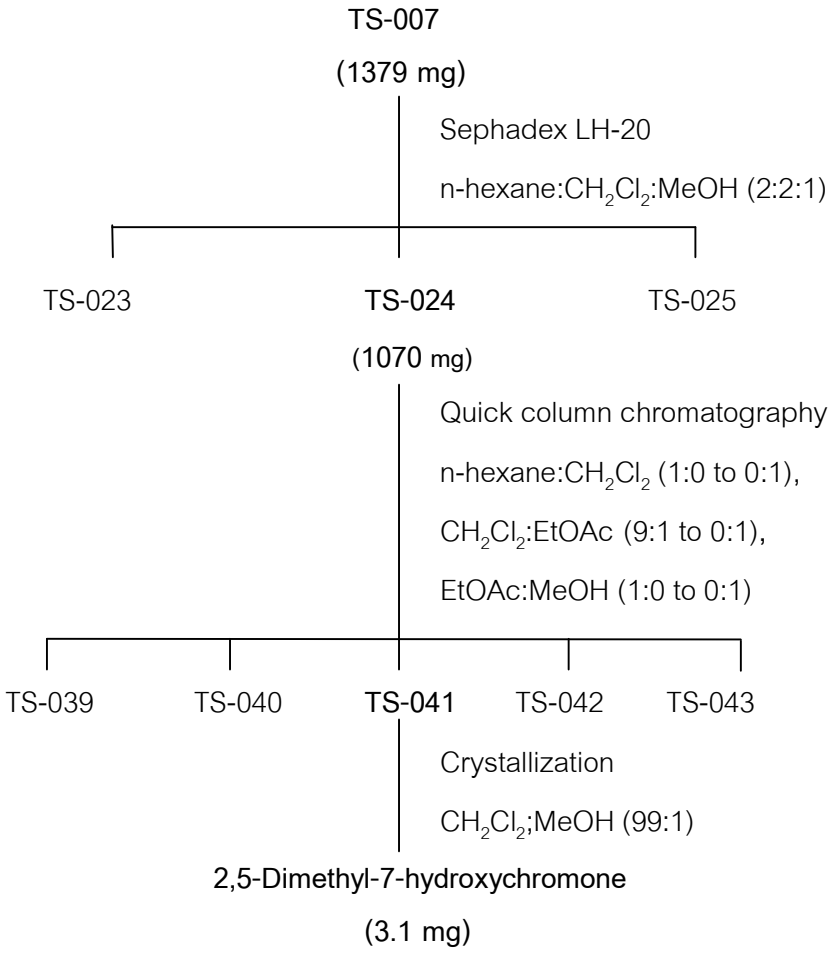

Scheme 14 Isolation of 2,5-dimethyl-7-hydroxychromone from the Tche-153 culture broth

3.10.4 Altenusin

The anti-*Candida albican*s fraction TS-013 (255 mg) was separated over a Sephadex LH-20 column (1 x 45 cm) using n-hexane:CH_2Cl_2:MeOH (2:2:1) as the eluent. The eluates (50 ml each) were collected and examined by TLC (silica gel, CH_2Cl_2:MeOH = 39:1). Fractions with similar chromatographic patterns were combined to yield six fractions: TS-026 - TS-031 (Table 18 and Scheme 16). The active fraction TS-029 (137mg) was repeatedly separated on a Sephadex LH-20 column (1 x 45 cm) using n-hexane:CH_2Cl_2:MeOH (2:2:1) as the eluent. The eluates (50 ml each) were collected and examined by TLC (silica gel, CH_2Cl_2:MeOH = 39:1), then combined to yield four fractions: TS-050 - TS-053 (Table 19 and Scheme 15).

Fraction TS-052 (35 mg) were crystallized from n-hexane:CH_2Cl_2:MeOH = 2:2:1 to give 10 mg of reddish prisms (R_f 0.65, silica gel, EtOAc:MeOH = 39:1). It was subsequently identified as altenusin **[43]** (Scheme 15).

Table 18 Fractions obtained from fraction TS-013 of the Tche-153 culture broth

Fraction code	Eluate volume (ml)	Weight (mg)
TS-026	50	41
TS-027	400	30
TS-028	50	18
TS-029	100	137
TS-030	50	9
TS-031	150	1

Table 19 Fractions obtained from fraction TS-029 of the Tche-153 culture broth

Fraction code	Eluate volume (ml)	Weight (mg)
TS-050	300	47
TS-051	200	33
TS-052	50	35
TS-053	50	19

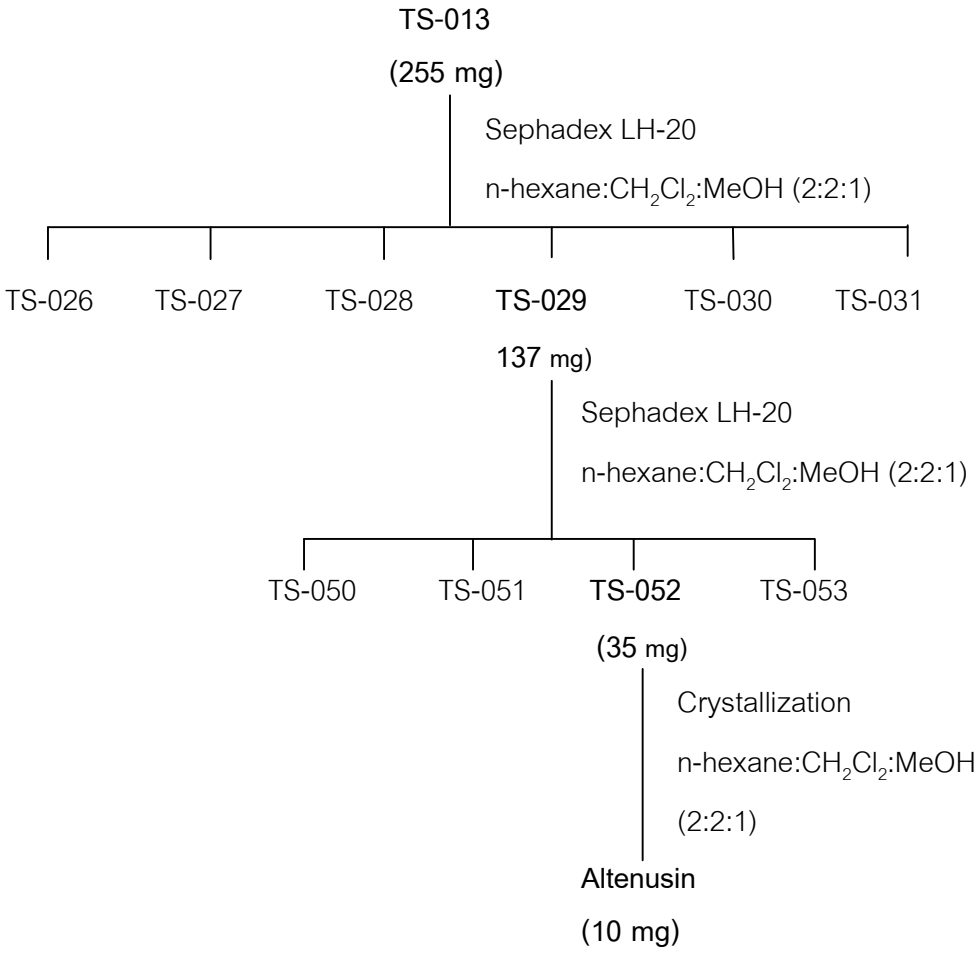

Scheme 16 Isolation of altenusin from the Tche-153 culture broth

3.11 Physical properties of the isolated compounds

3.11.1 1'-(2,6-Dihydroxyphenyl)butanone

1'-(2,6-Dihydroxyphenyl)butanone (9 mg) was obtained as colorless needles, soluble in chloroform.

EIMS : *m/z* (% relative intensity); Figure 31

180 $[M]^+$ (27), 165 (3), 147 (3), 138 (7), 137 (100)

^{1}H-NMR : δ ppm, 500 MHz, in $CDCl_3$; Figures 32-34, Table 20

^{13}C-NMR : δ ppm, 125 MHz, in $CDCl_3$; Figure 35, Table 20

3.11.2 1'-(2,6-Dihydroxyphenyl)-3'-hydroxybutanone

1'-(2,6-Dihydroxyphenyl)-3'-hydroxybutanone (3.7 mg) was obtained as colorless needles, soluble in chloroform.

ESI-TOF MS : $[M+Na]^+$ *m/z* 219; Figure 41

$[\alpha]^{25}_D$: -6.0 (*c* 0.085, $CHCl_3$)

^{1}H-NMR : δ ppm, 500 MHz, in $CDCl_3$; Figures 42-44, Table 21

^{13}C-NMR : δ ppm, 125 MHz, in $CDCl_3$; Figure 45, Table 21

3.11.3 Nodulisporin G

Nodulisporin G (13 mg) was obtained as yellow viscous liquid, soluble in chloroform.

HRESI-TOF MS : $[M+Na]^+$ *m/z* 413.2663 (calcd for $C_{25}H_{28}O_4\ Na^+$ 413.1207); Figure 50

$[\alpha]^{25}_D$: -1.7 (*c* 0.875, $CHCl_3$)

UV : λ_{max} nm (log ε), in methanol; Figure 52
221 (1.49), 271 (1.01), 346 (0.53)

IR : ν_{max} cm^{-1}, KBr disc; Figure 51
3400, 2927, 1648, 1579, 1463, 1349, 1228, 1059, 1018, 800

^{1}H-NMR : δ ppm, 500 MHz, in $CDCl_3$; Figures 53-56, Table 22

^{13}C-NMR : δ ppm, 125 MHz, in $CDCl_3$; Figure 57, Table 22

3.11.4 1'-(2,6-Dihydroxyphenyl)ethanone

1'-(2,6-Dihydroxyphenyl)ethanone (4.6 mg) was obtained as colorless needles, soluble in chloroform.

ESI-TOF MS : $[M+H]^+$ *m/z* 153; Figure 73

^{1}H-NMR : δ ppm, 500 MHz, in $CDCl_3$; Figures 74-75, Table 23

^{13}C-NMR : δ ppm, 125 MHz, in $CDCl_3$; Figure 76, Table 23

3.11.5 Phenylacetic acid

Phenylacetic acid (4.3 mg) was obtained as colorless needles, soluble in chloroform.

ESI-TOF MS : $[M+H]^+$ *m/z* 137; Figure 81

^{1}H-NMR : δ ppm, 500 MHz, in $CDCl_3$; Figures 82-83, Table 24

^{13}C-NMR : δ ppm, 125 MHz, in $CDCl_3$; Figure 84, Table 24

3.11.6 1,8-Dimethoxynaphthalene

1,8-Dimethoxy naphthalene (6.6 mg) was obtained as colorless needles, soluble in chloroform.

EIMS : *m/z* (% relative intensity); Figure 89

189 $[M+H]^+$ (12), 188 $[M]^+$ (100), 175 (37), 145 (89), 127 (22)

^{1}H-NMR : δ ppm, 500 MHz, in $CDCl_3$; Figures 90-91, Table 25

^{13}C-NMR : δ ppm, 125 MHz, in $CDCl_3$; Figure 92, Table 25

3.11.7 1,8-Dihydroxynaphthalene

1,8-Dihydroxynaphthalene (5.3 mg) was obtained as colorless needles, soluble in chloroform.

ESI-TOF MS : $[M+H]^+$ *m/z* 161; Figure 97

^{1}H-NMR : δ ppm, 500 MHz, in $CDCl_3$; Figures 98-99, Table 26

^{13}C-NMR : δ ppm, 125 MHz, in $CDCl_3$; Figure 100, Table 26

3.11.8 Altenusin

Altenusin (10 mg) was obtained as reddish prisms, soluble in methanol.

EIMS : *m/z* (% relative intensity); Figure 106

290 $[M]^+$ (100), 289 (2), 272 (37), 244(89), 215 (22), 201 (15)

^{1}H-NMR : δ ppm, 400 MHz, in CD_3OD; Figures 107-108, Table 27

^{13}C-NMR : δ ppm, 100 MHz, in CD_3OD; Figure 109, Table 27

3.11.9 Isoochracinic acid

Isoochracinic acid (6.5 mg) was obtained as colorless amorphous power, soluble in methanol.

ESI-TOF MS : $[M+Na]^+$ *m/z* 231; Figure 115

$[\alpha]^{25}_D$: -0.4 (*c* 0.46, MeOH)

^{1}H-NMR : δ ppm, 500 MHz, in CD_3OD; Figures 116-117, Table 28

^{13}C-NMR : δ ppm, 125 MHz, in CD_3OD; Figure 118, Table 28

3.11.10 Altenuic acid

Altenuic acid (33 mg) was obtained as colorless needles, soluble in DMSO.

HRESI-TOF MS : $[M+Na]^+$ *m/z* 345.0588 (calcd for $C_{25}H_{28}O_4\ Na^+$ 345.0581); Figure 123

$[\alpha]^{25}_D$: -2.2 (*c* 0.32, MeOH)

Melting point : 174-175 °C

UV : λ_{max} nm (log ε), in methanol; Figure 125

219 (1.69), 258 (0.74), 295 (0.30)

IR : ν_{max} cm^{-1}, KBr disc; Figure 124

3441, 2551, 1737, 1619, 1479, 1445, 1389, 1340, 1299, 1248, 1167, 1015, 848

^{1}H-NMR : δ ppm, 500 MHz, in DMSOd_6; Figures 126-127, Table 29

^{13}C-NMR : δ ppm, 125 MHz, in DMSOd_6; Figure 128, Table 29

3.11.11 2,5-Dimethyl-7-hydroxychromone

2,5-Dimethyl-7-hydroxychromone (3.1 mg) was obtained as colorless needles, soluble in methanol.

ESI-TOF MS : $[M+Na]^+$ *m/z* 191; Figure 135

^{1}H-NMR : δ ppm, 500 MHz, in CD_3OD; Figures 136-138, Table 30

^{13}C-NMR : δ ppm, 125 MHz, in CD_3OD; Figure 139, Table 30

3.12 Preparation of (R)-and (S)-MTPA esters of nodulisporin G

(R)–α-Methoxy-α-(trifluoromethyl)-phenylacetyl chloride (20 µl, 26 µM) was added to 2 mg of nodulisporin G in 400 µl dry pyridine. After being stirred at room temperature for 12 h, the mixture was extracted with CH_2Cl_2 (4 x 2 ml) and washed with 1M HCl (4 x 2 ml). The CH_2Cl_2 layer was dried with anhydrous Na_2SO_4. The residue was evaporated to dryness and purified to give S-(-)-MTPA ester. (S)-α-Methoxy-α-(trifluorometyl)-phenylacetyl chloride was also prepared using the same protocol to afford R-(+)-MTPA ester (Appendino *et a*l.,2005).

3.13 Determination of azole-synergistic activity against *Candida albicans* by disk diffusion assay.

Anti-*C. albicans* activity of test sample was determined by agar diffusion assay modified from antibiotic assay described in United States Pharmacopeia 32–National Formulary 27 (2009).

C. albicans ATCC 90028 was grown overnight on SDA at 37°C and suspended in sterile normal saline solution (0.85% NaCl). The turbidity of yeast suspension was adjusted to match that of 50%T at 580 nm using a spectrophotometer (BioSpec-1601, Shimadzu).

The yeast inoculum was added in a final concentration of 1% into molten SDA without and with ketoconazole at a sub-inhibitory concentration (0.125 µg/ml). The inoculated SDA (9 ml) was pipetted into 90-mm petri dish and allowed to harden. Ten µl of each test sample (1 mg of crude extract or 256 µg of pure compound in DMSO) and DMSO (control) were applied to paper disks placed on the inoculated agar surface. After keeping at room temperature for 1 h, the test plates were incubated at 37°C for 24 h. The clear zone of inhibition around the disk indicating antimicrobial activity of the compound was then measured.

3.14 Determination of azole-synergistic activity against *Candida albicans* by TLC-contact bioautography

TLC-contact bioautographic method, modified from previously described (Narasimhachari and Ramachandran, 1967), was used to detect active component in crude extract. The test fraction (1 mg) was applied to silica gel analytical TLC plate which was further developed by a suitable solvent system (CH_2Cl_2:MeOH = 39:1).

The assay plates were prepared as previously described in 3.13. Dried TLC plate was placed face down onto the inoculated agar surface. After keeping at room temperature for 1 h, the test plates were incubated at 37°C for 24 h. The clear inhibition zone around the chromatogram indicating antimicrobial activity of the active component was measured.

3.15. Determination of minimum inhibitory concentration (MIC) against *Candida albicans*

Compounds exhibiting activity from disk diffusion assay were determined for their MICs against *C. albicans* by broth microdilution method as previously described (NCCLS, 2002).

Test compound was dissolved in DMSO at a concentration of 25.6 mg/ml and further diluted in RPMI 1640 to 512 μg/ml. Then, it was serially diluted two-fold to 1 μg/ml and each dilution was dispensed in a volume of 100 μl into 96-well microtitre plate. A 200-μl of RPMI 1640 and a 100-μl of RPMI 1640 containing 1% DMSO were used as a sterility control and a growth control, respectively. Nystatin was used as a positive control. The experiment was done in triplicate.

C. albicans ATCC 90028 was grown overnight on SDA at 37°C and suspended in sterile normal saline solution (0.85% NaCl) to yield $1x10^6$ - $5x10^6$ CFU/ml. The yeast suspension was further diluted in RPMI1640 medium to yield $1x10^3$ - $5x10^3$ CFU/ml. A 100-μl inoculum was dispensed into each well that contained 100 μl of test compound. After incubation at 37 °C for 24 h, a 20 μl aliquot of p-iodonitrotetrazolium (INT) solution (1 mg/ml) was added into each well. The assay plates were further incubated for 24 h.

Violet color which developed in each well indicated the growth of test organism. The well showing no change in color indicated anticandidal activity of the test compound.

MIC was defined as the lowest concentration that showed no visible growth of *C. albicans*.

3.16 Determination of azole synergistic activity against *Candida albicans* by the microdilution chequerboard technique

Microdilution chequerboard method was used to determine the interaction of test compound with azole drugs including ketoconazole, fluconazole or itraconazole, according to the method described by Sun *et al*. (2008). The final drug concentrations after addition of 100 μL of the inoculum ranged from 256 to 4 μg/ml for test compound and 16 to 0.25 μg/ml for azole drugs. Plates were incubated at 37°C for 48 h, as described previously in **13.15.** The experiment was done in triplicate.

Fractional inhibitory concentration (FIC) index was used to indicate the effect of the combination. FIC index is the sum of the MIC-0 (no visible growth) of each drug when used in combination divided by the MIC-0 of the drug when used alone. Synergism, indifference and antagonism were defined as FIC indices of $\leq$0.5, >0.5 - 4 and >4, respectively (Odds, 2003).

CHAPTER IV

RESULTS AND DISCUSSION

4.1 Identification of the endophytic fungus *Nodulisporium* sp. Aann-134

Morphological characteristics

The Aann-134 fungus grew rapidly on PDA as a pale brown velvety colony (Figure 10). The reverse side was brown. On water agar with sterilized banana-leaf pieces, the Aann-134 fungus produced light brown hyphae. Conidiophores were long, asymmetrically branched and verrucose, as shown in Figure 11. These characteristics suggested that Aann-134 should be *Nodulisporium* sp. (Ellis, 1993).

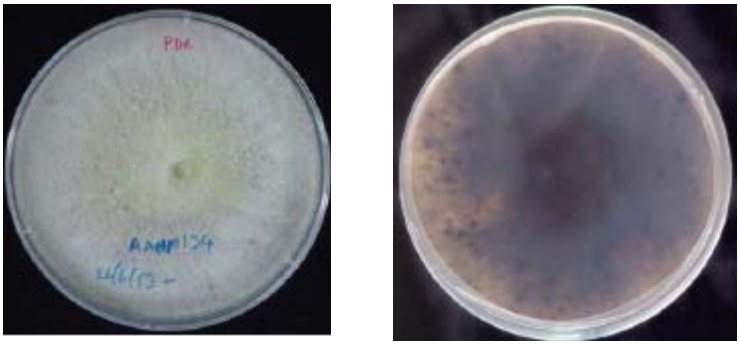

Figure 10 Colony morphology of *Nodulisporium* sp. Aann-134 grown on PDA at 25°C for 10 days. (Left) obverse side; (Right) reverse side.

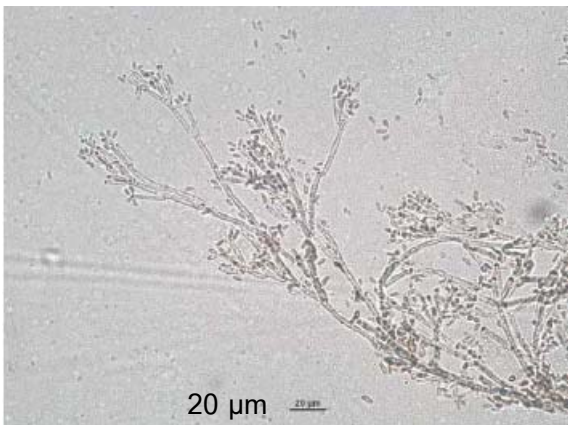

Figure 11 Microscopic morphology of *Nodulisporium* sp. Aann-134 grown on water agar with sterilized banana-leaf pieces at 25°C for 60 days.

DNA sequence based identification

The complete ITS1-5.8S-ITS2 DNA sequence of the endophytic fungus Aann-134 (Figure 12) was found to be perfectly matched (100% homology) with those of *Daldinia eschscholzii* strain HNY27-4C (FJ624265), isolate SUT168 (DQ322086), isolate MU 41 (AB641415) and strain KT32 (FR852577). This supported the identification of Aann-134 fungus as *Nodulisporium* sp. based on morphology as described earlier. *Nodulisporium* sp. has been known to be an anamorph of *Daldinia eschscholzii* (Farr *et al*., 1989).

Based on morphological characteristics and nucleotide sequence of the ribosomal RNA gene region, this endophytic fungus Aann134 was identified as *Nodulisporium* sp. Culture of *Nodulisporium* sp. Aann134 has been deposited at Department of Microbiology, Mahidol University, Thailand. The DNA sequence of the ITS1-5.8S-ITS2 region of this fungus has been submitted to the GenBank database with the accession number JN635501.

```
....|....| ....|....| ....|....| ....|....| ....|....|
        10         20         30         40         50
     18S                   ITS1
GGAGGGATCA TTACTGAGTT ATCTAAACTC CAACCCTATG TGAACTTACC
                      ITS1
GCCGTTGCCT CGGCGGGCCG CGTTCGCCCT GTAGTTTACT ACCTGGCGGC
                      ITS1
GCGCTACAGG CCCGCCGGTG GACTGCTAAA CTCTGTTATA TATACGTATC
          ITS1                                5.8S
TCTGAATGCT TCAACTTAAT AAGTTAAAAC TTTCAACAAC GGATCTCTTG
                      5.8S
GTTCTGGCAT CGATGAAGAA CGCAGCGAAA TGCGATAAGT AATGTGAATT

GCAGAATTCA GTGAATCATC GAATCTTTGA ACGCACATTG CGCCCATTAG
               5.8S                       ITS2
TATTCTAGTG GGCATGCCTG TTCGAGCGTC ATTTCAACCC TTAAGCCCCT
                      ITS2
GTTGCTTAGC GTTGGGAATC TAGGTCTCCA GGGCCTAGTT CCCCAAAGTC
                      ITS2
ATCGGCGGAG TCGGAGCGTA CTCTCAGCGT AGTAATACCA TTCTCGCTTT
                      ITS2
TGCAGTAGCC CCGGCGGCTT GCCGTAAAAC CCCTATATCT TTAGTGGTTG
     28S
ACCTCGAATC AG
```

Figure 12 Nucleotide sequence of the partial 18S rRNA gene, complete ITS1 region - 5.8S rRNA gene - ITS2 region, and partial 28S rRNA gene of the endophytic fungus *Nodulisporium* sp. Aann-134.

4.2 Identification of the endophytic fungus *Alternaria alternata* Tche-153

Morphological characteristics

The Tche-153 fungus grew on potato dextrose agar (PDA) as a gray cottony colony with brown diffusible pigment around the colony (Figure 13). The reverse side was brown. On water agar with sterilized banana-leaf pieces, the Tche-153 fungus produced brown catenate conidia on brown conidiophores. Conidia were obclavate with a short cylindrical beak, verrucose, with up to 8 transverse septa and a few longitudinal septa, overall length 25-49 μm and 8-12 μm thick in the broadest part (Figure 14). These characteristics suggested that the Tche-153 isolate should be *Alternaria alternata* (Ellis, 1993).

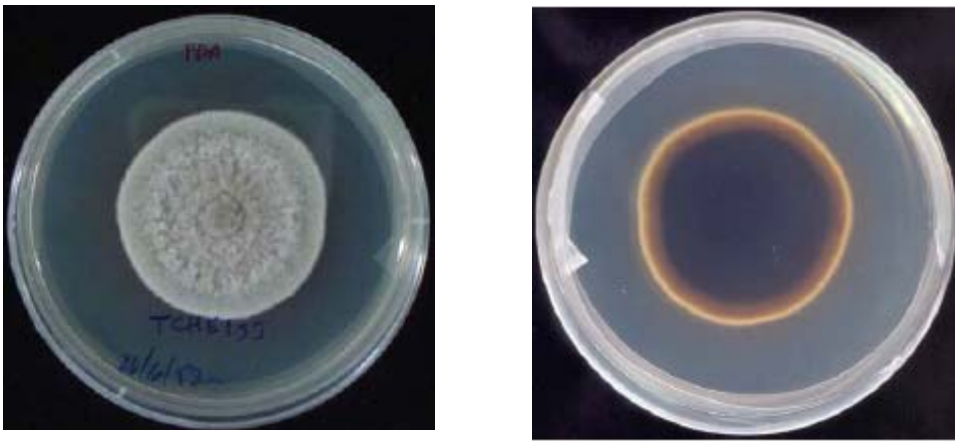

Figure 13 Colony morphology of *Alternaria alternata* Tche-153 grown on PDA at 25°C for 10 days. (Left) obverse side; (Right) reverse side.

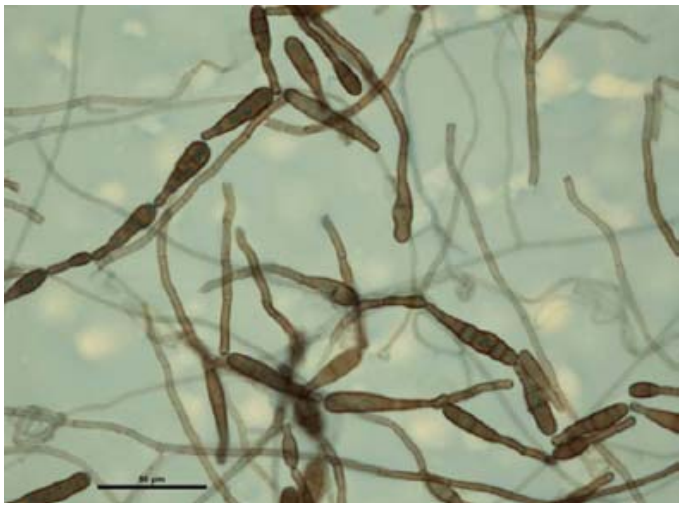

Figure 14 Microscopic morphology of *Alternaria alternata* Tche-153 grown on water agar with sterilized banana-leaf pieces at 25°C for 10 days.

DNA sequence based identification

The complete ITS1-5.8S-ITS2 DNA sequence of the endophytic fungus Tche-153 (Figure 15) was found to be perfectly matched (100% homology) with those of *A. alternata* (HM003680, GQ916545, GQ169766, DQ156341), *A. porri* (DQ156345), *A. tenuissima* (AF276656, DQ323692) and *A. longipes* (AF267137). All of the perfectly matched strains were not reference strains. Therefore, the ITS sequence data of *Alternaria* reference strains available in databases were retrieved with CLC Mainworkbench 5.6 (CLC bio A/S, Aarhus, Denmark) and aligned with that of the Tche-153 fungus. It was found that complete ITS sequence of Tche-153 showed the highest homology (99.79%) to that of *A. alternata* ATCC 28329 (AF229459) and 99.59% homology to those of *A. alternata* ATCC MYA-4642 (HQ263343), *A. alternata* ATCC 13963 (AY625056) and *A. tenuissima* ATCC 16423 (AF229476).

Based on morphological characteristics and nucleotide sequence of the ribosomal RNA gene region, this endophytic fungus Tche-153 was identified as *Alternaria alternata*. Culture of *A. alternata* Tche-153 has been deposited at Department of Microbiology, Mahidol University, Thailand. The DNA sequence of the ITS1-5.8S-ITS2 region of this fungus has been submitted to the GenBank database with the accession number JN210895.

```
....|....| ....|....| ....|....| ....|....| ....|....|
         10         20         30         40         50
        18S                          ITS1
CTGCGGAGGG ATCATTACAC AAATATGAAG GCGGGCTGGA ATCTCTCGGG
                      ITS1
GTTACAGCCT TGCTGAATTA TTCACCCTTG TCTTTTGCGT ACTTCTTGTT
                      ITS1
TCCTTGGTGG GTTCGCCCAC CACTAGGACA AACATAAACC TTTTGTAATT
           ITS1                                5.8S
GCAATCAGCG TCAGTAACAA ATTAATAATT ACAACTTTCA ACAACGGATC
                      5.8S
TCTTGGTTCT GGCATCGATG AAGAACGCAG CGAAATGCGA TAAGTAGTGT
                      5.8S
GAATTGCAGA ATTCAGTGAA TCATCGAATC TTTGAACGCA CATTGCGCCC
                 5.8S                          ITS2
TTTGGTATTC CAAAGGGCAT GCCTGTTCGA GCGTCATTTG TACCCTCAAG
                      ITS2
CTTTGCTTGG TGTTGGGCGT CTTGTCTCTA GCTTTGCTGG AGACTCGCCT
                      ITS2
TAAAGTAATT GGCAGCCGGC CTACTGGTTT CGGAGCGCAG CACAAGTCGC
                      ITS2
ACTCTCTATC AGCAAAGGTC TAGCATCCAT TAAGCCTTTT TTCAACTTTT
                   28S
GACCTCGGAT CAGGTAGGGA TACCCGCTGA ACTTAAGCAT AT
```

Figure 15 Nucleotide sequence of the partial 18S rRNA gene, complete ITS1 region - 5.8S rRNA gene - ITS2 region, and partial 28S rRNA gene of the endophytic fungus *Alternaria alternata* Tche-153.

4.3 Structure determination of secondary metabolites isolated from the endophytic fungus *Nodulisporium* sp. Aann-134

The crude EtOAc extract (1 mg per disk) of *Nodulisporium* sp. Aann-134 primarily exhibited antifungal activity and ketoconazole-synergistic activity against *Candida albicans* with inhibition zone diameters of 7.39 and 19.31 mm, respectively. The extract was further purified by bioassay-guided fractionation using a chromatographic combination of Sephadex LH-20 and silica gel columns to afford seven compounds. Extensive analyses of NMR spectral data (^{1}H and ^{13}C; 2D ^{1}H-^{1}H COSY, HMQC, and HMBC) and mass spectral data in combination with literature data comparison, all seven compounds were identified as one new resorcinol derivative and three known resorcinol derivatives, two naphthalene derivatives, and phenylacetic acid.

4.3.1 Structure determination of 1'-(2,6-dihydroxyphenyl)butanone

The compound was obtained as colorless needles from fraction AC019 of the EtOAc extract (0.2 % w/w yield) and fraction ACC019 of the MeOH extract (0.1% w/w yield) (Schemes 5 and 12), respectively. The low-resolution EIMS spectrum (Figure 31) showed the molecular ion peak $[M]^{+\bullet}$ at *m/z* 180. The ^{13}C-NMR spectrum (Table 20 and Figure 35) displayed eight carbon signals which were classified by HSQC (Figure 37-38) as one methyl carbon at δ 13.88, two methylene carbons at δ 17.79 and 46.66, two aromatic methine carbon signals at δ 108.40 (2C) and 135.67, two quaternary aromatic carbon signals at δ 110.07 and 161.18 (2C), and a ketone carbonyl carbon at δ 207.87. Therefore, the molecular formula $C_{10}H_{12}O_3$ was proposed based on these mass spectral and ^{13}C-NMR data. The ^{1}H-NMR spectrum (Table 20 and Figures 32-34) of the compound displayed typical character of a symmetrically 1,2,3-trisubstituted benzene ring at δ 6.39 (2H, *d*, *J* = 8.1 Hz, H-3/H-5*)* and 7.22 (1H, *t*, *J* = 8.1 Hz, H-4). The resorcinol moiety was proposed from the evidence of these proton signals and the downfield shifts of the oxygenated aromatic carbons at δ 161.18 (C-2/C-6). In addition, the n-butanone moiety was suggested by the ketone carbonyl carbon at δ 207.87 (C-1') and the proton signals at δ 0.99 (3H, *t*, *J* = 7.3 Hz, H_3-4'), 1.74 (2H, *h*, *J* = 7.3 Hz, H_2-3') and 3.12 (2H, *t*, *J* = 7.3 Hz, H_2-2'). Analysis of the ^{1}H-^{1}H COSY spectrum (Figure 36) confirmed the connectivities from H-3/H-5 to H-4 and H_2-2' to H_2-3' to H_3-4'. The ^{1}H and ^{13}C-NMR data of the compound were completely assigned from the HSQC (Figures 37-38) and the HMBC spectra (Figures 39-40) showing the long-range correlations between H-3/H-5 with C-1 (δ 110.07), C-2/C-6 and C-1'; between H-4 with C-2/C-6 and C-3/C-5 (δ 108.40); between H_2-2' with C-1' and C-1 , and between H_2-3' with C-1', of which the location of the butan-1-one side chain was suggested at C-1 of the resorcinol ring. The HMBC long-range correlations were shown in Figure 16 and summarized in Table 20. Based upon these spectral data, the compound was identified as a resorcinol derivative 1'-(2,6-dihydroxyphenyl)butanone **[20]** which was previously isolated from *Nodulisporium* sp. (Dai *et al*., 2006).

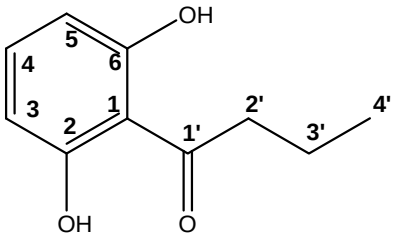

1'-(2,6-Dihydroxyphenyl)butanone **[20]**

Table 20 NMR spectral data of 1'-(2,6-dihydroxyphenyl)butanone (in $CDCl_3$, 500 MHz)

Position	δ_H (ppm), *J* (Hz)	δ_C (ppm)	^{1}H-^{1}H COSY	HMBC correlation ^{1}H to ^{13}C
1		110.07		
2		161.18		
3	6.39 (1H, *d*, *J* = 8.1)	108.40	4	1, 2, 1'
4	7.22 (1H, *t*, *J* = 8.1)	135.67	3, 5	2/6, 3/5
5	6.39 (1H, *d*, *J* = 8.1)	108.40	4	1, 6, 1'
6		161.18		
1'		207.87		
2'	3.12 (2H, *t*, *J* = 7.3)	46.66	3'	1, 1'
3'	1.74 (2H, *m*, *J* = 7.3)	17.79	2', 4'	1'
4'	0.99 (3H, *t*, *J* = 7.3)	13.88	3'	
2,6-OH	9.62 (2H, *s*)			

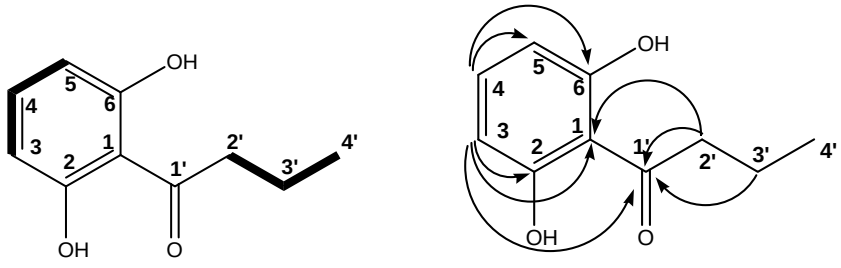

Figure 16 ^{1}H-^{1}H COSY (bold line) and key HMBC correlations (arrow) for 1'-(2,6-dihydroxyphenyl)butanone in $CDCl_3$

4.3.2 Structure determination of 1'-(2,6-dihydroxyphenyl)-3'-hydroxybutanone

The compound was obtained as colorless needles from fraction AC035 of the EtOAc extract (1.23 % w/w yield) (Scheme 7). The high-resolution ESI-TOF MS (Figure 41) showed the pseudomolecular ion peak $[M+Na]^+$ at *m/z* 219.0627 (calculated for $C_{10}H_{12}O_4Na^+$ at m/z 219.0628), consistent with the molecular formula $C_{10}H_{12}O_4$. The ^{13}C-NMR spectrum (Table 21 and Figure 45) displayed eight carbon signals which were classified by DEPT 135 (Figure 46) as one methyl carbon signal at δ 23.1; one methylene carbon signals at δ 51.4; one oxygenated methine carbon at δ 73.72; two aromatic methine carbon signals at δ 108.99 (2C) and 136.75; two quaternary aromatic carbon signals at δ 111.53, 161.10(2C) and a ketone carbonyl carbon at δ 206.28. The ^{1}H-NMR spectrum (Table 21 and Figures 42-44) of the compound displayed typical character of a symmetrically 1,2,3-trisubstituted benzene ring similar to the previously described resorcinol derivatives **[20]** at δ 6.50 (2H, *d, J* = 8.1 Hz, H-3/H-5*)* and 7.30 (1H, *t, J* = 8.1 Hz, H-4). Furthermore, one methyl proton signal at δ 1.37 (3H, *d, J* = 6.3 Hz, H_3-4') together with non-equivalent methylene proton signals at δ 3.20 (1H, *dd, J* =16.0, 2.9 Hz, H-2'a) and 3.35 (1H, *dd, J* =16.0, 9.3 Hz, H-2'b) and one oxygenated methine proton signal at δ 4.50 (1H, *qdd, J* = 9.3, 6.3, 2.9, Hz, H-3') were consistent with a -CH_2-CHO-CH_3 moiety. This moiety and the carbonyl carbon at δ 206.30 (C-1') were combined to form a 3'-hydroxybutanone side chain. Finally, a two-proton signal at δ 9.96 was assigned to two phenolic hydroxyl protons. Analysis of the ^{1}H-^{1}H COSY spectrum (Figure 47) confirmed the connectivities from H-3/H-5 to H-4 and H-3' to H_2-2' to H_3-4'. The ^{1}H-NMR and ^{13}C-NMR data of the compound were completely assigned from the HMQC spectrum (Figure 48) and the HMBC spectrum (Figure 49) showing the long-range correlations between H-3/H-5 with C-1 (δ 111.53), C-2/C-6 (δ 161.10) and C-1', of which the location of the butanone side chain was suggested at C-1 of the resorcinol ring; between H-4 with C-2, C-6; and between H_2-2' and H-3' with C-1' ,C-4'. The HMBC long-range correlations were shown in Figure 17 and summarized in Table 21. Based upon these spectral data, the compound was identified as a resorcinol derivative 1'-(2,6-dihydroxyphenyl)-3'-hydroxybutanone **[19]** which was previously isolated from *Nodulisporium* sp. (Dai *et al*., 2006).

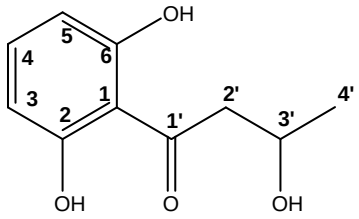

1'-(2,6-Dihydroxyphenyl)-3'-hydroxybutanone **[19]**

Table 21 NMR Spectral data of 1'-(2,6-dihydroxyphenyl)-3'-hydroxybutanone (in $CDCl_3$, 500 MHz)

Position	δ_H (ppm), *J* (Hz)	δ_C (ppm)	^1H-^1H COSY	HMBC correlation ^1H to ^{13}C
1		111.53		
2		161.10		
3	6.50 (1H, *d*, *J* = 8.1)	108.99	4	1, 1', 2
4	7.30 (1H, *t*, *J* = 8.1)	136.75	3/5	2, 6
5	6.50 (1H, *d*, *J* = 8.1)	108.99	4	1, 1', 6
6		161.10		
1'		206.28		
2'	a 3.20 (1H, *dd*, *J* = 16.0, 2.9)	51.44	2'b	1'
	b 3.35 (1H, *dd*, *J* = 16.0, 9.3)		2'a, 3'	3', 1', 4'
3'	4.50 (1H, *qdd*, *J* = 9.3, 6.3, 2.9)	66.61	2'b, 4'	1', 4'
4'	1.37 (3H, *d*, *J* = 6.3)	23.10	3'	2', 3'
2,6-OH	10.06 (2H, *s*)			

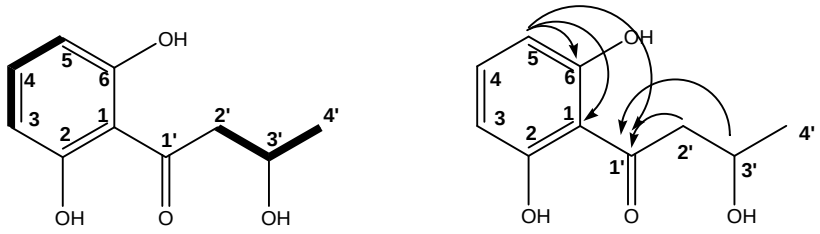

Figure 17 ^1H-^1H COSY (bold line) and key HMBC correlations (arrow) for 1'-(2,6-dihydroxyphenyl)-3'-hydroxybutanone in $CDCl_3$

4.3.3 Structure determination of nodulisporin G

The compound was obtained as a viscous oil from fraction ACC007-4 of the EtOAc/MeOH extract (0.22 % w/w yield) (Scheme 10). The high resolution ESI-TOF-MS (Figure 50) showed the pseudomolecular ion $[M+Na]^+$ *m/z* 413.2663 (calcd. for $C_{20}H_{22}O_8Na^+$ 413.1207), consistent with the molecular formula $C_{20}H_{22}O_8$. The UV spectrum showed bands at 221, 271 and 346 nm (Figure 52). The IR spectrum displayed bands at 3441, 1737, and 1619 cm^{-1} (Figure 51) characteristic for hydroxyl group and carbonyl group, respectively. The ^{13}C-NMR spectrum (Table 22 and Figure 57) showing only ten carbon signals implying the symmetric character of the structure. The carbon signals were classified by DEPT 135 (Figure 58) as one methyl carbon at δ 19.79 (C-4'); one methylene carbon at δ 42.78 (C-2'); one oxygenated methine carbon at δ 72.77 (C-3'); three methine aromatic carbons at δ 106.26 (C-3), 108.12 (C-5), and 137.11 (C-4); one quaternary aromatic carbon at δ 106.99 (C-1); two oxygenated quaternary aromatic carbons at δ 160.66 (C-2) and 161.07 (C-6), and one ketone carbon at δ 197.46 (C-1'). The ^{1}H-NMR spectrum (Table 22 and Figure 53-56) in $CDCl_3$ displayed a character of the asymmetrically 1,2,3-trisubstituted benzene ring different from the previously described resorcinol derivatives **[19]** at δ 6.34 (1H, *dd, J* = 8.3, 1.0 Hz, H-5), 6.40 (1H, *dd, J* = 8.3, 1.0 Hz, H-3), and 7.26 (1H, *t, J* = 8.3 Hz, H-4). Furthermore, one methyl proton signal at δ 1.42 (3H, *d, J* = 6.3 Hz, H_3-4') together with non-equivalent methylene proton signals at δ 2.65 (1H, *dd, J* =17.2, 3.5 Hz, H-2'a) and 2.57 (1H, *dd, J* =17.1, 12.2 Hz, H-2'b) and one oxygenated methine proton signal at δ 4.47 (1H, *qdd, J* = 6.2, 3.5, 12.2 Hz, H-3') were consistent with a $-CH_2-CHO-CH_3$ moiety. This moiety and the carbonyl carbon at δ 197.46 (C-1') were combined to form a 3'-hydroxybutanone side chain. Finally, a one-proton singlet at δ 11.63 was assigned to a phenolic proton. Analysis of the ^{1}H-^{1}H COSY (Figure 59) spectrum confirmed the connectivities from H-3 to H-4 to H-5 and H-3' to H_2-2' to H_3-4'. The ^{1}H-NMR and ^{13}C-NMR data were completely assigned from the HMQC spectrum (Figure 60) and the HMBC spectrum (Figures 61-64) showing the following long-range correlations between H-3 with C-1 (δ 106.99), C-2 (δ 160.66), C-5 (δ 108.12) and C-1'; between H-4 with C-2 (δ 160.66) and C-6 (δ 161.07); between H-5 with C-1 (δ 106.99) ,C-3 (δ 106.26), and C-

6 (δ 161.10), between H_2-2' with C-1, C-1', C-3' and C-4'; between H_3-4' with C-1', C-3'; and between 6-OH with C-1, C-4, C-5, and C-6. The long-range correlation between H_2-2' with C-1 confirmed the 3'-hydroxybutanone substituting at C-1 of the resorcinol nucleus. According to the structural symmetry, these data were accounted for 2 symmetrical units of $C_{10}H_{11}O_4$. The HMBC long-range correlations were shown in Figure 18 and summarized in Table 22. Finally, the two units were proposed to connect through a peroxide bridge based on the different chemical shifts of the oxygenated quaternary aromatic carbons at δ 160.66 (C-2) and 161.07 (C-6). From the described evidence, the compound was identified as a new dimeric resorcinol compound, for which the trivial name nodulisporin G **[62]** was proposed.

The absolute configuration of the hydroxybutanone chain at C-3' was assigned using the modified Mosher's method (Appendino *et al*., 2005). Reaction of nodulisporin G with Mosher's reagents, (*R*)- and (*S*)-methoxytrifluoromethylphenylacetic (MTPA) chloride yielded the (*S*)-MTPA ester **[62S]** and (*R*)-MTPA ester **[62R]**, respectively. The difference in chemical shift values ($\Delta\delta SR$) of the corresponding protons in the diastereomeric esters, (*S*)-MTPA ester **[62S]** and (*R*)-MTPA ester **[62R]**, led to the assignment of the *S* absolute configuration for C-3' (Figure 19).

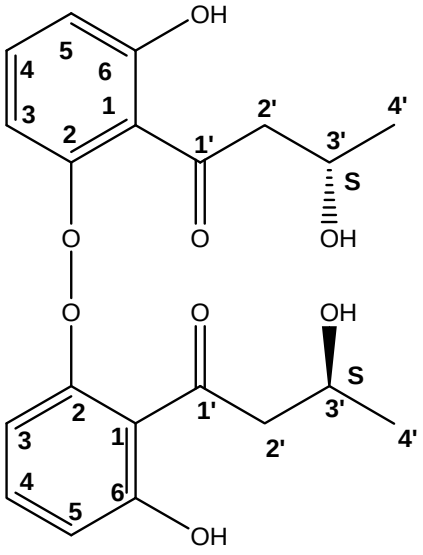

Nodulisporin G **[62]**

Table 22 NMR Spectral data of nodulisporin G (in $CDCl_3$, 500 MHz)

Position	δH (ppm), J (Hz)	δC (ppm)	^{1}H-^{1}H COSY	HMBC correlation ^{1}H to ^{13}C
1		106.99		
2		160.66		
3	6.34 (2H, *dd, J* = 8.3, 1.0)	106.26	4	1, 2, 5,1'
4	7.26 (2H, *t, J* = 8.3)	137.11	3, 5	2, 6
5	6.40 (2H, *dd, J* = 8.3, 1.0)	108.12	4	1, 3, 6
6		161.07		
1'		197.46		
2'	a 2.65 (2H, *dd, J* =17.1, 12.2)	42.78	3'	1, 1', 3', 4'
	b 2.57 (2H, *dd, J* =17.1, 3.5)			
3'	4.47 (2H, *qdd, J* = 6.3, 3.5, 12.2)	72.77	2', 4'	
4'	1.42 (6H, *d, J* = 6.3)	19.79	3'	2', 3'
6OH	11.63 (1H, *s*)			1, 5, 6

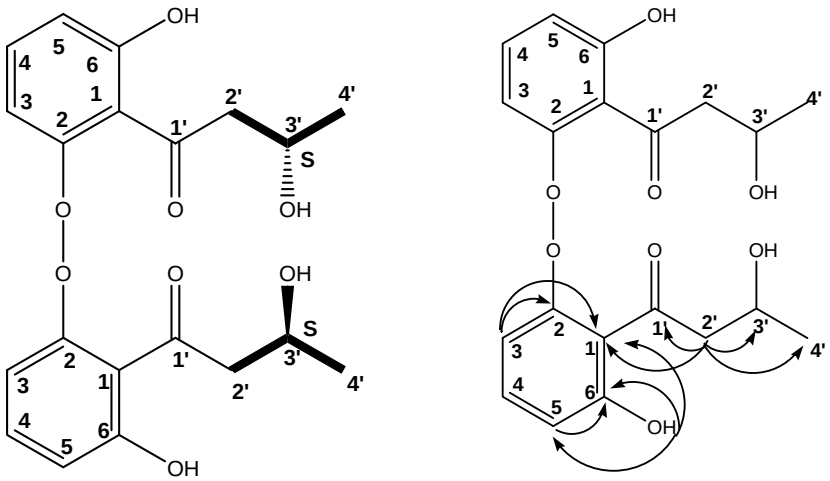

Figure 18 ^{1}H-^{1}H COSY (bold line) and key HMBC correlations (arrow) for nodulisporin G.

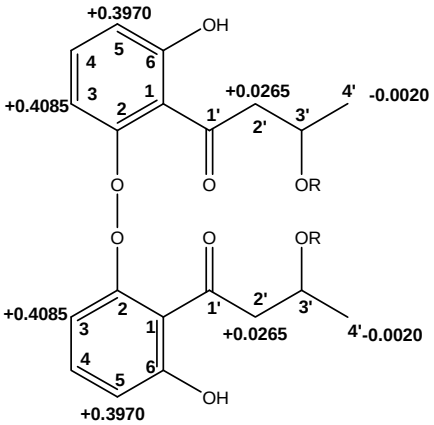

62S, R = (*R*)-MTPA

62R, R = (*S*)-MTPA

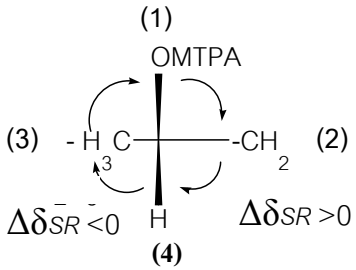

S- Configuration

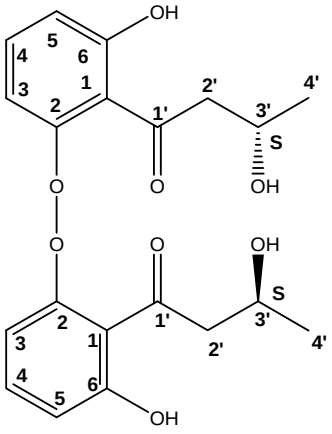

Nodulisporin G

Figure 19 $\Delta\delta_{SR}$ values ($\Delta\delta_{SR} = \delta_S - \delta_R$) for the MTPA esters **62*S*** and **62*R*** of nodulisporin G

.

4.3.4 Structure determination of 1'-(2,6-dihydroxyphenyl)ethanone

The compound was obtained as colorless needles from fraction AC026 of the EtOAc extract (0.09 % w/w yield) and fraction ACC014 of the MeOH extract (0.07 % w/w yield) (Schemes 6 and 11). The low-resolution ESI-TOF MS (Figure 73) showed the pseudomolecular ion peak $[M+H]^+$ at *m/z* 153. The ^{1}H-NMR (Figures 74-75) and ^{13}C-NMR (Figure 76) spectra showed characteristic signals of a symmetrically 1,2,3-trisubstituted benzene ring similar to those of 1'-(2,6-dihydroxy-phenyl)butanone **[20]** at δ_H 6.39 (2H, *d, J* = 8.0 Hz, H-3/H-5) / δ_C 108.31 (C-3/C-5), δ_H 7.25 (1H, *t, J* = 8.0 Hz, H-4) / δ_C135.98 (C-4), δ_C161.27 (C-2/C-6), and δ_C 110.23 (C-1). The remaining signals observed at δ_H 2.73 (3H, *s*, H_3-2') / δ_C 33.43 and δ_C 205.15 were ascribed for an acetyl moiety. The ^{1}H-NMR and ^{13}C-NMR data of the compound were completely assigned from the HSQC spectrum (Figure 77) and the HMBC spectrum (Figures 78-80) which showed the following long-range correlations between H-3/H-5 with C-1, C-2/C-6, and C-1'; between H-4 with C-2/C6; and between H_3-2' with C-1 and C-1'. The long-range correlation between H_3-2' and C-1 indicated that the acetyl moiety attached to the aromatic nucleus at C-1. The NMR data of the compound were summarized in Table 25. Based upon these spectral data, the compound having the molecular formula $C_8H_8O_3$ was identified as a resorcinol derivative 1'-(2,6-dihydroxyphenyl)ethanone **[60]**. The HMBC long-range correlations were shown in Figure 20 and summarized in Table 23.

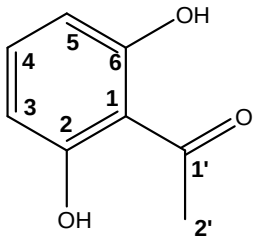

1'-(2,6-Dihydroxyphenyl)ethanone **[60]**

Table 23 NMR spectral data of 1'-(2,6-dihydroxyphenyl)ethanone (in $CDCl_3$, 500 MHz)

Position	δ_H (ppm), *J* (Hz)	δ_C (ppm)	HMBC correlation ^1H to ^{13}C
1		110.23	
2		161.27	
3	6.39 (1H, *d*, *J* = 8.0)	108.31	1, 2, 1'
4	7.25 (1H, *t*, *J* = 8.0)	135.98	2, 6
5	6.39 (1H, *d*, *J* = 8.0)	108.31	1, 6, 1'
6		161.27	
1′		205.15	
2′	2.73 (2H, *s*)	33.43	1, 1'
2,6-OH	9.49 (2H, *s*)		

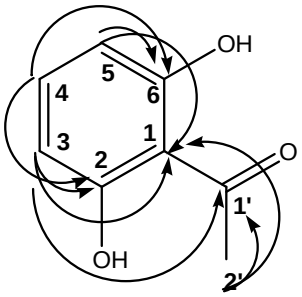

Figure 20 Key HMBC correlations (arrow) for 1'-(2,6-dihydroxyphenyl)ethanone

4.3.5 Structure determination of phenylacetic acid

The compound was obtained as colorless needles from fraction AC045 of the EtOAc extract (0.14 % w/w yield) (Scheme 7). The low-resolution ESI-TOF MS spectrum (Figure 81) showed the pseudomolecular ion peak $[M+H]^+$ at *m/z* 137. The ^{13}C-NMR spectrum (Table 24 and Figure 84) displayed six carbon signals which were classified by correlations in the HSQC spectrum (Figures 85-86) as belonging to one methylene carbon at δ 40.86, five aromatic methine carbons at δ 129.35 (2C), 128.65 (2C) and 127.35, one quaternary aromatic carbon at δ 133.26, and a carbonyl carbon at δ

176.66. The ^{1}H-NMR spectrum (Table 24 and Figures 82-83) displayed typical characteristic of a monosubstituted benzene ring at δ 7.28-7.33 (5H). The acetic acid moiety was ascribed by the carbonyl carbon signal at δ 176.66 (C-2') and a two-proton singlet at δ 3.65 (2H, *s*, H-1'). The ^{1}H-NMR and ^{13}C-NMR data were completely assigned from the HSQC spectrum (Figures 85-86) and the HMBC spectrum (Figures 87-88) which showed the long-range correlations between H-2/H-6 with C-1, C-4, and C-1'; between H-3/H-5 with C-1; between H-4 with C-2/C6; and between H_2-1' with C-1, C-2/C-6, and C-2'. The last set of long-range correlations indicated that the acetic acid moiety attached to the aromatic nucleus at C-1. Its NMR data were summarized in Table 26. Based upon these spectral data, the compound having the molecular formula $C_8H_8O_2$ was identified as phenylacetic acid **[61]**. The HMBC long-range correlations were shown in Figure 21 and summarized in Table 24.

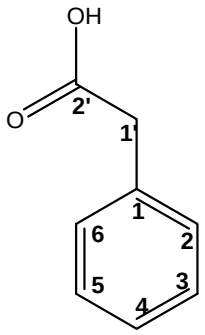

Phenylacetic acid **[61]**

Table 24 NMR Spectral data of phenylacetic acid (in $CDCl_3$, 500 MHz)

Position	δ_H (ppm), *J* (Hz)	δ_C (ppm)	HMBC correlation ^1H to ^{13}C
1		133.26	
2		129.35	1, 1', 4
3		128.65	1
4	7.28-7.33 (5H)	127.35	2, 6
5		128.65	1
6		129.35	1, 1', 4
1'	3.65 (2H, *s*)	40.86	1, 2, 6, 2'
2'		176.66	

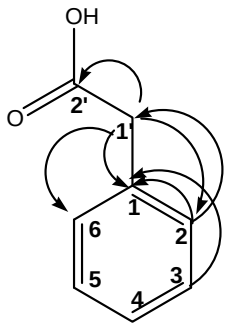

Figure 21 Key HMBC correlations (arrow) for phenylacetic acid

4.3.6 Structure determination of 1,8-dimethoxynaphthalene

The compound was obtained as colorless needles from fraction AC002 of the EtOAc extract (0.12 % w/w yield), fraction ACC002 of the hexane extract (0.12% w/w yield) and fraction ACC007 of the MeOH extract (0.2% w/w yield) (Schemes 4, 8 and 9), respectively. Its low-resolution EIMS (Figure 89) showed the molecular ion peak $[M]^{+\bullet}$ at *m/z* 188. Its ^{13}C-NMR spectrum (Table 25 and Figure 92) showed seven signals which were classified by DEPT 135 (Figure 93) as a methyl carbon signal at δ 55.44 (2 C); three aromatic methine carbon signals at δ 105.23, 119.83 and 125.32 (each one representing, 2C); and three quaternary carbon signals at δ 116.63, 156.10 (2 C) and 156.38. Based on the above mass spectral and ^{13}C-NMR data, its molecular formula

$C_{12}H_{12}O_2$ was determined. Its ^{1}H-NMR spectrum (Table 25 and Figures 90-91) displayed typical characteristic of the 1,2,3-trisubstitued benzene moiety at δ 6.78 (2H, *dd*, *J* = 8.2, 1.3 Hz, H-2/H-7), 7.28 (2H, *t*, *J* =8.2 Hz, H-3/H-6) and 7.32 (1H, *dd*, *J* = 8.2,1.3 Hz, H-4/H-5). The proton singlet at δ 3.78 was readily assigned to two methoxy protons at (1-OCH_3/8-OCH_3). The ^{1}H and ^{13}C NMR data accounted for only half of the carbon and hydrogen compositions given by the molecular formula, demonstrating that the compound possess a highly symmetrical structure. Analysis of its ^{1}H-^{1}H COSY (Figure 94) spectrum established the connectivity from H-4 to H-3 to H-2; and H-5 to H-6 to H-7. The ^{1}H-NMR and ^{13}C-NMR data of the compound (Table 25) were completely assigned from the HMQC spectrum (Figure 95) and the HMBC spectrum (Figure 96) showing long-range correlations between H-2/H-7 with C-1/C-8 (δ 156.10), C-4/C-5 (δ 119.83) and C-8a (δ 116.63); between H-3/H-6 with C-1/C-8, C-2/C-7 (δ 105.23), C-4/C-5, and C-4a (δ 156.38) and between OCH_3 with C-1/C-8. The later correlation indicated that the two methoxy groups should be placed at C-1 and C-8. The long-range correlations from the HMBC spectrum were illustrated in Figure 22 and summarized in Table 25. Based upon these spectral data, the compound was identified as 1,8-dimethoxynaphthalene **[18]** which was previously isolated from *Nodulisporium* sp. (Dai *et al*., 2006).

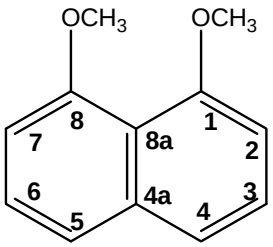

1,8-dimethoxynaphthalene **[17]**

Table 25 NMR Spectral data of 1,8-dimethoxynaphthalene (in $CDCl_3$, 500 MHz)

Position	δ_H (ppm), *J* (Hz)	δ_C (ppm)	^1H-^1H COSY	HMBC correlation ^1H to ^{13}C
1		156.10		
2	6.78 (1H, *dd, J* = 8.2, 1.3)	105.23	3, 4	1, 4, 8a
3	7.28 (1H, t, J = 8.2)	125.32		1, 2, 4, 4a
4	7.32 (1H, *dd, J* = 8.2, 1.3)	119.83	3, 2	2, 4a, 8a
5	7.32 (1H, *dd, J* = 8.2, 1.3)	119.83	6, 7	7, 4a, 8a
6	7.28 (1H, t, J = 8.2)	125.32		8, 7, 5, 4a
7	6.78 (1H, *dd, J* = 8.2, 1.3)	105.23	6, 5	8, 5, 8a
8		156.10		
4a		156.38		
8a		116.63		
1 OCH_3	3.78	55.44		1
8 OCH_3	3.78	55.44		8

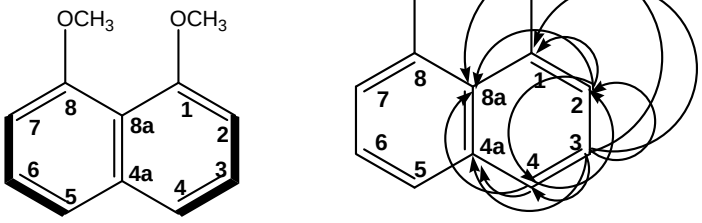

Figure 22 ^1H-^1H COSY (bold line) and key HMBC (arrow) correlations for 1,8-dimethoxynaphthalene

4.3.7 Structure determination of 1,8-dihydroxynaphthalene

The compound was obtained as colorless needles from fraction ACC015 in 0.18 % w/w yield of the MeOH extract (Scheme 11). Its low-resolution ESI-TOF MS (Figure 97) showed the pseudomolecular ion peak $[M+H]^+$ at *m/z* 161. The ^{1}H-NMR (Figures 98-99) and 125 MHz ^{13}C-NMR (Figure 100) spectra of compound ACC015 in $CDCl_3$ closely resembled those of AC002 with characteristic of 1,2,3-trisubstituted benzene ring at δ_H 6.78 (2H, *dd, J* = 8.2,0.9 Hz, H-2/H-7) / δ_C 109.35 (C-2/C-7); δ_H 7.28 (2H, *t, J* = 8.2 Hz, H-3/H-6) / δ_C126.68 (C-3/C-6); δ_H 7.36 (2H, dd, J = 8.2,0.8 Hz, H-4/H-5) / δ_C 120.46 (C-4/C-5), δ_C152.76 (C-1/C-8), δ_C 114.52 (C-8a), and δ_C 137.01 (C-4a). The main difference was the absence of the methoxyl groups and the presence hydroxyl proton at δ_H 7.63. The proton singlet at δ 7.63 was readily assigned to two hydroxy protons at 1-OH/8-OH. The ^{1}H and ^{13}C NMR data accounted for only a part of the carbon and hydrogen compositions given by the molecular formula. This observation demonstrated that the compound was a highly symmetrical structure. Analysis of its ^{1}H-^{1}H COSY (Figure 101) spectrum recorded in $CDCl_3$ established the connectivity from H-3/H-6 to H-4/H-5 to H-2/H-7. The ^{1}H-NMR and ^{13}C-NMR data of the compound (Table 26) were completely assigned from the HSQC spectrum (Figure 102) and the HMBC spectrum (Figure 103-105) showing long-range correlations between H-2/H-7 with C-1/C-8 (δ 156.10), C-4/C-5 and C-8a; between H-3/H-6 with C-1/C-8, C-2/C-7, C-4/C-5, and C-4a; between H-4/H-5 with C-1/C-8, C-2/C-7, C-4a, and C-8a; and between OH with C-1/C-8, C-2/C-7. The later correlation indicated that the two hydroxyl groups should be placed at C-1 and C-8. The long-range correlations from the HMBC spectrum were illustrated in Figure 23 and summarized in Table 26. Based upon these spectral data, the compound was identified as 1,8-dihydroxynaphthalene **[63]** which was previously isolated from *Papulaspora immerse* H. (Gallo *et al*., 2010).

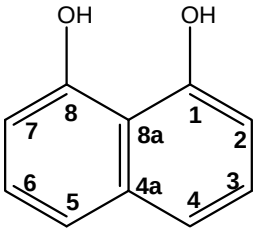

1,8-dihydroxynaphthalene **[63]**

Table 26 NMR Spectral data of 1,8-dihydroxynaphthalene (in $CDCl_3$, 500 MHz)

Position	δ_H (ppm), *J* (Hz)	δ_C (ppm)	^1H-^1H COSY	HMBC correlation ^1H to ^{13}C
1		152.76		
2	6.78 (1H, *dd*, *J* =8.2, 0.9)	109.35	3/6	1, 4, 8a
3	7.28 (1H, *t*, *J* = 8.2)	126.68	4/5,2	1, 2, 4, 4a
4	7.36 (1H, *dd*, *J* = 8.2, 0.9)	120.46	3/6	2, 4a, 8a
5	7.36 (1H, *dd*, *J* = 8.2, 0.9)	120.46	3/6	7, 4a, 8a
6	7.28 (1H, *t*, *J* = 8.2)	126.68	4/5,2	8, 7, 5, 4a
7	6.78 (1H, *dd*, *J* =8.2, 0.9)	109.35	3/6	8, 5, 8a
8		152.76		
4a		137.01		
8a		114.52		
1-OH	7.63			1/8
8-OH	7.63			1/8

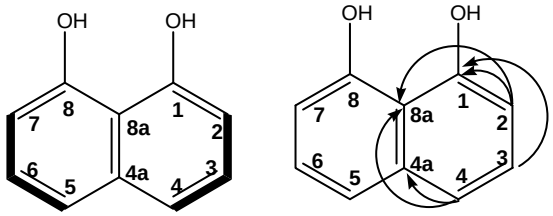

Figure 23 ^1H-^1H COSY (bold line) and key HMBC (arrow) correlations for 1,8-dihydroxynaphthalene

4.4 Structure determination of secondary metabolites isolated from the endophytic fungus *Alternaria alternata* Tche-153

The crude EtOAc extract (1 mg per disk) of the fungal endophyte *A. alternata* Tche-153 primarily exhibited ketoconazole-synergistic activity against *C. albicans* with an inhibition zone diameter of 23.59 mm. The extract was further purified by bioassay-guided fractionation using a chromatographic combination of Sephadex LH-20 and silica gel columns to afford four compounds. Extensive analyses of NMR spectral data (^{1}H and ^{13}C; 2D ^{1}H-^{1}H COSY, HMQC, and HMBC) and mass spectral data in combination with literature data comparison, led to the identification of four isolated compounds as three salicylic acid derivatives altenusin, isoochracinic acid and altenuic acid and a chromone derivative, 2,5-dimethyl-7-hydroxychromone, respectively.

4.4.1 Structure determination of altenusin

The compound was obtained as reddish prisms from fraction TS052 of the EtOAc extract (0.1% w/w yield) (Scheme 16). The low-resolution EIMS spectrum (Figure 106) showed the molecular ion peak $[M]^{+\bullet}$ at *m/z* 290. The ^{13}C-NMR spectrum (Table 27 and Figure 109) displayed fifteen carbon signals of two methyl carbons at δ 19.50 and 56.00, four aromatic methine carbon signals at δ 101.00, 111.00, 117.00 and 118.00, nine quaternary aromatic carbon signals at δ 107.00, 127.50, 135.50, 143.00, 145.00, 148.00, 165.00, 166.00 and 175.00 ppm. The low-field signal at δ 175.00 can be assigned to the carbon atom of a carboxyl group. This was further confirmed by the presence of a fragment ion at *m/z* 244 $[M\text{-}CO_2\text{-}H]^{+}$in the positive EI-MS. Therefore, the molecular formula $C_{15}H_{14}O_6$ was proposed based on these mass spectral and ^{13}C-NMR data. The ^{1}H-NMR spectrum (Table 27 and Figures 107-108) displayed six signals at δ 1.90 (3H, *s,* H_3-2'), 3.80 (3H, *s*, 5-OCH_3), 6.11 (1H, *d*, *J* = 3.0 Hz, H-6), 6.37 (1H, *d*, *J* = 2.7 Hz H-4*)*, 6.43 (1H*, s*, H-6'), 6.52 (1H, *s*, H-3'), aromatic methine proton at δ 6.11 (1H, *d*, *J* = 2.7 Hz, H-6) *meta*-coupled to another aromatic proton at δ 6.37 (1H, *d*, *J* = 3.0 Hz H-4*)*. Two aromatic singlets at δ 6.52 and 6.43 were assigned to H-6' and H-3', respectively. A methoxy signal was seen at δ 3.80 and an aromatic methyl at δ 1.90. The ^{1}H-NMR and ^{13}C-NMR data of the compound were completely assigned from the

HMQC spectrum (Figure 110) and the HMBC spectrum (Figures 111-114) showing the long-range correlations between H-4 with C-2 (δ 107.00), C-3 (δ 166.0), C-5 (δ 165.0) and C-6 (δ 111.0); between H-6 with C-2, C-4, (δ 101.0), between 5-OCH_3 with C-5, respectively, thereby establishing the structure of one aromatic ring. Furthermore, from the correlations of the aromatic methyl group 2'-CH_3 with C-1' (δ 135.5), C-3' (δ 118.0) and C-2' (δ 127.5), between H-6' with C-4' (δ 145.0) and C-2' and between H-3' with C-1' and C-5' (δ 143.0), respectively, the structure of the second aromatic ring was deduced. The correlation of H-6 with C-1' and H-6' with C-1 (δ 148.0), established the C1-C1' bond between both rings. The long-range correlations from the HMBC spectrum were shown in Figure 24 and summarized in Table 29. Based upon these spectral data, the compound was identified as a salicylic acid derivative altenusin (3,4',5'-trihydroxy-5-methoxy-2'-methyl[1,1'-biphenyl]-2-carboxylic acid) **[43]** which was previously isolated from *Alternaria* sp. (Aly *et al*., 2008 a; Cota *et al*., 2008); *Penicillium* (Nakanishi *et al*., 1995).

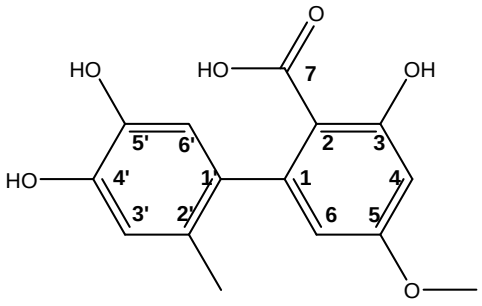

Altenusin [43]

Table 27 NMR spectral data of altenusin in (CD_3OD, 500 MHz)

Position	δ_H (ppm), *J* (Hz)	δ_C (ppm)	HMBC correlation ^1H to ^{13}C
1		148.00	
2		107.00	
3		165.90	
4	6.37 (1H, *d*, *J* = 2.7)	101.00	2, 3, 5, 6
5		165.00	
6	6.11 (1H, *d*, *J* = 2.7)	111.00	2, 4, 1'
7		175.00	
1'		135.50	
2'		127.5	
3'	6.52 (1H, *s*)	118.00	1', 5'
4'		145.00	
5'		143.00	
6'	6.43 (1H, *s*)	117.00	1, 2', 4'
2'-CH_3	1.90 (3H, *s*)	19.50	1', 2',3'
5-OCH_3	3.80 (3H, *s*)	56.00	5

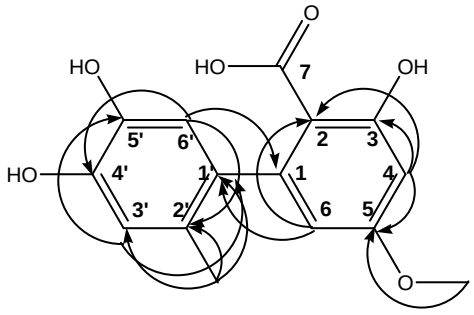

Figure 24 Key HMBC correlations (arrow) for altenusin **[43]**

4.4.2 Structure determination of isoochracinic acid

The compound was obtained as a colorless solid from fraction TS017 of the EtOAc extract (in 0.07% w/w yield) (Scheme 14). The low-resolution ESI-TOF MS (Figure 115) showed the pseudomolecular ion peak $[M+Na]^+$ at *m/z* 231. The ^{13}C-NMR

spectrum (Table 28 and Figure 118) displayed ten carbon signals which were classified by DEPT 135 (Figure 119) as one methylene carbon at δ 40.23; four methine carbon signals at δ 78.67, 113.92, 117.02 and 137.74; and five quaternary carbon signals at δ 112.56, 152.47, 158.31, 171.31 and 172.87. The low-field signals at δ = 171.31 and 172.87 were assigned to the carbonyl carbons of a lactone group (C-7) and a carboxyl group (C-3') respectively. The low-field signal at δ 78.67 was assigned to an oxygenated carbon atom (C-1'). Therefore, the molecular formula $C_{10}H_8O_5$ having seven degrees of unsaturation, was proposed based on these mass spectra and ^{13}C-NMR data. The ^{1}H-NMR spectrum (Table 28 and Figures 116-117) displayed a typical characteristic of a 1,2,3-trisubstituted aromatic ring by the signals at δ 6.85 (1H, *dd*, *J* = 8.1, 0.6 Hz, H-4), 7.02 (1H,*dd, J* = 7.7, 0.6 Hz, H-6) and 7.52 (1H, *dd*, *J* = 8.1, 7.7 Hz, H-5). The ABX system of the aliphatic protons was observed at δ 2.75 (1H, *dd, J* = 16.7, 7.9 Hz, H-2'a); 3.00 (1H, *dd J* = 16.7, 4.9 Hz, H-2'b) and 5.77 (1H, *dd*, *J* = 7.9, 4.9 Hz, H-1'), Analysis of the ^{1}H-^{1}H COSY spectrum (Figure 120) confirmed the connectivity from H-1' to H-2'a and H-2'b, and H-6 to H-5 and H-4 as shown in Figure 24. The ^{1}H-NMR and ^{13}C-NMR data were completely assigned from the HMQC spectrum (Figure 121) and the HMBC spectrum (Figure 122) showing the long-range correlations in the aromatic ring between H-6 with C-1 (δ 152.47), C-5 (δ 137.74), C-4 (δ 117.02), and C-2 (δ 112.56); H-5 with C-1, C-4, and C-3 (δ 158.31); and H-4 with C-6 (δ 113.96), C-3, and C-2. Moreover, the HMBC correlations between H-1' with C-7 (δ 171.36), C-1 and H-2' with C-1' (δ 78.87), C-1 and C-3' (δ 172.87) indicated the attachment of a γ-lactone ring to the aromatic ring, and the carboxylic moiety to C-2', respectively. The long-range correlations from the HMBC spectrum were shown in Figure 25 and summarized in Table 28. Based upon these spectral data, compound TS017 was identified as a salicylic derivative isoochracinic acid **[54]** which was previously isolated from *Alternaria kikuchiana* and *Mycosphaerella fijiensis* (Kameda and Namiki, 1947; Stierle *et al*.,1991).

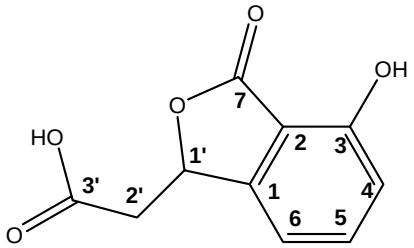

isoochracinic acid [54]

Table 28 NMR Spectral data of isoochracinic acid (CD_3OD, 500 MHz)

Position	δ_H (ppm),*J*(Hz)	δ_C (ppm)	^1H-^1H COSY	HMBC correlation ^1H to ^{13}C
1		152.47		
2		112.56		
3		158.31		
4	6.85 (1H, *dd*, *J* = 8.1, 0.6)	117.02	5	2, 3, 6
5	7.52 (1H, *dd*, *J* = 8.1, 7.7)	137.74	4, 6	1, 3, 4
6	7.02 (1H, *d*d, *J* = 7.7, 0.6)	113.96	5	1, 2, 4, 5
7		171.36		
1'	5.77 (1H, *dd*, *J* = 7.9, 4.9)	78.87	2'a, 2'b	1, 7
2'	a) 2.75 (1H, *dd*,, *J* = 16.7, 7.9)	40.23	1'	1, 1', 3'
	b) 3.00 (1H, *dd*, *J* =16.7, 4.9)		1'	1, 1', 3'
3'-COOH		172.87		

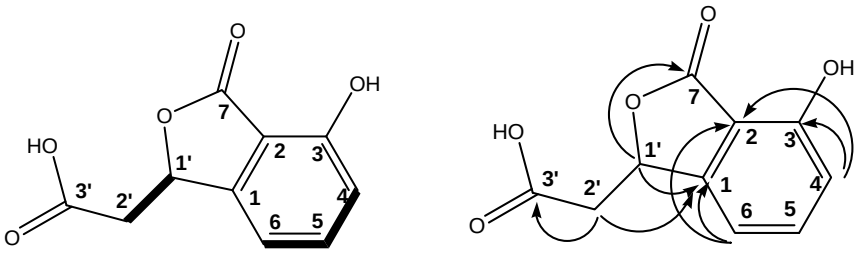

Figure 25 ^1H-^1H COSY (bold line) and key HMBC correlations (arrow) for isoochracinic acid.

4.4.3 Structure determination of 1'R*,4'S*-altenuic acid

The compound was obtained as colorless needles from fractions TS018-TS020 of the EtOAc extract (0.33 % w/w yield) (Scheme 14). The high resolution ESI-TOF-MS spectrum (Figure 123) showed the pseudomolecular ion peak $[M+Na]^+$ at *m/z* 345.0588 $[M+Na]^+$ (calcd. for $C_{15}H_{14}O_8Na$, 345.0581). The UV spectrum (Figure 125) showed bands at 219, 258 and 295 nm while the IR spectrum (Figure 124) displayed bands at 3441 (broad), 1737, and 1619 cm^{-1} characteristic for carboxylic hydroxy group and carbonyl groups, respectively. The ^{1}H-NMR spectrum (Table 29 and Figures 126-127) displayed two meta-coupled aromatic protons δ 6.45 (1H, *d* ,*J* = 2.0 Hz, H-4) and 6.78 (1H, *d, J* = 2.0 Hz, H-6) indicating a tetra-substituted aromatic ring, methyl protons at δ 1.69 (3H, *s*, H_3-7'), methoxy protons at δ 3.80 (3H, *s*, 5-OCH_3), two pairs of methylenes proton at δ 2.50 (1H, *d*, *J* =16.0 Hz, H-5'a), 2.76 (1H, *d*, *J* = 16.0 Hz, H-5'b) and 2.95 (1H, *d, J* =18.0 Hz, H-2'a), 3.79 (1H, *d*, *J* =18.0 Hz, H-2'b); and one hydroxyl proton at δ 10.97. The ^{13}C-NMR spectrum (Table 29 and Figure 128) displayed fifteen carbon signals which were classified by DEPT 135 (Figure 129) as one methyl carbon at δ 21.86 (H_3-7') and one methyoxyl carbon at δ 56.02 (5-OCH_3); two methylene carbons at δ 39.0 (H_2-5') and 40.6 (H_2-2'); two oxygenated quaternary carbons at δ 88.07 (C-4'), 88.79 (C-1'); two aromatic methine carbons at δ 101.10 (C-6) and 102.15 (C-4); two aromatic quaternary carbons at δ 105.15 (C-2) and 149.23 (C-1); two oxygenated aromatic quaternary carbons at δ 158.17 (C-3) and 165.26 (C-5); and carbonyl carbons at δ 165.75, 169.95 and 172.25. The ^{1}H-NMR and ^{13}C-NMR data of the compound were completely assigned from the HMQC spectrum (Figure 130) and the HMBC spectrum (Figures 131-134) showing the long-range correlations between H-4 with C-2, C-3, C-5, and C-6 as well as H-6 with C-2, C-4, and C-5, the aromatic hydroxyl group to C-2, C-3, and C-4, the methoxyl proton with C-5, thereby establishing the structure of the tetrasubstituted aromatic ring. Furthermore, HMBC correlations between the nonequivalent methylene protons H_2-2' with C-1', C-3', and C-4' together with the nonequivalent methylene protons H_2-5' with C-1', C-4', and C-6' and 7'-CH_3 with C-1', C-

4', and C-5' were observed. Based upon these spectral data, three structures (**A**, **B**, and **C**) were possible as shown below.

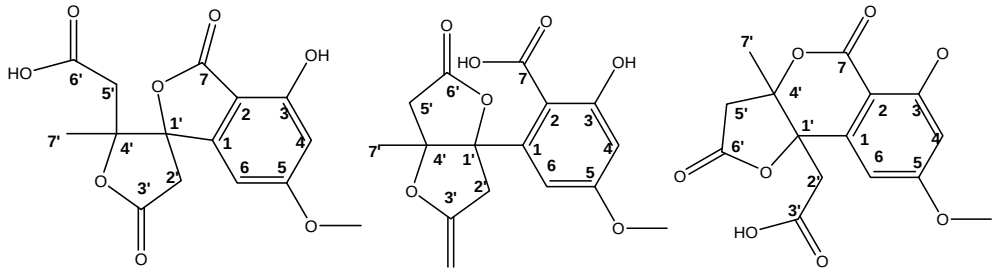

A B C

Table 29 NMR Spectral data of altenuic acid in (DMSO-d_6, 500 MHz)

Position	δ_H (ppm),J(Hz)	δ_C (ppm)	^{1}H-^{1}H COSY	HMBC correlation ^{1}H to ^{13}C
1		149.23		
2		105.15		
3		158.17		
4	6.45 (1H, *d*, J = 2.0)	102.15	6	2, 6, 5, 3
5		165.75		
6	6.78 (1H, *d*, J = 2.0)	101.10	4	2, 5, 4, 1'
7		165.26		
5-OCH_3	3.80 (3H, *s*)	56.02		5
1'		88.79		
2'	a 2.95 (1H, *d*, J = 18.0)	40.6	2'b	1', 3', 4'
	b 3.79 (1H, *d*, J = 18.0)		2'a	1, 3'
3'		172.25		
4'		88.07		
5'	a 2.50 (1H, *d*, J = 16.0)	39.0	5'b	4', 6', 7'
	b 2.76 (1H, *d*, J = 16.0)		5'a	1', 4', 6'
6'-COOH		169.95		
7'	1.69 (3H, *s*)	21.86		1', 4', 5'
3-OH	10.97 (OH)			2, 3, 4

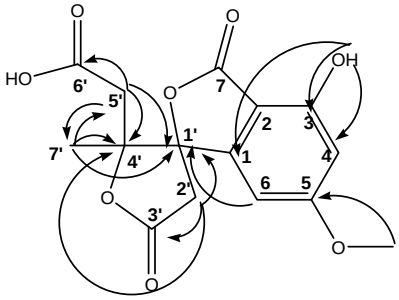

Figure 26 Key HMBC correlations (arrow) for altenuic acid

Chemical structure of the compound could not be assembled by analysis of NMR data, therefore a single crystal of the compound was prepared for X-ray crystallographic analysis. The compound crystallized in the Monoclinic space group C2/C unit cell dimensions: a = 27.606 (7) Å, b = 6.2710 (14) Å, c = 18.701 (6) Å, alpha = 90.00 , beta = 114.98 (2), gamma = 90.00, volume = 2934.6 (14) $Å^3$. The structure and the relative configuration were finally solved by X-ray crystallographic analysis, and molecular packing as shown in Figure 26. The compound was identified as 1'R*,4'S*-altenuic acid **[53]**. Altenuic acids were previously obtained as a mixture of altenuic acids I, II, and III form (Rosett *et al.*, 1957), Altenuic acid II was later identified as 1'S,4'S-altenuic acid (Williams & Thomas, 1973).

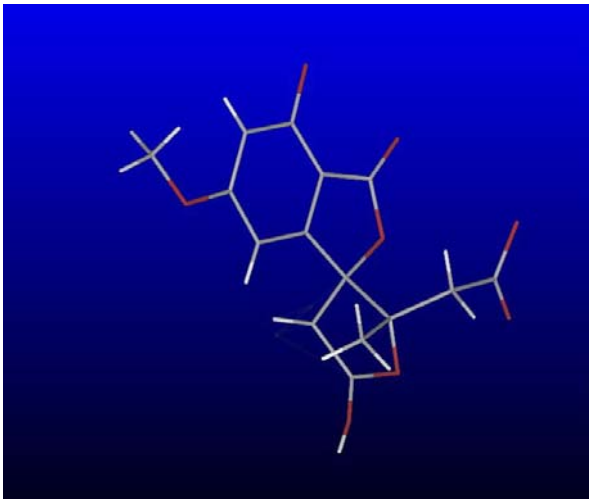

Figure 27 X-ray crystal structure of altenuic acid; Molecular packing

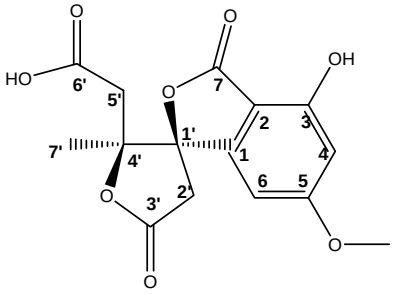

1'*S*,4'*S* Altenuic acid

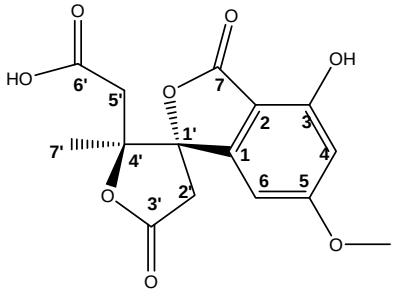

1'*R**,4'*S** Altenuic acid

4.4.4 Structure determination of 2,5-dimethyl-7-hydroxychromone

The compound was obtained as colorless needles from fraction TS041 of the EtOAc extract (0.03% w/w yield) (Scheme 15). The low-resolution ESI-TOF MS (Figure 135) showed the pseudomolecular ion peak $[M+H]^+$ at *m/z* 191. The ^{1}H-NMR spectrum (Table 30 and Figures 136-138) displayed two meta-coupled aromatic δ 6.62 (1H, *dd*, *J* = 2.6,1.0 Hz*,* H-6*)*, 6.64 (1H*, d*, *J* = 2.6 Hz, H-8) indicating a tetra-substituted aromatic ring, two aromatic methyl protons were observed at δ 2.32 (3H, *d*, *J* = 0.7 Hz, 2-CH_3) and 2.72 (3H, *s*, 5-CH_3), and the upfield chemical shift of the vinyl proton at δ 5.98 (1H, *d*, *J* = 0.7 Hz, H-3), indicated it to reside at C-3. The ^{13}C-NMR spectrum (Table 30 and Figure 139) displayed eleven carbon signals which were classified by DEPT 135 (Figure 140) as two methyl carbons at δ 19.80 (2-CH_3) and 23.07 (5-CH_3); three methine carbons at δ 101.67 (C-8), 111.41 (C-3), and 118.02 (C-6); four quaternary aromatic carbons at δ 115.62 (C-4a), 143.65 (C-5), 161.48 (C-8a), 163.13 (C-7), and two low-field quaternary carbons at δ = 166.62 (C-2), and 182.05 (C-4), can be assigned to the β and carbonyl ketone carbon atom of an α,β-unsaturated carbonyl substructure. Therefore, the molecular formula $C_{11}H_{10}O_3$ was proposed based on these mass and ^{13}C-NMR data. The ^{1}H-NMR and ^{13}C-NMR data of compound TS041 were completely assigned from the HMQC spectrum (Figure 141) and the HMBC spectrum (Figure 142-143) showing the long-range correlations between 5-CH_3 with C-4a (δ 115.62), C-5 (δ 143.68), and C-6 (δ 118.02); between H-8 with C-6 (δ 118.02) and C-7 (δ 163.13); between H-6 with C-4a (δ 115.62) and C-8 (δ 101.67) and between 2-CH_3 with C-2 (δ 166.62) and C-3 (δ 111.14), respectively. The long-range correlations from the HMBC spectrum of TS041 were

shown in Figure 28 and summarized in Table 30. Based on the spectral data, the compound was identified as 2,5-dimethyl-7-hydroxy-chromone **[50]** which was previously isolated from *Alternaria* sp. (Aly *et al.* 2008 a).

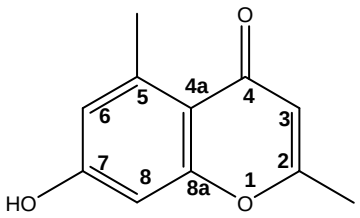

2,5-Dimethyl-7-hydroxychromone **[50]**

Table 30 NMR Spectral data of 2,5-dimethyl-7-hydroxychromone (CD_3OD, 500 MHz)

Position	δ_H (ppm), *J* (Hz)	δ_C (ppm)	HMBC correlation ^1H to ^{13}C
2		166.62	
3	5.98 (1H, *d*, *J* = 0.7)	111.41	2, 4a, 2-CH_3
4		182.05	
4a		115.62	
5		143.65	
6	6.62 (1H, *dd*, *J* = 2.6,1.0)	118.02	4a, 8, 5-CH_3
7		163.13	
8	6.64 (1H, *d*, *J* = 2.6)	101.67	6, 7, 4a,8a
8a		161.48	
2-CH_3	2.32 (3H, *d*, *J* = 0.7)	19.80	2, 3
5-CH_3	2.72 (3H, *s*)	23.07	4a, 5, 6

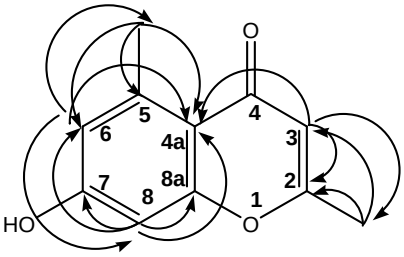

Figure 28 Key HMBC correlations (arrow) for 2,5-dimethyl-7-hydroxychromone **[50]**

4.5 Anti-*C. albicans* activity of 1,8-dihydroxynaphthalene and 1'-(2,6-dihydroxyphenyl) butanone

By disk diffusion assay 1,8-dihydroxynaphthalene **[63]** and 1'-(2,6-dihydroxy phenyl)butanone **[20]** at the amount of 256 µg/disk exhibited activity against *C. albicans* with inhibition zone diameter of 14.99±0.38 and 25.68±0.02 mm, respectively. In the presence of a subinhibitory concentration of ketoconazole at 0.125 µg/ml, 1,8-dihydroxynaphthalene and 1'-(2,6-dihydroxyphenyl)butanone produced clear inhibition zone diameter of 29.50±0.07 and 36.55±0.03 mm, respectively, as shown in Fig. 29 while the other isolated metabolites [**18,62**] at the same concentration were completely inactive. This suggested that 1,8-dihydroxynaphthalene; 1'-(2,6-dihydroxyphenyl) butanone and azole drug combination might be synergistic against *C. albicans*. Therefore, the chequerboard technique was used to analyze the interaction of 1,8-dihydroxynaphthalene; 1'-(2,6-dihydroxyphenyl)butanone and representative azole drugs, including fluconazole. As shown in Table 31, 1,8-dihydroxynaphthalene; 1'-(2,6-dihydroxyphenyl)butanone and showed strong synergistic activity with fluconazole against *C. albicans* with the FIC index ranging from 0.25-0.375. MICs of fluconazole and 1,8-dihydroxynaphthalene were >64 and 256 µg/ml when used alone and were dramatically reduced to 8 and 32 µg/ml when used in combination, respectively. MICs of fluconazole and 1'-(2,6-dihydroxyphenyl)butanone were >64 and 128 µg/ml when used alone and were dramatically reduced to 8 and 3 µg/ml when used in combination, respectively.

Table 31 MICs (μg/ml) of AC019 (1'-(2,6-dihydroxyphenyl)butanone **[20]**), ACC015 (1,8-dihydroxynaphthalene **[63]**) and fluconazole (FCZ) by chequerboard assay indicating synergistic activity against *C. albicans*

Compound code	*Candida albicans* ATCC 90028				
	Without FCZ	With FCZ	FCZ alone	FCZ in combination	FIC Index**
AC019	128	3	>64	8	0.375
ACC015	256	32	>64	8	0.25

***** MIC producing optically clear inhibition

****** FIC index is Fractional Inhibitory Concentration index defined as the sum of the MIC of each drug when used in combination divided by the MIC of the drug when used alone. Synergism, indifference and antagonism were defined as FIC indices of ≤0.5, >0.5 - 4 and >4, respectively (Odds, 2003).

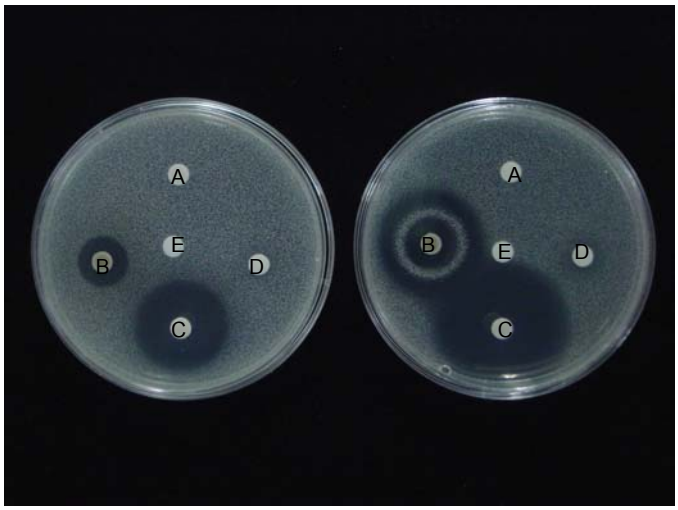

Figure 29 Disk diffusion assay determining synergistic activity with ketoconazole against *C. albicans* of the isolated secondary metabolites (256 μg per disk, each) from *Nodulisporium* sp. Aann-134: the left SDA plate without ketoconazole, the right SDA plate with a subinhibitory concentration of ketoconazole (0.125 μg/ml), A = 1,8-dimethoxy naphthalene [**18**], B = 1,8-dihydroxynaphthalene [**63**], C = 1'-(2,6-dihydroxyphenyl)butanone [**20**], D = nulisporin G **[62]** and E = dimethylsulfoxide (control).

4.6 Anti-*C. albicans* activity of altenusin [43]

By disk diffusion assay altenusin [**43**] at the amount of 256 µg/disk exhibited activity against *C. albicans* with unclear inhibition zone diameter of 8.34±0.03 mm. In the presence of a subinhibitory concentration of ketoconazole at 0.125 µg/ml, altenusin produced clear inhibition zone diameter of 19.18±1.23 mm, as shown in Fig. 30 while the other isolated metabolites [**50, 53 and 54**] at the same concentration were completely inactive. This suggested that altenusin and azole drug combination might be synergistic against *C. albicans*. Therefore, the chequerboard technique was used to analyze the interaction of altenusin and three representative azole drugs, including ketoconazole, fluconazole and itraconazole. As shown in Table 32, altenusin showed strong synergistic activity with all three selected azole drugs against *C. albicans* with the FIC index ranging from 0.078-0.188. Among three azole drugs, combination of altenusin with ketoconazole showed the highest synergistic activity with FIC index 0.078. MIC-0s of ketoconazole and altenusin were 16 and 256 µg/ml when used alone and were dramatically reduced to 0.25 and 16 µg/ml when used in combination, respectively. The synergistic activity determined by the chequerboard technique confirmed the result of the preliminary disk diffusion assay. The correspondence of results obtained from the two methods found in this study was in agreement with the previous study of Curvularide B (Chomcheon *et al*, 2010). These results demonstrated that the simple disk diffusion assay using culture medium containing subinhibitory concentration of drug could be used as a preliminary method to screen on a large number of test compounds for synergistic activity against *C. albicans*.

Table 32 MICs (μg/ml) of altenusin and selected azole drugs by chequerboard assay indicating synergistic activity against *C. albicans*

	Azole drug alone			MIC-0 of each compound in combination		
Azole drugs	MIC-2[a]	MIC-0[b]		Azole drugs	Altenusin **[43]**[c]*	FIC index
Ketoconazole	0.25	16		0.25	16	0.078
Fluconazole	2	>64		1	32	0.141
Itraconazole	2	>64		4	32	0.188

[a]MIC-2 is defined as the minimum inhibitory concentration that causes a prominent decrease in turbidity as compared with the growth control.

[b]MIC-0 is defined as the minimum inhibitory concentration that gives rise to no visible growth.

[c]MIC-0 of altenusin alone was 256 μg/ml.

Figure 30 Disk diffusion assay determining synergistic activity with ketoconazole against *C. albicans* of the isolated secondary metabolites (256 μg per disk, each) from *A. alternata* Tche-153: the left SDA plate without ketoconazole, the right SDA plate with a subinhibitory concentration of ketoconazole (0.125 μg/ml), A = altenuic acid [**53**], B = 2,5 dimethyl-7-hydroxychromone [**50**], C = altenusin [**43**], and D = dimethylsulfoxide (control).

CHAPTER V

CONCLUSION

The endophytic fungus, *Nodulisporium* sp., isolated from leaf of *Artemisia annua* L. The extract was further purified by bioassay-guided fractionation using a chromatographic combination of silica gel columns and Sephadex LH-20 to afford one new compound, nodulisporin G **[62]** (13 mg), and six known compounds, 1'-(2,6-dihydroxy phenyl)butanone **[20]** (9 mg), 1'-(2,6-dihydroxyphenyl)-3'-hydroxybutanone **[19]** (3.7 mg), 1'-(2,6-dihydroxyphenyl)ethanone **[60]** (4.6 mg), phenylacetic acid **[61]**. (4.3 mg), 1,8-dimethoxy naphthalene **[18]** (6.6 mg), and 1,8-dihydroxynaphthalene **[63]**, (5.3 mg), Their structures were elucidated by spectroscopic methods and comparison with literature data of naphthalene and resorcinol derivatives. Resocinol derivative 1'-(2,6-dihydroxyphenyl)butanone **[20]** and naphthalene derivative 1,8-dihydroxy naphthalene **[63]** can be exhibiting synergistic activity with fluconazole against *Candida albicans* with MICs 8 µg/ml and fractional inhibitory concentration indices 0.375 and 0.250, respectively while the related resocinol derivatives **[62, 19** and **60]**, naphthalene derivative **[18]**, and phenylacetic acid **[61]** were completely inactive.

The endophytic fungus, *Alternaria alternata* isolated from leaf of *Terminalia chebula* Retz. The extract was further purified by bioassay-guided fractionation using a chromatographic combination of silica gel columns and Sephadex LH-20 to afford four known compounds, altenusin **[43]** (10 mg), isoochracinic acid **[54]** (6.5 mg), and altenuic acid **[53]** (33 mg), together with a chromone, 2,5-dimethyl-7-hydroxychromone **[50]** (3.1 mg). Their structures were elucidated by spectroscopic methods and comparison with literature data of salicylic acid and chromone derivatives. The fractionation of the culture broth from the tropical endophytic fungus *A. alternata* provided altenusin **[43]** showing significant synergistic activity with fluconazole against *C. albicans* in low concentrations with the fractional inhibitory concentration indices 0.141 while the related salicylic derivatives **[53** and **54]** were completely inactive. The biphenyl basic skeleton of altenusin **[43]** containing a salicylic moiety and a catechol moiety might be speculated as an important part for its bioactivity. As this is the first discovery that

(13 mg), a biphenyl salicylic acid derivative exhibited significant synergistic activity with azole drugs against *C. albicans*, altenusin **[43]** may serve as a potential lead candidate of the drug discovery program for more potent azole-synergistic drugs to effectively combat the widespread Candidiasis.

This discovery of endophytic fungal metabolites with potent azole-synergistic activity is of significance for the development of analogs with different simple chemical skeletons that could serve as new effective azole-synergists to treat the invasive candidiasis.

REFERENCES

Aly, A. H., *et al*. 2008a. Cytotoxic metabolites from the fungal endophyte *Alternaria* sp. and their subsequent detection in its host plant *Polygonum senegalense*. J. Nat. Prod. 71: 972–980.

Ambera, K., Aijaza, A., Immaculatab, X., Luqmana, K. A., and Nikhata, M. 2010. Anticandidal effect of Ocimum sanctum essential oil and its synergy with fluconazole and ketoconazole. Phytomedicine 17: 921–925.

Appendino, G., *et al*. 2005. Cytotoxic Germacrane Sesquiterpenes from the Aerial Parts of *Santolina insularis*. J. Nat. Prod. 68: 853-857.

Bunyapraphatsara, N., and Chokechaijaroenporn, O. 2000. Thai Medicinal Plants. Vol 1 and 4. Faculty of Pharmacy, Mahidol University and National Center for Genetic Engineering and Biotechnology, Bangkok. Public limited company.

Chomcheon, P.,*et al*. 2010. Curvularides A–E: antifungal hybrid peptide–polyketides from the endophytic fungus *Curvularia geniculata*. Chem. Eur. J. 16: 11178–11185.

Cota, B. B., *et al*. 2008. Altenusin, a biphenyl isolated from the endophytic fungus *Alternaria* sp., inhibits trypanothione reductase from *Trypanosoma cruzi*. FEMS Microbiol. Lett. 285: 177–182.

Dai, J., Krohn, K., Draeger, S., And Schulz, B. 2009. New naphthalene-chroman coupling products from the endophytic fungus, *Nodulisporium* sp. from *Erica arborea*. Eur J. Org. Chem. 2009: 1564–1569.

Dai, J., *et al*. 2006. Metabolites from the Endophytic Fungus *Nodulisporium* sp. From *Juniperus cedre*. Eur. J. Org. Chem. 15: 3498–3506.

Eilenberg, H., *et al*. 2010. Induced production of antifungal naphthoquinones in the pitchers of the carnivorous plant *Nepenthes khasiana*. J. Exp. Bot. 61(3): 911–922.

Ellis, M. B. 1993. Dematiaceous Hyphomycetes. CAB International, Oxon: 464–466.

Eyberger, A. L., Dondapati, R., and Porter, J. R., 2006. Endophyte fungal isolates from *Podophyllum peltatum* produce podophyllotoxin. J. Nat. Prod. 69: 1121–1124.

Farr, D. F., Bills, G. F., Chamuris, G. P., and Rossman, A. Y.1989. Fungi on Plant and Plant Products in the United States. St Paul: American Phytopathological Society Press.

Feser, GE. ME., Raulli, R. E., and Cihlar, R. L. 1998. Synergy of Nitric Oxide and Azoles against *Candida* Species In Vitro. Antimicrob. Agents Chemother. 42(9): 2342–2346.

Gallo, M. B. C., *et al*. 2010. Chemical Constituents of *Papulaspora immersa*, an Endophyte from *Smallanthus sonchifolius* (Asteraceae), and Their Cytotoxic Activity. Chem. Biodivers. 7(12): 2941–2950.

Gangadevi, V. and J. Muthumary. 2007. Preliminary studies on cytotoxic effect of fungal taxol on cancer cell lines. Afr. J. Biotechnol. 6(12): 1382-86.

Gangadevi, V., and Muthumary, J. 2008. Isolation of *Colletotrichum gloeosporioides,* a novel endophytic taxolproducing fungus from the leaves of a medicinal plant, *Justicia gendarussa.* Mycologia Balcanica 5: 1– 4.

Ghannoum, M. A. 1997. Future of antimycotic therapy. Dermatol. Ther. 3: 104–111.

Ghannoum, M. A., *et al*. 1995. In vitro determination of optimal antifungal combinations against *Cryptococcus neoformans* and *Candida albicans.* Antimicrob. Agents Chemother. 39(11): 2459–2465.

Gligorov, J., *et al*. 2011. Prevalence and treatment management of oropharyngeal candidiasis in cancer patients: results of the French candidoscope study. Int. J. Radiat. Oncol. Biol. Phys. 80: 532-539.

Greenspan, D. 1994. Treatment of oral candidiasis in HIV infection. Oral Surg. Oral Med. Oral Pathol. 78: 211-5.

Gunatilaka, A. A. L. 2006. Natural products from plant-associated microorganisms: Distribution, structural diversity, bioactivity and implication of their occurence. J. Nat. Prod. 69 : 509-526.

Guo, N., *et al*. 2009. In vitro and in vivo interactions between fluconazole and allicin against clinical isolates of fluconazole resistant *Candida albicans* determined by alternative methods. FEMS Immunol. Med. Mic. 58: 193–201.

Guo, Q., Sun, S., Yu, J., Li, Y., and Cao, L. 2008. Synergistic activity of azoles with amiodarone against clinically resistant *Candida albicans* tested by chequerboard and time–kill methods. J. Med. Microbiol. 57: 457–462.

Gu, W. 2009. Bioactive metabolites from *Alternaria brassicicola* ML-P08, an endophytic fungus residing in *Malus halliana* World J. Microbiol. Biotechnol. 25 (9): 1677-1683.

Hirai, K., Wada, Y., and Watanuki, M. 1990. Altenusin for active oxygen removal and its use in therapy. *Kokai Tokkyo Koho*. Patent written in Japanese. Application: JP 88–151200 19880621.

Kameda, K., and Namiki, M. 1947. New phthalide from a fungus, *Alternaria kikuchiana,* Chem. Lett.: 1491–1942.

Karwa, R., and Wargo, K. A. 2009. Efungumab: a novel agent in the treatment of invasive candidiasis. Ann. Pharmacother. 43: 1818–23.

Kashiwada, Y., Nonaka, G. I., and Nishioka, I. 1984. Studies on rhubarb (Rhei I Rhizome).V. Isolation and characterization of chromone and chromanone derivatives. Chem. Pharm. Bull. **32**(9): 3493-3500.

Kimura, Y., Mizuno, T., Nakajima, H., and Hamasaki, T. 1992. Altechromones A and B, new plant growth regulators produced by the fungus, *Alternaria* sp. Biosci. Biotech. Biochem. 56(10): 1664-1665.

Kriengkauykiat, J., Ito, J. I., and Dadwal, S. S. 2011. Epidemiology and treatment approaches in management of invasive fungal infections. Clin. Epidemiol. 3: 175-191.

Kusari, S., Lamshöft, M., Zühlke, S., and Spiteller, M. 2008. An endophytic fungus from *Hypericum perforatum* that produces hypericin. J. Nat. Prod. 71: 159-162.

Lee, C. K., Lee, P. H., and Kuo, Y. H. 2001. The chemical constituents from the aril of *Cassia fistula* L. J. Chin. Chem. Soc. 48: 1053–1058.

Li, J. Y., Strobel, G. A., Sidhu, R., Hess, W. M., and Ford, E. 1996. Endophytic taxol producing fungi from bald cypress *Taxodium distichum*. Microbiol. **42**(8): 2223-2226.

Lim, C. S. Y., Rosli, R., Seow, H. F., and Chong, P. P. 2011. *Candida* and invasive candidiasis: back to basics. Eur. J. Clin. Microbiol. Infect. Dis.

Liu, L., Liu, S., Chen, X., Guo, L., and Che, Y. 2009. Pestalofones A-E, bioactive cyclo hexanone derivatives from the plant endophytic fungus *Pestalotiopsis fici*. Bioorg. Med. Chem.17(2): 606-13.

Li, Y., *et al*. 2008. *In vitro* interaction between azoles and cyclosporin A against clinical isolates of *Candida albicans* determined by the chequerboard method and time–kill curves. J. Antimicrob. Chemother. 61: 577–585.

Marr, K. A., White, T. C., van Burik, J. A., and Bowden, R. A. 1997. Development of fluconazole resistance in *Candida albicans* causing disseminated infection in a patient undergoing marrow transplantation. Clin. Infect. Dis. 25: 908-910.

Nakanishi, S., *et al*. 1995. Isolation of myosin light-chain kinase inhibitors from microorganisms dehydroaltenusin, altenusin, atrovenetinone, and cyclooctasulfur. Biosci. Biotechnol. Biochem. 59(7): 1333–1335.

Narasimhachar, N., and Ramachandran, S. 1967. A simple bioatuographic technique for identifying biologically active material on thin-layer chromatograms. J. Chromatogr. A 27: 494.

National Committee for Clinical Laboratory Standards. 2002. Reference Method for Broth Dilution Antifungal Susceptibility Testing of Yeasts; Approved Standard M27-A2. 2nd edn. National Committee for Clinical Laboratory Standards.

Nishi, I., Sunada, A., Toyokawa, M., Asari, S., and Iwatani, Y. 2009. In vitro antifungal combination effects of micafungin with fluconazole, voriconazole, amphotericin B, and flucytosine against clinical isolates of *Candida* species. J. Infect. Chemother. 15: 1–5.

Odds, F. C. 2003. Synergy, antagonism, and what the chequerboard puts between them. J. Antimicrob. Chemother. 52: 1.

Oyama, M., *et al*. 2004. Fungal metabolites as potent protein kinase inhibitors: identification of a novel metabolite and novel activities of known metabolites. Lett. Drug. Des. Discov. 1: 24–29.

Patton, L. L., Bonito, A. J., and Shugars, D. A. 2001. A systematic review of the effectiveness of antifungal drugs for the prevention and treatment of oropharyngeal candidiasis in HIV-positive patients. Oral Surg. Oral Med. Oral Pathol. Oral Radiol. Endod. 92: 170-179.

Pfaller, M..A., Boyken, L., Hollis, R. J., Messer, S. A., Tendolkar, S., and Diekema, D. J. 2005. In vitro susceptibilities of clinical isolates of *Candida* species, *Cryptococcus neoformans*, and *Aspergillus* species to itraconazole: global survey of 9,359 isolates tested by clinical and laboratory standards institute broth microdilution methods. J Clin Microbiol. 43: 3807–3810.

Pfaller, M. A., Castanheira, M., Messera, S. A., Moet, G. J., and Jones, R. N. 2010. Variation in *Candida* spp. distribution and antifungal resistance rates among bloodstream infection isolates by patient age: report from the SENTRY Antimicrobial Surveillance Program (2008–2009). Diagn. Microbiol. Infect. Dis. 68: 278-283.

Pfaller, M. A., Moet, G. J., Messer, S. A., Jones, R. N., and Castanheira, M. 2011. Geographic variations in species distribution and ehinocandin and azole antifungal resistance rates among *Candida* bloodstream infection isolates: report from the SENTRY Antimicrobial Surveillance Program (2008 to 2009). J. Clin. Microbiol. 49: 396-399.

Pongcharoen, W., *et al*. 2008. Metabolites from the endophytic fungus *Xylaria* sp. PSU-D14. Phytochemistry. 69: 1900-1902.

Prachya, S., *et al*. 2007. Cytotoxic mycoepoxydiene derivatives from an endophytic fungus *Phomopsis* sp. isolated from *Hydnocarpus anthelminthicus*. Planta. Med. 73: 1418–1420.

Puri, S. C., *et al*. 2006. The endophytic fungus *Trametes hirsuta* as a novel alternative source of podophyllotoxin and related aryl tetralin lignans. J. Biotechnol. 122: 494–510.

Puri, S. C., Verma, V., Amna, T., Qazi, G. N., and Spiteller, M. 2005. An endophytic fungus from *Nothapodytes foetida* that produces camptothecin. J. Nat. Prod. 68: 1717–1719.

Quan, H., *et al*. 2006. Potent *in vitro* synergism of fluconazole and berberine chloride against clinical isolates of *Candida albicans* resistant to fluconazole. Antimicrob. Agents Chemother. 50: 1096–1099.

Rex, J. H., Rinaldi, M. G., and Pfaller, M. A. 1995. Resistance of Candida species to fluconazole. Antimicrob. Agents Chemother. 39: 1–8.

Ricci, M., Blasi, P., Giovagnoli, S., Perioli, L., Vescovi, C., and Ross,i. C. 2004. Leucinostatin-A loaded nanospheres: characterization and *in vivo* toxicity and efficacy evaluation. Int. J. Pharm. 275: 61–72.

Roland, W., Webe, S., Kapp, R., Paululat, T., Mösker, E., and Anke, H. 2007. Anti-*Candida* metabolites from endophytic fungi. Phytochemistry 68: 886–892.

Rosett, T., Sankhala, R. H., Stickings, C. E., Taylor, M. E. U., and Thomas, R. 1957. Studies in the biochemistry of micro-organisms. 103. Metabolites of *Alternaria tenuis* Auct.: Culture filtrate products. Biochem. J. 67(3): 390-400.

Rukayadi, Y., Lee, K., Lee, M. S., Yong, D., and Hwang, J. K. 2009. Synergistic anticandidal activity of xanthorrhizol in combination with ketoconazole or amphotericin B. FEMS. Yeast. Res. 9: 1302–1311.

Sangamwar, A. T., Deshpande, U. D., Pekamwar, S. S., and Vadvalkar, S. M. 2007. Improving decision making for drug candidates: A computational approach for benzthiazoles as antifungal. Indian J. Biotechnol. 6: 389–396.

Sharma, M., Manoharlal, R., Negi, A. S., and Prasad, R. 2010. Synergistic anticandidal activity of pure polyphenol curcumin I in combination with azoles and polyenes generates reactive oxygen species leading to apoptosis. FEMS. Yeast Res. 10: 570–578.

Singh, S. B., *et al*. 2003. Isolation, structure, and HIV-1-integrase inhibitory activity of structurally diverse fungal metabolites. J. Ind. Microbiol .Biotechnol. 30 : 721–731.

Stierle, A., and Stobel, G. 1995. The search for a taxol-producing microorganism among the endophytic fungi of the pacific yew, *Taxus brevifolia*. J. Nat. Prod. 58(9): 1315-1324.

Stierle, A., Strobel, G. A., and Stierle, D. 1993. Taxol and taxane production by *Taxomyces andreanae*, an endophytic fungus of Pacific yew. Science 260: 214-216.

Stierle, A., Upadhyay, R., Hershenhorn, J., Strobel, G. A., and Molina, G. 1991. The phytotoxins of *Mycosphaerella fijiensis*, the causative agent of black Sigatoka disease of bananas and plantains. Experientia 47: 853–859.

Strobel, G. A. 2002. Rainforest endophytes and bioactive products. Crit. Rev. Biotechnol. 22(4): 315–333.

Strobel, G. A., and Daisy, B. 2003. Bioprospecting for microbial endophytes and their natural products. Microbiol. Mol. Biol. Rev. 67: 491–502.

Strobel, G. A., Hess, H. M., Frod, E., Sidhu, R. S., and Yang, X. 1996. Taxol from fungal endophytes and issue of biodiversity. J. Ind. Microbiol .Biotechnol. 17(5-6): 417-423.

Strobel, G. A., Miller. R. V., Martinez-Millee, C., Condron, M. M., Teplow, D. B., and Hess, W. M. 1999. Cryptocandin, a potent antimycotic from the endophytic fungus *Cryptosporiopsis* cf. *quercina*. Microbiol. 145: 1919–1926.

Strobel, G. A., Yang, X., Sears, J., Kramer, R., Sidhu, R.,S., and Hess, W. M. 1996. Taxol from Pestalotiopsis microspora, an endophytic fungus of Taxus wallachiana. Microbiol. 142: 435–440.

Sun, L. M., Cheng, A. X., Wu, X. Z., Zhang, H. J. and Lou, H. X. 2010. Synergistic mechanisms of retigeric acid B and azoles against *Candida albicans*. J. App. Microbiol. 108: 341–348.

Sun, S., Li, Y., Guo, Q., Shi, C., Yu, J., and Ma, L. 2008. *In vitro* interactions between tacrolimus and azoles against *Candida albicans* determined by different methods. Antimicrob. Agents Chemother. 52: 409–417.

Suthep, W., *et al*. 2004. Endophytic fungi with anti-microbial, anti-cancer and anti-malarial activities isolated from Thai medicinal plants. World J. Microbiol. Biotechnol. 20: 265–272.

Tan, R. X., and Zou, W. X. 2001. Endophytes: a rich source of functional metabolites. Nat. Prod. Rep. 18: 448-459.

Tempone, A. G., *et al*. 2007. Amphibian secretions for drug discovery studies: a search for new antiparasitic and antifungal compounds. Lett. Drug. Des. Discov. 4: 67–73.

Wang, F., *et al*. 2008. Seven new prenylated indole diketopiperazine alkaloids from holothurian-derived fungus *Aspergillus fumigatus*. Tetrahedron 64: 7986–7991.

Wang, F. W., *et al*. 2006. Neoplaether, a new cytotoxic and antifungal endophyte metabolite from *Neoplaconema napellum* IFB–E016. FEMS Microbiol Lett. 261: 218–223.

Wani, M. C., Taylor, H. L., Wall, M. E, Coggon p., and McPhail, A. T. 1971. Plant antitumor agents. VI. The isolation and structure of taxol, a novel antileukemic and antitumor agent from *Taxus brevifolia*. J. Am. Chem. Soc. 93: 2325-2327.

White, T. J., Bruns, T., Lee, S., and Taylor, J. 1990. Amplification and direct sequencing of fungal ribosomal RNA genes for phylogenetics. PCR Protocols: A Guide to Methods and Applications (Innis MA, Gelfand DH, Sninsky JJ & White TJ, eds), pp. 315–322. Academic Press, San Diego.

Williams, D. J., and Thomas, R. 1973. Crystal structure of (±) altenuic acid II. Tetrahedron Lett. 9: 639-640.

Wiyakrutta, S., *et al*. 2004. Endophytic fungi with anti-microbial, anti-cancer and anti-malarial activities isolated from Thai medicinal plants. World J. Microbiol. Biotechnol. 20: 265–272.

Yang, X., Zhang, L., Guo, B., and Guo, S. 2004. Preliminary study of vincristine-producing endophytic fungus isolated from leaves of *Catharanthus roseus*. Zhongcaoyao 35: 79–81.

Zhang, Y., Wang, S., Li, X. M., Cui, C. M., Feng, C., and Wang, B. G. 2007. New sphingolipids with a previously unreported 9-methyl-C20-sphingosine moiety from a marine algus endophytic fungus *Aspergillus niger* EN-13. Lipids 42(8): 759-764.

Zhang, Z., Schwartz, S., Wagner, L., and Miller, W. 2000. A greedy algorithm for aligning DNA sequences. J. Comput. Biol. 7: 203–214.

APPENDICES

APPENDIX A

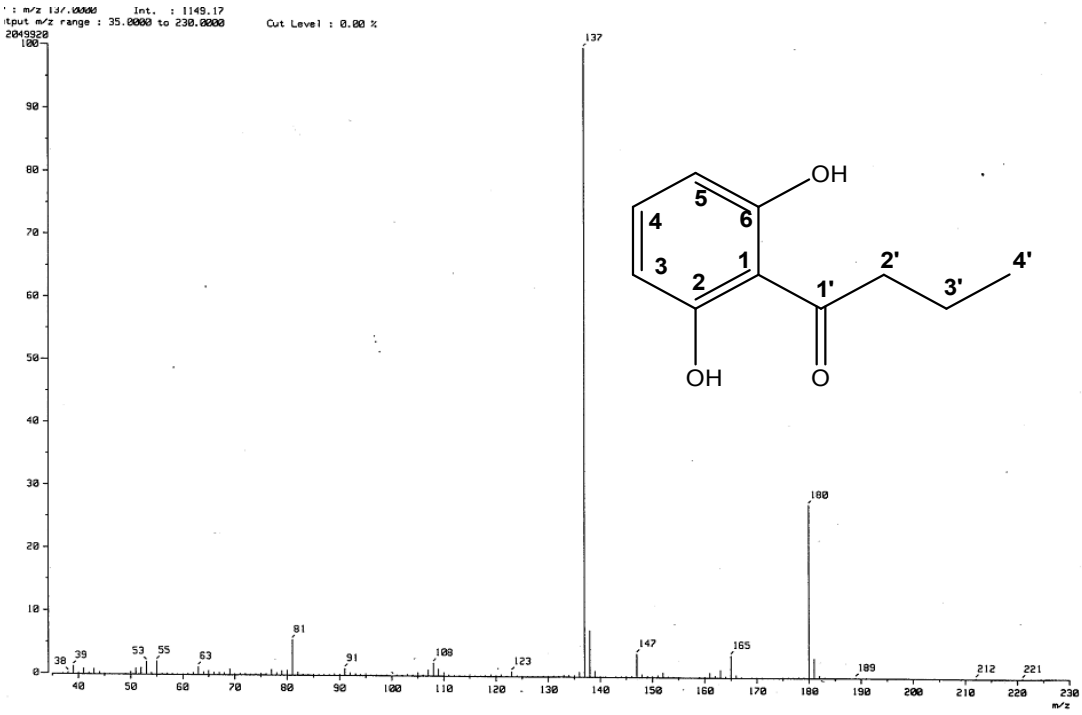

Figure 31 EIMS spectrum of 1'-(2,6-Dihydroxyphenyl)butanone

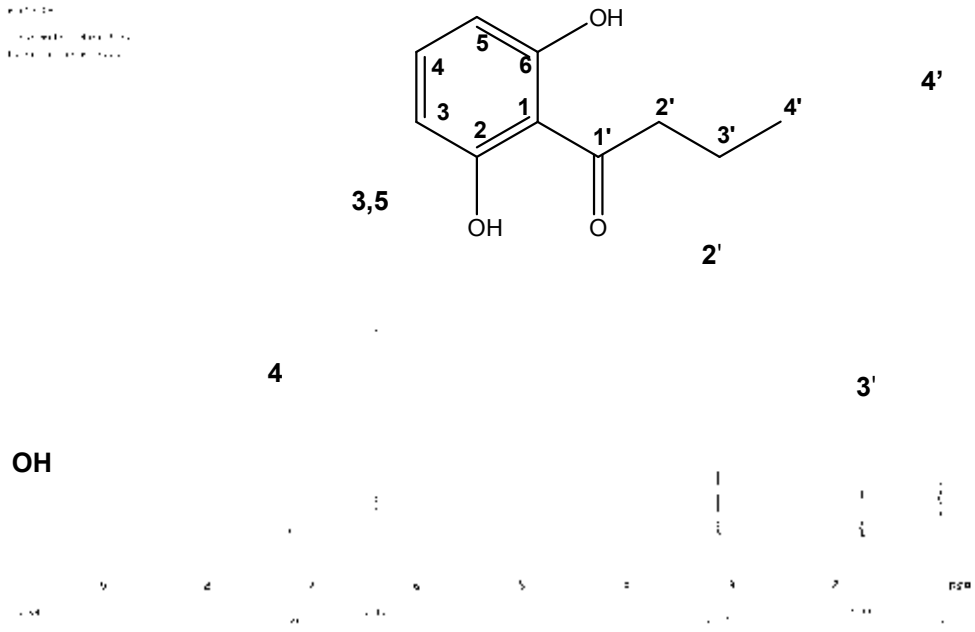

Figure 32 ^{1}H-NMR spectrum of 1'-(2,6-Dihydroxyphenyl)butanone (500 MHz, $CDCl_3$)

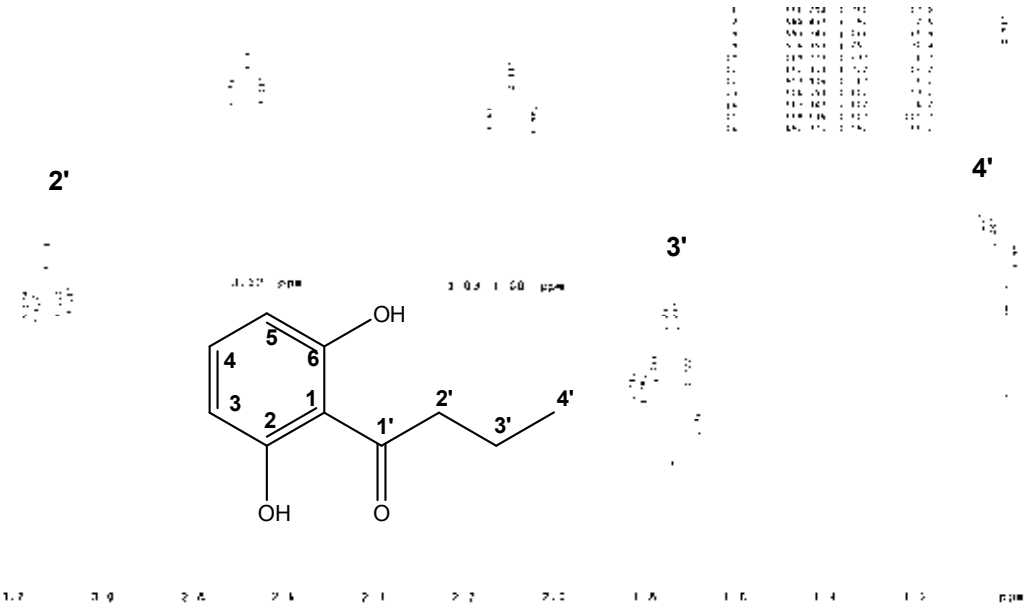

Figure 33 Expanded ^{1}H-NMR spectrum of 1'-(2,6-Dihydroxyphenyl)butanone (500 MHz, $CDCl_3$)

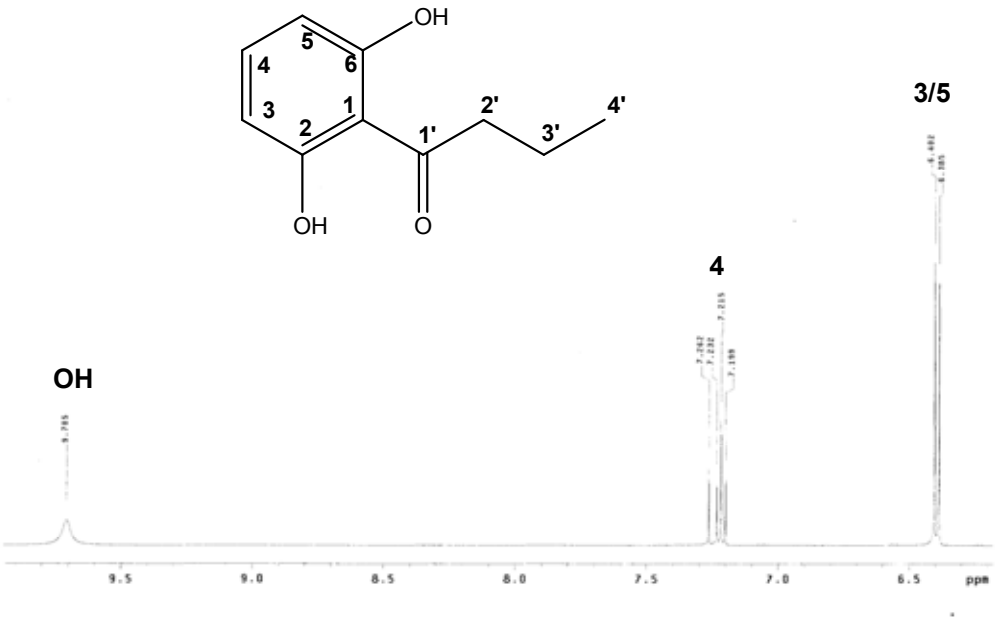

Figure 34 Expanded ^{1}H-NMR spectrum of 1'-(2,6-Dihydroxyphenyl)butanone (500 MHz, $CDCl_3$)

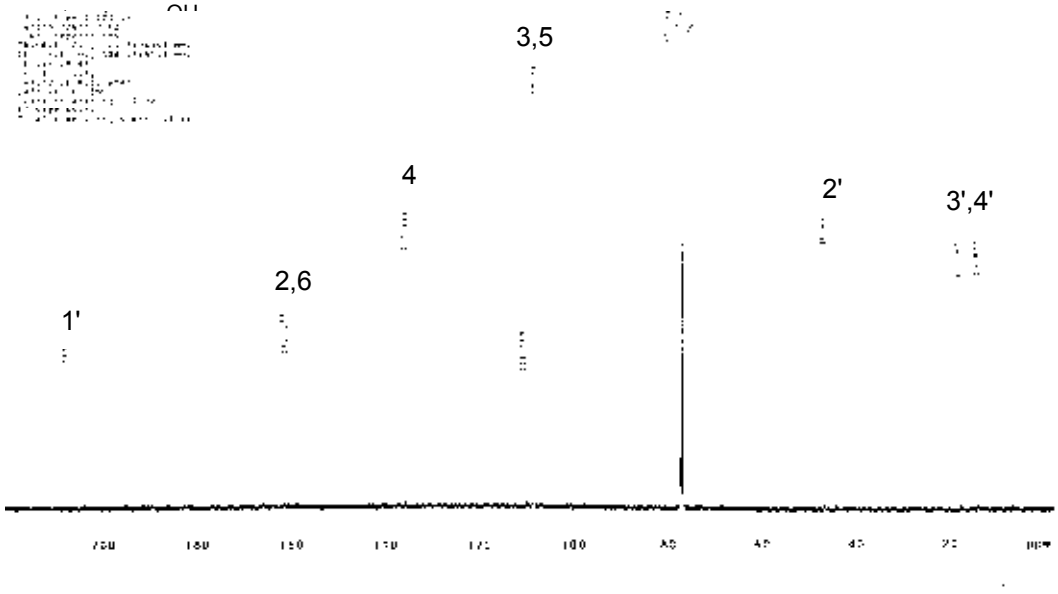

Figure 35 ^{13}C-NMR spectrum of 1'-(2,6-dihydroxyphenyl)butanone (125 MHz, $CDCl_3$)

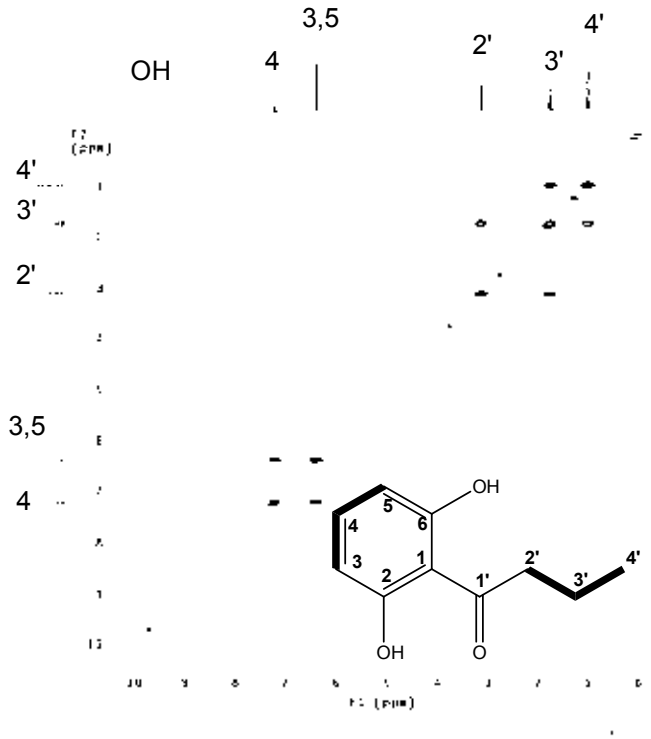

Figure 36 ^{1}H-^{1}H COSY spectrum of 1'-(2,6-Dihydroxyphenyl)butanone ($CDCl_3$)

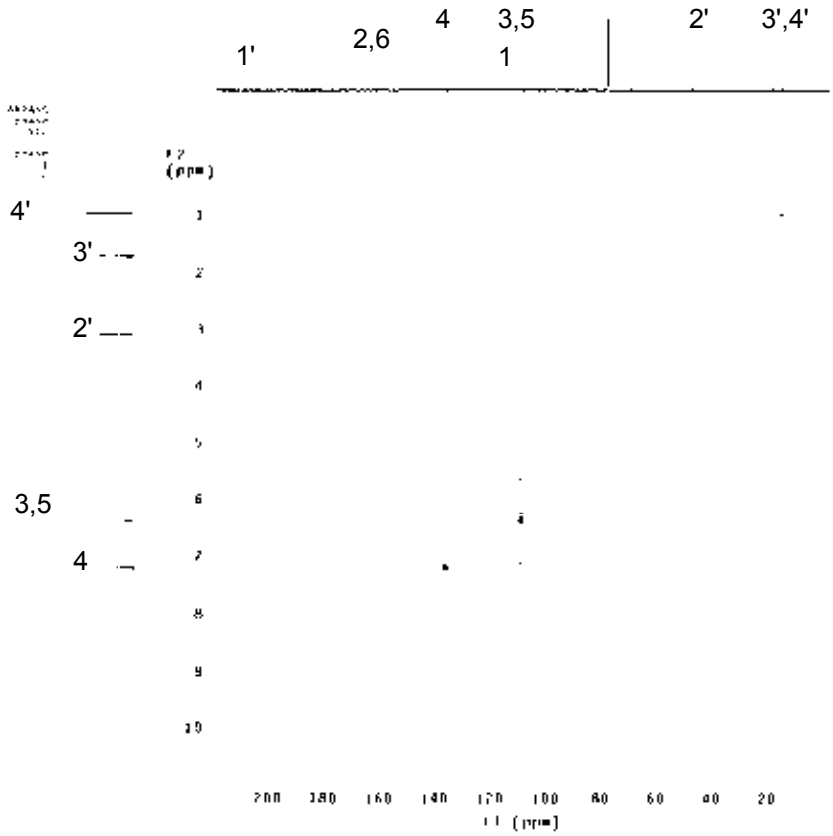

Figure 37 HSQC spectrum of 1'-(2,6-Dihydroxyphenyl)butanone ($CDCl_3$)

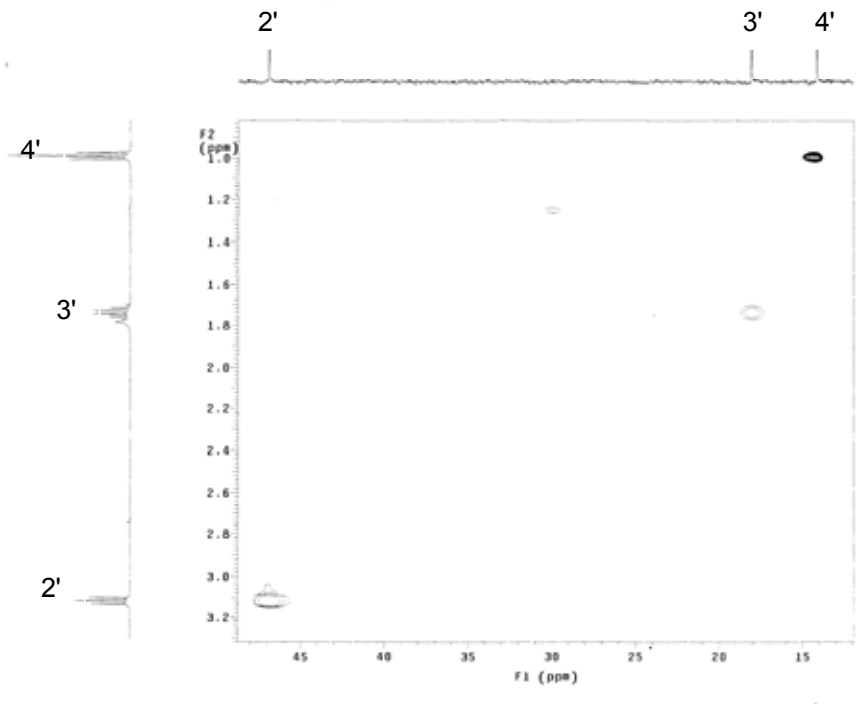

Figure 38 HSQC spectrum of 1'-(2,6-Dihydroxyphenyl)butanone ($CDCl_3$)

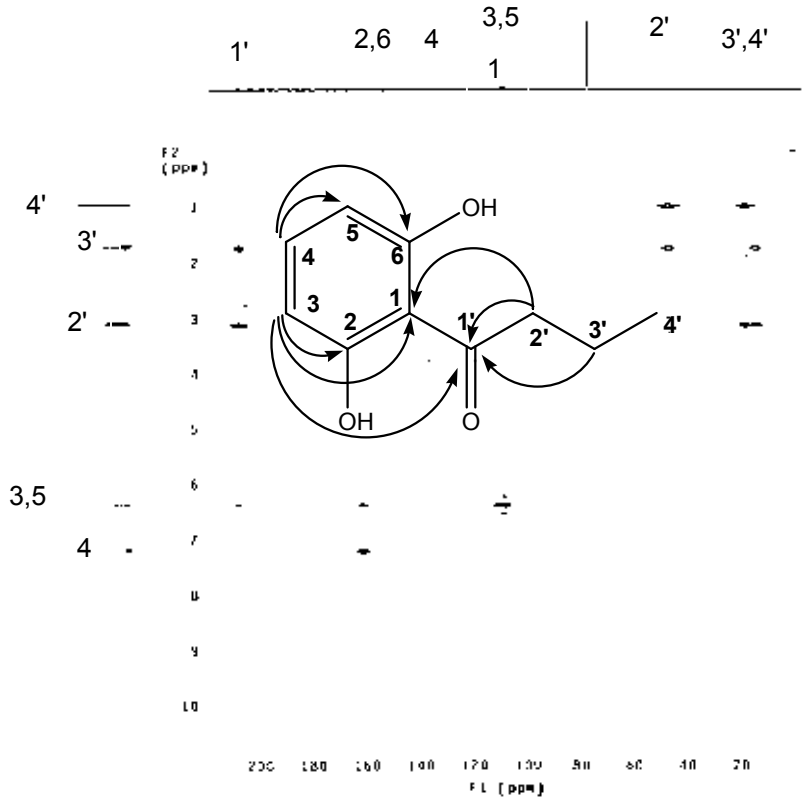

Figure 39 HMBC spectrum of 1'-(2,6-Dihydroxyphenyl)butanone ($CDCl_3$)

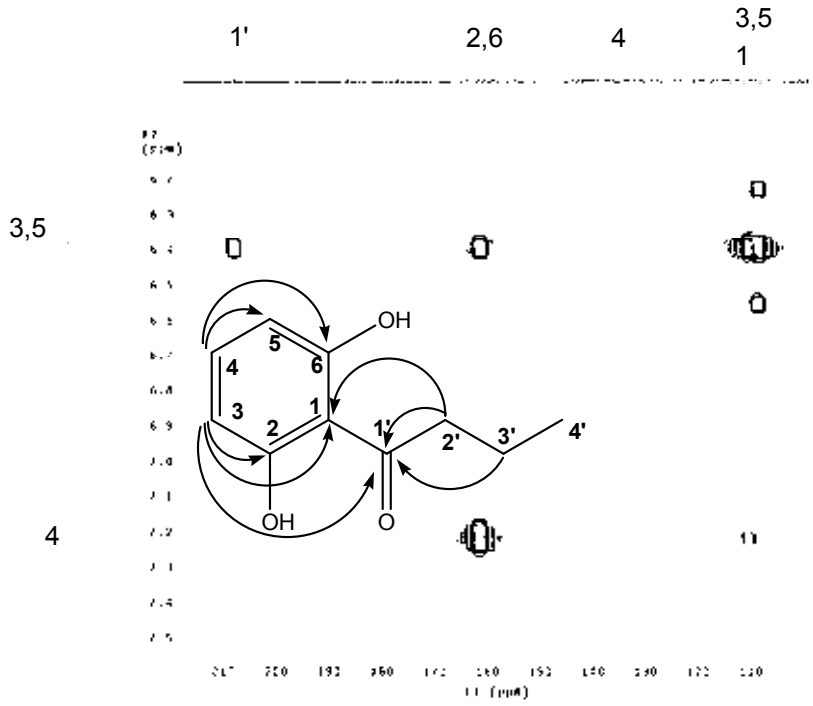

Figure 40 Expanded HMBC spectrum of 1'-(2,6-Dihydroxyphenyl)butanone ($CDCl_3$)

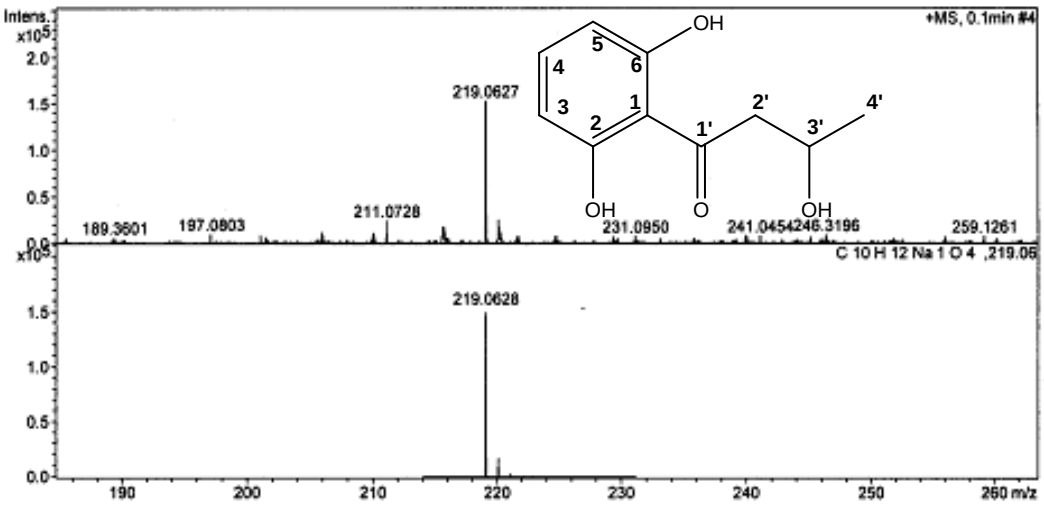

Figure 41 ESI-TOF MS spectrum of 1'-(2,6-Dihydroxyphenyl)-3'-hydroxybutanone

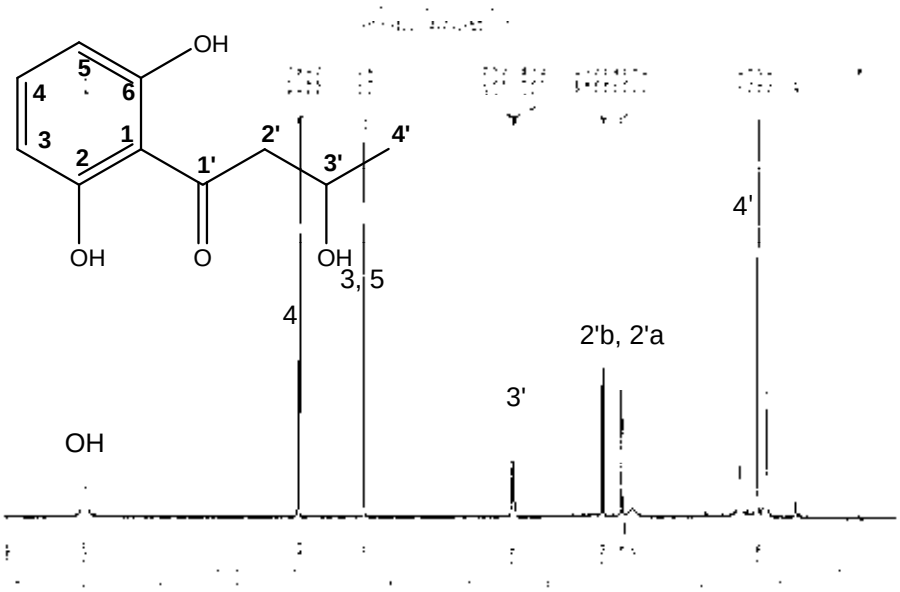

Figure 42 ^{1}H-NMR spectrum of 1'-(2,6-Dihydroxyphenyl)-3'-hydroxybutanone (500 MHz, $CDCl_3$)

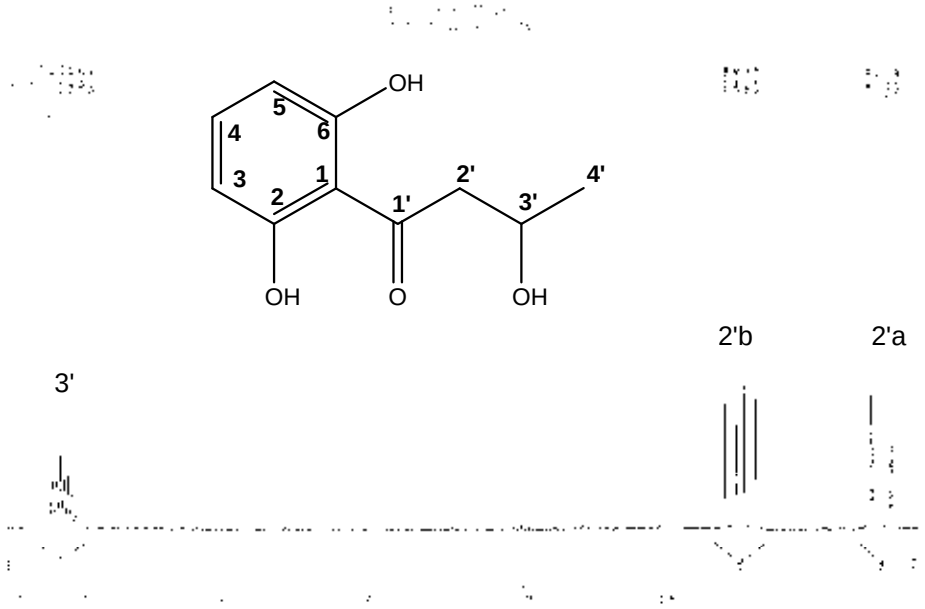

Figure 43 Expanded ^{1}H-NMR spectrum of 1'-(2,6-Dihydroxyphenyl)-3'-hydroxybutanone (500 MHz, $CDCl_3$)

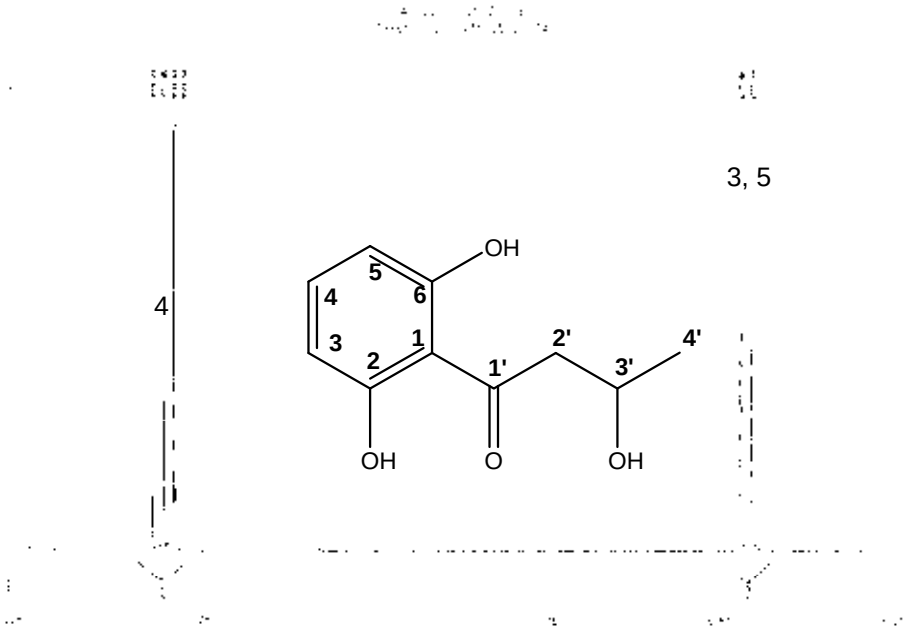

Figure 44 Expanded ^{1}H-NMR spectrum of 1'-(2,6-Dihydroxyphenyl)-3'-hydroxybutanone (500 MHz, $CDCl_3$)

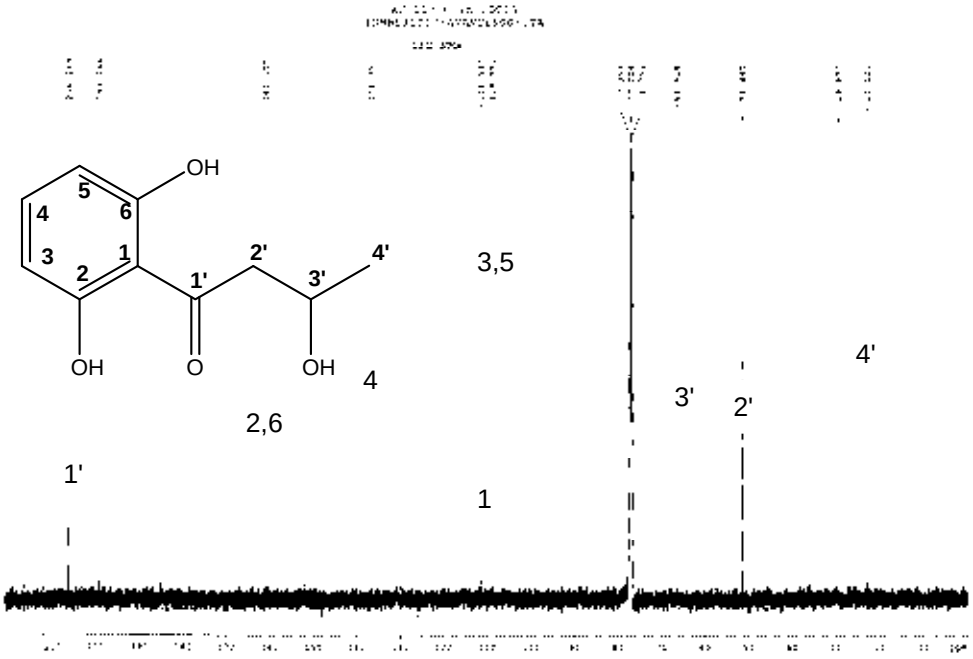

Figure 45 ^{13}C-NMR spectrum of 1'-(2,6-Dihydroxyphenyl)-3'-hydroxybutanone (125 MHz, $CDCl_3$)

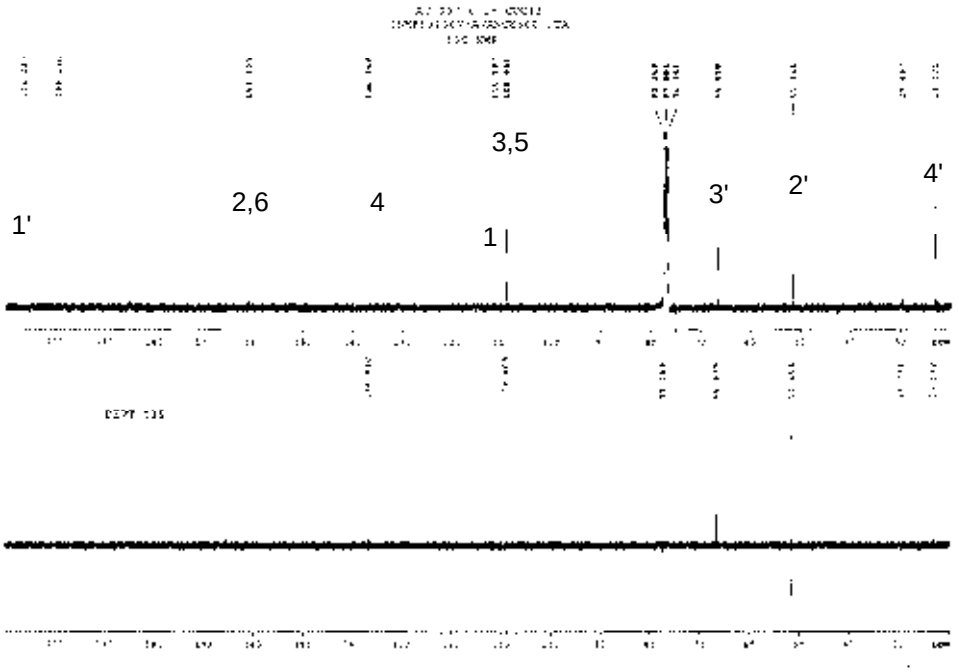

Figure 46 DEPT 135 spectrum of 1'-(2,6-Dihydroxyphenyl)-3'-hydroxybutanone (125 MHz, $CDCl_3$)

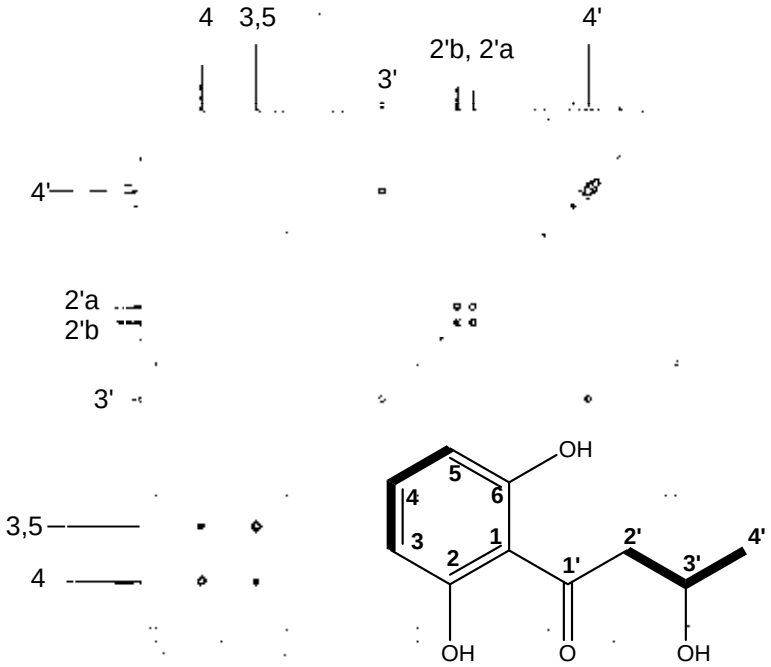

Figure 47 ^{1}H-^{1}H COSY spectrum of 1'-(2,6-Dihydroxyphenyl)-3'-hydroxybutanone

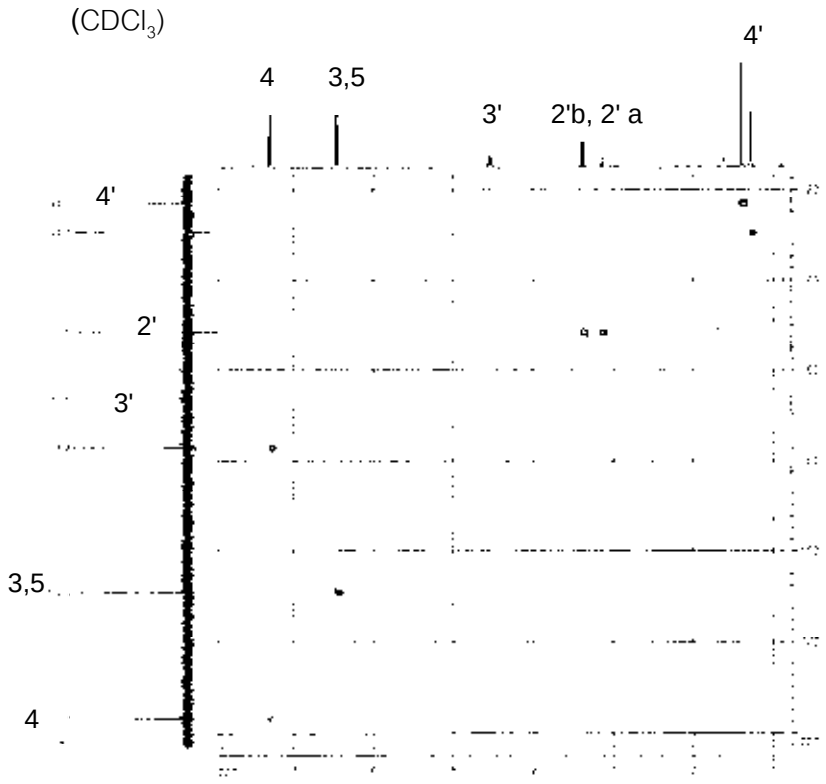

Figure 48 HMQC spectrum of 1'-(2,6-Dihydroxyphenyl)-3'-hydroxybutanone ($CDCl_3$)

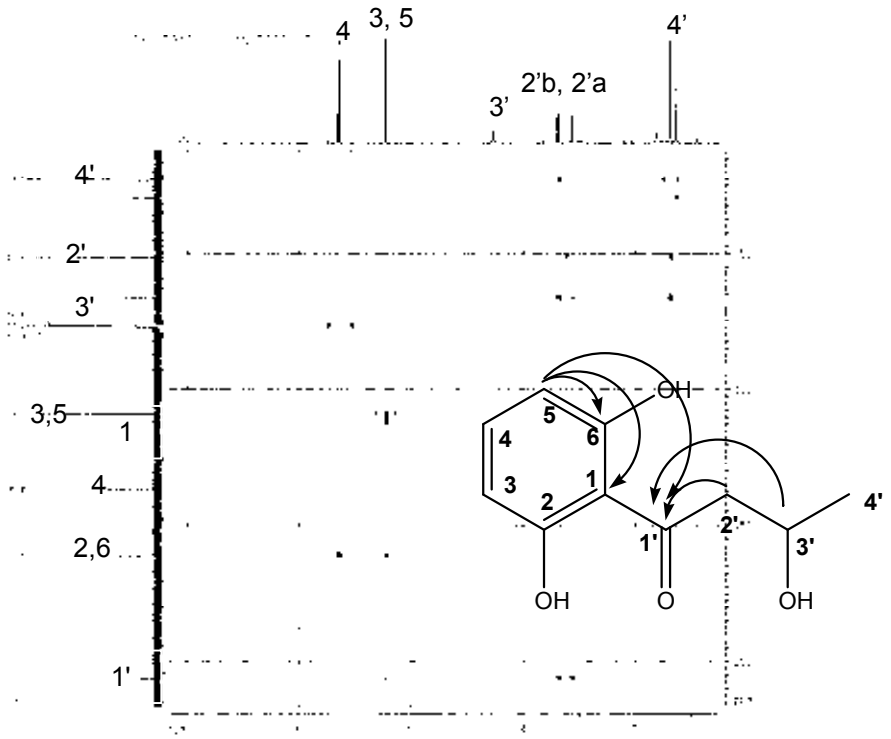

Figure 49 HMBC spectrum of 1'-(2,6-Dihydroxyphenyl)-3'-hydroxybutanone ($CDCl_3$)

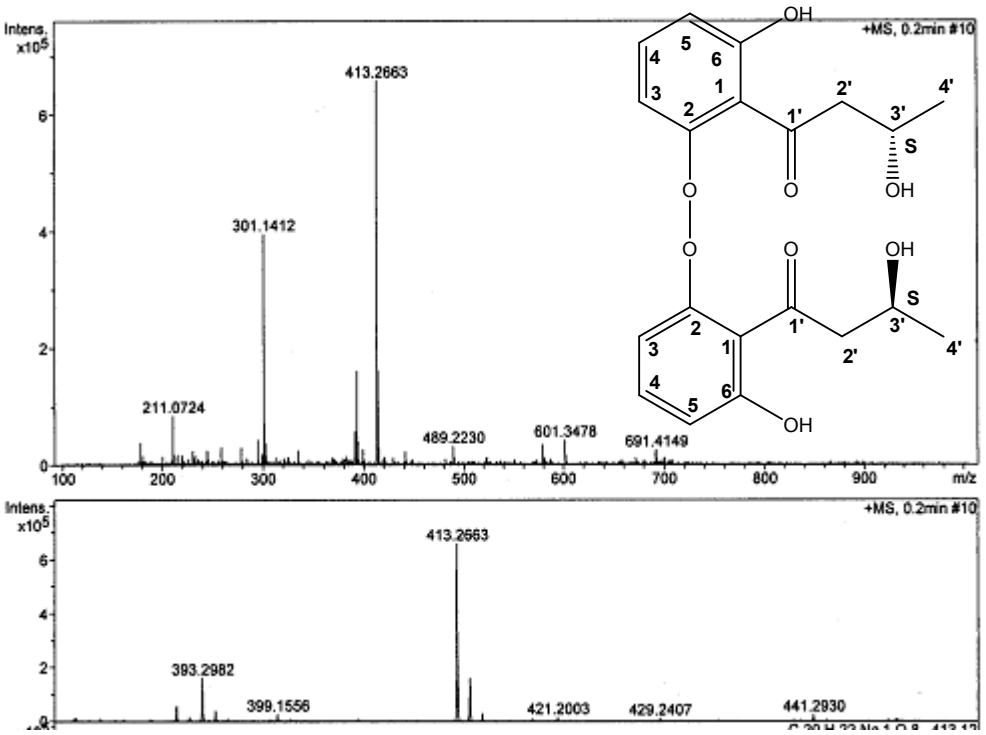

Figure 50 ESI-TOF MS spectrum of Nodulisporin G

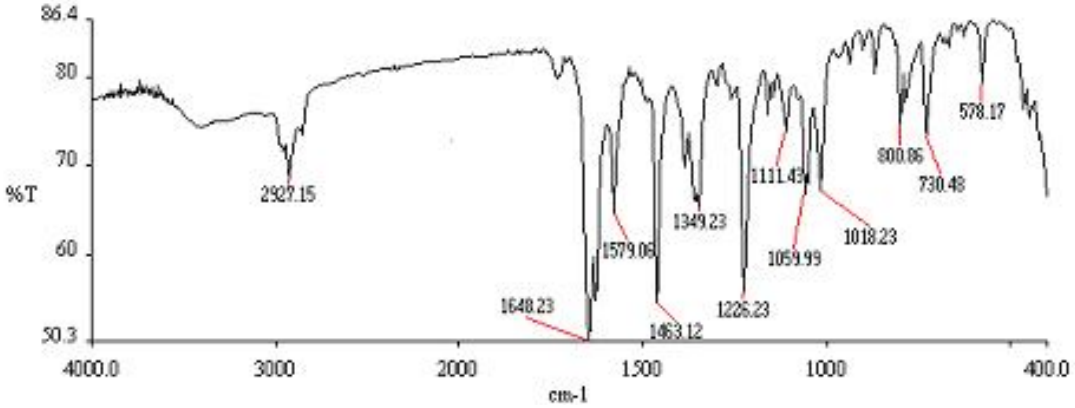

Figure 51 The IR spectrum of Nodulisporin G

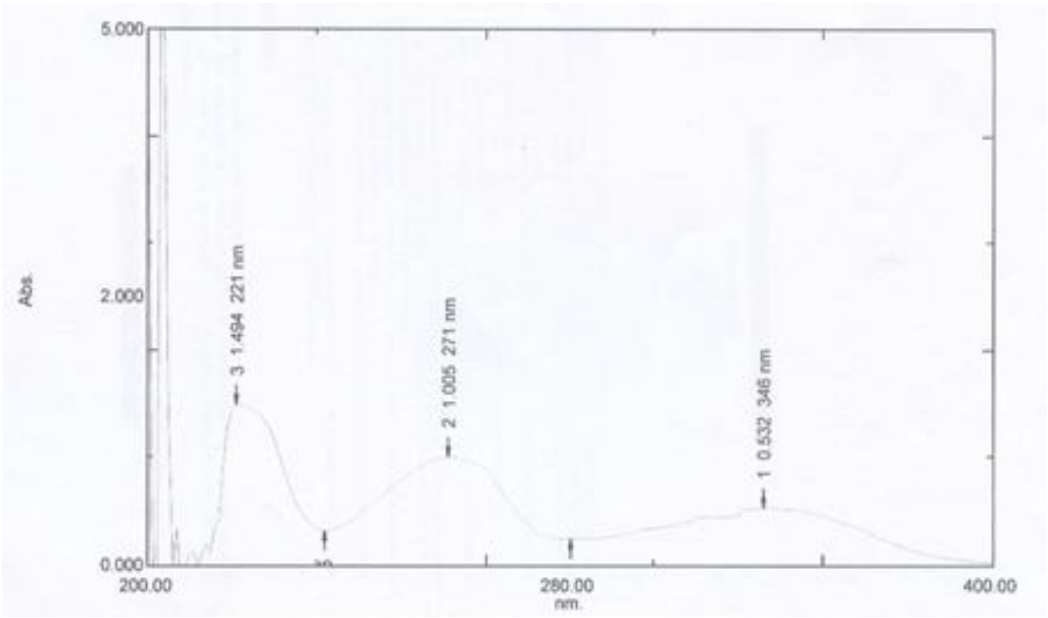

Figure 52 The UV spectrum of Nodulisporin G

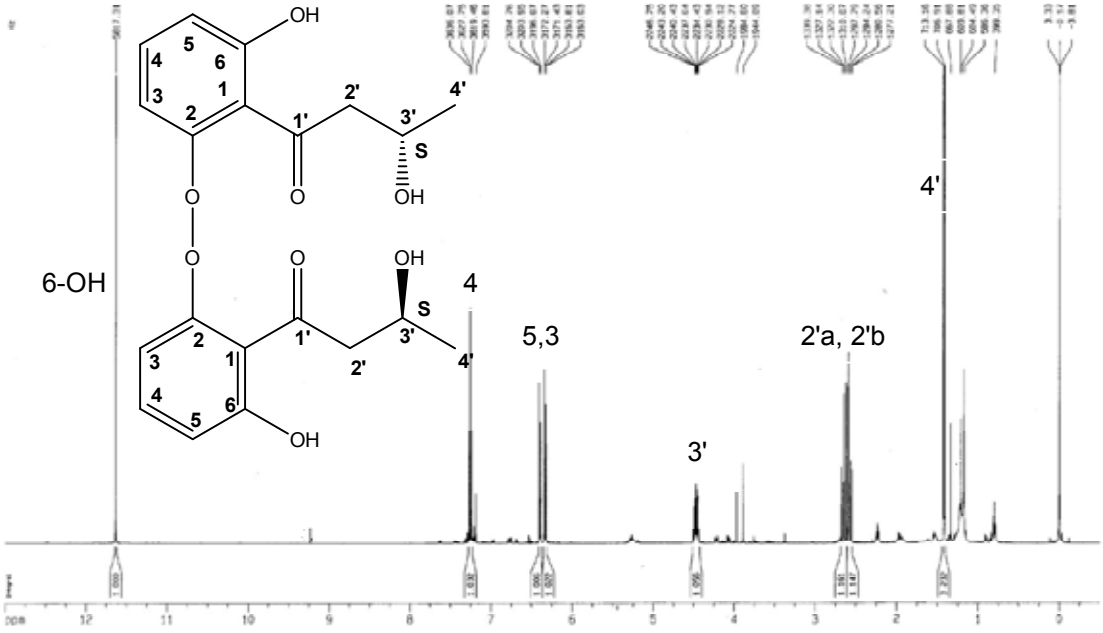

Figure 53 ^{1}H-NMR spectrum of Nodulisporin G (500 MHz, $CDCl_3$)

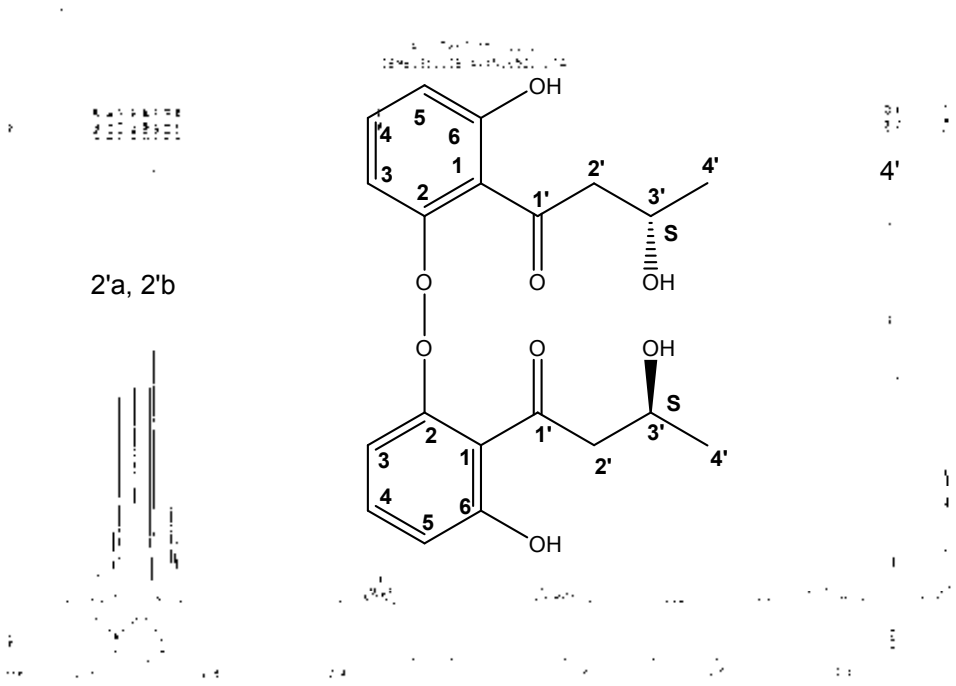

Figure 54 Expanded ^{1}H-NMR spectrum of Nodulisporin G (500 MHz, $CDCl_3$)

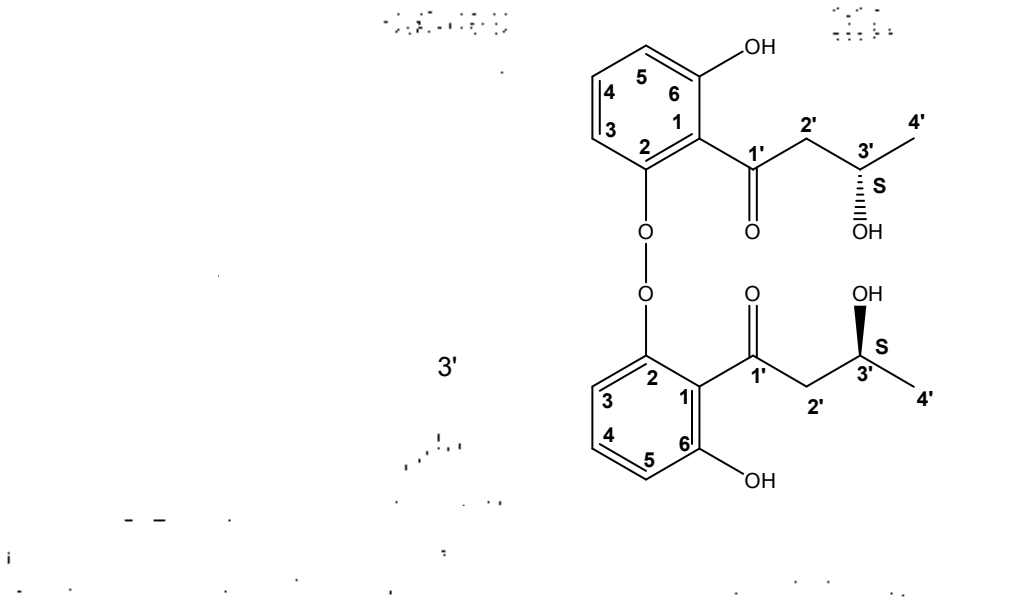

Figure 55 Expanded ^{1}H-NMR spectrum of Nodulisporin G (500 MHz, $CDCl_3$)

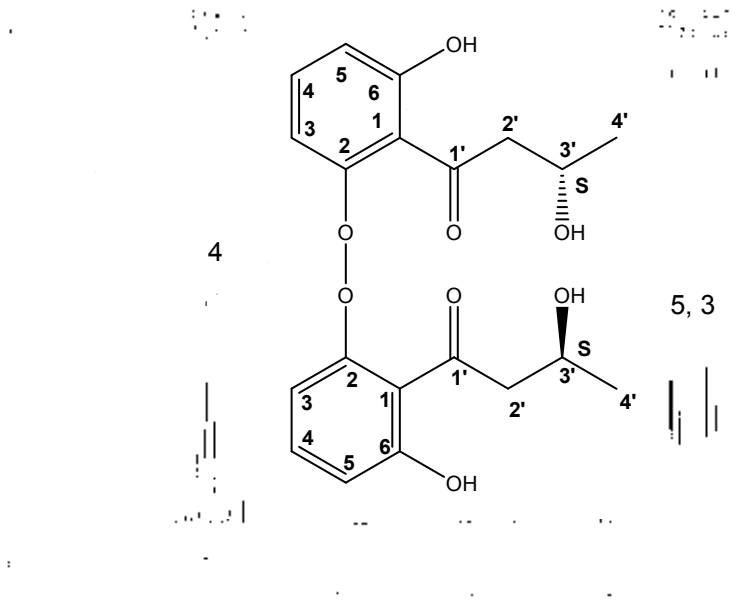

Figure 56 Expanded ^{1}H-NMR spectrum of Nodulisporin G (500 MHz, $CDCl_3$)

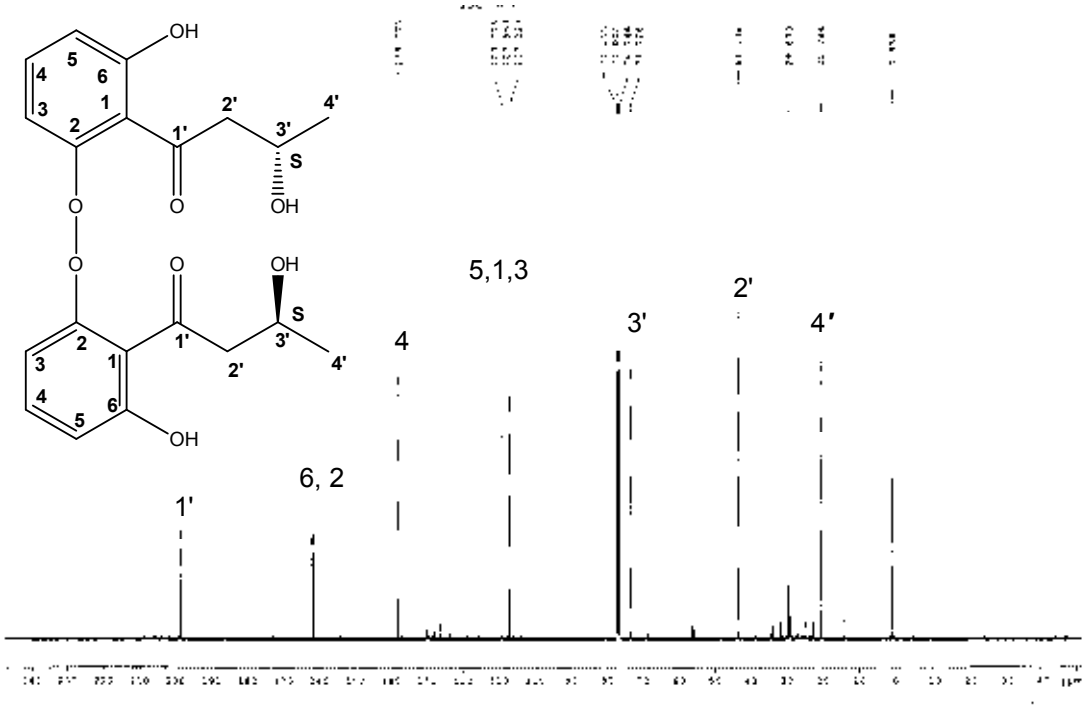

Figure 57 ^{13}C-NMR spectrum of Nodulisporin G (125 MHz, $CDCl_3$)

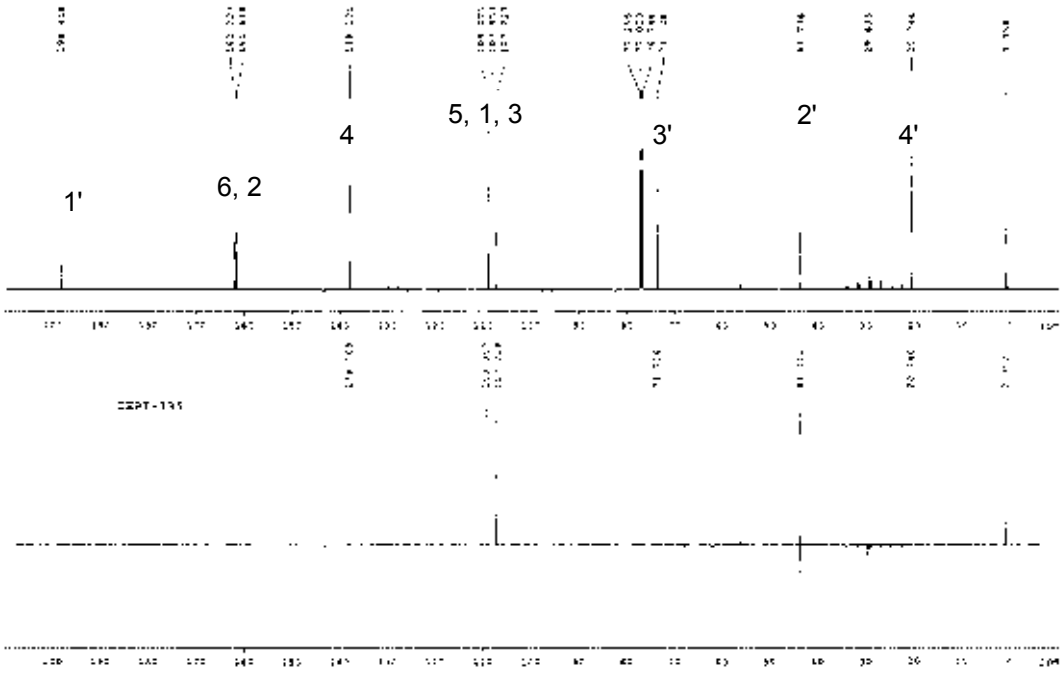

Figure 58 DEPT 135 spectrum of Nodulisporin G (125 MHz, $CDCl_3$)

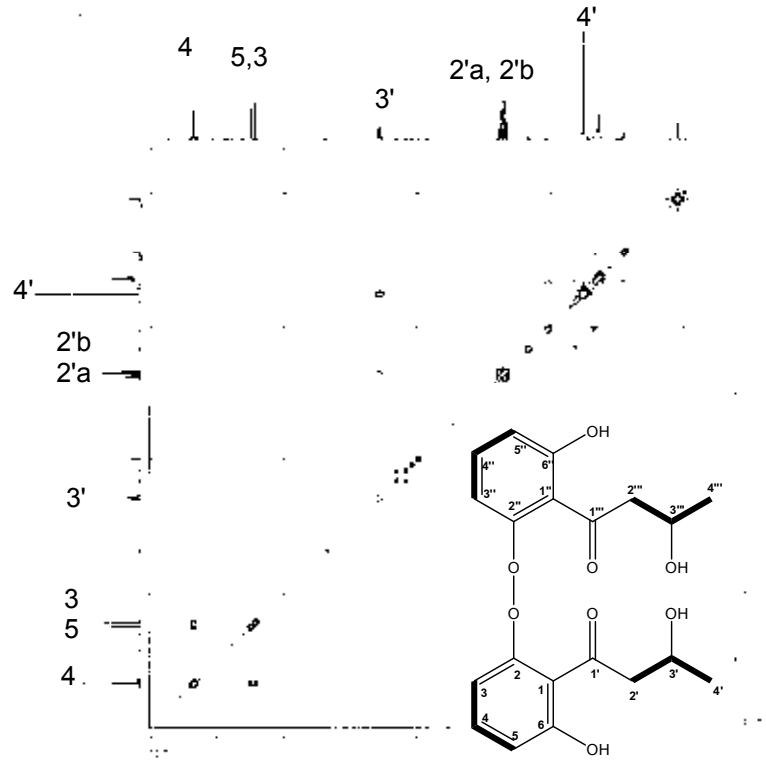

Figure 59 ^{1}H-^{1}H COSY spectrum of Nodulisporin G ($CDCl_3$)

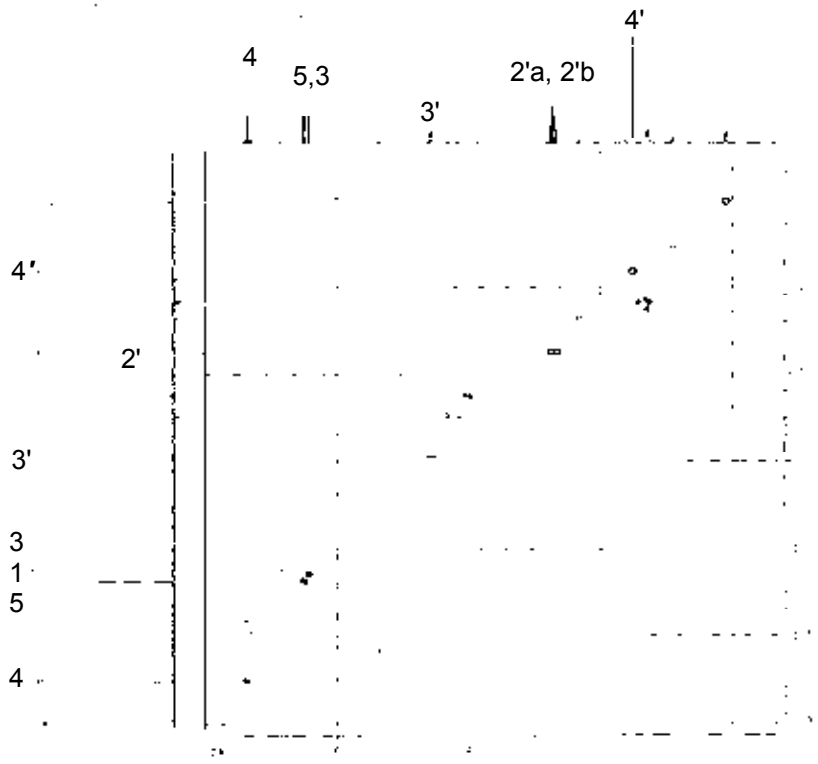

Figure 60 HMQC spectrum of Nodulisporin G ($CDCl_3$)

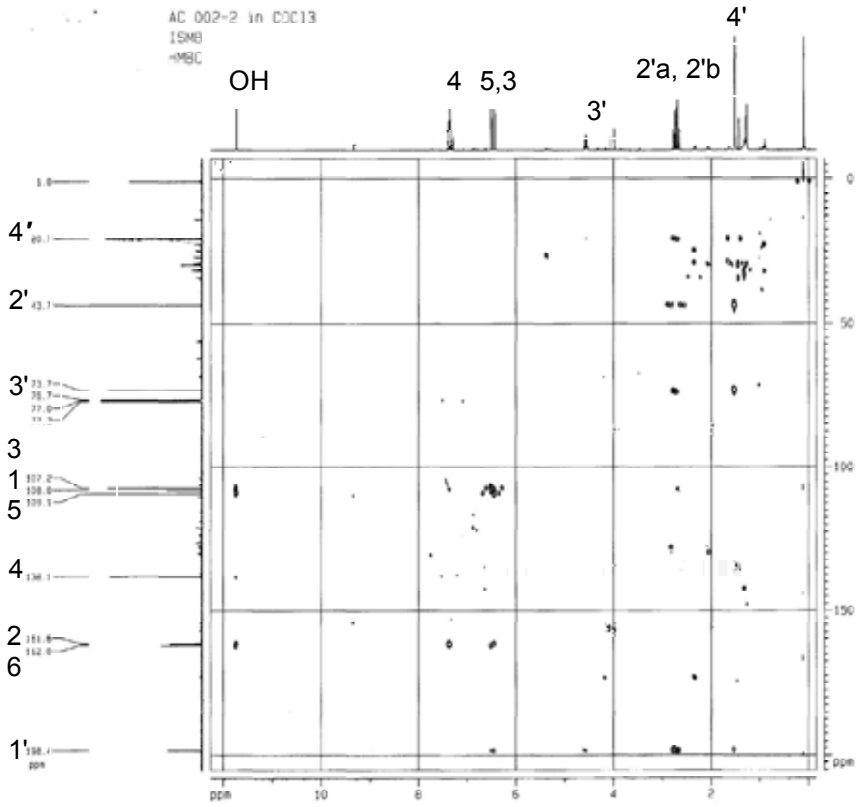

Figure 61 HMBC spectrum of Nodulisporin G ($CDCl_3$)

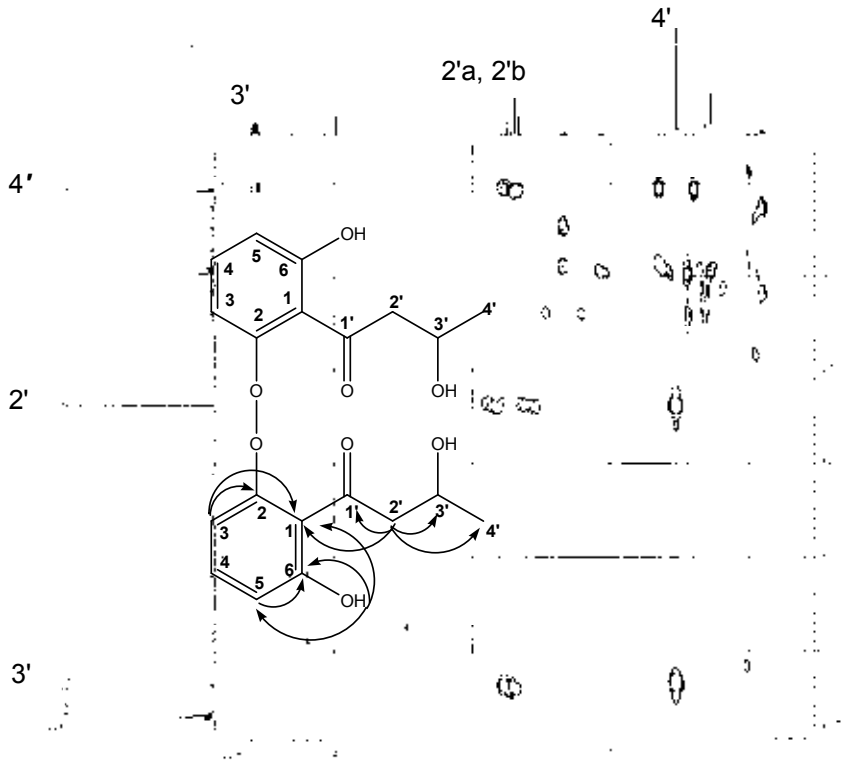

Figure 62 Expanded HMBC spectrum of Nodulisporin G ($CDCl_3$)

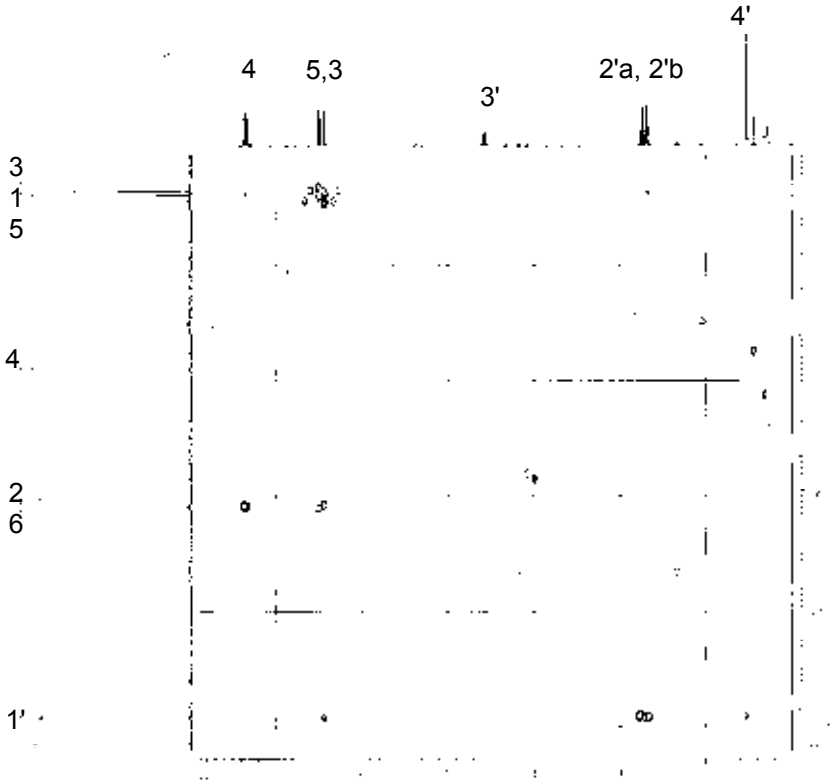

Figure 63 Expanded HMBC spectrum of Nodulisporin G ($CDCl_3$)

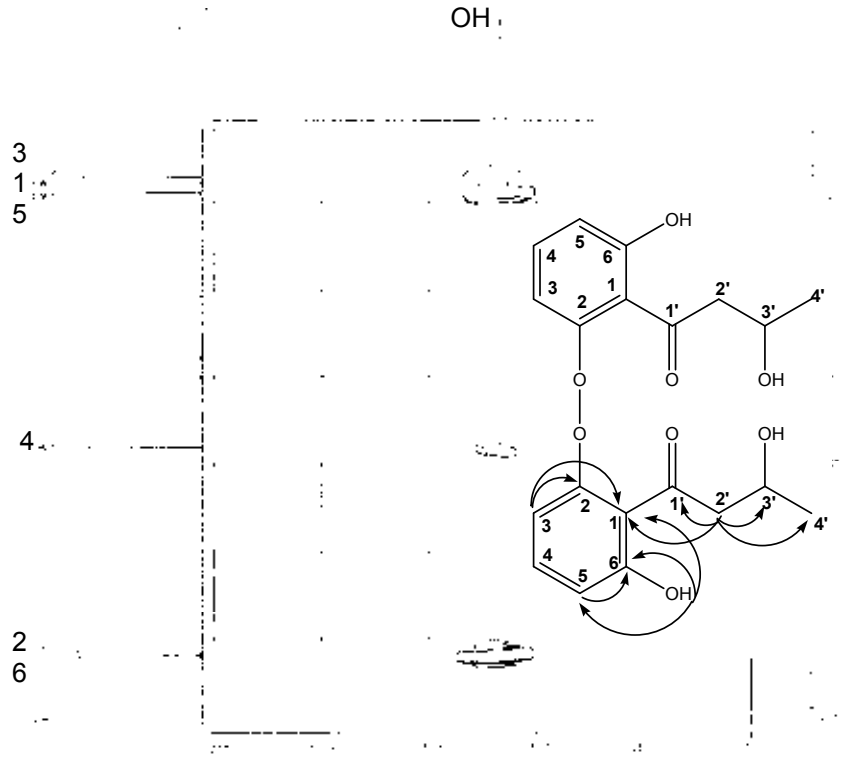

Figure 64 Expanded HMBC spectrum of Nodulisporin G ($CDCl_3$)

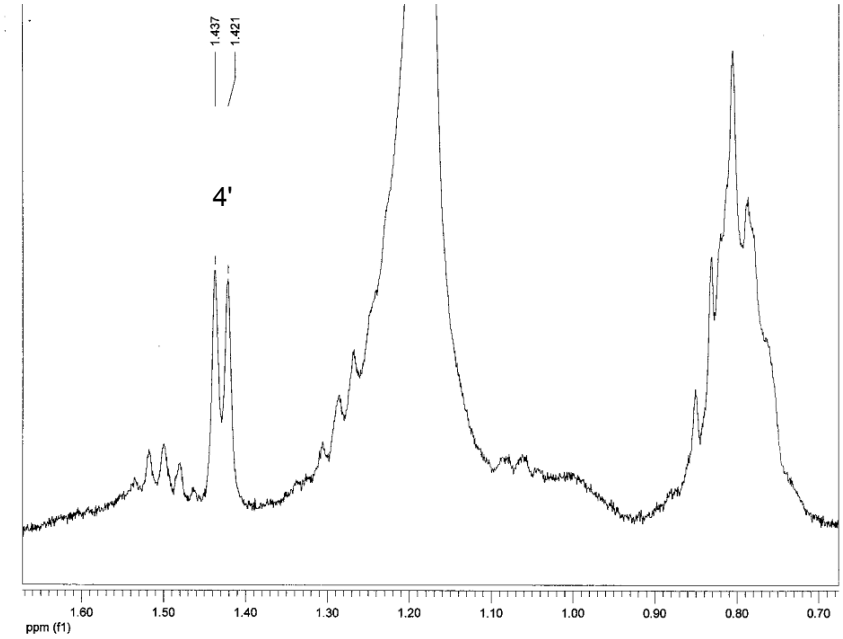

Figure 65 Expanded region ^{1}H-NMR spectrum of Nodulisporin G (*S)*-MTPA ester (400 MHz, $CDCl_3$)

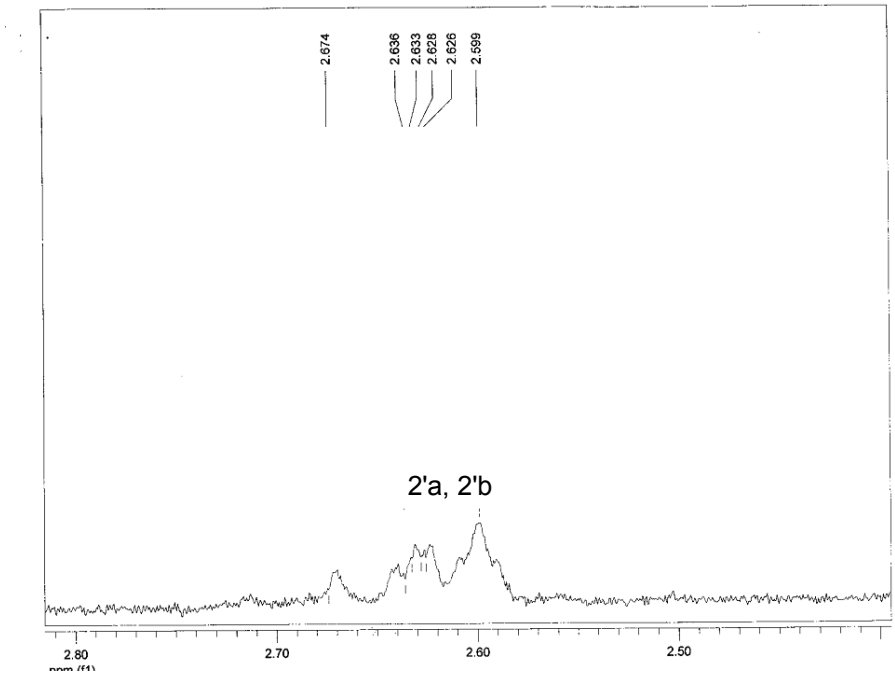

Figure 66 Expanded region ^{1}H-NMR spectrum of Nodulisporin G (*S)*-MTPA ester (400 MHz, $CDCl_3$)

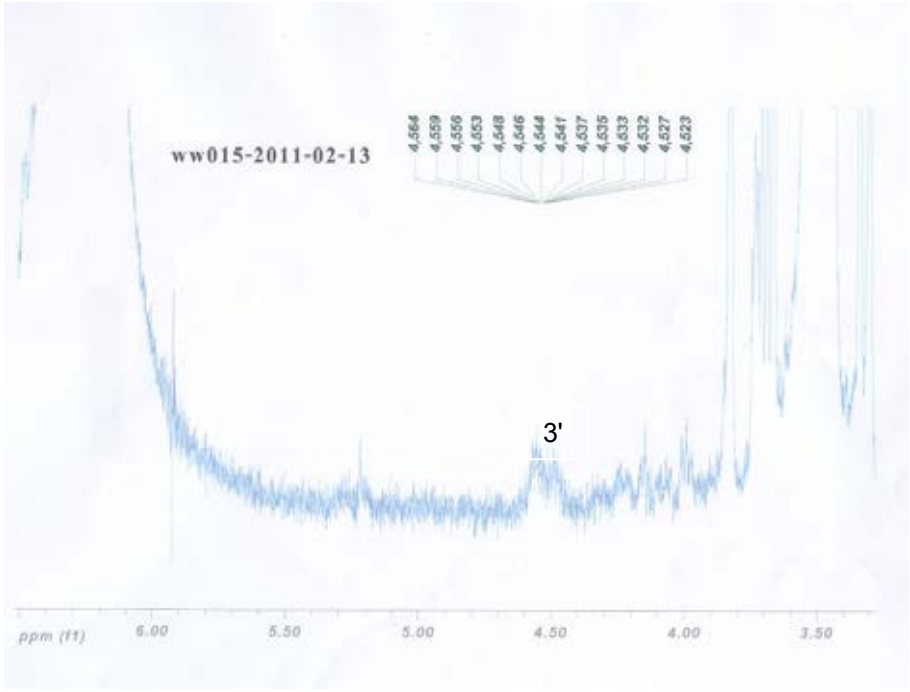

Figure 67 Expanded region ^{1}H-NMR spectrum of Nodulisporin G (*S*)-MTPA ester (400 MHz, $CDCl_3$)

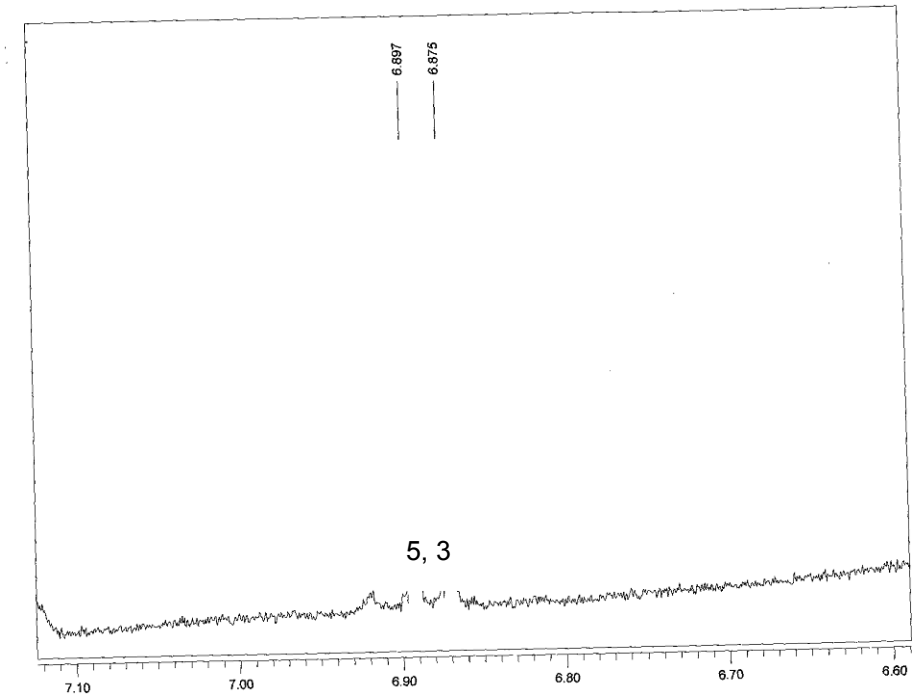

Figure 68 Expanded region ^{1}H-NMR spectrum of Nodulisporin G (*S*)-MTPA ester (400 MHz, $CDCl_3$)

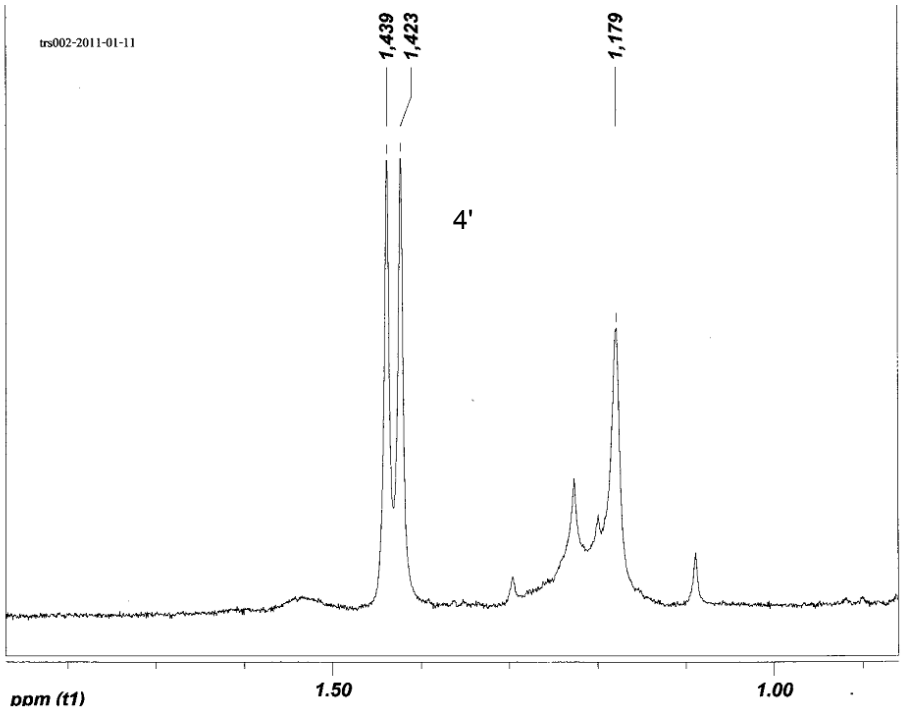

Figure 69 Expanded region ^{1}H-NMR spectrum of Nodulisporin G (*R)*-MTPA ester (400 MHz, $CDCl_3$)

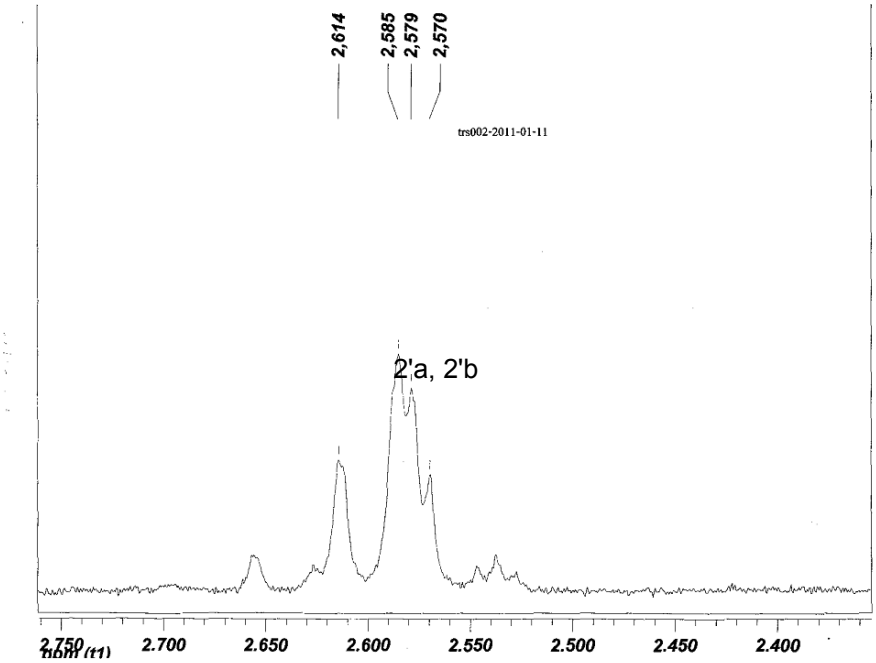

Figure 70 Expanded region ^{1}H-NMR spectrum of Nodulisporin G (*R)*-MTPA ester (400 MHz, $CDCl_3$)

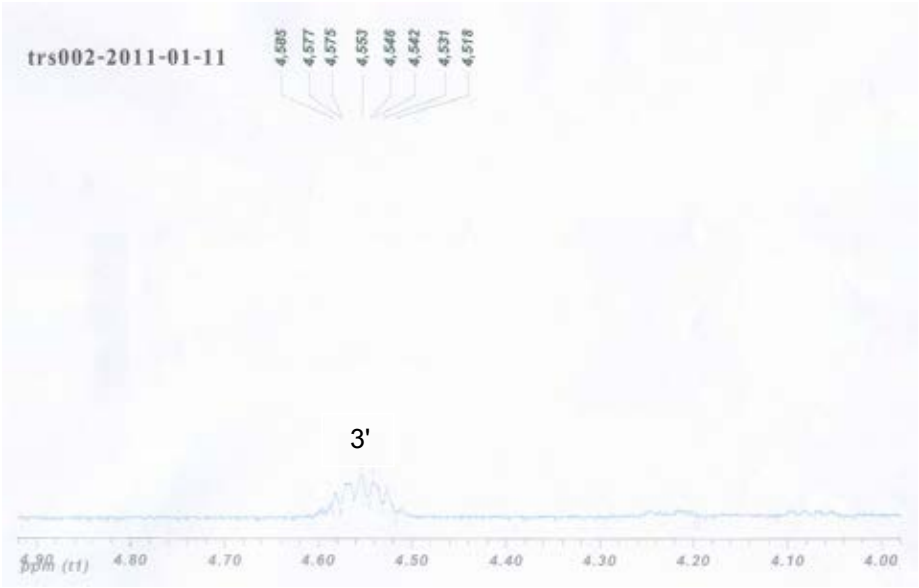

Figure 71 Expanded region ^{1}H-NMR spectrum of Nodulisporin G (*R*)-MTPA ester (400 MHz, $CDCl_3$)

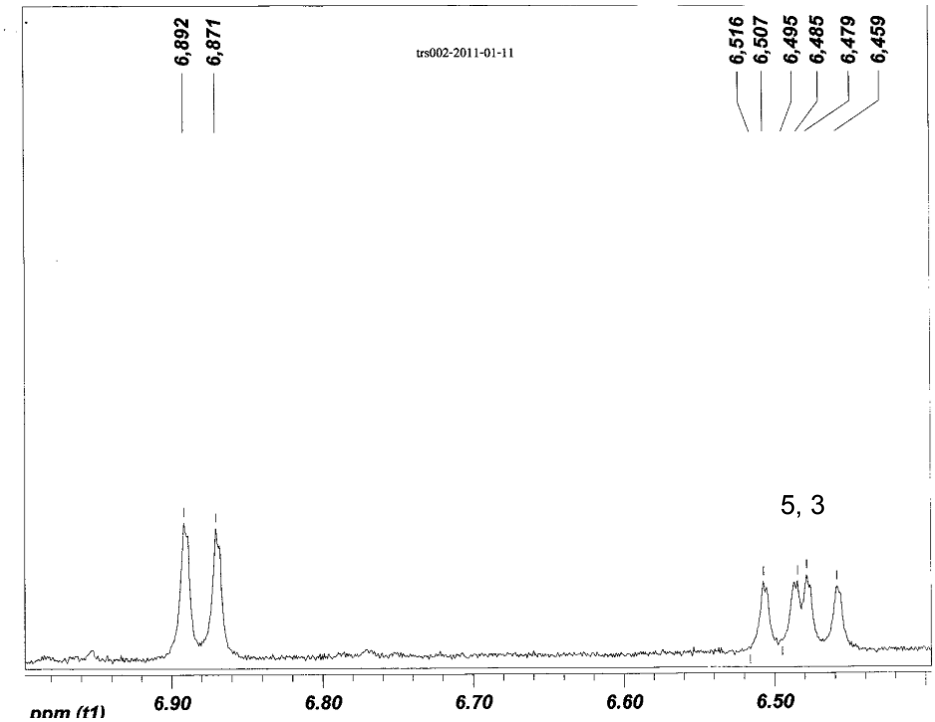

Figure 72 Expanded region ^{1}H-NMR spectrum of Nodulisporin G (*R*)-MTPA ester (400 MHz, $CDCl_3$)

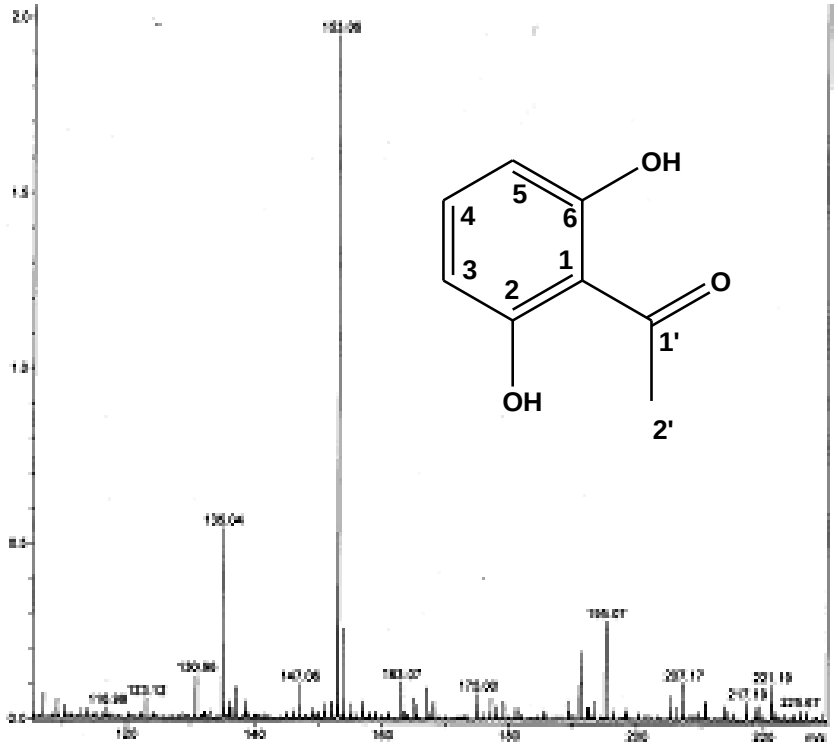

Figure 73 EIMS spectrum of 1'-(2,6-Dihydroxyphenyl)ethanone

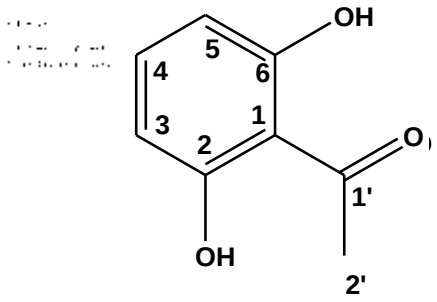

2'

4 3, 5

OH

Figure 74 ^{1}H-NMR spectrum of 1'-(2,6-Dihydroxyphenyl)ethanone (500 MHz, $CDCl_3$)

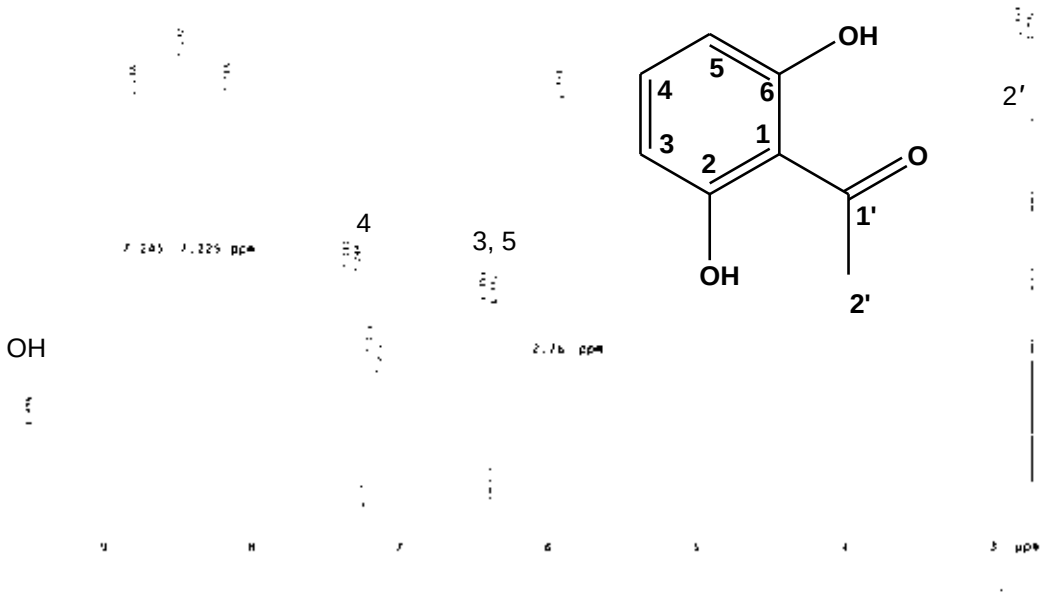

Figure 75 Expanded ^{1}H-NMR spectrum of 1'-(2,6-Dihydroxyphenyl)ethanone (500 MHz, $CDCl_3$)

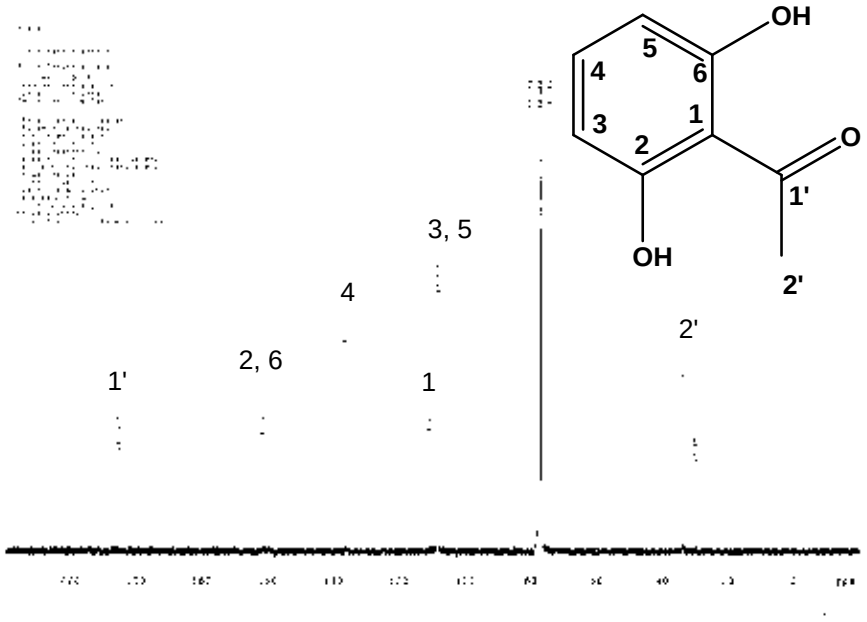

Figure 76 ^{13}C-NMR spectrum of 1'-(2,6-Dihydroxyphenyl)ethanone (125 MHz, $CDCl_3$)

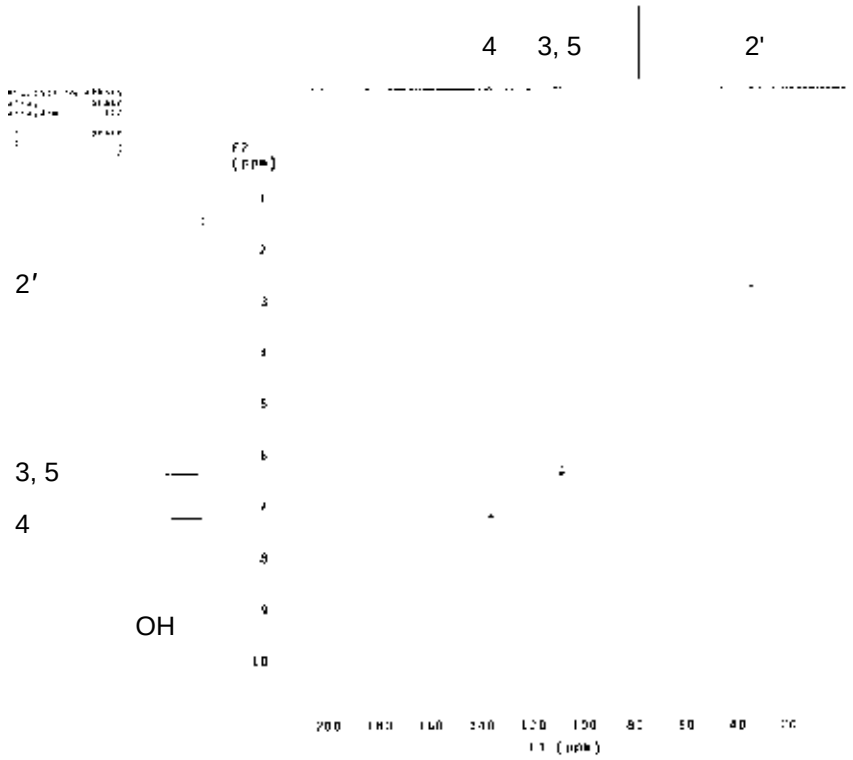

Figure 77 HSQC spectrum of 1'-(2,6-Dihydroxyphenyl)ethanone ($CDCl_3$)

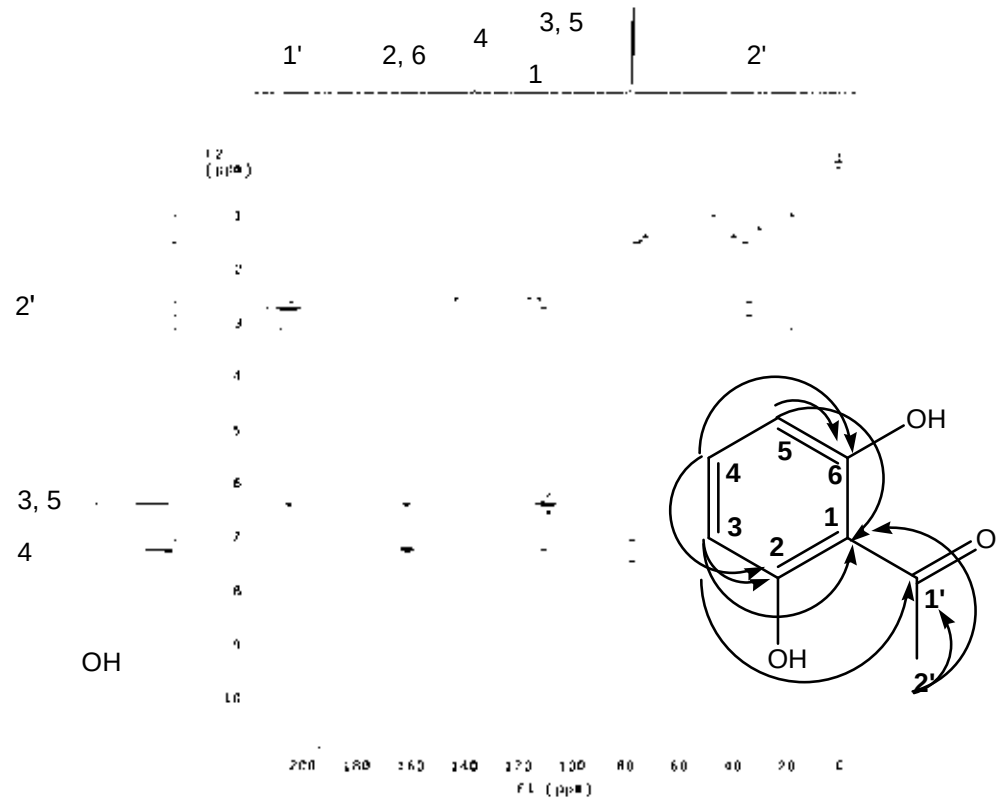

Figure 78 HMBC spectrum of 1'-(2,6-Dihydroxyphenyl)ethanone ($CDCl_3$)

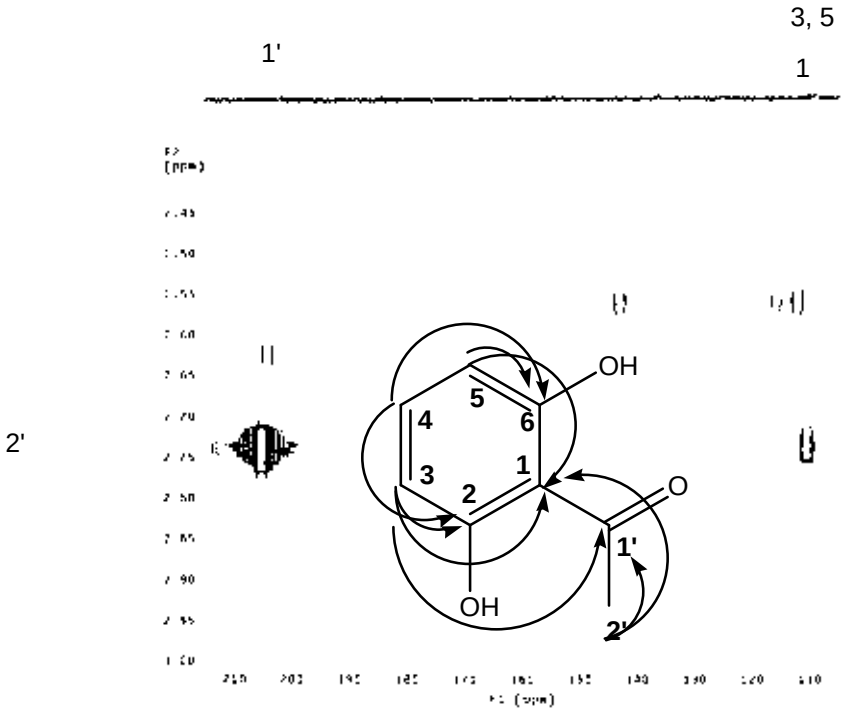

Figure 79 Expanded HMBC spectrum of 1'-(2,6-Dihydroxyphenyl)ethanone ($CDCl_3$)

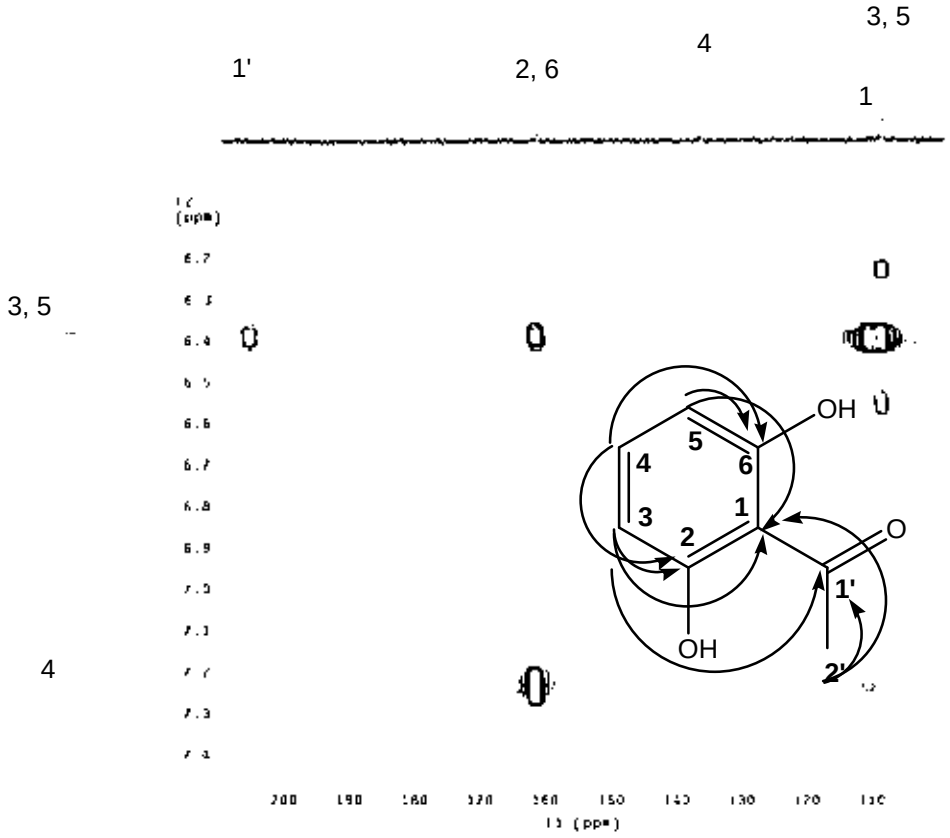

Figure 80 Expanded HMBC spectrum of 1'-(2,6-Dihydroxyphenyl)ethanone ($CDCl_3$)

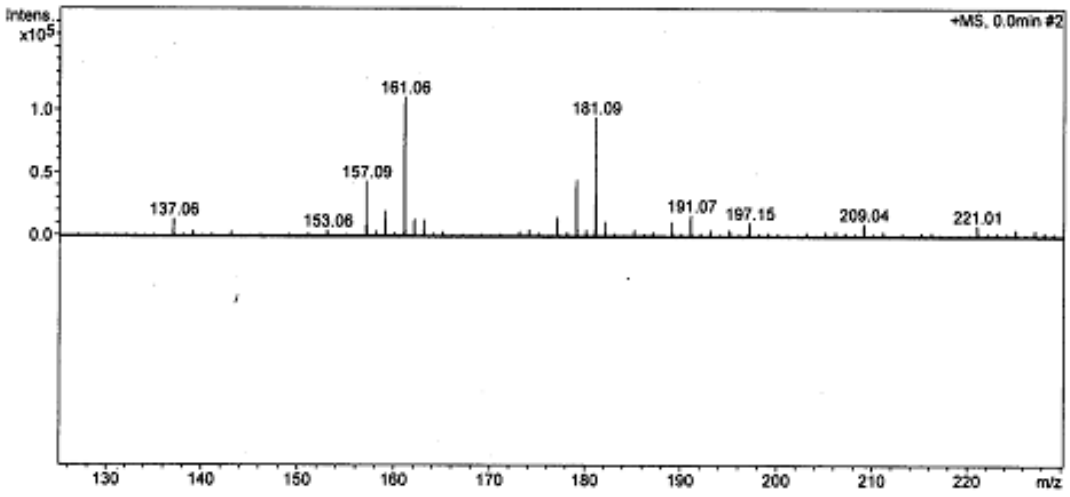

Figure 81 EIMS spectrum of phenylacetic acid

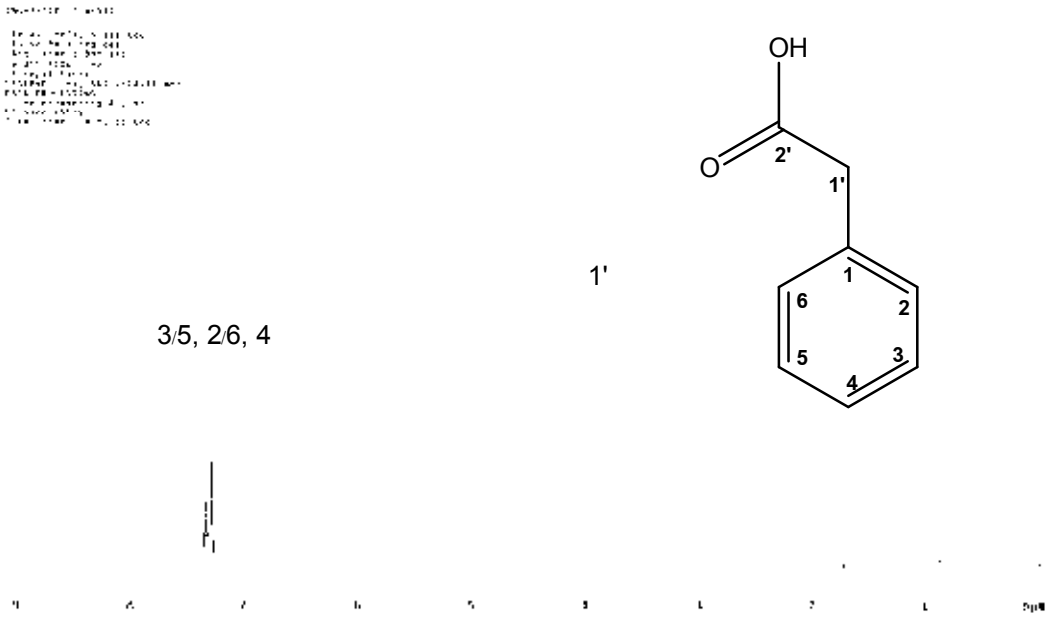

Figure 82 ^{1}H-NMR spectrum of phenylacetic acid **(500 MHz, $CDCl_3$)**

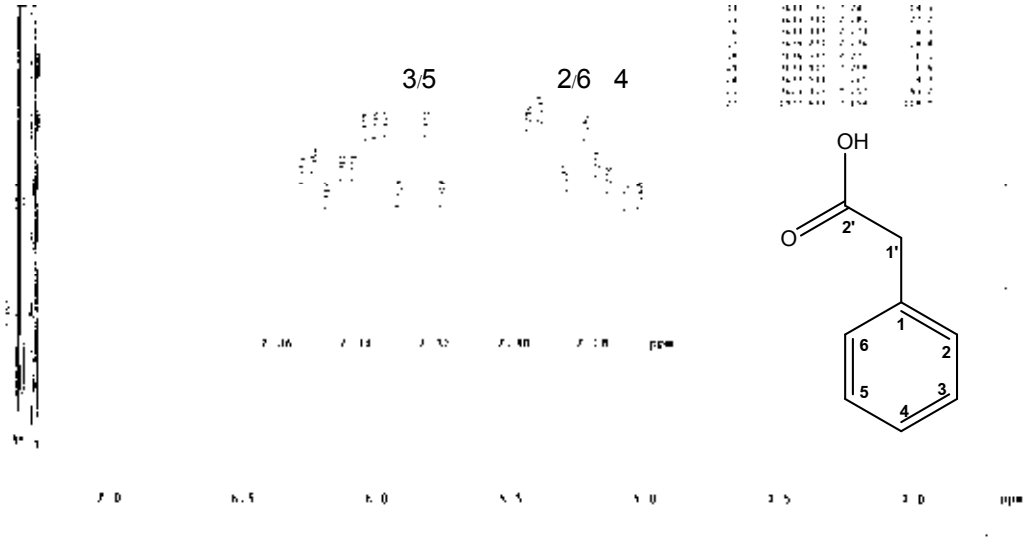

Figure 83 Expanded ^{1}H-NMR spectrum of phenylacetic acid (500 MHz, $CDCl_3$)

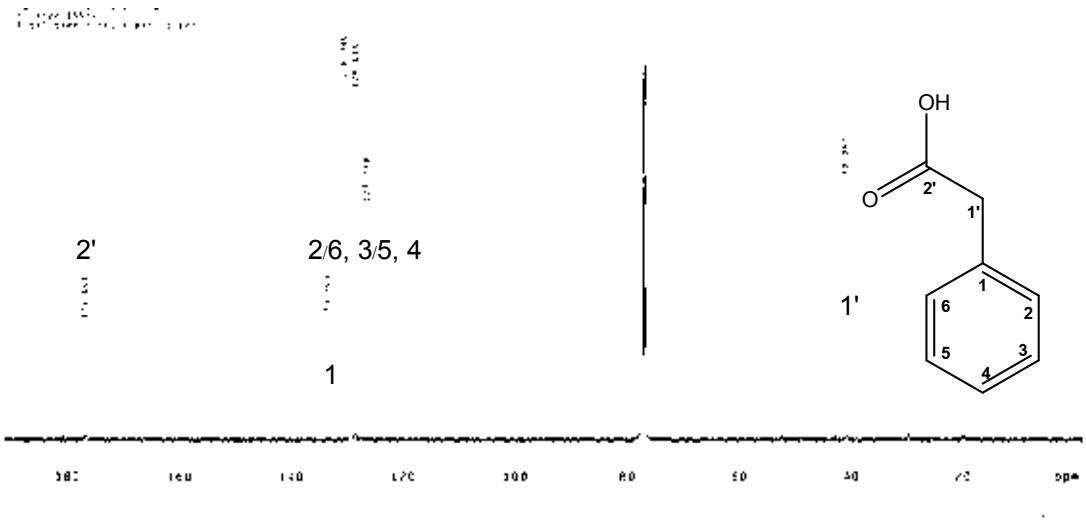

Figure 84 ^{13}C-NMR spectrum of phenylacetic acid (125 MHz, $CDCl_3$)

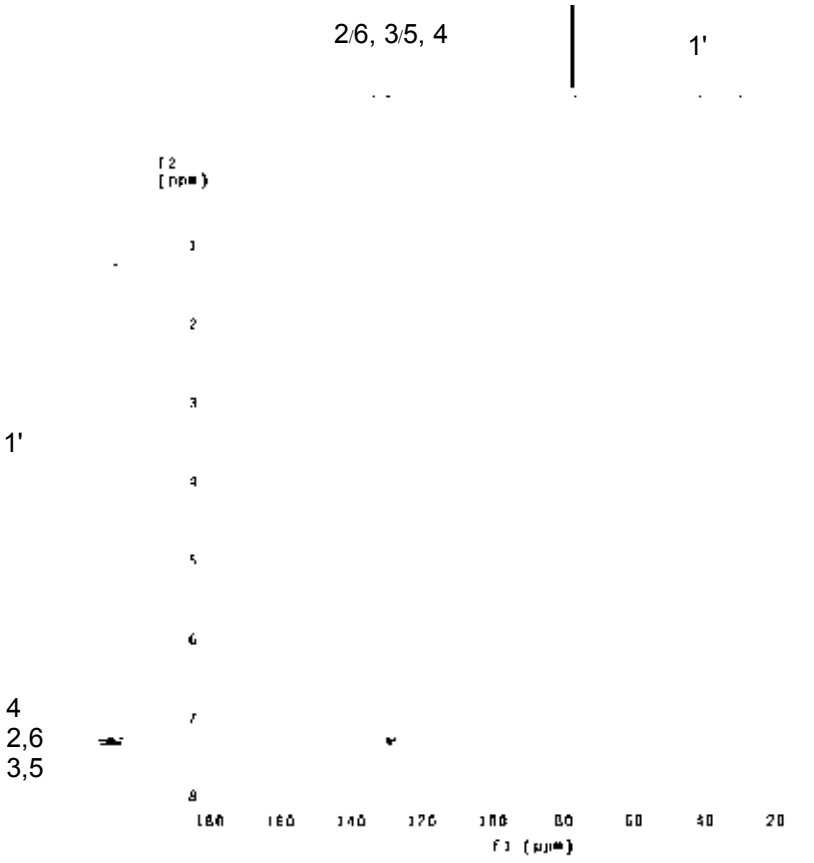

Figure 85 HSQC spectrum of phenylacetic acid ($CDCl_3$)

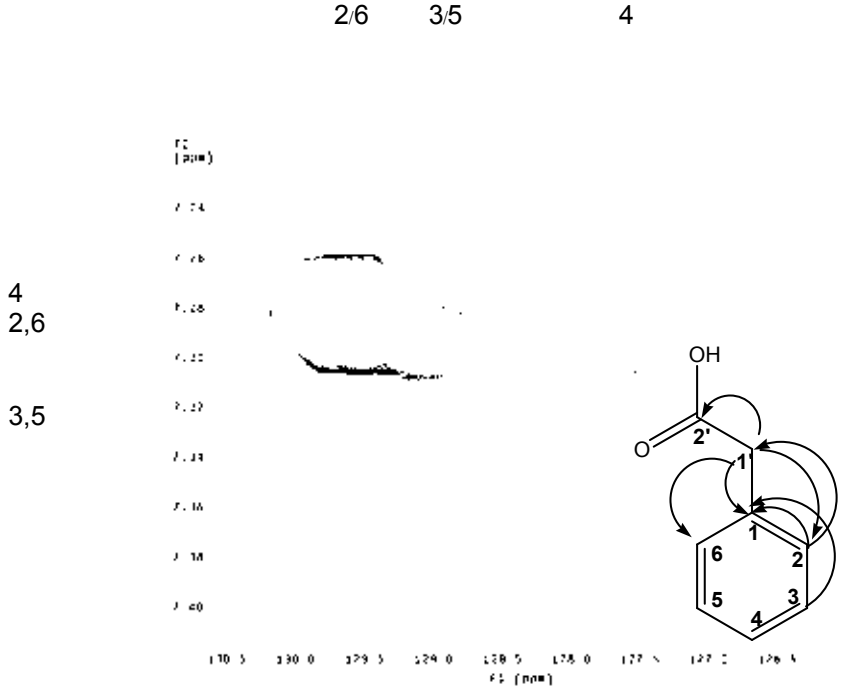

Figure 86 Expanded HSQC spectrum of phenylacetic acid ($CDCl_3$)

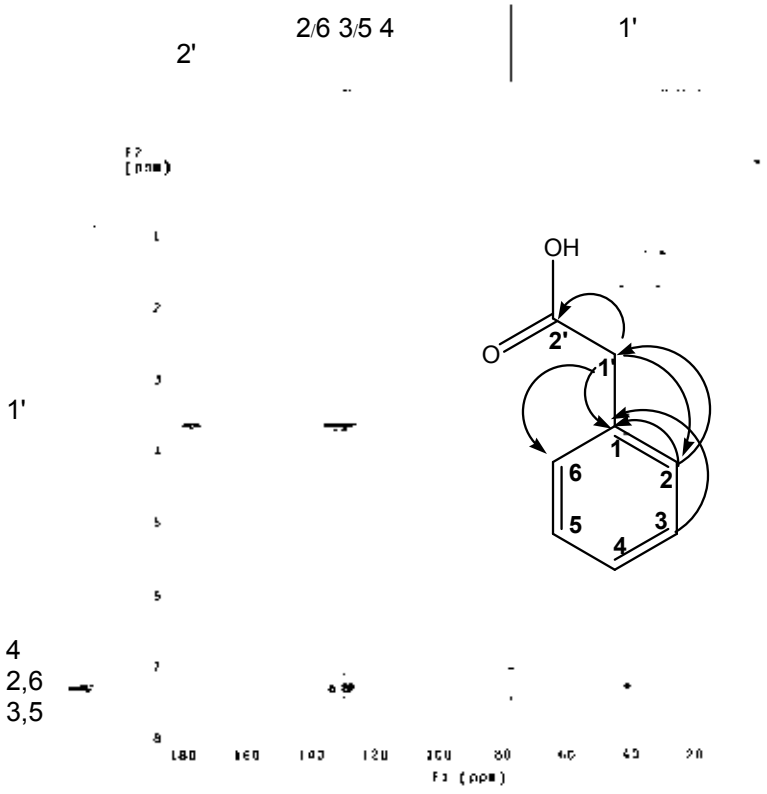

Figure 87 HMBC spectrum of phenylacetic acid ($CDCl_3$)

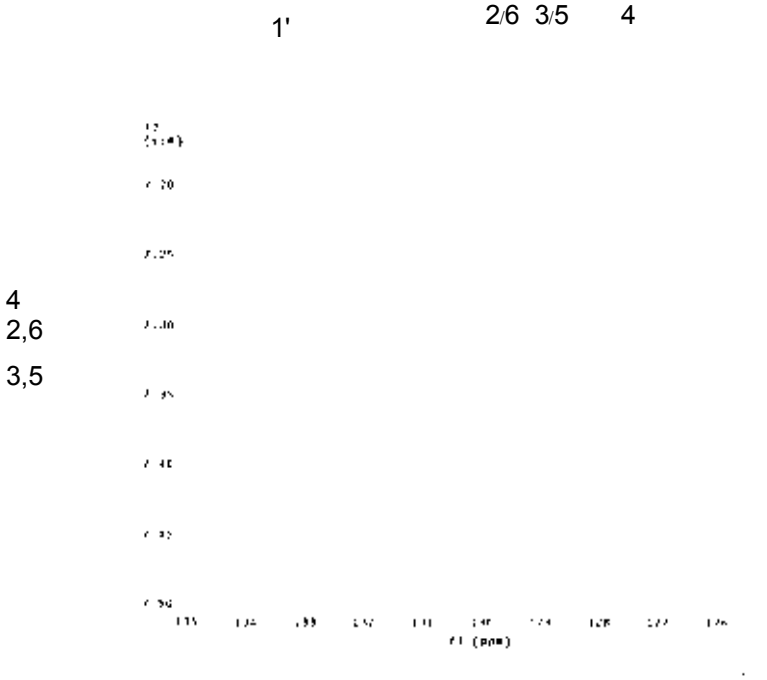

Figure 88 Expanded HMBC spectrum of phenylacetic acid ($CDCl_3$)

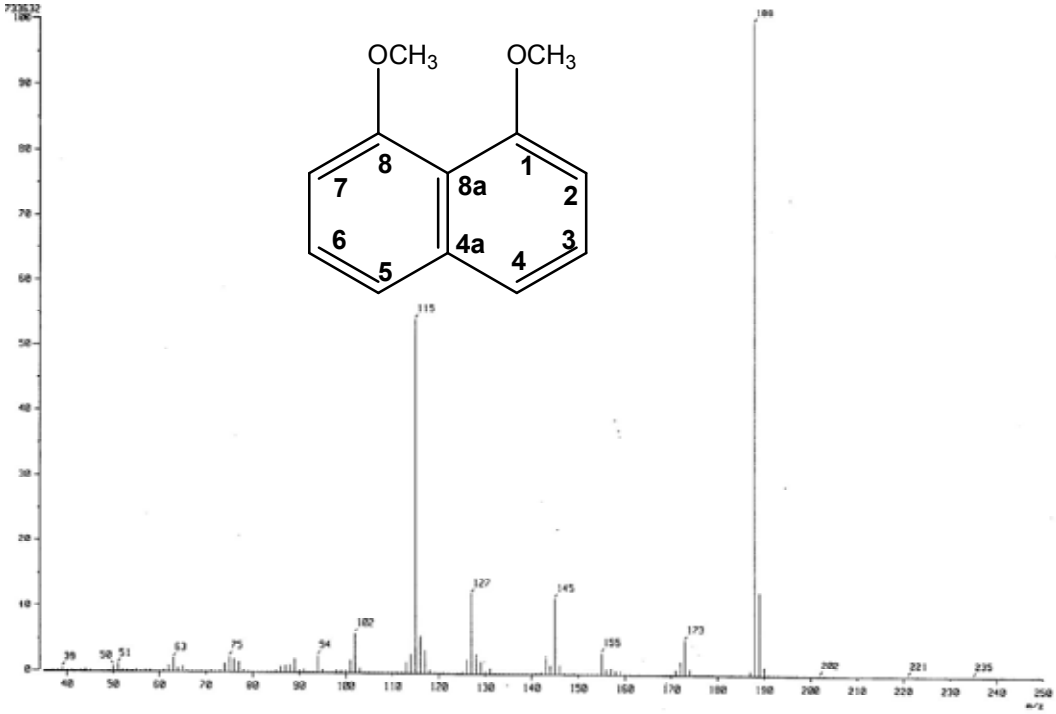

Figure 89 EIMS spectrum of 1,8-dimethoxynaphthalene

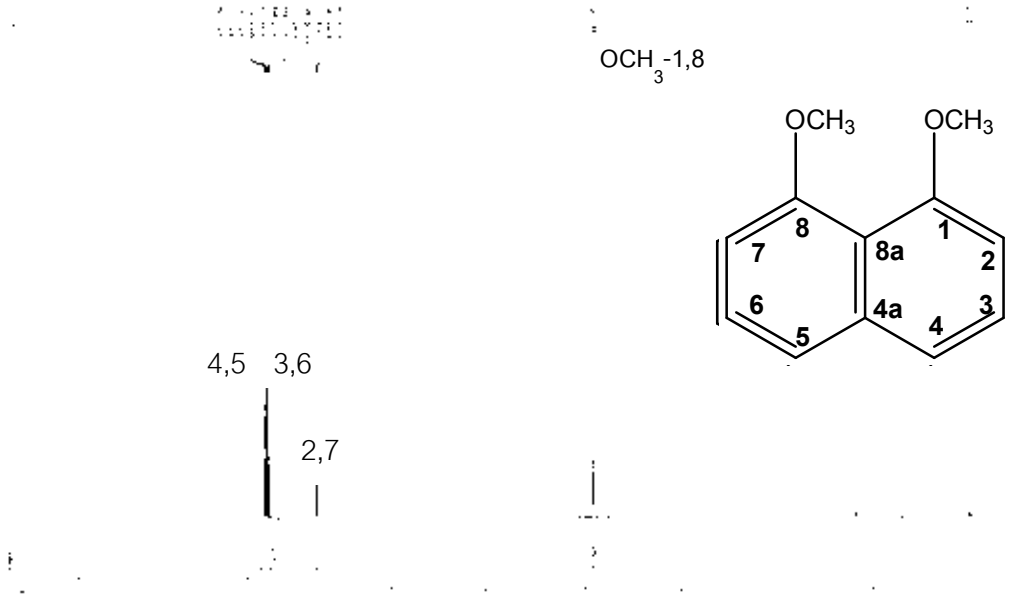

Figure 90 ^{1}H-NMR spectrum of 1,8-dimethoxynaphthalene (500 MHz, $CDCl_3$)

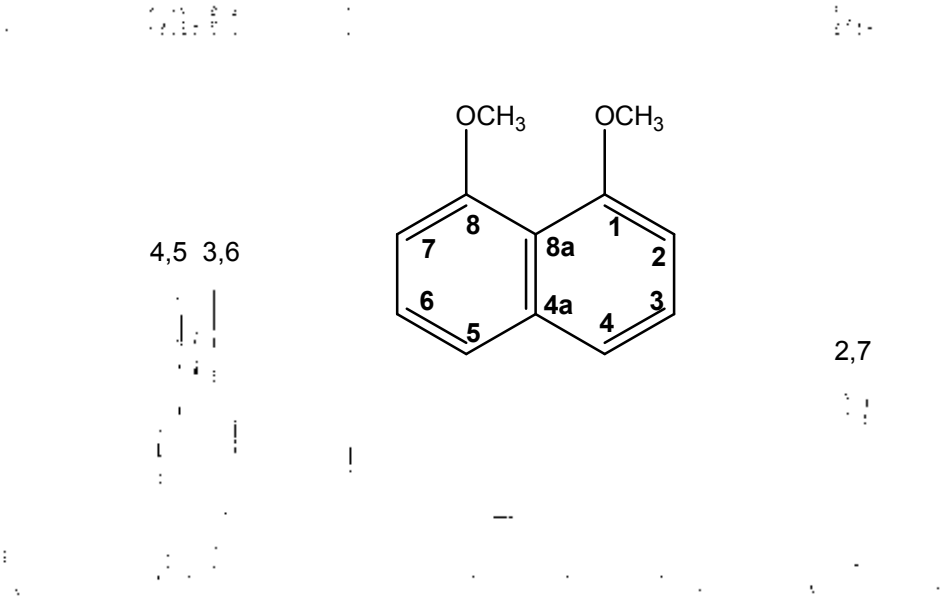

Figure 91 Expanded ^{1}H-NMR spectrum of 1,8-dimethoxynaphthalene (500 MHz, $CDCl_3$)

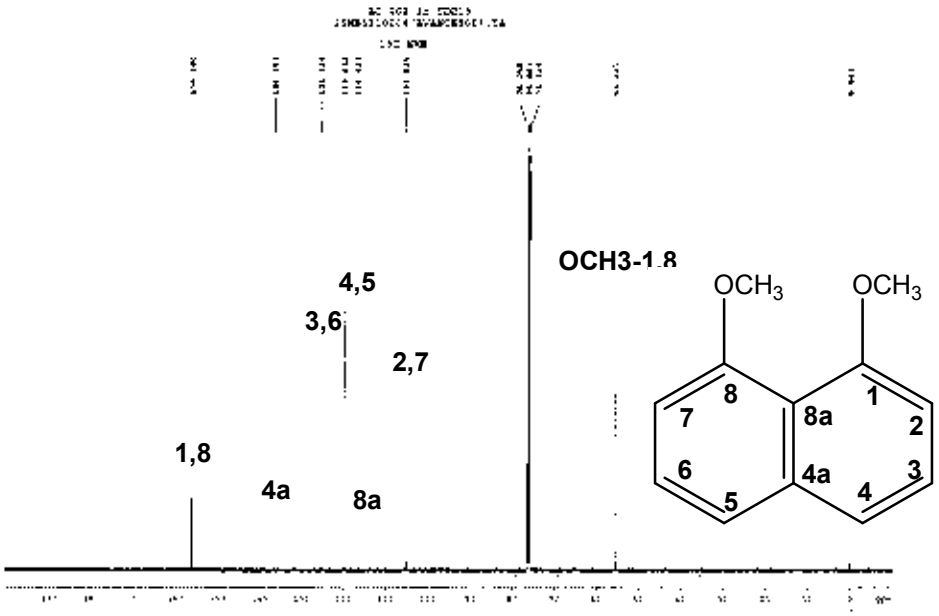

Figure 92 ^{13}C-NMR spectrum of 1,8-dimethoxynaphthalene125 MHz, $CDCl_3$)

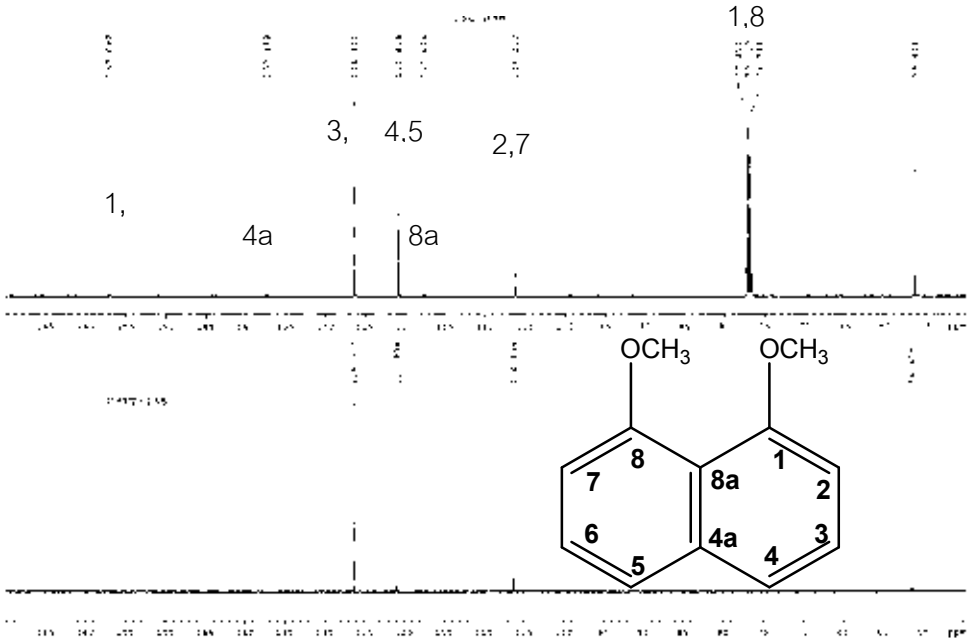

Figure 93 DEPT 135 spectrum of 1,8-dimethoxynaphthalene (125 MHz, $CDCl_3$)

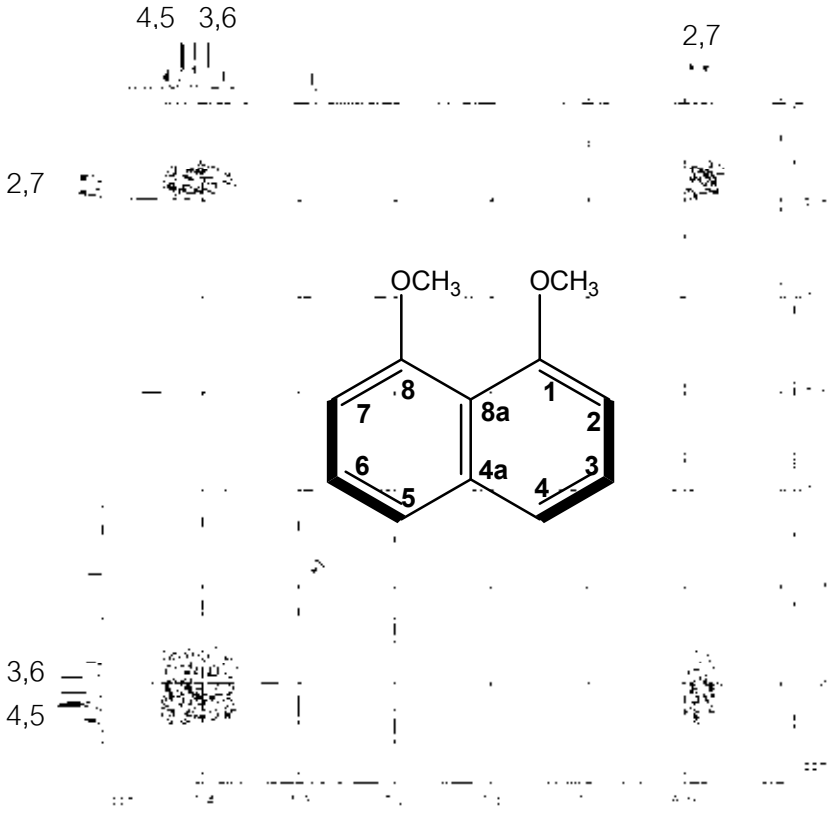

Figure 94 ^1H-^1H COSY spectrum of 1,8-dimethoxynaphthalene ($CDCl_3$)

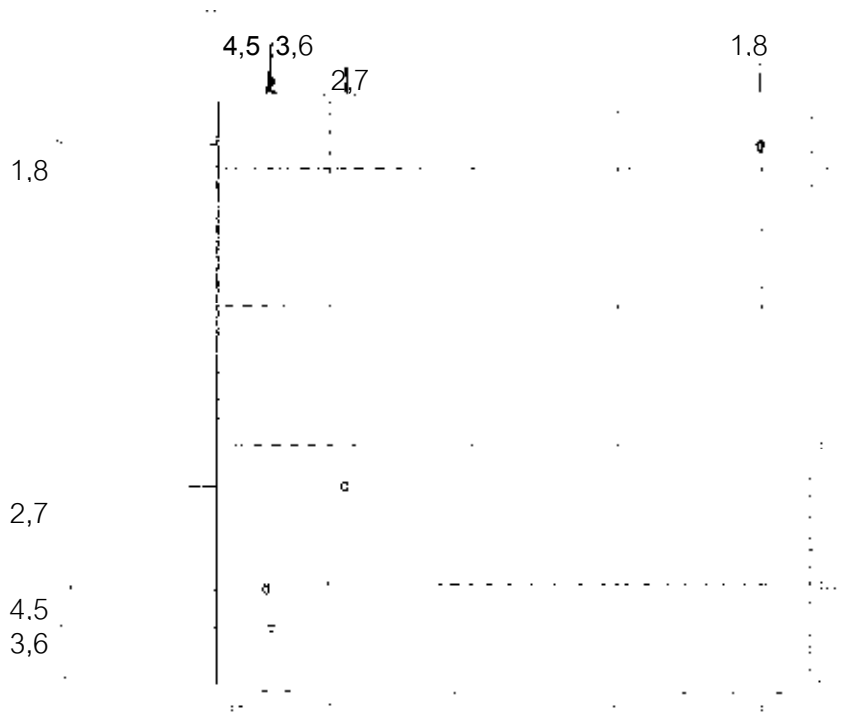

Figure 95 HMQC spectrum of 1,8-dimethoxynaphthalene ($CDCl_3$)

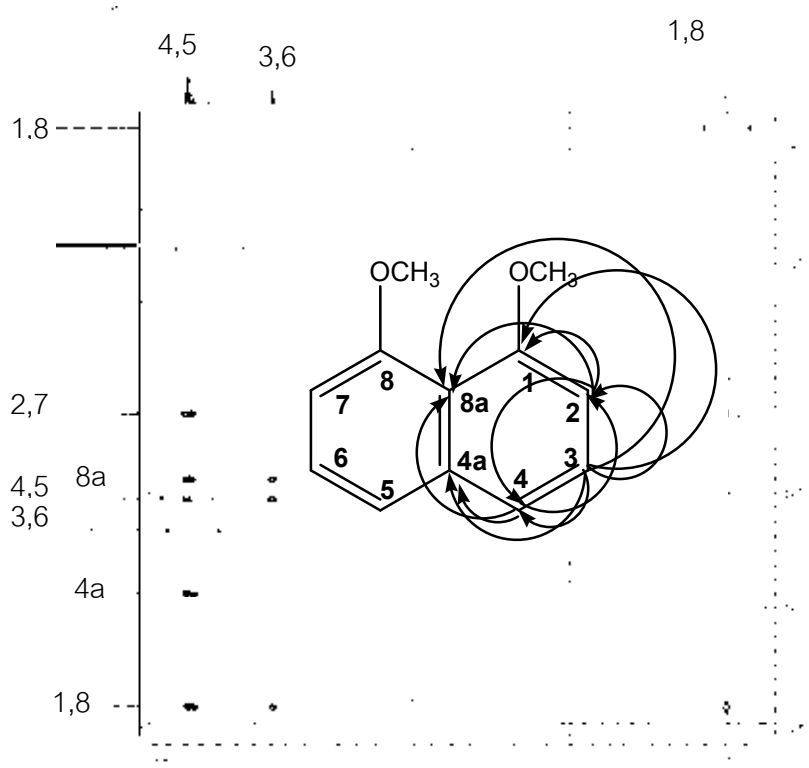

Figure 96 HMBC spectrum of 1,8-dimethoxynaphthalene ($CDCl_3$)

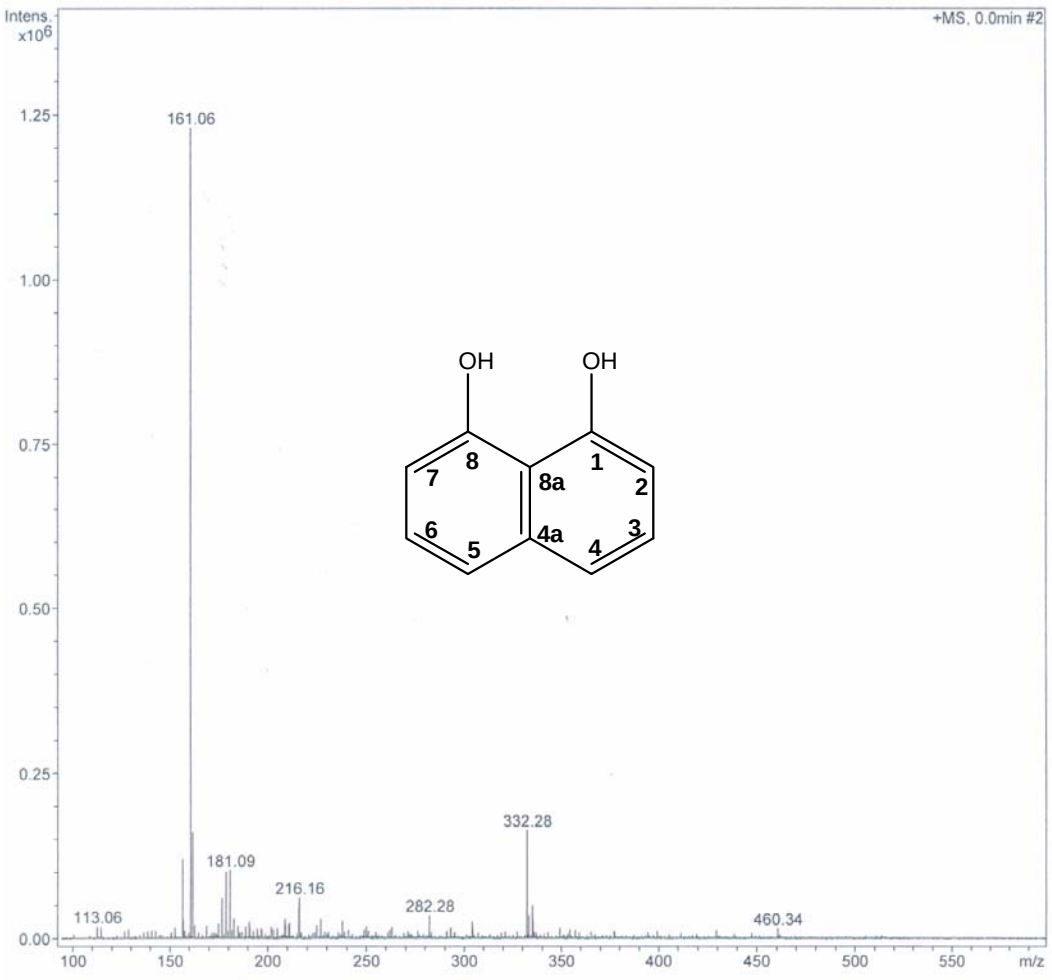

Figure 97 ESI-TOF MS spectrum of 1,8-dihydroxynaphthalene

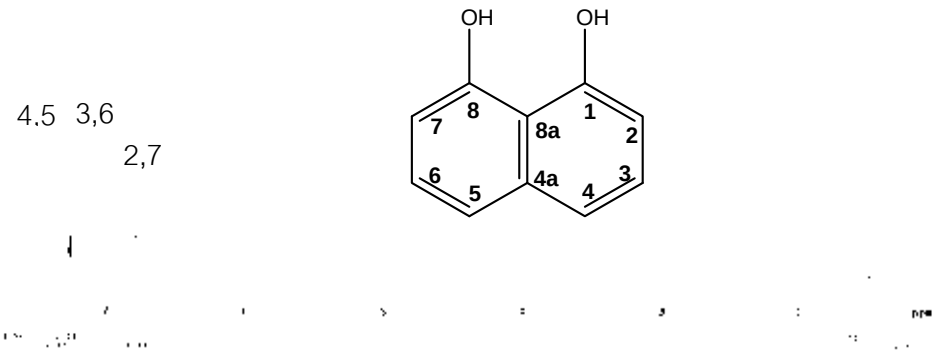

Figure 98 ^{1}H-NMR spectrum of 1,8-dihydroxynaphthalene (500 MHz, $CDCl_3$)

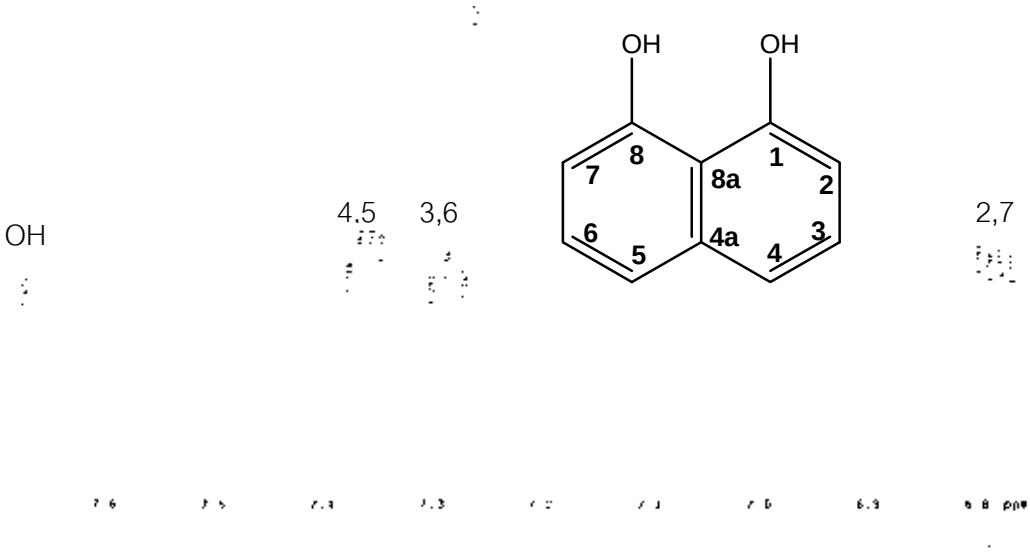

Figure 99 Expanded ^{1}H-NMR spectrum of 1,8-dihydroxynaphthalene (500 MHz, $CDCl_3$)

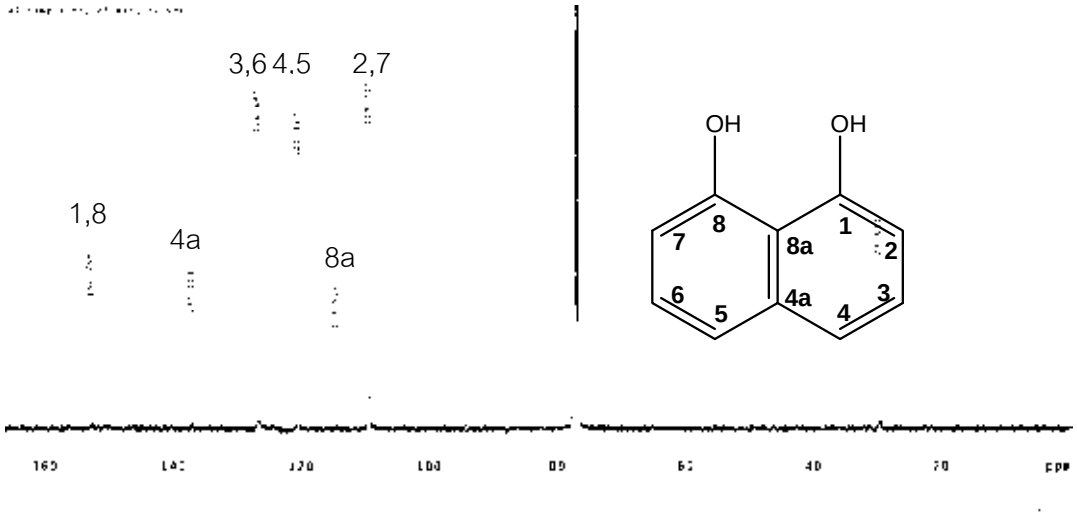

Figure 100 ^{13}C-NMR spectrum of 1,8-dihydroxynaphthalene (125 MHz, $CDCl_3$)

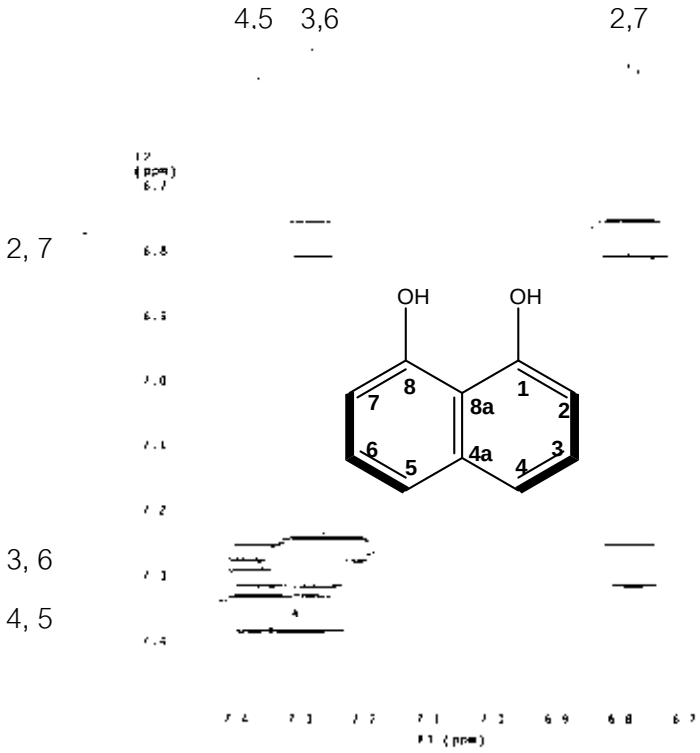

Figure 101 Expanded ^{1}H-^{1}H COSY spectrum of 1,8-dihydroxynaphthalene ($CDCl_3$)

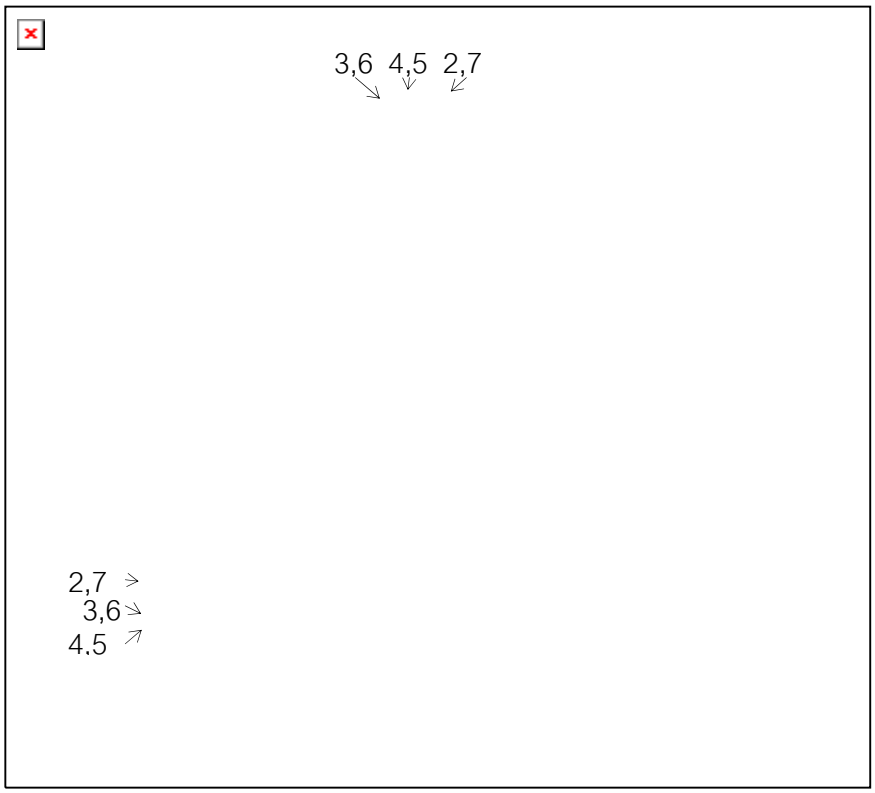

Figure 102 HMQC spectrum of 1,8-dihydroxynaphthalene ($CDCl_3$)

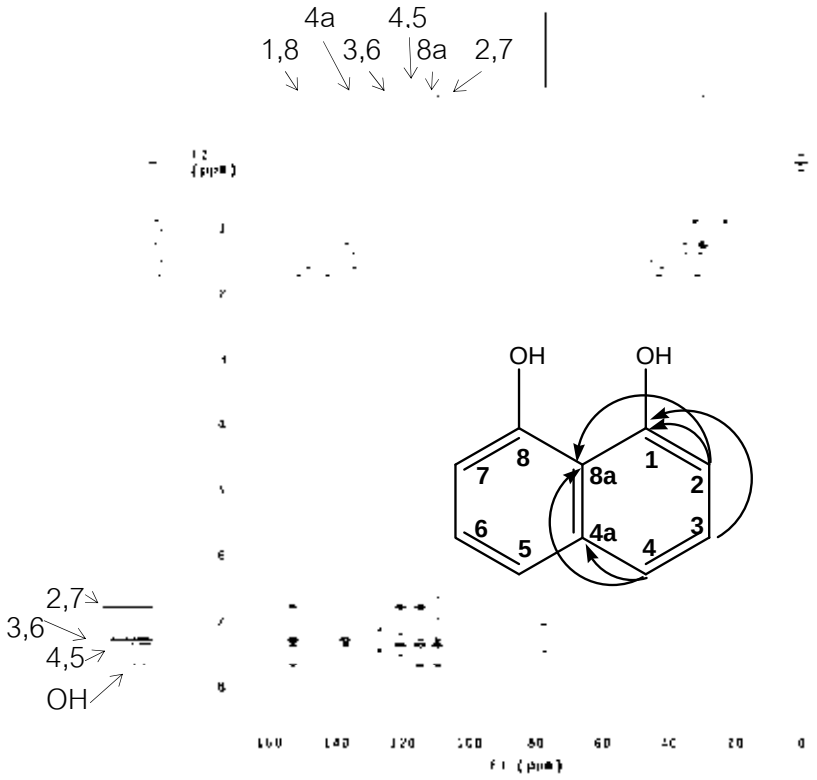

Figure 103 HMBC spectrum of 1,8-dihydroxynaphthalene ($CDCl_3$)

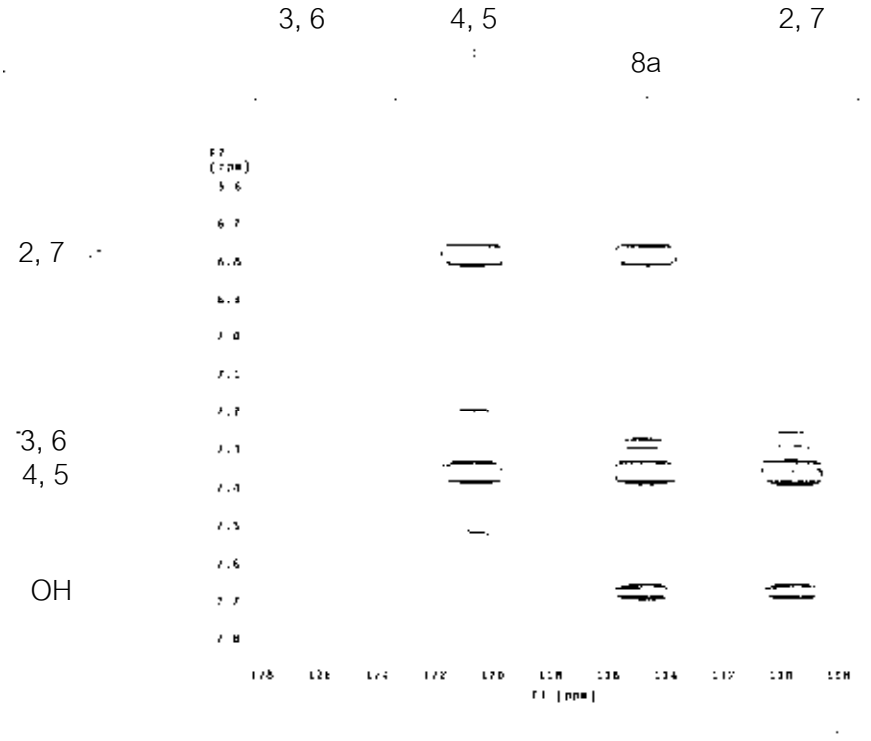

Figure 104 Expanded HMBC spectrum of 1,8-dihydroxynaphthalene ($CDCl_3$)

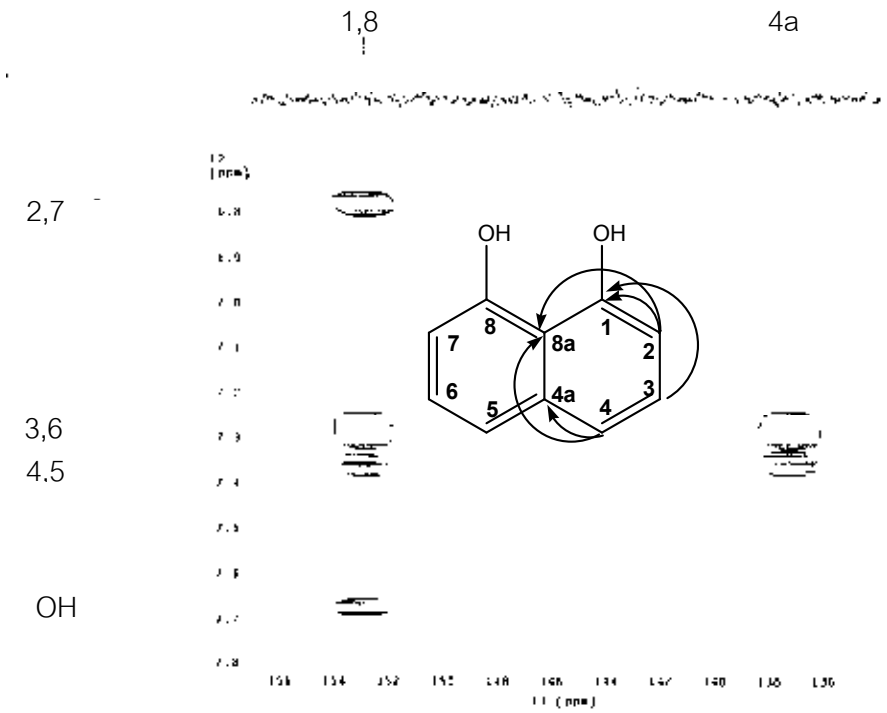

Figure 105 Expanded HMBC spectrum of 1,8-dihydroxynaphthalene ($CDCl_3$)

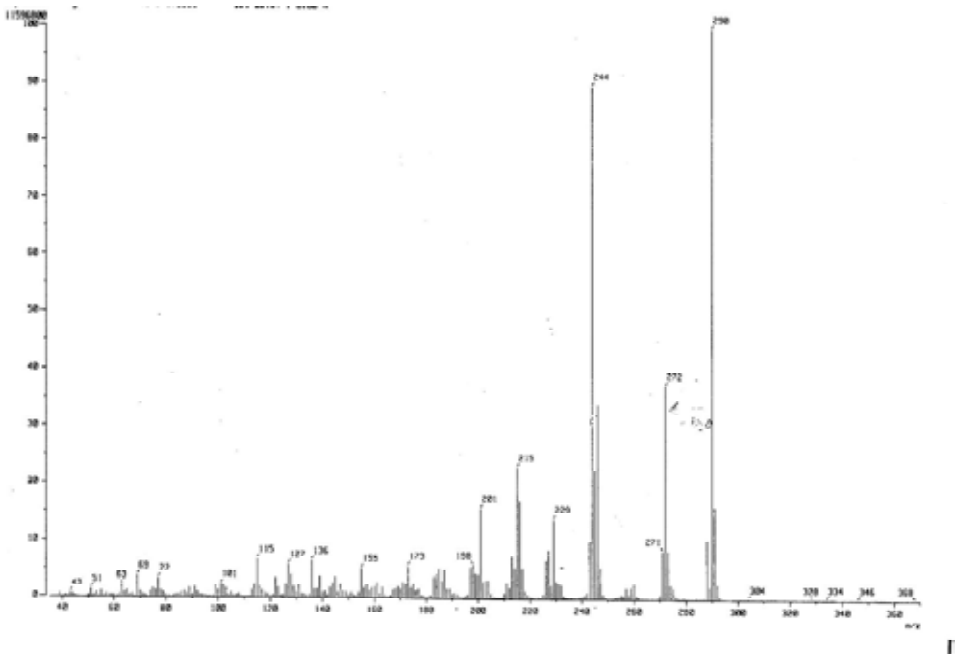

Figure106 EIMS spectrum of altenusin

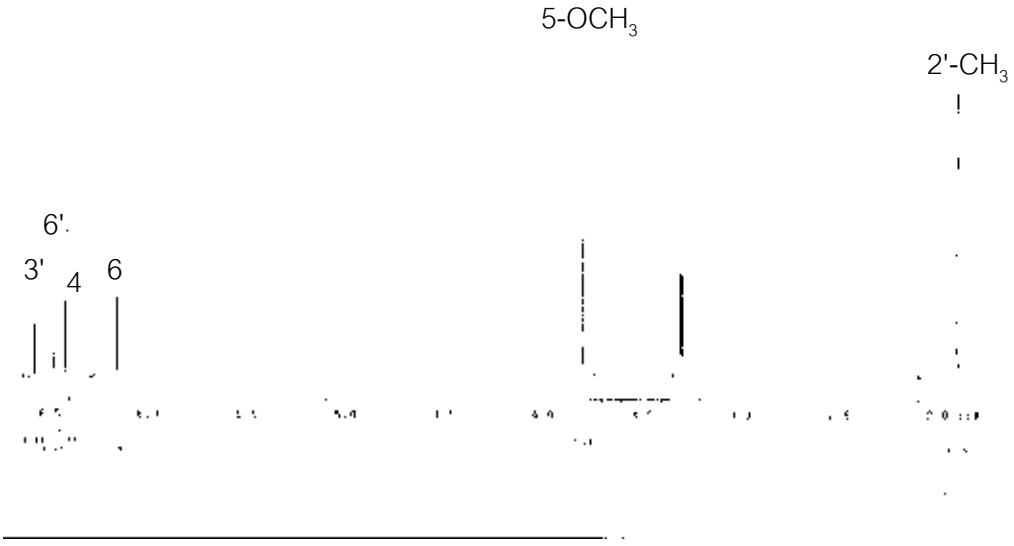

Figure107 ^{1}H-NMR spectrum of altenusin (500 MHz, $CDCl_3$)

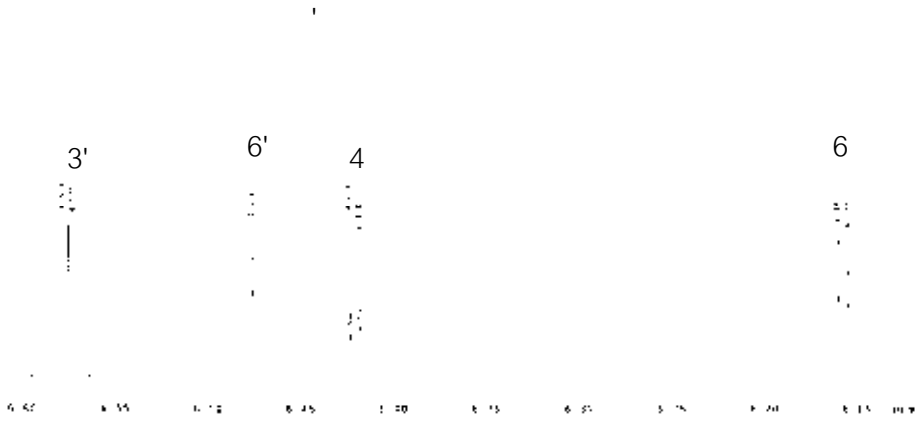

Figure108 Expanded ^{1}H-NMR spectrum of altenusin (500 MHz, $CDCl_3$)

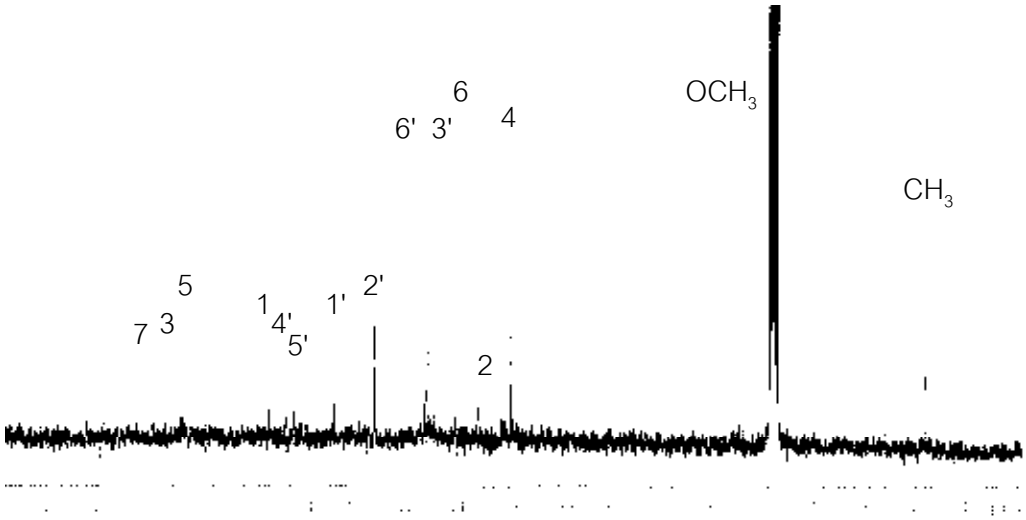

Figure109 ^{13}C-NMR spectrum of altenusin (75 MHz, CD_3OD)

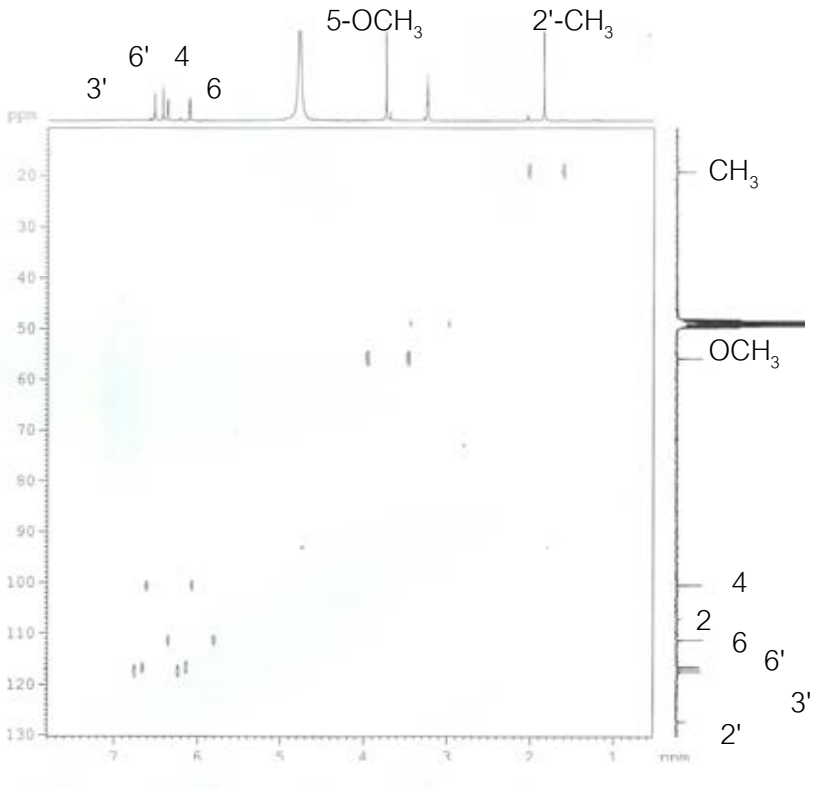

Figure 110 HMQC spectrum of altenusin (CD_3OD)

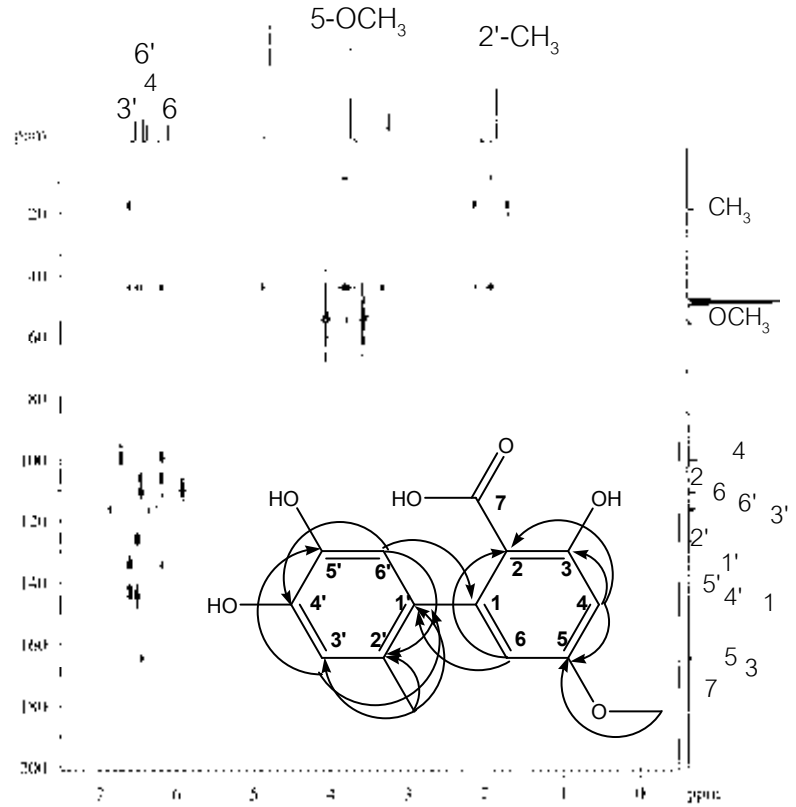

Figure 111 HMBC spectrum of altenusin (CD_3OD)

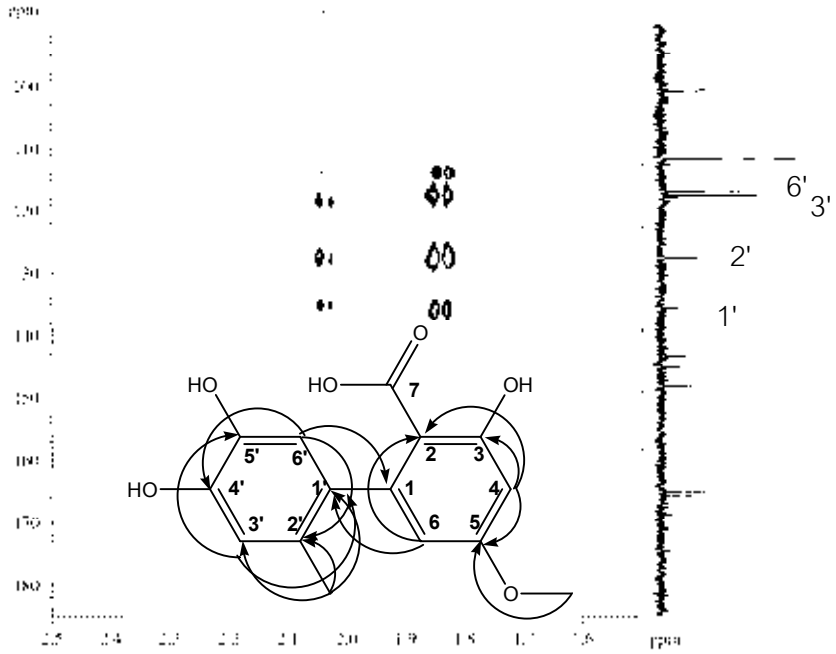

Figure112 Expanded HMBC spectrum of altenusin (CD_3OD)

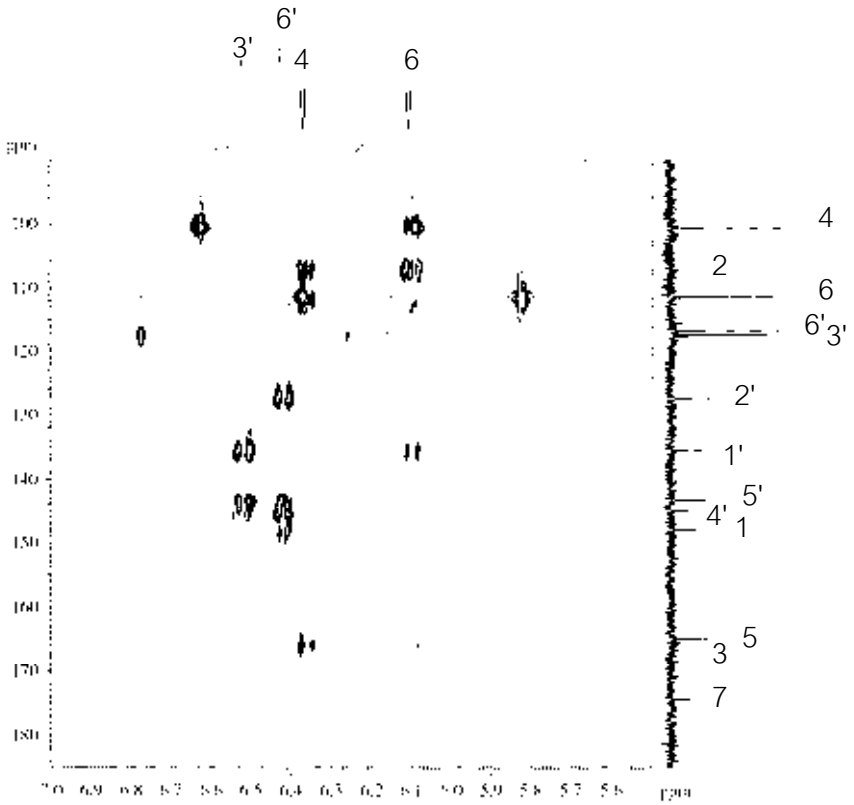

Figure 113 Expanded HMBC spectrum of altenusin (CD_3OD)

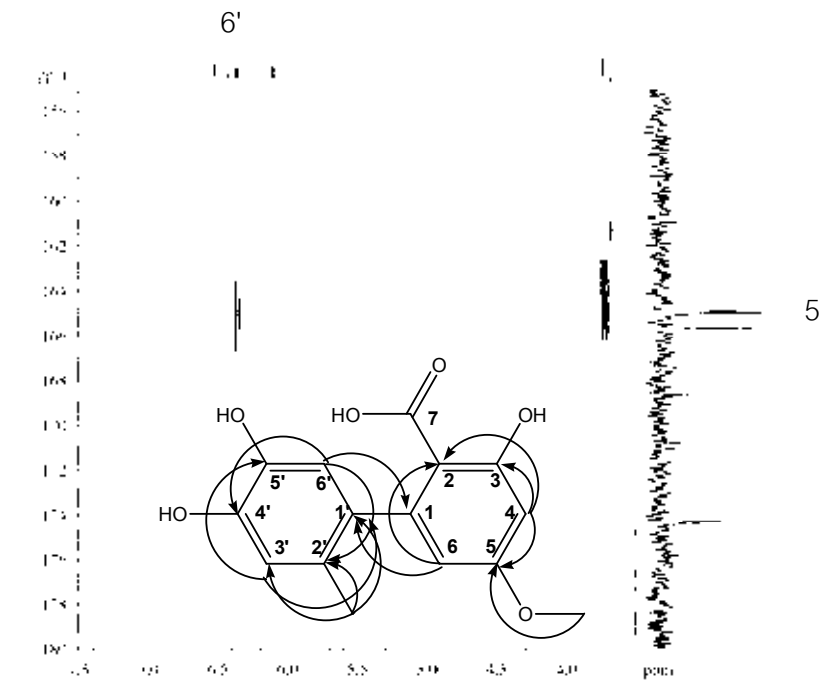

Figure114 Expanded HMBC spectrum of altenusin (CD_3OD)

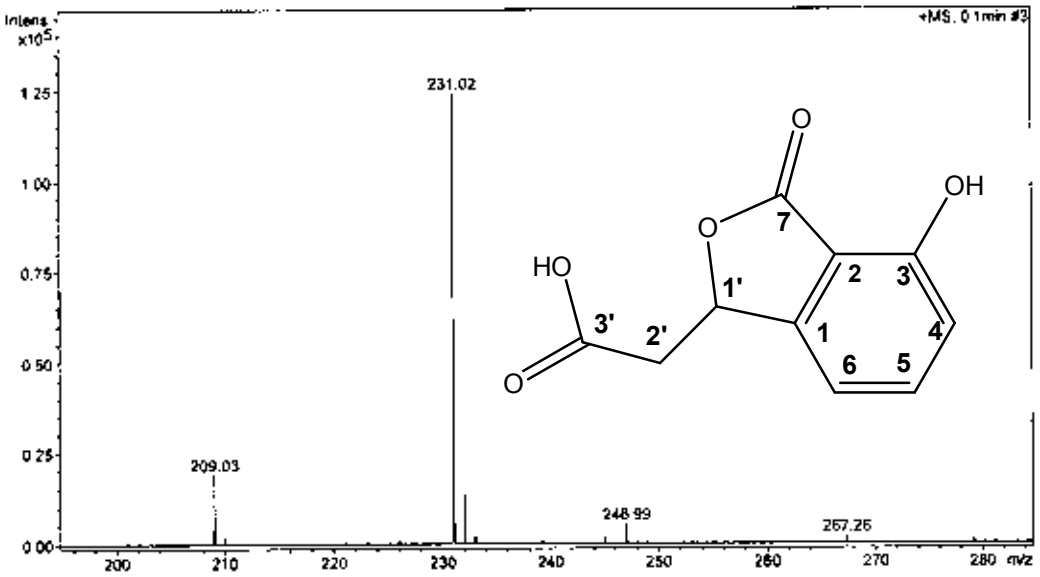

Figure 115 ESI-TOF MS spectrum of Isoochracinic acid

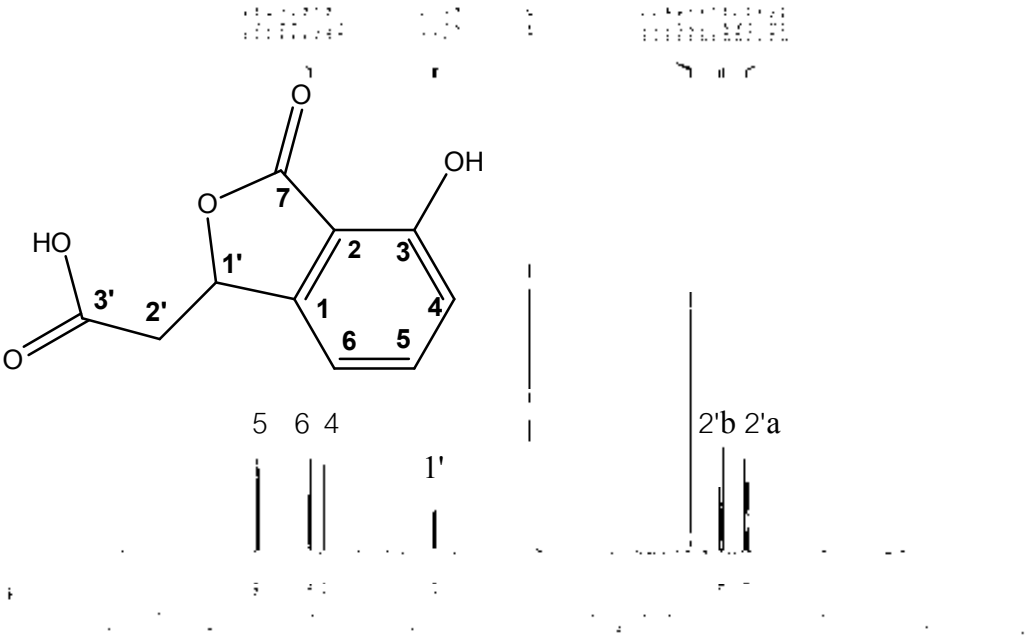

Figure 116 ^{1}H-NMR spectrum of Isoochracinic acid (500 MHz, CD_3OD)

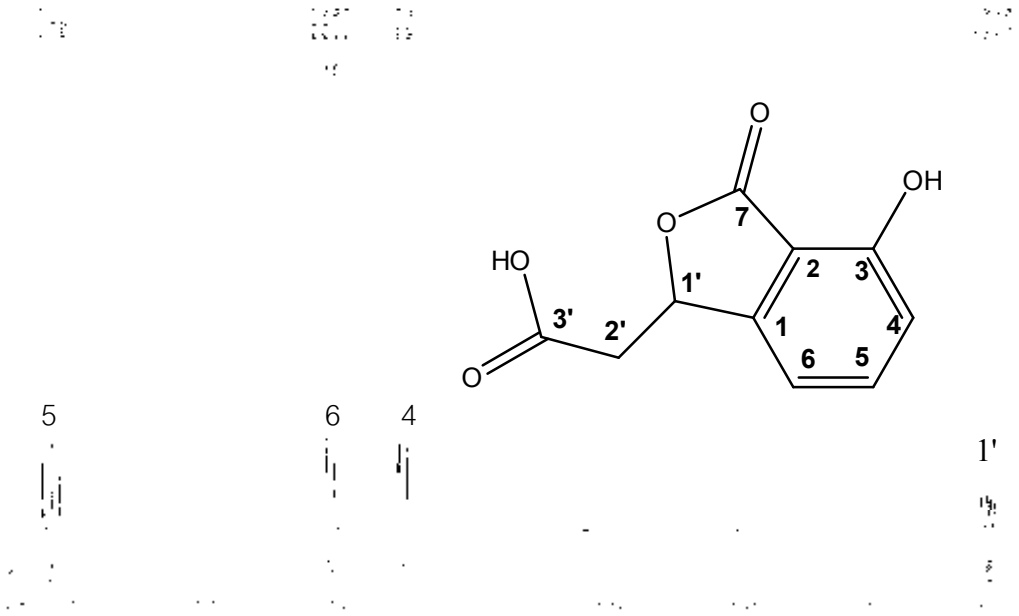

Figure 117 Expanded ^{1}H-NMR spectrum of Isoochracinic acid (500 MHz, CD_3OD)

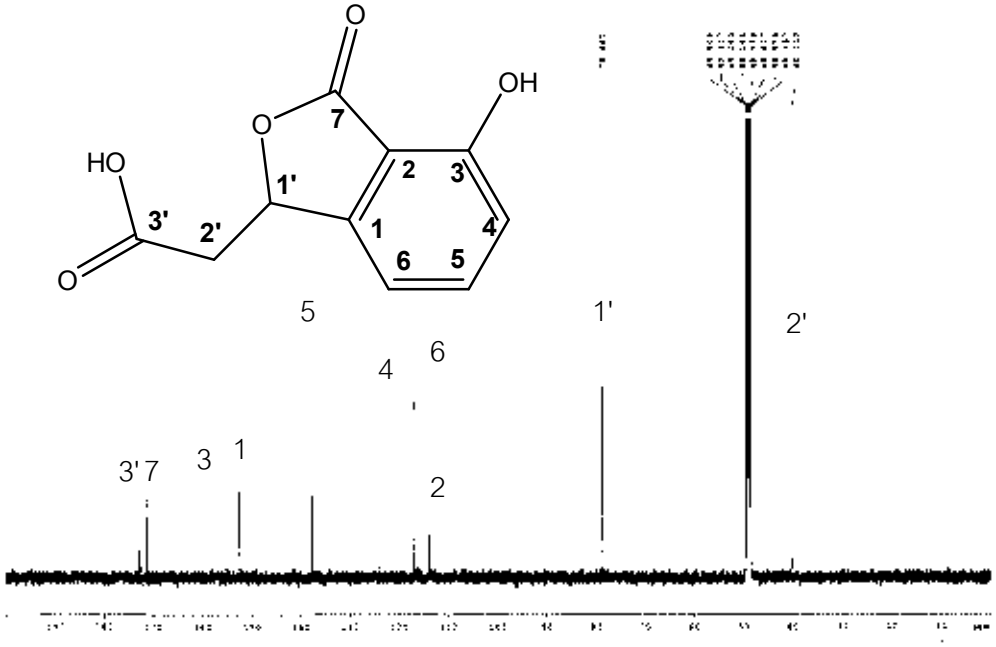

Figure 118 ^{13}C-NMR spectrum of Isoochracinic acid (125 MHz, CD_3OD)

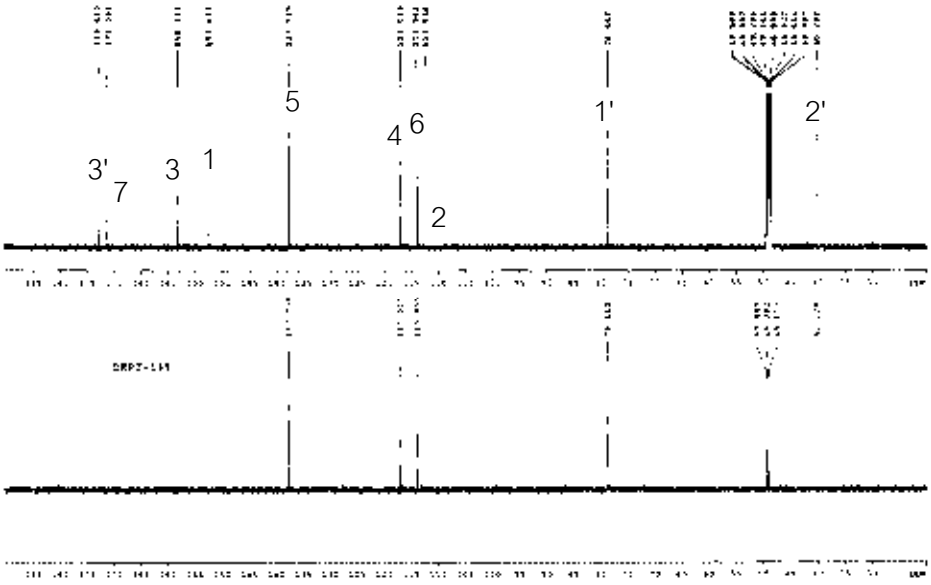

Figure 119 DEPT 135 spectrum of Isoochracinic acid (125 MHz, CD_3OD)

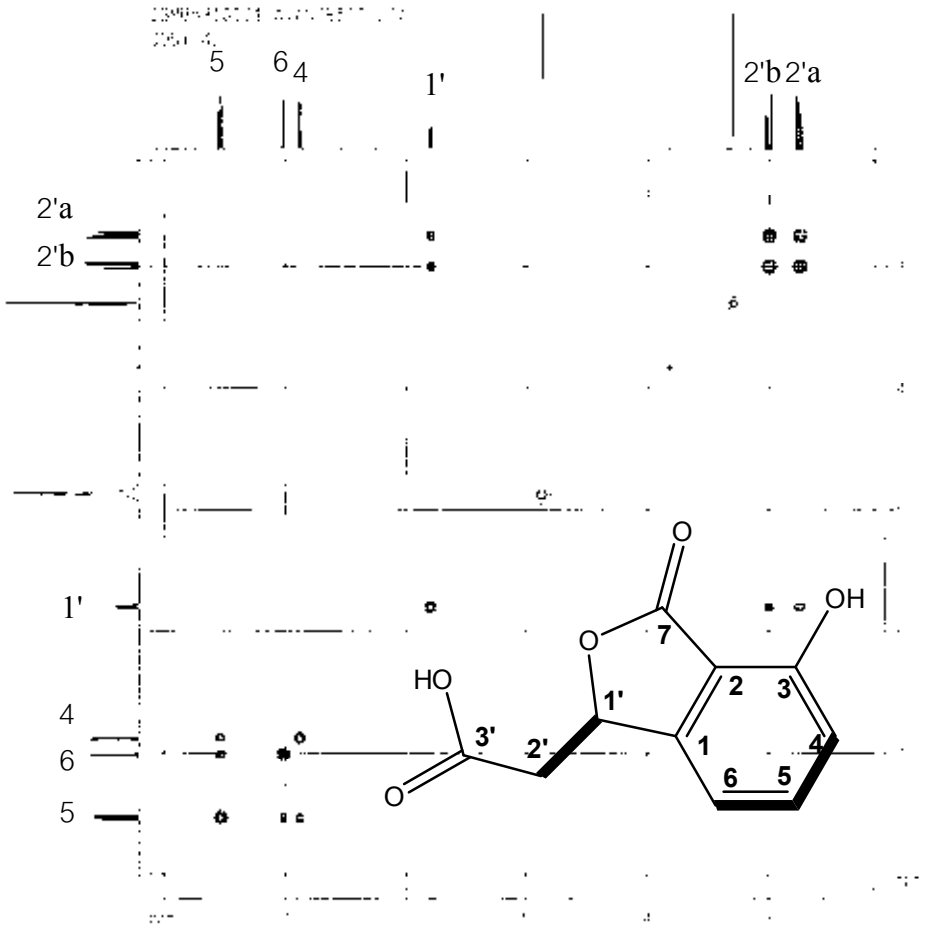

Figure 120 ^1H-^1H COSY spectrum Isoochracinic acid (CD_3OD)

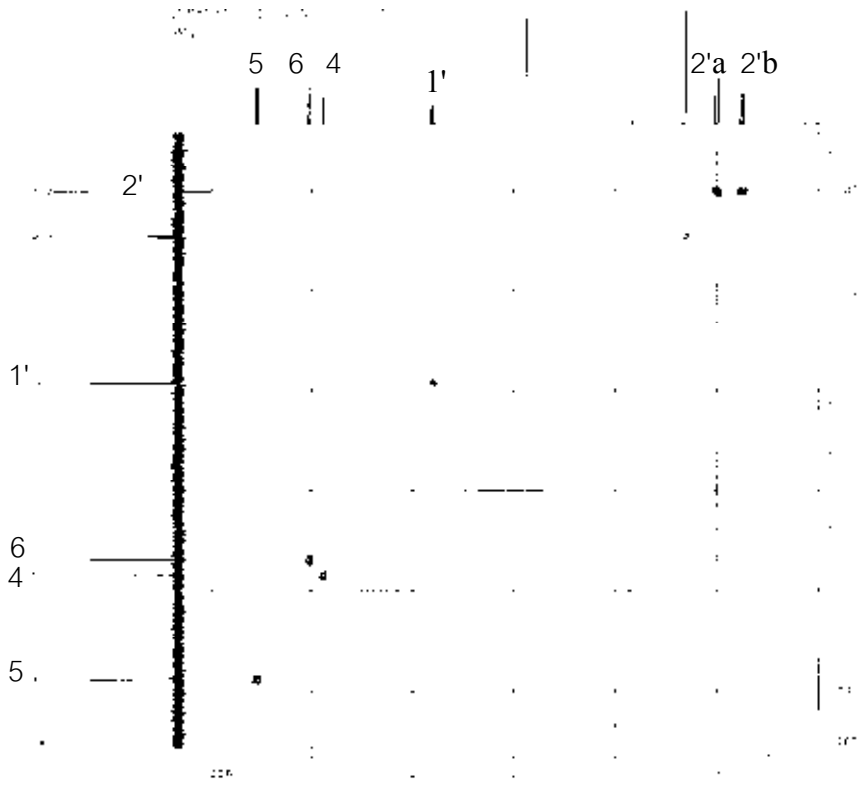

Figure 121 HMQC spectrum Isoochracinic acid (CD_3OD)

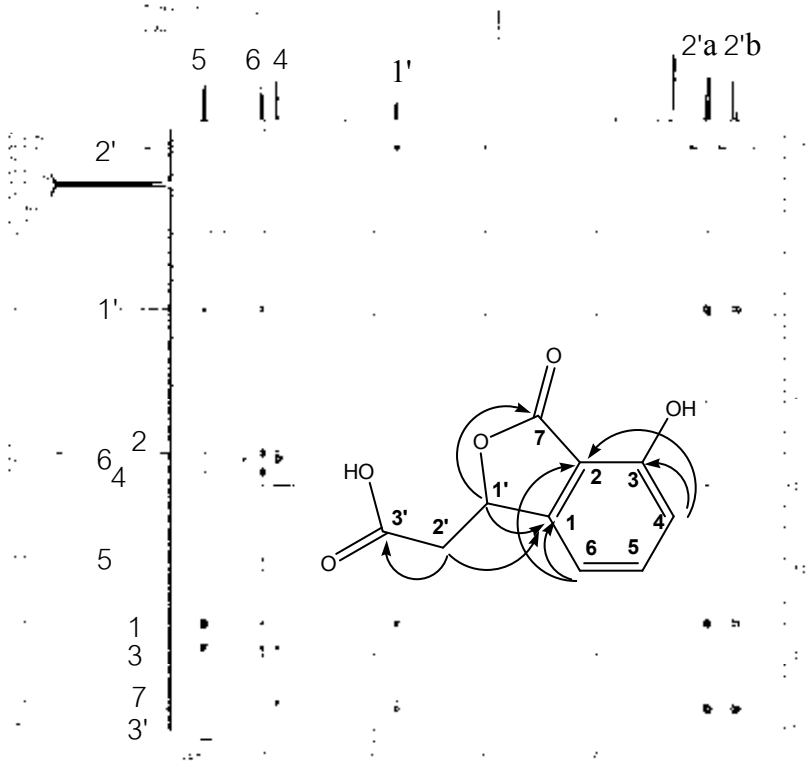

Figure 122 HMBC spectrum Isoochracinic acid (CD_3OD)

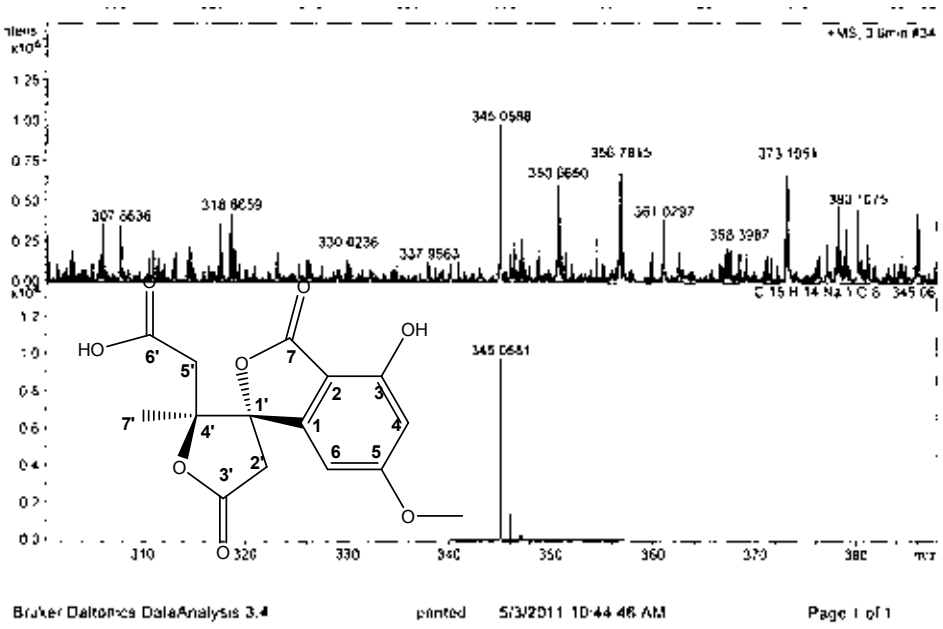

Figure 123 ESI-TOF MS spectrum of altenuic acid

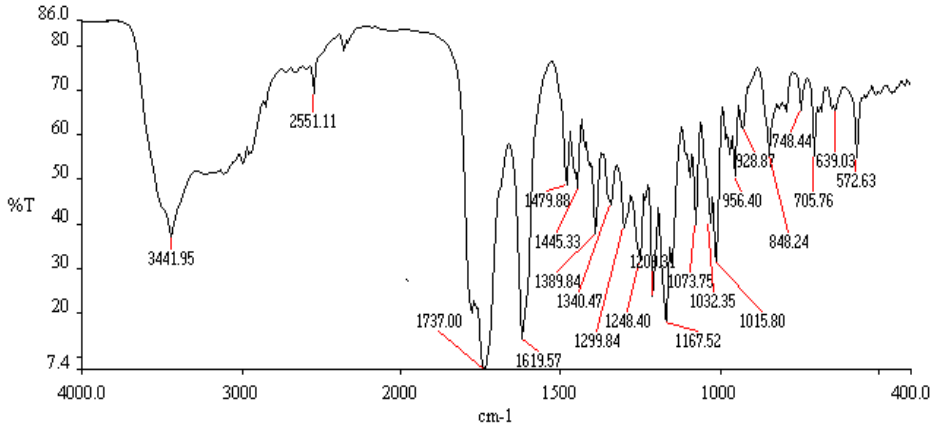

Figure124 The IR spectrum of altenuic acid

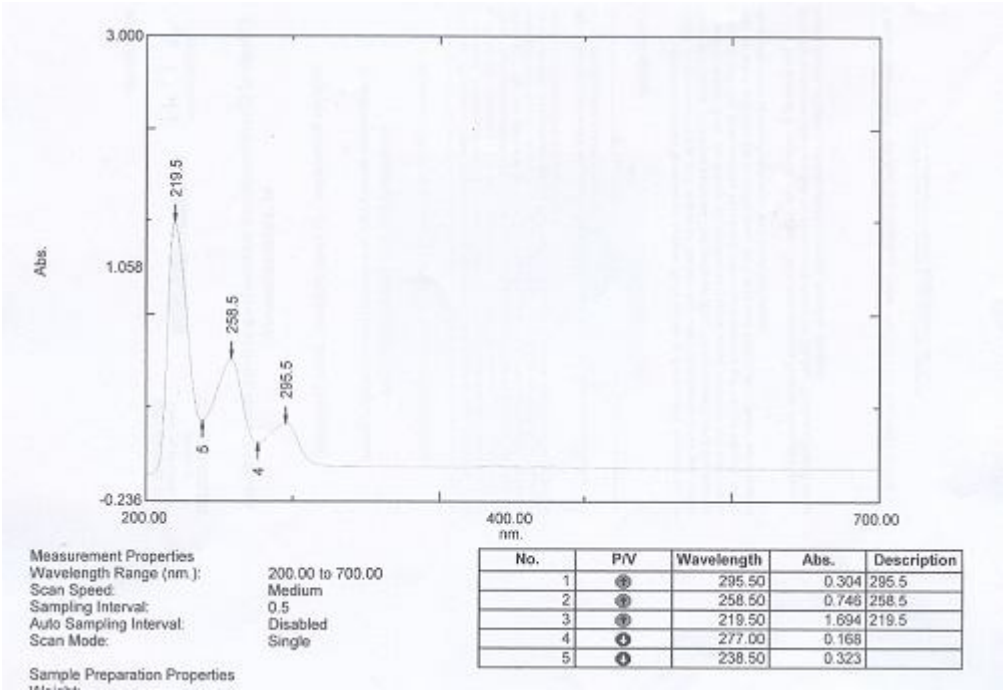

Figure 125 The UV spectrum of altenuic acid

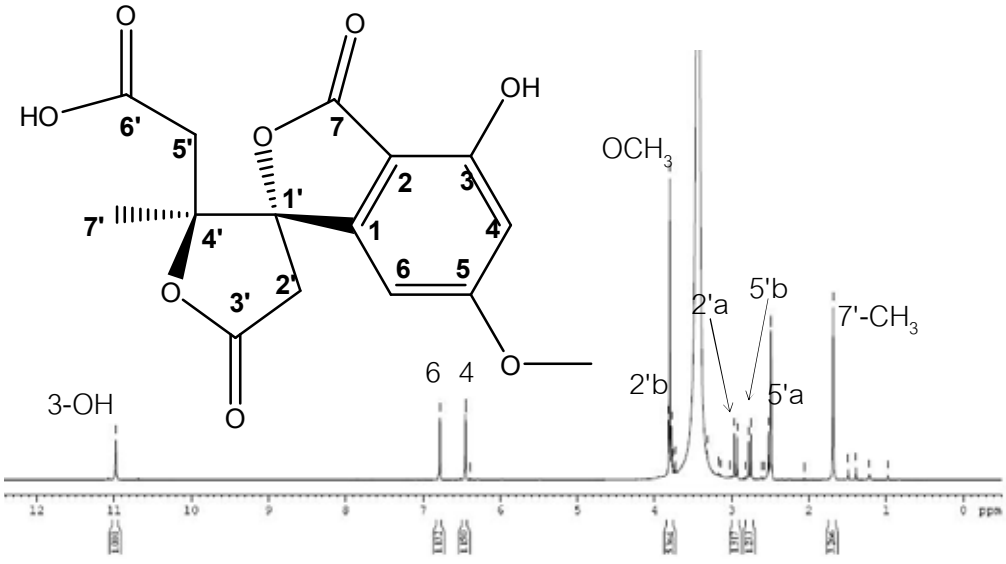

Figure 126 ^{1}H-NMR spectrum of altenuic acid (500 MHz, DMSOd_6)

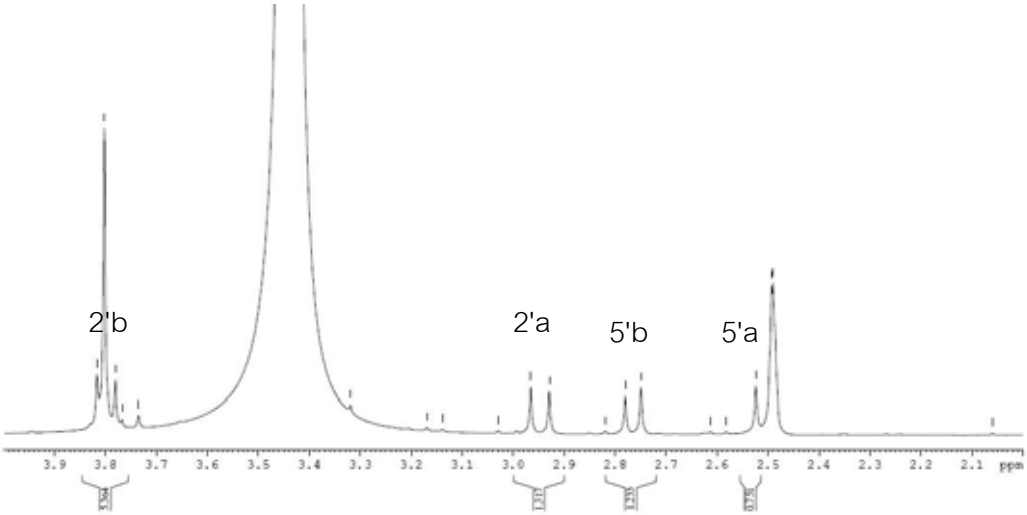

Figure 127 Expanded ^{1}H-NMR spectrum of altenuic acid (500 MHz, DMSOd_6)

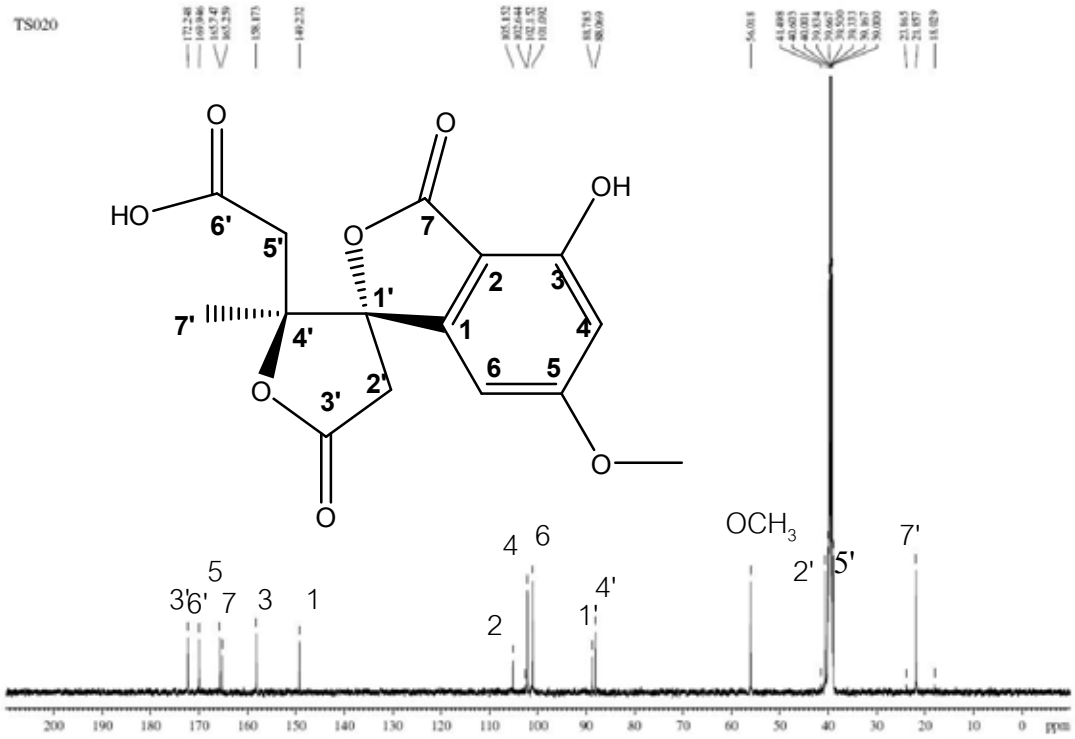

Figure 128 ^{13}C-NMR spectrum of altenuic acid (125 MHz, DMSOd_6)

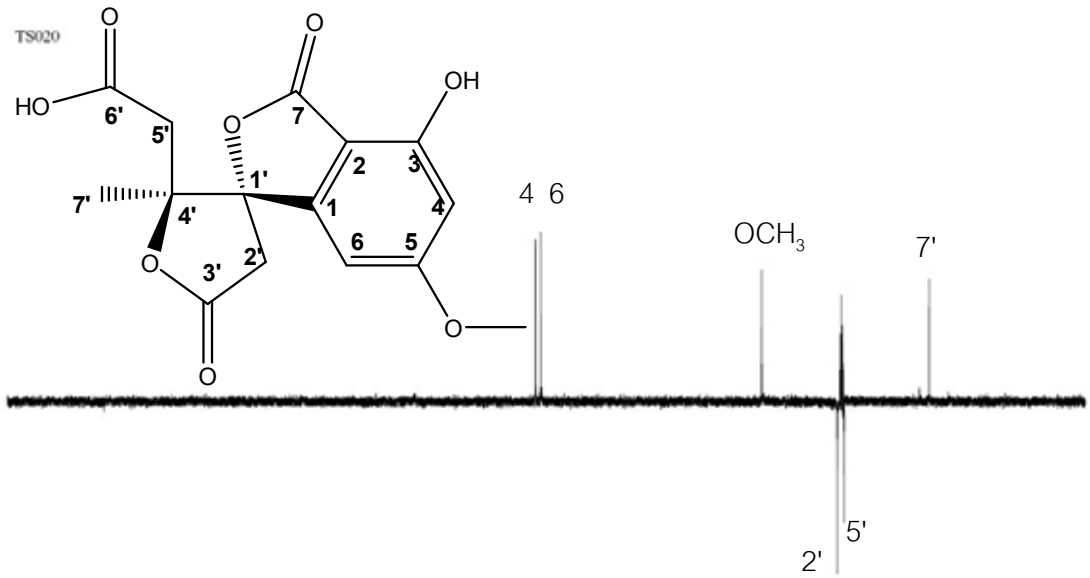

Figure 129 DEPT 135 spectrum of altenuic acid (125 MHz, DMSOd_6)

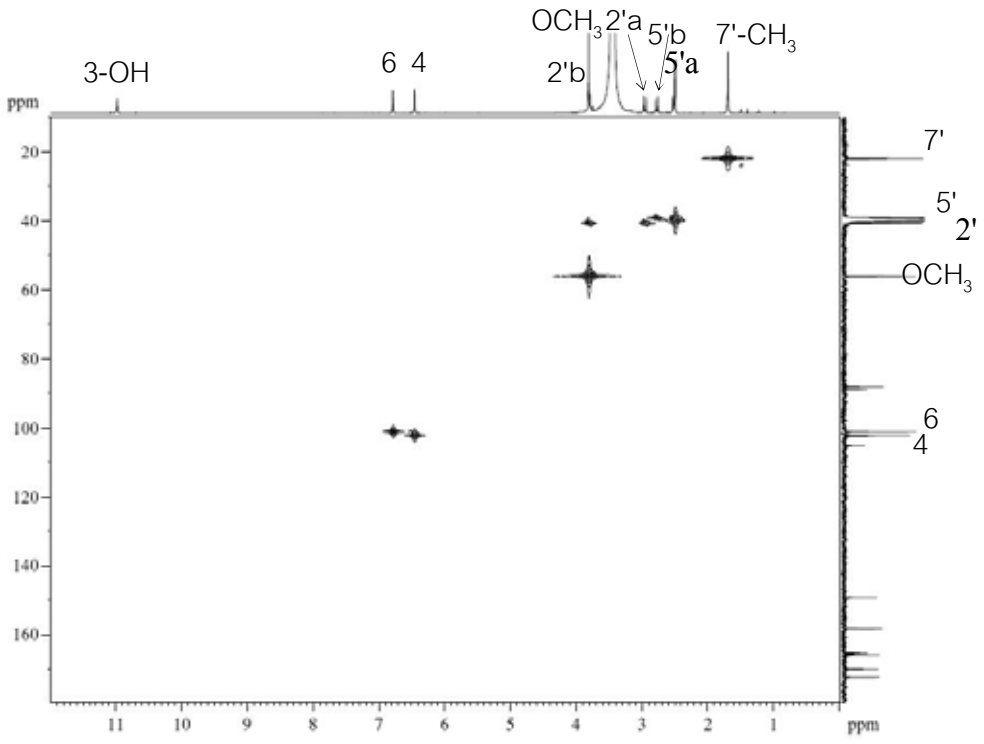

Figure 130 HMQC spectrum of altenuic acid (DMSOd_6)

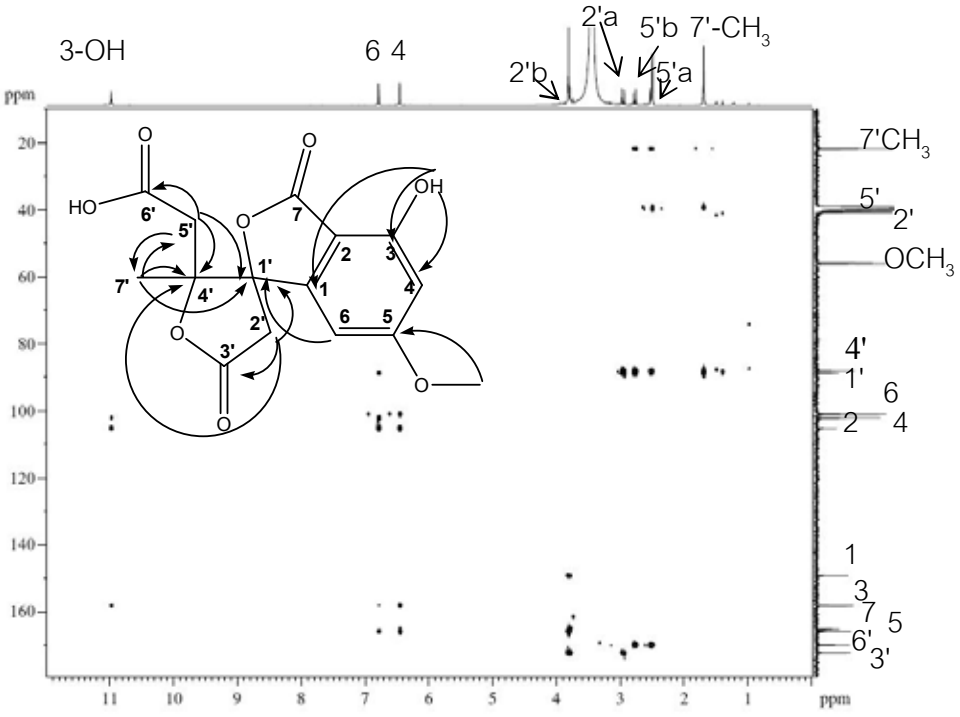

Figure 131 HMBC spectrum of altenuic acid (DMSOd_6)

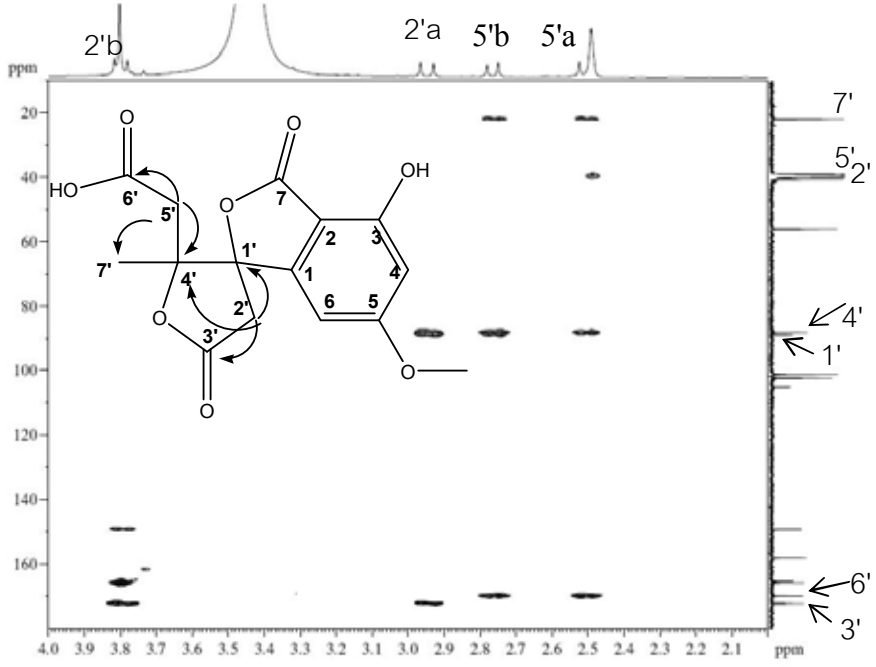

Figure 132 Expanded HMBC spectrum of altenuic acid (DMSOd_6)

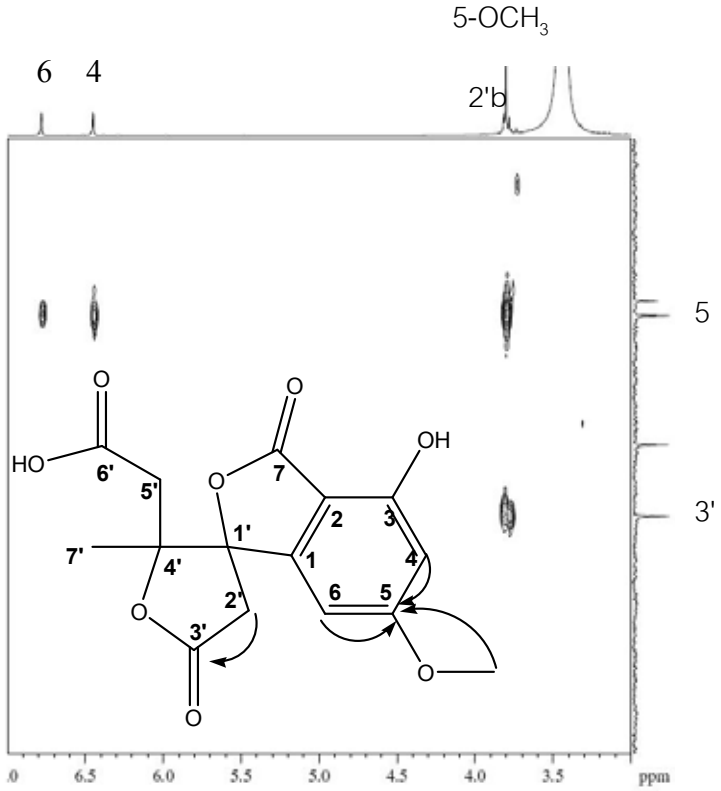

Figure 133 Expanded HMBC spectrum of altenuic acid (DMSOd_6)

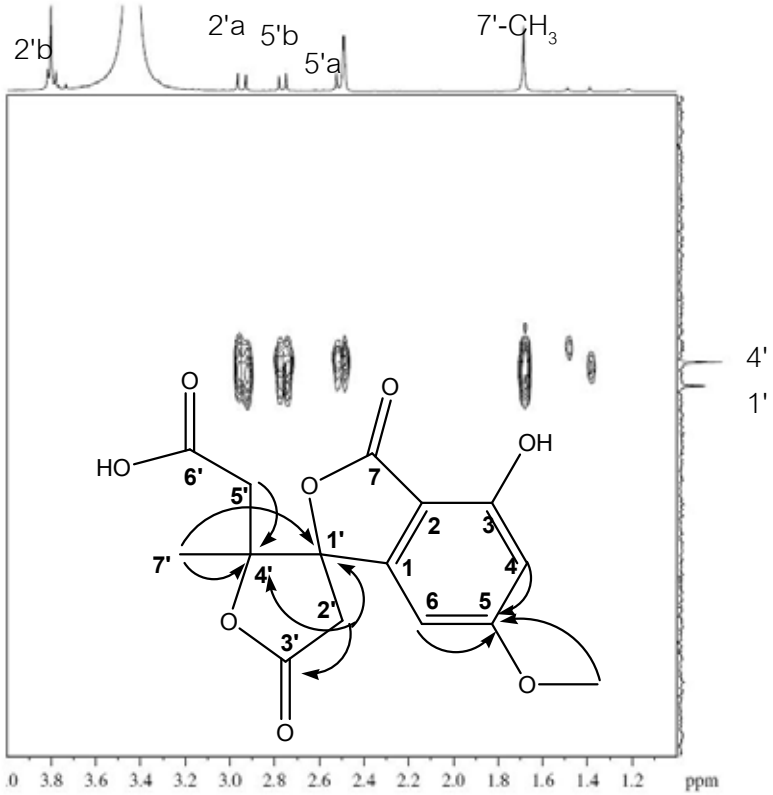

Figure 134 Expanded HMBC spectrum of altenuic acid (DMSOd_6)

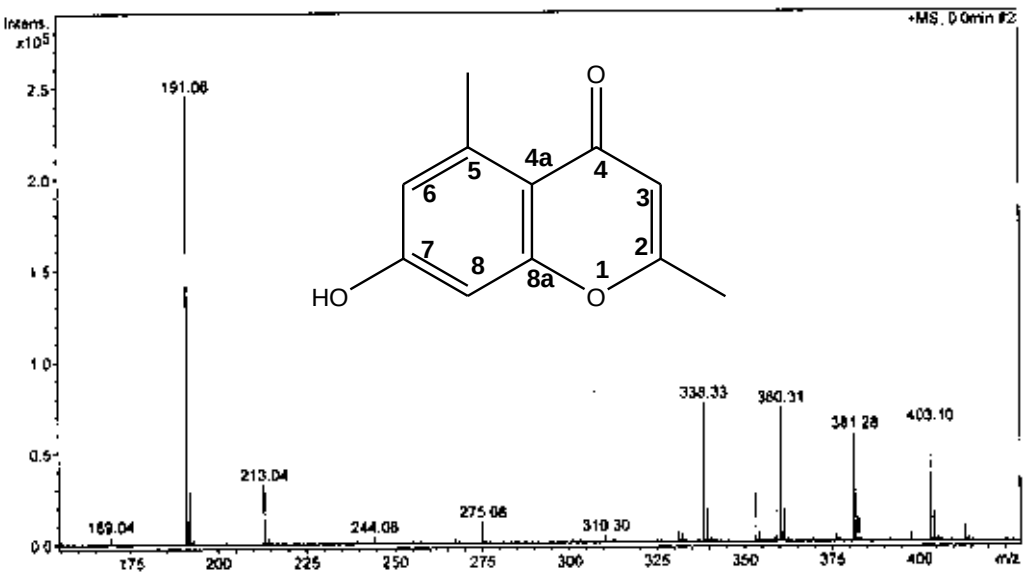

Figure 135 ESI-TOF MS spectrum of 2,5-dimethyl-7-hydroxychromone

Figure 136 ^{1}H-NMR spectrum of 2,5-dimethyl-7-hydroxychromone (500 MHz, CD_3OD)

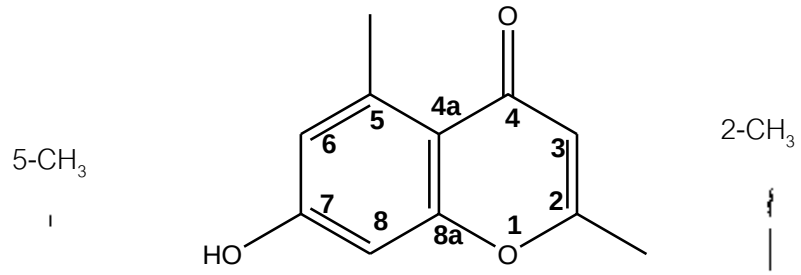

Figure 137 ^{1}H-NMR spectrum of 2,5-dimethyl-7-hydroxychromone (500 MHz, CD_3OD)

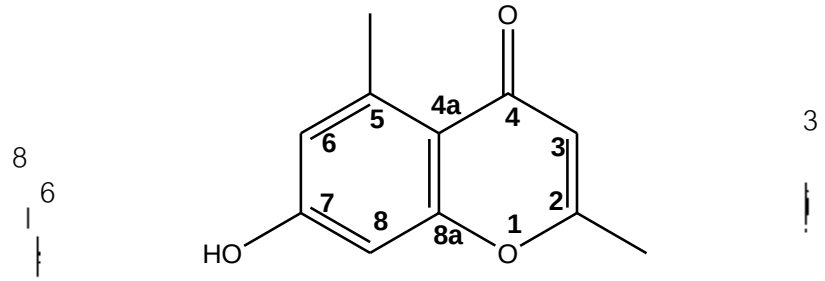

Figure 138 Expanded ^{1}H-NMR spectrum of 2,5-Dimethyl-7-hydroxychromone (500 MHz, CD_3OD)

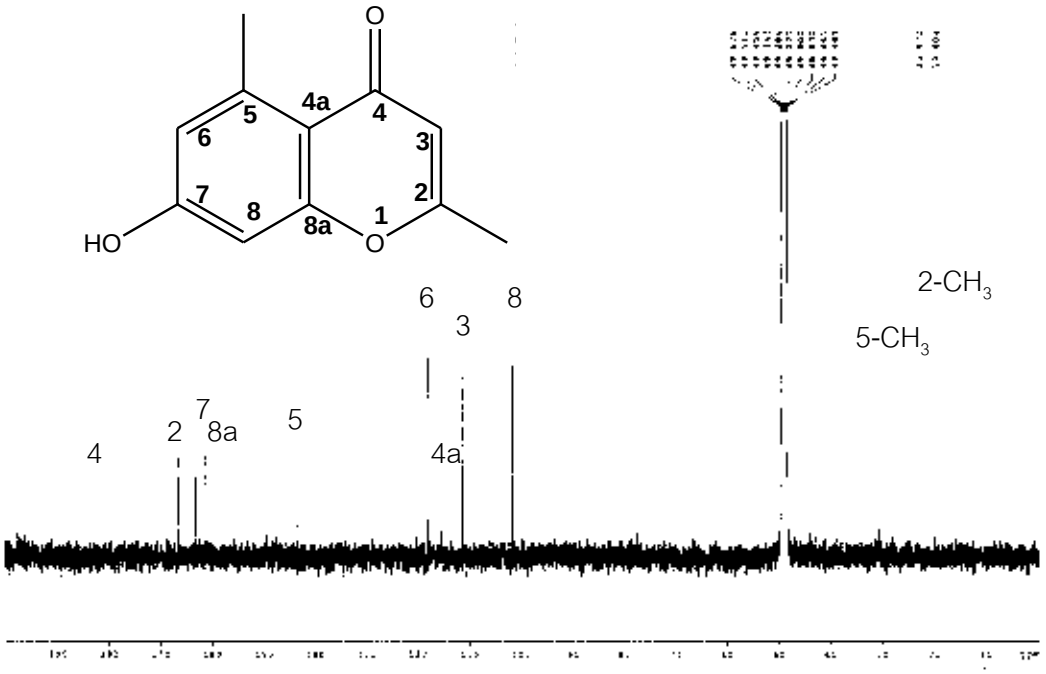

Figure 139 ^{13}C-NMR spectrum of 2,5-dimethyl-7-hydroxychromone (125 MHz, CD_3OD)

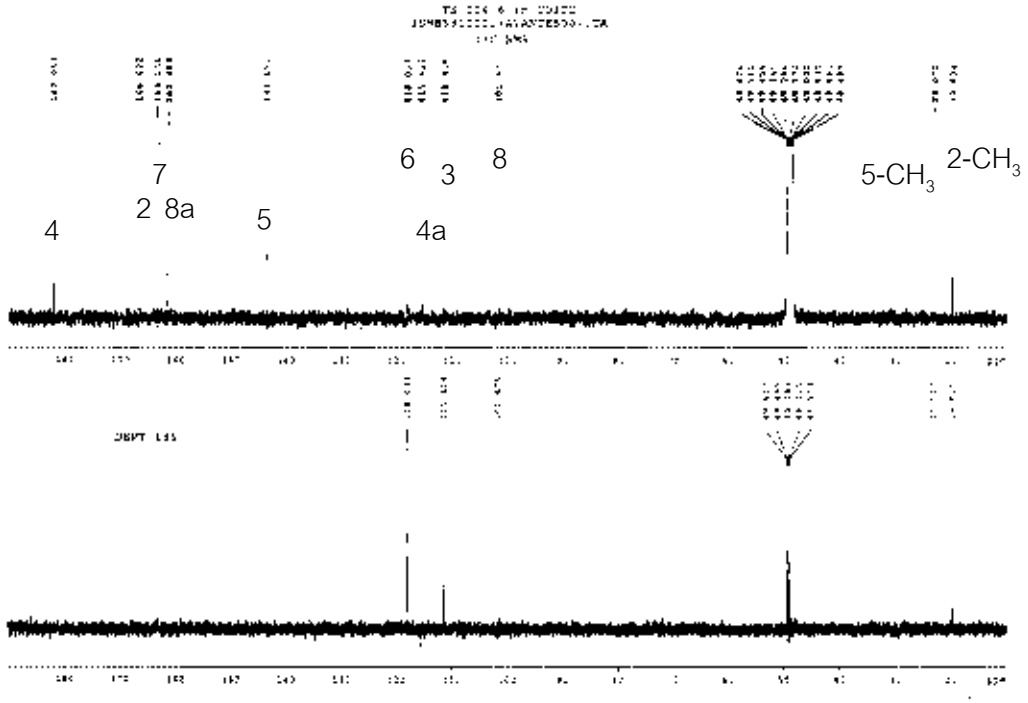

Figure 140 DEPT 135 spectrum of 2,5-dimethyl-7-hydroxychromone (125 MHz, CD_3OD)

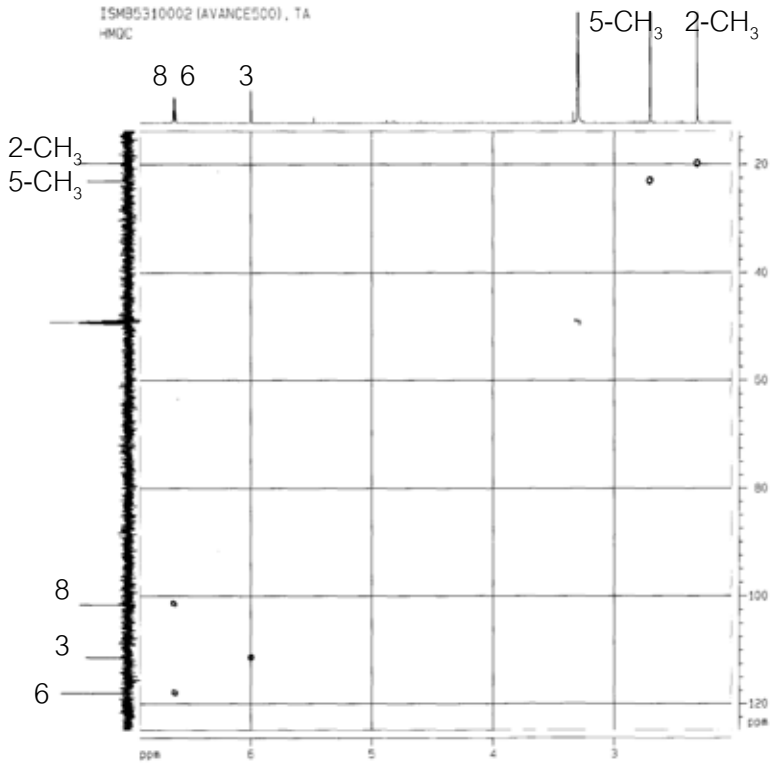

Figure 141 HMQC spectrum of 2,5-dimethyl-7-hydroxychromone (CD_3OD)

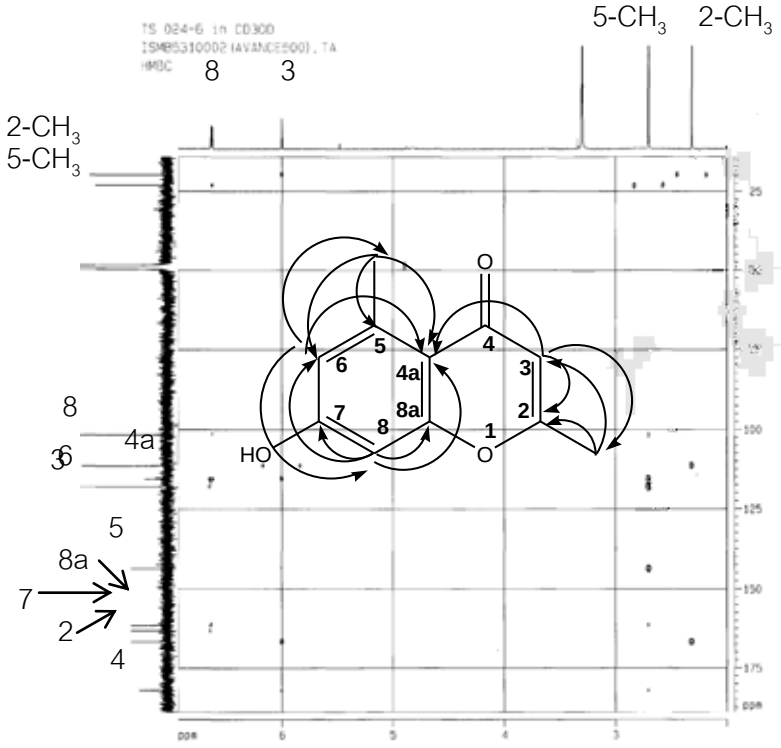

Figure 142 HMBC spectrum of 2,5-dimethyl-7-hydroxychromone (CD_3OD)

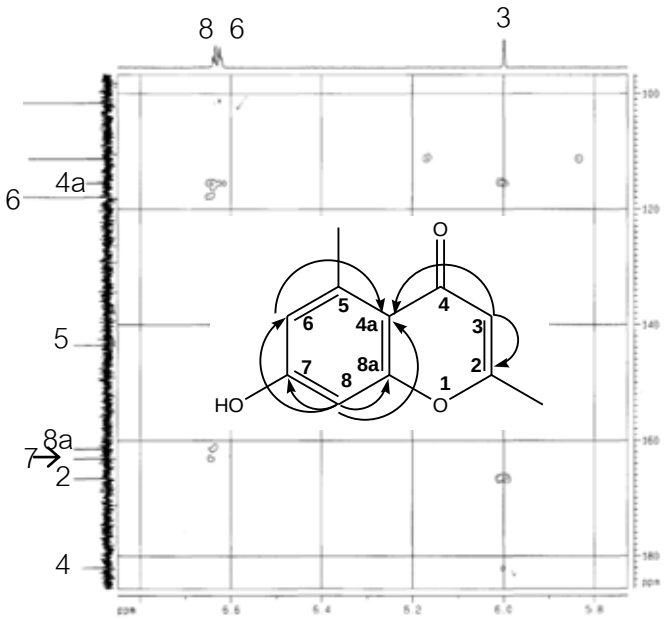

Figure 143 Expanded HMBC spectrum of 2,5-dimethyl-7-hydroxychromone (CD_3OD)

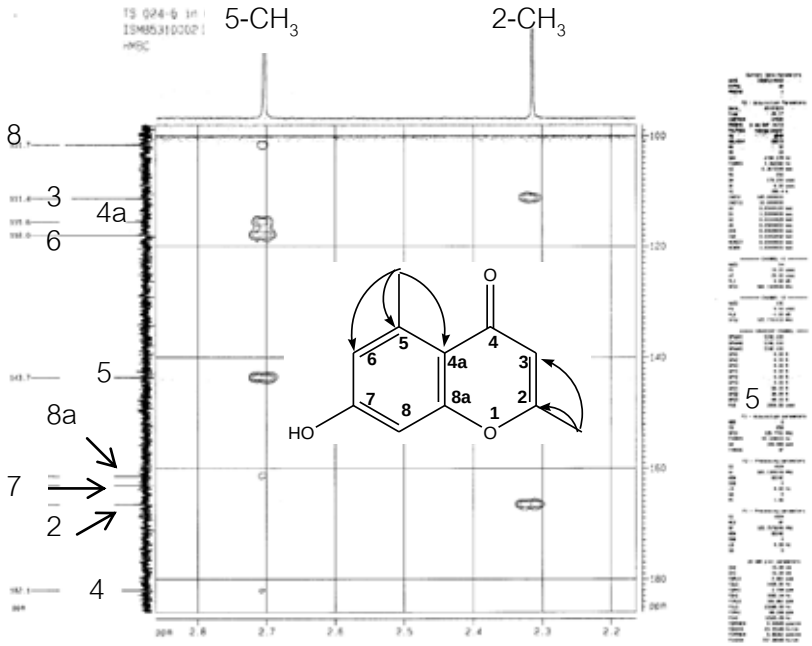

Figure 144 Expanded HMBC spectrum of 2,5-dimethyl-7-hydroxychromone (CD_3OD)

APPENDIX B

1. Czapek Yeast autolysate Broth (CzYB)

Czapek solution A	50	ml
Czapek solution B	50	ml
Yeast extract	5	g
Sucrose	30	g
Zinc solution	1	ml
Copper solution	1	ml
Distilled water to	1000	ml

2.Yeast Extract Sucrose Broth (YSB)

Yeast extract	20	g
Sucrose	150	g
$MgSO_4.7H_2O$	0.5	g
Distilled water to	1000	ml

VITA

Mrs. Jatuporn Phaopongthai was born on August 21,1956 in Ratchaburi Province, Thailand. She graduated from the Faculty of Education, Srinakharinwirot University in 1980 with Bachelor Degree of Education (Chemistry). She received her Master Degree of Science (Chemistry) in 1994 from the Faculty of Science, Chulalongkorn University, Thailand. During her Ph.D. study, she received scholarships from the Graduate School, Chulalongkorn University and Rajamangala University of Technology Thanyaburi. She has been working as Assistant Professor at the Deparment of Chemistry, Faculty of Science and Technology, Rajamangala University of Technology Thanyaburi, Phathumthanee, Thailand.

Jatuporn Phaopongthai Thesis

ORIGINALITY REPORT

26%	14%	25%	7%
SIMILARITY INDEX	INTERNET SOURCES	PUBLICATIONS	STUDENT PAPERS

PRIMARY SOURCES

1	Submitted to Higher Education Commission Pakistan Student Paper	2%
2	Chin-Cheng Liu. "Arisanschinins A–E, Lignans from Schisandra arisanensis ... Publication	1%
3	www.freepatentsonline.com Internet Source	1%
4	Angelica Soares. "In vitro Antiviral Effect of Meroditerpenes Isolated from the… Publication	1%
5	Warunee Jirawattanapong. "Synthesis of glabridin derivatives as tyrosinase in… Publication	1%
6	Chomcheon, P.. "Aromatase inhibitory, radical scavenging, and antioxidant a… Publication	1%
7	jbcs.sbq.org.br Internet Source	1%
8	Kasettrathat, C.. "Cytotoxic and antiplasmodial substances from marine-deriv… Publication	1%
9	Zhou, P.. "Coumarins and bicoumarin from Ferula sumbul: anti-HIV activity a… Publication	1%
10	Ki Kim. "New Benzamide Derivatives and NO Production Inhibitory Compoun… Publication	1%
11	www.ism2.univ-cezanne.fr Internet Source	1%
12	ethesis.unifr.ch Internet Source	1%
13	Submitted to Mahidol University Student Paper	< 1%
14	Chantana Aromdee. "Effect of the derivatives of andrographolide on the mo… Publication	< 1%
15	Narumon Boonman. "Acanthamoebicidal activity of Fusarium sp. Tlau3, an e… Publication	< 1%
16	Ki Kim. "New Cytotoxic Tetrahydroprotoberberine-Aporphine Dimeric and A… Publication	< 1%

17	aac.asm.org Internet Source	< 1%
18	Anatole Azebaze. "Xanthones from the Seeds of Allanblackia monticola and… Publication	< 1%
19	Priyanka Bagri. "New flavonoids from Punica granatum flowers", Chemistry … Publication	< 1%
20	L. Sun. "In Vitro Activities of Retigeric Acid B Alone and in Combination with… Publication	< 1%
21	H. Quan. "Potent In Vitro Synergism of Fluconazole and Berberine Chloride… Publication	< 1%
22	Gary A. Strobel. "Rainforest Endophytes and Bioactive Products", Critical R… Publication	< 1%
23	Takekuma, S.i.. "An efficient preparation, crystal structures, and properties … Publication	< 1%
24	Han, Q.B.. "Xanthones with growth inhibition against HeLa cells from Garcin… Publication	< 1%
25	Antia, B.S.. "Itaconic acid derivatives and diketopiperazine from the marine-… Publication	< 1%
26	Zhiyong Guo. "1H and13C NMR signal assignments of Paecilin A and B, tw… Publication	< 1%
27	Liu, R.. "Isolation and purification of coumarin compounds from the root of P… Publication	< 1%
28	Vilailak Prachyawarakorn. "Diketopiperazines and Phthalides from a Marine… Publication	< 1%
29	Ahn, E.M.. "Prenylated flavonoids from Moghania philippinensis", Phytochem… Publication	< 1%
30	Z.-L. Li. "Triterpenoids from the husks of Xanthoceras sorbifolia Bunge", Jo… Publication	< 1%
31	Submitted to King Saud University Student Paper	< 1%
32	stratingh.eldoc.ub.rug.nl Internet Source	< 1%
33	lib.ugent.be Internet Source	< 1%
34	Hegazy, M.E.F.. "Biotransformation of sesquiterpenoids having @a,@b-un… Publication	< 1%
35	Ian-Lih Tsai. "Cytotoxic Neolignans from the Stem Wood of Machilus obova… Publication	< 1%
		< 1%

36	Ferreira, D.. "Biflavanoid proguibourtinidin carboxylic acids and their biflava… Publication	< 1%
37	www.ncbi.nlm.nih.gov Internet Source	< 1%
38	DellaGreca, M.. "Cinnamic acid amides and lignanamides from Aptenia cord… Publication	< 1%
39	www.vremea-online.ro Internet Source	< 1%
40	Liu, H.. "Norclerodane diterpenoids from rhizomes of Dioscorea bulbifera",… Publication	< 1%
41	Submitted to University of Macau Student Paper	< 1%
42	Guimaraes, D.O.. "Diketopiperazines produced by endophytic fungi found … Publication	< 1%
43	Mei You. "Glycosides from the Methanol Extract of Notopterygium incisum"… Publication	< 1%
44	www.mushroomhunter.net Internet Source	< 1%
45	Hernandez-Guerrero, C.J.. "Cytotoxic dibromotyrosine-derived metabolites… Publication	< 1%
46	"Nigerasperones A~C, New Monomeric and Dimeric Naphtho-γ-pyrones fr… Publication	< 1%
47	scholar.lib.vt.edu Internet Source	< 1%
48	Jin-Shan Tang. "Complete assignments of1H and13C NMR spectral data of… Publication	< 1%
49	Ping-Chung Kuo. "Eurycomalin A, a new dimeric dihydrobenzofuran fromEu… Publication	< 1%
50	Maneekarn Chinworrungsee. "Cytotoxic activities of trichothecenes isolated… Publication	< 1%
51	Muangsin, N.. "Austrocortinin: Crystal structure of a natural anthraquinone p… Publication	< 1%
52	"A New Benzophenone from Lindera fruticosa", Bulletin of the Korean Chem… Publication	< 1%
53	Ji-Feng Liu. "Two New Phenylpropanoid Derivatives and Other Constituent… Publication	< 1%
54	M.-A. Ouyang. "Water-soluble constituents from aerial roots of Ficus microc… Publication	< 1%
55	Farzana Shaheen. "New α-Glucosidase Inhibitors and Antibacterial Compo…	< 1%

	Publication	< 1%
56	Jussara Pinheiro Barbosa. "In vitroAntiviral Diterpenes from the Brazilian Br… Publication	< 1%
57	www.sc.mahidol.ac.th Internet Source	< 1%
58	www.dtic.mil Internet Source	< 1%
59	M. Hussain. "Synthesis and Antimicrobial Activities of Some Isocoumarin an… Publication	< 1%
60	Wei-Xin Sun. "Chemical Constituents of Daphne giraldii Nitsche", Journal of… Publication	< 1%
61	Submitted to Institute of Graduate Studies, UiTM Student Paper	< 1%
62	ntur.lib.ntu.edu.tw Internet Source	< 1%
63	Submitted to Texas Christian University Student Paper	< 1%
64	Damager, I.. "Synthesis and characterisation of novel chromogenic substra… Publication	< 1%
65	Khalid Mohammed Khan. "Synthesis and Biological Screening of 7-Hydroxy… Publication	< 1%
66	koreacrystal.or.kr Internet Source	< 1%
67	Jingqiu Dai. "Metabolites from the Endophytic FungusNodulisporium sp. fro… Publication	< 1%
68	Simirgiotis, M.J.. "Identification of phenolic compounds from the fruits of the… Publication	< 1%
69	Kurono, M.. "A practical semi-synthesis of tautomycin using a hydrolysate o… Publication	< 1%
70	Ojika, M.. "Aplyronine A, a potent antitumor macrolide of marine origin, and … Publication	< 1%
71	www.jic.ac.uk Internet Source	< 1%
72	Zhong-shan Cheng. "Biodiversity and biotechnological potential of mangrov… Publication	< 1%
73	www.lookchemical.com Internet Source	< 1%
74	A. K. Sinha. "Microwave-assisted rapid synthesis of methyl 2,4,5-trimethoxy… Publication	< 1%

75	www.ohiolink.edu Internet Source	< 1%
76	opus.tu-bs.de Internet Source	< 1%
77	www.mdpi.org Internet Source	< 1%
78	Katsuyoshi Matsunami. "Megastigmane glucosides and an unusual monote… Publication	< 1%
79	Submitted to Drexel University Student Paper	< 1%
80	www.bionewsonline.com Internet Source	< 1%
81	Ndom, J.C.. "Secondary metabolites from Senecio burtonii (Compositae)", P… Publication	< 1%
82	Clark, R.J.. "New Isocyano and Isothiocyanato Terpene Metabolites from th… Publication	< 1%
83	Wen-Yong Liu. "Pyrrole alkaloids from Bolbostemma Paniculatum", Journal … Publication	< 1%
84	Xiang Wan. "Biotransformation of caffeic acid by Momordica charantia perox… Publication	< 1%
85	Lim, J.H.. "Combination effects of cephalexin and gentamicin on Edwardsie… Publication	< 1%
86	Amel Hadj-Bouazza. "New Acyclonucleosides: Synthesis and Anti-HIV Act… Publication	< 1%
87	Zhang, Y.. "Ergosterimide, a new natural Diels-Alder adduct of a steroid an… Publication	< 1%
88	Lemmich, J.. "Monoterpene, chromone and coumarin glucosides of Diplolo… Publication	< 1%
89	Garcia, Abraham Ramirez-Apan, Teresa Ant. "Absolute configuration assig… Publication	< 1%
90	Gonzalez, M.J.T.G.. "Stilbenes and other constituents of Knema austrosiam… Publication	< 1%
91	www.bentham-mps.org Internet Source	< 1%
92	etd.uovs.ac.za Internet Source	< 1%
93	www.chemie.uni-hamburg.de Internet Source	< 1%
94	Kato, K.. "2,2'-Isopropylidenebis[(4S,5R)-4,5-di(2-naphthyl)-2-oxazoline] lig…	< 1%

	Publication	< 1%
95	Rashid, M.A.. "New nitrogenous constituents from the South African marine… Publication	< 1%
96	www-pub.iaea.org Internet Source	< 1%
97	Eun-Kyoung Song. "Diarylheptanoids with Free Radical Scavenging and He… Publication	< 1%
98	Yi Zhang. "New Sphingolipids with a Previously Unreported 9-Methyl-C20-s… Publication	< 1%
99	Wang, L.. "Ring-opening polymerization of l-lactide catalyzed by robust mag… Publication	< 1%
100	Jia Guo. "Three New Phenolic Compounds from the Lichen Thamnolia verm… Publication	< 1%
101	Subhash Jain. "Novel Fluorinated Spiro [Indole-indazolyl-thiazolidine]-2,4′-d… Publication	< 1%
102	www.znaturforsch.com Internet Source	< 1%
103	Meffo Yemele Bouberte. "Tithoniamarin and tithoniamide: a structurally uniqu… Publication	< 1%
104	www.sbfgnosia.org.br Internet Source	< 1%
105	www.patents.com Internet Source	< 1%
106	edoc.bib.ucl.ac.be:81 Internet Source	< 1%
107	Feng Wang. "Two new aromatic compounds from the resin of Styrax tonkin… Publication	< 1%
108	www.coursehero.com Internet Source	< 1%
109	en.wikipedia.org Internet Source	< 1%
110	www.math.titech.ac.jp Internet Source	< 1%
111	"Pubescenes, Jatrophane Diterpenes, fromEuphorbia pubescens,with Mult… Publication	< 1%
112	Craig, D.. "Additive Pummerer reactions of vinylic sulfoxides. Synthesis of @… Publication	< 1%
113	L. Yan. "The alternative oxidase of Candida albicans causes reduced fluco… Publication	< 1%

114	Nahrstedt, A.. "Amygdalin acyl derivatives, cyanogenic glycosides from the… Publication	< 1%
115	George R. Pettit. "Isolation, structure, and synthesis of combretastatin A-2,… Publication	< 1%
116	mdpi.org Internet Source	< 1%
117	intl-aac.asm.org Internet Source	< 1%
118	Sonwa, M.M.. "Chemical study of the essential oil of Cyperus rotundus", Ph… Publication	< 1%
119	www.faqs.org Internet Source	< 1%
120	Qing-Jian Zhang. "Three new Diels-Alder type adducts from the stem bark o… Publication	< 1%
121	Bharat Bashyal. "Tricinonoic acid and tricindiol, two new irregular sesquiterp… Publication	< 1%
122	Li, X.C.. "Phenolic compounds from the aqueous extract of Acacia catechu… Publication	< 1%
123	www.weathercity.com Internet Source	< 1%
124	Lescop, C.. "Synthesis of Novel Nucleosides with a Fused Cyclopropane R… Publication	< 1%
125	Ankli, A.. "Cytotoxic cardenolides and antibacterial terpenoids from Crossop… Publication	< 1%
126	Jijun Xue. "Studies on Flavans. III. The Total Synthesis of (±)-7,4′-Dihydrox… Publication	< 1%
127	Nadine Muller. "Synthesis of pyrimidinones by action of benzamidine on a b… Publication	< 1%
128	Ligang Zhou. "Antibacterial phenolic compounds from the spines of Gledits… Publication	< 1%
129	www.eczakademi.org Internet Source	< 1%
130	www.filecatch.com Internet Source	< 1%
131	Wang, X.. "Analysis of the constituents in the rat plasma after oral administra… Publication	< 1%
132	edoc.ub.uni-muenchen.de Internet Source	< 1%
133	J. L. Seidel. "Neotropical ant gardens", Journal of Chemical Ecology, 06/19…	< 1%

[redacted]	Publication	< 1%
134	Otsuka, H.. "Stereochemistry of megastigmane glucosides from Glochidion… Publication	< 1%
135	Blanca Rivero-Cruz. "Smooth Muscle Relaxant Action of Benzyl Benzoates… Publication	< 1%
136	"Antitubercular and Antiplasmodial Constituents ofAbrus precatorius", Plant… Publication	< 1%
137	Maurice Awouafack. "Antimicrobial Prenylated Dihydrochalcones from Erios… Publication	< 1%
138	Nakatani, S.. "Melleumin A, a novel peptide lactone isolated from the culture… Publication	< 1%
139	Marko Vogler. "Dianhydrohexitole-Based Benzamidines: An Efficient Synthe… Publication	< 1%
140	Wendong Wang. "Synthesis of N - Glycoside Analogs via Thionolactones †"… Publication	< 1%
141	Tolls, J.. "Extraction and isolation of linear alcohol ethoxylates from fish", Jou… Publication	< 1%
142	Daniela Weber. "Endophytic Fungi, Occurrence and Metabolites", Physiolo… Publication	< 1%
143	Pierre Emmanuel Charles. "Serum procalcitonin measurement contribution … Publication	< 1%
144	H. M. T. B. Herath. "Dactyloidin, a New Diaryl Nonanoid from Myristica Dac… Publication	< 1%
145	Peng, J.. "The new bioactive diterpenes cyanthiwigins E-AA from the Jamai… Publication	< 1%
146	Suaifan, G.A.R.Y.. "Effects of steric bulk and stereochemistry on the rates o… Publication	< 1%
147	Yuan-Wah Leong. "Phenanthrenes, dihydrophenanthrenes and bibenzyls fr… Publication	< 1%
148	Zhi-Qi Yin. "Acetophenone Derivatives and Sesquiterpene fromEuphorbia e… Publication	< 1%
149	Sudo, H.. "10-O-acylated iridoid glucosides from leaves of Premna subsca… Publication	< 1%
150	Fatima Chaaib. "Antifungal and Antioxidant Compounds from the Root Bark … Publication	< 1%
151	Guillermo Schmeda-Hirschmann. "A new antifungal and antiprotozoal depsi… Publication	< 1%

EXCLUDE QUOTES	ON	EXCLUDE MATCHES	OFF
EXCLUDE BIBLIOGRAPHY	ON		